Odontogenic Induction Capacity of In Vitro Expanded Dental Mesenchymal Cells in Whole Tooth Bioengineering

Yang, L.

Awarding institution:
King's College London

A thesis submitted to King's College London for the degree of

Doctor of Philosophy

Odontogenic Induction Capacity of *In Vitro* Expanded Dental Mesenchymal Cells in Whole Tooth Bioengineering

Liu Yang

Centre for Craniofacial & Regenerative Biology

Dental Institute

King's College London

September, 2017

Supervised firstly by:

Prof. Paul Sharpe

Centre for Craniofacial & Regenerative Biology, Dental Institute, King's College London, UK.

and secondly by:

Dr. Isabelle Miletich

Centre for Craniofacial & Regenerative Biology, Dental Institute, King's College London, UK.

Examined by:

Dr. Bing Hu

Peninsula Schools of Medicine and Dentistry, Plymouth University, UK.

and by:

Dr. Claire Higgins

Department of Bioengineering, Imperial College London, UK.

Statement of originality

I declare that all the work presented in this thesis, unless otherwise acknowledged, is my own. This project provides an original contribution to the knowledge of this subject.

Signed 杨柳 Yang Liu Date 01/Apr/2018

Acknowledgements

I would like to express my sincerest thanks to my supervisor Prof. Paul Sharpe for this exciting project and for his outstanding supervision and inspiring advices on it. Thanks also go to my secondary supervisor Dr. Isabelle Miletich, coordinator Prof. Gordon Proctor and my MPhil/PhD upgrade examiner Prof. Abigail Tucker for their great advices on the project and my study. My heartfelt gratitude goes to Dr. Ana Angelova Volponi, Dr. Yvonne Pang for their patient and meticulous guidance and assistance on the project and in the lab. I am especially thankful to Yang Ma, Ana Caetano who not only had intensively worked on this project with me, but also become really good friends outside of work. Great appreciation to Dr. Christopher Healy for the micro-CT scan, Prof. Paul Sharpe and Mrs. Dhivya Chandrasekaran for the surgeries of mouse subrenal transplantation, Val Yianni for help on sample preparations of RNA sequencing and FACS, Dr. Shelly Abraham for qPCR training. My deepest sadness on hearing of the passing of Shelly, may her soul rest in peace. Thank all the other current and former Sharpe group members for consistent support, they are Jing, Maja, Basem, Vitor, Mushriq, Abeer, Tian, Zhengwen, Rebecca, Lucia, Arshiya. A big thank you to Angela for her terrific admin work. Appreciation to CFD technical team and New Hunt's House BSU team for providing excellent technical support. I'm grateful to many friends for keeping me from getting too homesick, especially my 3-year flat mate Hadeel who has been like a big sister to me. I'm also deeply indebted to my parents who consistently and unconditionally support me. Last but not least, I am grateful and honored to be sponsored by King's College London and China Scholarship Council.

Abstract

Whole tooth bioengineering has been achieved in mice using non-cultured embryonic dental mesenchymal cells (DMCs). *In vitro* expanded postnatal DMCs can also contribute to tooth formation but only as cells that respond to inductive signals. Since large cell numbers are required for clinical application, enabling *in vitro* expanded cell populations to induce *de novo* odontogenesis is the main challenge. To investigate if cultured DMCs can contribute to tooth formation as inductive cells, genetically-labelled cultured embryonic or postnatal DMCs were mixed with wild-type fresh inductive embryonic DMCs in different ratios, and then recombined with responsive epithelium. It is shown that although unable to initiate, cultured embryonic DMCs do not lose their ability to contribute to tooth induction; while postnatal pulp cells can neither initiate nor contribute. Micro-environmental modification of proliferating embryonic DMCs via 3D culture and co-culture systems were attempted to restore or retain the odontogenic induction ability. Although with increased expression of odontogenic genes *Pax9* and *Msx1*, 3D cultured and co-cultured cells failed to initiate odontogenesis. Embryonic DMCs cultured for short periods (within 48 hours) maintained tooth inducing ability. Gene expression profiling was carried out with RNA sequencing data of cultured DMCs collected at different time points to study the molecular basis of the progressively reduced inductivity. In combination with gene expression comparisons between epithelial odontogenic and non-odontogenic tissues, the *Wnt* signalling pathway and *Dlk1* were found to have a strong correlation with maintenance of odontogenic induction capacity.

Table of Contents

List of Figures

List of Tables

List of Abbreviations

2D	Two dimensional
3D	Three dimensional
α-MEM	alpha Minimal Essential Medium
Barx1	BarH-like homeobox 1
BMP	Bone Morphogenetic Protein
BMSCs	Bone marrow derived Mesenchymal Stem Cells
BSA	Bovine Serum Albumin
CDKN1A	Cyclin-dependent kinase inhibitor 1A
cDNA	complementary deoxyribonucleic acid
CiPSCs	Chemically induced Pluripotent Stem Cells
DAPI	4',6-diamidino-2-phenylindole
Dl1	Distal less homeobox 1
Dl2	Distal less homeobox 2
Dl5	Distal less homeobox 5
Dl6	Distal less homeobox 6
DMEM	Dulbecco's Modified Eagle's medium
dNTP	deoxy-ribonucleoside triphosphate
DPBS	Dulbecco's phosphate-buffered saline
DPSCs	Dental Pulp Stem Cells
DSP	Dentin Sialoprotein
DSPP	Dentin sialophosphoprotein
E(number)	Embryonic day
EDA	Ectodysplasin-A
EDAR	Ectodysplasin-A receptor
EpSCs	Epithelial Stem Cells

ERMs	Epithelial Rest of Malassez
ES	Embryonic Stem
FBS	Fetal Bovine Serum
FGF	Fibroblast Growth Factor
GAPDH	Glyceraldehyde 3-phosphate dehydrogenase
GFP	Green Fluorescent Protein
Gli1	GLI family zinc finger 1
Gli2	GLI family zinc finger 2
Gli3	GLI family zinc finger 3
H&E	Hematoxylin and Eosin
HH	Hedgehog
IF	Immunofluorescence
IMS	Industrial Methylated Spirit
iOS	induced Odontogenic Stem
iPS	induced Pluripotent Stem
L-15	Leibovitz's L-15
Lef1	Lymphoid enhancer binding factor 1
Lh6	LIM homeobox 6
Lhx7	LIM homeobox 7
M-MLV	Moloney Murine Leukemia Virus
MSCs	Mesenchymal Stem Cells
Msx1	Msh homeobox 1
mTmG	membrane-Tomato/membrane-Green
NTC	No Template Control
P(number)	Passage
Pax9	Paired box 9
PBS	Phosphate-Buffered Saline
PBST	Phosphate Buffered Saline Tween-20

PCT	Progenitor Cell Targeted
PDLSCs	Periodontal ligament stem cells
PFA	Paraformaldehyde
PiPSCs	Protein induced Pluripotent Stem Cells
Pitx2	Paired-like homeodomain transcription factor
qPCR	quantitative Polymerase Chain Reaction
RNA	Ribonucleic acid
RT	Reverse Transcription/Transcriptase
Runx2	Runt-related transcription factor 2
SCAPs	Stem Cells from Apical Papilla
SHEDs	Stem cells from Human Exfoliated Deciduous tooth
SHH	Sonic hedgehog
Sostdc1	Sclerostin domain containing 1
TGFβ	Transforming growth factor β
TGPCs	Tooth Germ Progenitor Cells
TNF	Tumor necrosis factor
WNT	Wingless-type MMTV integration site family
Wnt10a	Wingless-type MMTV integration site family, member 10a
Wnt10b	Wingless-type MMTV integration site family, member 10b
Wnt5a	Wingless-type MMTV integration site family, member 5a
Wnt5b	Wingless-type MMTV integration site family, member 5b

Chapter I General Introduction

1.1 Clinical problem

Tooth loss is a common dental problem worldwide, with periodontal disease as the leading cause, following others such as caries and trauma. Multiple functions of teeth including mastication, articulation and aesthetics, result in vast demands for the treatment of tooth loss.

At present, clinically, missing teeth are restored by removable dentures, fixed bridges and dental implants which all involve non-biological materials, and thus not only do they cause foreign body sensation and reaction in mouth, but they also have limited lifespan that may lead to regular replacement or re-treatment which are time and money consuming for patients; Moreover, although implants minimize the discomfort and causes no damage to the adjacent teeth compared with the other two prostheses, failure can occur due to bone loss around the implant during the long term chewing movement, since implants rigidly connect with alveolar bone through “osseointegration” and lack the periodontal ligament to absorb masticatory forces.

To avoid these drawbacks of artificial teeth, stem-cell based tooth regeneration has been suggested as an alternative, thanks to progress in regenerative medicine, stem cell biology and tissue engineering. Currently, the general concept of tooth bioengineering is “to mimic the nature tooth development process *in vitro* or *in vivo* using stem cells” (Otsu et al., 2014).

1.2 Tooth development

To mimic the natural process, it is essential to have a comprehensive understanding of how the embryo makes teeth.

1.2.1 Embryonic odontogenesis

In common with the other ectodermal appendages, e.g. hair follicles and many exocrine glands (mammary, sweat and salivary glands), embryonic development of teeth involves two groups of cells: epithelial cells derived from oral ectoderm which differentiate into ameloblasts to form enamel, and mesenchymal cells derived from cranial neural crest (ectomesenchyme) which differentiate into odontoblasts to form dentin and all other cells to form the rest of a tooth such as pulp, cementum, periodontal ligament and even alveolar bone. Sequential and reciprocal interactions between the two participants throughout the process are the key drive and regulation of tooth formation.

The process of tooth germ development can be divided into four main phases, initiation, morphogenesis, differentiation and mineralization, root development and eruption. In the first phase, initiation, locally thickened oral ectoderm forms dental lamina (epithelium) which is capable of inducing underlying mesenchyme to become odontogenic. The tooth forming capacity then shifts from epithelium to mesenchyme, the induced odontogenic mesenchyme sends signals back to induce epithelium to form dental placodes. The following phase is morphogenesis in which epithelium further invaginates into the underlying mesenchyme and forms a “bud”, accordingly this is called “bud stage”, while mesenchymal cells condense around the bud, where dynamic changes of shape and size can be observed in the cells at the condensed mesenchyme area (Mammoto et al., 2011). As this phase proceeds, epithelium continuously extends to surround the

condensing mesenchyme (dental papilla) and forms a cap shape, hence this period is named “cap stage” during which the tooth crown morphogenesis is initiated and regulated by a signalling centre that develops at the tip of the late “bud”, known as the primary enamel knot (epithelium). With further extension of epithelium, comes the “bell stage”, and also commences the next phase: cytodifferentiation, during which epithelial and mesenchymal cells at the interface differentiate into ameloblasts and odontoblasts respectively and subsequently (by the late bell stage) form enamel and dentin through mineralization. Location related heterogeneity can be observed in the mesenchymal cells in the tooth germ: cells at the interface between epithelium and mesenchyme differentiate into odontoblasts, others differentiate into pulp cells, whereas during bell stage the dental follicle cells differentiate into periodontal tissues, including the periodontal ligament, cementum and alveolar bone. Additionally, it has been reported that the balance between neural crest- and non-neural crest- derived cell populations changes in the dental mesenchyme during advancing development which might due to vascularization bringing circulating cells to the forming tooth and migration of cells from periodontal to dental mesenchyme during odontogenesis (Chai et al., 2000). Different populations that exist in the dental pulp stem cells also imply heterogeneity in dental mesenchymal condensates (An et al., 2018, Sharpe, 2016). Tooth root development starts after the bell stage leading to tooth eruption by coordination with bone resorption. Humans have two dentitions; the permanent tooth germ develops with the same process after the deciduous tooth germ completely detached from the dental lamina. (Figure I-1. upper diagram) In addition, the extracellular matrix (ECM) layer, whose main components are laminin, collagen IV, nidogen and sulfated proteoglycan, and the basement membranes (BM) between the dental epithelium and mesenchyme, which are specialized extracellular matrices that mainly consist of various forms of laminin, type IV collagen, perlecan, and nidogen, are both considered to be involved with

cell proliferation and differentiation. During tooth morphogenesis, extracellular matrices are dramatically changed. Type IV collagen and laminin molecules are evenly distributed in the dental basement membranes during early mouse embryonic development and disappear when the membranes are degraded by enzymes (Fukumoto and Yamada, 2005).

Humans have two sets of incisors, canines and premolars and one set of molars, while mice have just one set of teeth with only molars at the back and continuously growing incisors at the front of the mouth separated by a toothless area which is called diastema (Tucker and Sharpe, 2004). Although different in tooth type, pattern and replacement, it has been shown that human and mouse teeth share similar development pattern and signalling networks (Lin et al., 2007). Thus, in this research, murine molars are selected to be a simplified model of human teeth. For mice, tooth development initiates from embryonic day 10 (E10), and the bud, cap and bell stages on E12.5 (early bud) and E13.5 (bud), E14.5 (early cap) and E15.5 (cap), E16.5 (early bell), E17.5 (bell) and E18.5 (late bell) respectively.

1.2.2 Cell signalling and gene regulation in tooth development

Most of the paracrine signal molecules mediating the epithelium-mesenchyme interactions during odontogenesis belong to four conserved protein families: transforming growth factor β (TGFβ), fibroblast growth factor (FGF), Hedgehog (HH) family and WNT family. These signals regulate the relative gene expression in epithelial and mesenchymal cells via different signalling pathways such as bone morphogenetic protein (Bmp), Fgf, sonic hedgehog (Shh) and Wnt. Ectodysplasin-A (EDA) which belongs to tumor necrosis factor (TNF) family was found to function in tooth organogenesis through the Eda pathway together with its receptor EDAR. Mutations in EDA and EDAR can cause ectodermal dysplasia, a genetic condition involving dysgenesis of at least two ectodermal derivatives, such as hair, nails,

teeth, and sweat glands, which highlights a common pathway for appendage formation (Salas-Alanis et al., 2015). The genes regulated by these signals encode growth factors, transcription factors, signals, signal receptors which render the epithelial or mesenchymal cells be able to induce, respond or differentiate. (Thesleff, 2003, Tucker and Sharpe, 2004, Jussila and Thesleff, 2012, Li et al., 2013b) (Figure I-1, lower diagram)

At the initiation stage, the paired-related homeobox gene *Pitx2* is expressed in oral ectoderm, establishing the dentition pattern through the mutual up-regulation with *Fgf8* and down-regulation with *Bmp4* (Liu et al., 2003). The thickened oral ectoderm, dental lamina, sends signals such as BMP4, FGF8, SHH, WNT10b, TNF (EDA and EDAR) to induce odontogenic ability in the underlying mesenchyme. The induced odontogenic mesenchyme express transcription factors such as LIM homeodomain genes *Lhx6, Lhx7,* BarH-like homeobox 1 (*Barx1*), distal less homeobox genes *Dl1, Dl2, Dl5, Dl6,* paired box gene 9 (*Pax9*), Msh homeobox genes *Msx1, Msx2,* GLI-Kruppel family member *Gli1, Gli2, Gli3*, and also reciprocal signals including ACTIVIN, BMP4 and FGFs are sent back to epithelium to promote the formation of dental placodes. During the morphogenesis stage, dental placodes (epithelium) express transcription factors such as *Msx2*, lymphoid enhancer binding factor 1 (*Lef1*) and *p21* also known as cyclin-dependent kinase inhibitor 1A (*CDKN1A*) and signal receptor *Edar*. Signal molecules involving BMP4, FGF8, SHH, WNT sent from dental placode induce expression of new genes including *Lef1* and runt homologue gene *Runx2* and maintain the earlier expressed genes in mesenchyme to regulate its condensation. The condensed mesenchyme then releases signals of BMP4, FGF (3,10) and WNT (5a,5b) to induce the formation of enamel knots in the epithelium. Enamel knots, as signalling centres, produce BMP (2,4,7), FGF (3,4,9,20), SHH, WNT(3,6,10a,10b) and TNF (Eda, Edar) to

regulate the cell differentiation in both epithelium and mesenchyme. (Jussila and Thesleff, 2012, Thesleff, 2003, Tucker and Sharpe, 2004)

Deficiency of the transcription factors such as *Pax9, Msx1, Msx2, Dlx1, Dlx2, Gli2, Gli3, Lef1,* and *Runx2* leads to hypodontia. *Follistatin, Sprouty* and Sclerostin domain containing 1 (*Sostdc1*) are important antagonists or inhibitors of signal molecules ACTIVIN, FGF and BMP respectively and deletion of these genes give rise to extra teeth (Tummers and Thesleff, 2009).

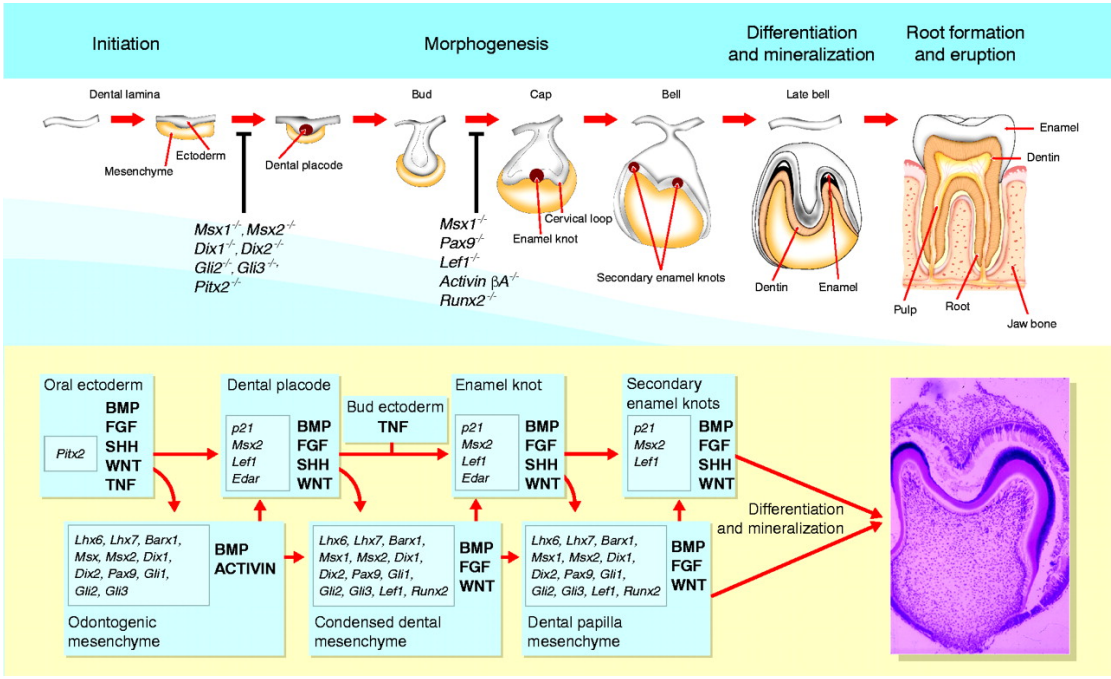

Figure I-1. Diagrams of stages and signalling networks of tooth development.

Upper diagram shows the stages of tooth development, deficiency of certain genes can lead to arrest of tooth development at different stages. Lower diagram illustrates the simplified signalling networks of odontogenesis, boldfaces represent signalling molecules and italics represent the transcription factors expressed in the tissue compartments. The inhibitors of the major signalling pathways are not shown here. Adapted from (Thesleff, 2003)

1.3 Whole Tooth bioengineering scheme

According to the study on tooth development, in the blueprint of clinical tooth regeneration, patient-derived epithelial and mesenchymal cells will be expanded *in vitro* to generate sufficient cells and then combined to mimic the nature tooth development to form an early stage (bud or cap stage) tooth primordium (Volponi et al., 2010). The next step could be either transplantation of the primordium into the location of the missing tooth (Ikeda et al., 2009), or generation of a bioengineered tooth unit *in vitro* composed of a mature tooth, periodontal ligament and alveolar bone following surgical engraftment (Oshima et al., 2011). The developed and erupted tooth from the bioengineered primordium or the survived graft of the bioengineered tooth unit will be the replacement of the missing tooth. (Figure I-2).

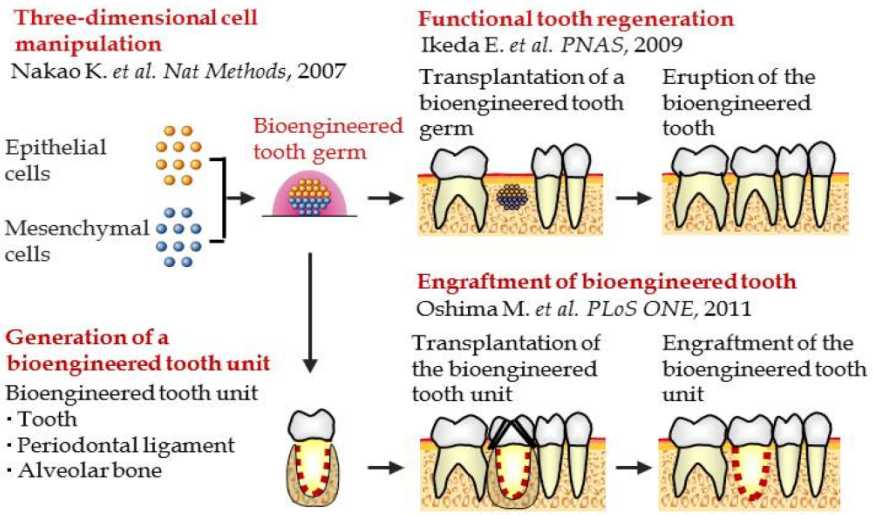

Figure I-2. Schematic of tooth regeneration.

Suitable adult sources of epithelial and mesenchymal cells are expanded and combined to form an early stage tooth primordium which is subsequently either directly transplanted in the location of the missing tooth or cultured to form a tooth unit to replace the missing tooth. (Oshima and Tsuji, 2014b)

Scaffold-based tooth regeneration is an approach seeding single cells on pre-designed biodegradable dental scaffolds with correct morphology. Scaffolds can provide environment for guiding and assisting the generation of extracellular matrix (ECM) which can mimic the natural dental ECM to enable cell adhesion and differentiation. This method can be used to generate tissues with a uniform cellular distribution and has been applied in clinical applications of bone and cartilage regenerative therapy. However, so far this approach is not satisfying for whole tooth bioengineering, given the much more complex structures. In addition to cell sources and factors required, the physical and chemical properties, biocompatibility and controllability of the materials used to produce scaffolds are also in need of further study (Zhang et al., 2013, Oshima and Tsuji, 2014a).

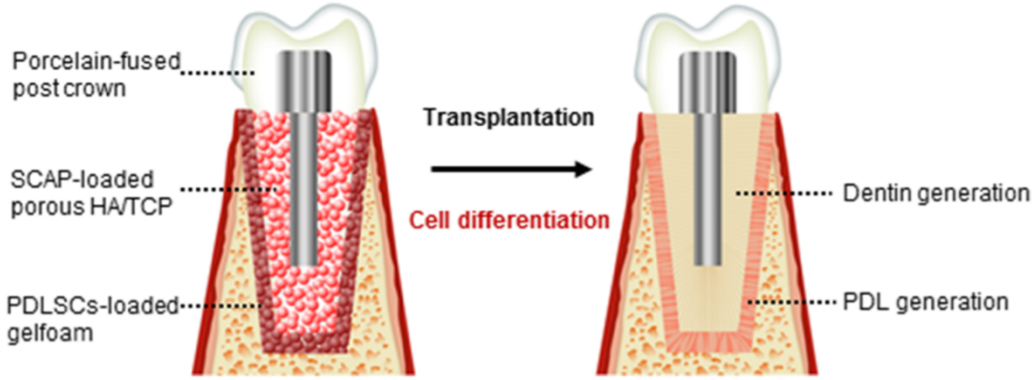

Figure I-3. Schematic of scaffold-based bioengineered dental root.

Bioengineered root regeneration using a root-shaped hydroxyapatite/tricalcium phosphate (HA/ TCP) carrier, which was loaded with SCAP cells that were covered with gelfoam/PDLSCs, has been reported to form a root-like structure to which a porcelain crown was attached, resulting in normal tooth function. (Reprinted from (Oshima and Tsuji, 2014a))

1.4 Stem cell sources for tooth tissue regeneration

Distinguished from artificial teeth, as the sources for tooth regeneration, stem cells are totally biological; they are generally defined as “clonogenic cells capable of both self-renewal and multilineage differentiation” (Weissman, 2000). Based on the stage of ontogenesis in which they appear, stem cells can be classified into three main categories: embryonic stem (ES) cells, fetal and adult stem cells (Pappa and Anagnou, 2009). Induced pluripotent stem (iPS) cell as a novel source has drawn much attention in recent research of regenerative medicine (Otsu et al., 2014).

1.4.1 Embryonic stem cells

ES cells are pluripotent stem cells derived from the inner cell mass of the blastocyst which forms at an early stage of embryo development, approximately 5 days after conception in human; they are capable of differentiating into all derivations of the three primary germ layers: ectoderm, endoderm and mesoderm; they can expand rapidly and if cultured in optimal conditions with feeder layers and leukemia inhibitory factor (LIF), they will stay youthfully immortal (Thomson et al., 1998).

Since ES cells are pluripotent stem cells, they have been directed to differentiate into several kinds of cell types, e.g. neural, cardiac, endothelial (vascular), pancreatic (Islet-like), hepatic, hematopoietic and bone cells (Yu and Thomson, 2010); in oral and maxillofacial field, they have been used in the regeneration of alveolar bone and periodontal tissue (Kang et al., 2008, Inanc et al., 2009). Specially in tooth regeneration, (Ning et al., 2010) provides evidence that ES cells can be induced to differentiate into dental epithelial-like cells by ameloblasts serum-free conditioned medium, while (Ohazama et al., 2004) demonstrated that

when mouse ES cells were recombined with inductive E10 tooth germ epithelial cells, they expressed a combination of three genes: *Msx1*, *Lhx7*, *Pax9* which is unique to odontogenic mesenchymal cells indicating they are responsive to odontogenic signals; moreover, although the recombinations formed only fragile bone and soft tissue without intact tooth structure, gene *DSPP* (dentin sialophosphoprotein), which is mainly expressed in odontoblasts, was detected in histological analysis suggesting tooth cell differentiation had occurred.

However, although ES cells are promising and useful in tooth regeneration, their application in the clinic is still hindered because of three main problems: ethical concerns for using human embryos, immune rejection caused by allogeneic transplantation, and the possibility of tumorigenesis due to the potential immortality of ES cells.(Otsu et al., 2014)

1.4.2 Fetal stem cells

As the name suggests, fetal stem cells originate from the fetus, a recognizable developing mammal with basic outlines of its organs after embryonic stage and before birth. The human fetal period normally starts from the ninth week to birth while in mouse this begins on the tenth to eleventh day. (Carlson, 2013) These cells can be collected from the fetus proper or from the supportive extra-embryonic structures. (Pappa and Anagnou, 2009)

Stem cells from fetus proper, e.g. fetal blood, bone marrow, liver and kidney, have greater expansion potential and multipotency than their adult counterparts; and with less tumorigenesis possibility and ethical controversy than ES cells. However, the use of stillborn fetus is restricted since it is not completely “ethical problem free” and with limited source; moreover, allogeneic immune rejection is still an

unsolved issue (O'Donoghue and Fisk, 2004). In regenerative dentistry research, tooth germ cells are the most widely used fetal stem cells. Mouse E14.5 molar tooth rudiments gave rise to normal tooth development including eruption after being transferred into the soft tissue of the diastema of the maxilla of adult mice (Ohazama et al., 2004); re-associated mouse E14.5 tooth germ epithelial and mesenchymal cells formed fully functional teeth at adult mice tooth extraction site (Nakao et al., 2007, Ikeda et al., 2009). These findings all indicate that fetal dental stem cells can function normally in corresponding adult environment.

Fetal stem cells from supportive extra-embryonic structures such as umbilical cord, amniotic fluid, and placenta, are more inclined to be classified into adult stem cells since they are obtained postnatally which avoids ethical contention. (Li et al., 2013a) demonstrated that human umbilical mesenchymal stem cells can differentiate into odontoblast-like cells when cultured with conditioned medium of rat tooth germ cells which made this kind of fetal stem cells a promising candidate cell source for tooth regeneration.

1.4.3 Adult stem cells

Adult stem cells, also known as somatic or postnatal stem cells, are unspecialized cells found throughout both juvenile and adult animals and human bodies. They reside in particular areas called “stem cell niches” of each organ or tissues to generate corresponding cells for tissue maintenance and repair while keep self-renewing. To date, adult stem cells have been identified in many organs and tissue, including brain, bone marrow, peripheral blood, blood vessels, skeletal muscle, skin, teeth, heart, gut, liver, ovarian epithelium, and testis. (Young and Black, 2004) For tooth repair and regeneration, adult stem cell sources can be divided into two

categories which are stem cells from dental and non-dental tissue (Otsu et al., 2014) .

1.4.3.1 Dental adult stem cells

1.4.3.1.1 Adult dental mesenchymal stem cells (Figure I-4)

Mesenchymal Stem Cells (MSCs) were first described as the adherent, fibroblastoid cell population isolated from adult bone marrow which can generate multiple connective tissue cell types, thus Marrow Stromal Cells was an interchangeable name for them (Caplan, 1994). Later they were discovered in many other tissue including dental tissue; moreover evidence showed that they can even transdifferentiate into epithelial and neuroecdermal cell lineages, so sometimes they are also referred as Multipotent Stromal Cells (Phinney and Prockop, 2007).

Stem cells derived from dental tissue share the common features of MSCs: plastic-adherent, expression of MSC marker genes and differentiation into mesenchymal cell lineages (osteoblasts chondrocytes and adipocytes) *in vitro* (Egusa et al., 2012). For MSC markers, according to the criteria suggested by the International Society for Cellular Therapy (ISCT) to distinguish MSCs from other cells in the bone marrow compartment: expression of CD73, CD90 and CD105, which were selected to include surface antigens that are absent from most hematopoietic cells; lack expression of CD34, CD45, CD14 or CD11b, CD79a or CD19 and HLA-DR surface molecules, which were selected to include surface antigens that are expressed by hematopoietic cells (Dominici et al., 2006). However, cell populations from different dental origins differ in some respects such as expression of individual marker genes, proliferation rate and multipotency (Volponi et al., 2010).

Dental pulp stem cells (DPSCs)

DPSCs are the first MSCs isolated from adult dental tissue. They were first obtained from human impacted third molars exhibiting high expansion rates with capability of producing "sporadic but densely calcified nodules" *in vitro* and generating dentin-pulp like structure *in vivo* (Gronthos et al., 2000). Subsequent studies of DPSCs revealed that they can also differentiate into odontoblasts, adipocytes, chondrocytes, osteoblasts, endotheliocytes and even neurons which made them not only a candidate stem cell source for tooth regeneration but also for other areas in regenerative medicine (d'Aquino et al., 2007, Graziano et al., 2008, Koyama et al., 2009, Yalvac et al., 2009, Yu et al., 2010, Volponi and Sharpe, 2013).

Stem cells from human exfoliated deciduous teeth (SHEDs)

SHEDs were first isolated from the remnant pulps of human exfoliated deciduous incisors of 7-8 year old children (Miura et al., 2003). When cultured *in vitro*, they had similar multipotency to DPSCs while after *in vivo* transplantation, they can form dentin, bone and dental pulp-like structures but not dentin-pulp complexes. They presented even higher proliferation rates and increased population doublings compared with DPSCs and can aggregate into spheres. Moreover, at the gene level, higher expression in SHEDs was observed for genes that participate in pathways related to cell proliferation and extracellular matrix (Nakamura et al., 2009). They were thus suggested to be ideal stem cell source for tooth repair and bone induction (Cordeiro et al., 2008).

Periodontal ligament stem cells (PDLSCs)

PDLSCs isolated from human periodontal ligament which can be obtained during tooth extraction surgeries were capable of separately regenerating all periodontal tissue including cementum, periodontal ligament and alveolar bone (Seo et al., 2004). The location from where PDLSCs originated might affect their

differentiation characteristics: PDLSCs on the alveolar bone surface (a-PDLSCs) displayed superior bone regeneration than the ones on the tooth root surface (r-PDLSCs) (Wang et al., 2011).

Dental follicle stem cells (DFSCs), Stem cells from apical papilla (SCAPs) and Tooth germ progenitor cells (TGPCs)

Dental MSCs can also be found in developing dental tissue such as apical papillae, dental follicles and tooth germ mesenchymes which can be acquired from developing third molar tooth germ at different stages in human adults. Since third molar/wisdom tooth extractions due to orthodontics or tooth impaction are common surgeries in the clinic, they are accessible stem cell sources (Morsczeck et al., 2005, Sonoyama et al., 2006, Ikeda et al., 2008).

Apical papilla refers to the papilla tissue located at the tip of a developing tooth root. SCAPs demonstrated higher expansion ability than DPSCs with similar multipotency and produced dentin and periodontal ligament when co-transplanted with DPSCs into the tooth sockets of minipigs (Sonoyama et al., 2006). Dental follicles are loose connective tissue sacs containing a developing tooth. DFSCs were capable of differentiating into osteoblasts/cementoblasts, adipocytes and neurons *in vitro* and generating cementum and periodontal ligament *in vivo* (Yao et al., 2008, Honda et al., 2010). TGPCs obtained from the third molar tooth germ at the late bell stage displayed high proliferation activity and the capability to differentiate *in vitro* into lineages of the three germ layers including osteoblasts, neural cells and hepatocytes (Ikeda et al., 2008).

Because of the immature status of the origins of these cell populations described above, stem cells derived from developing tooth germs were considered to possess embryonic-like properties such as high expansion capacity and greater

multipotency. However, further study of these cell sources was required to determine their characteristics and application in regenerative medicine/dentistry (Volponi et al., 2010, Egusa et al., 2012).

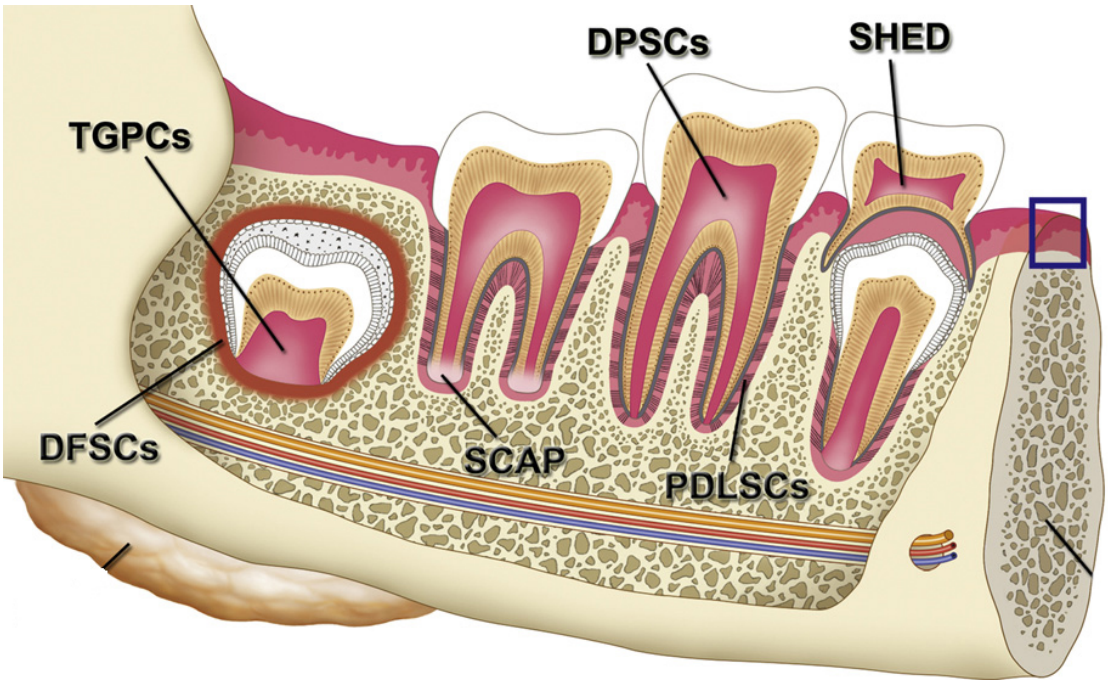

Figure I-4. Sources of adult mesenchymal stem cells in dental tissue.

DPSCs: dental pulp stem cells; SHED: stem cells from human exfoliated deciduous teeth; PDLSCs: periodontal ligament stem cells; DFSCs: dental follicle stem cells; SCAP: stem cells from the apical papilla; TGPCs: tooth germ progenitor cells. Adapted from (Egusa et al., 2012)

1.4.3.1.2 Adult dental epithelial stem cells (EpSCs)

Odontogenic adult EpSCs are located at the apical end of continuously growing incisors of mice. They can generate transit amplifying progeny differentiating into enamel-forming ameloblasts (Harada et al., 1999).

In human, no corresponding adult EpSCs exist since enamel-producing ameloblasts were lost after tooth eruption (Smith and Warshawsky, 1977). However, epithelial rests of Malassez (ERMs), the dormant epithelial remnants during root development, can form enamel-like tissue when recombined with primary dental pulp cells (Shinmura et al., 2008). Furthermore, a recent study showed that ovine ERMs have a unique EpSC population that can be induced to transdifferentiate into mesenchymal cell lineages, indicating they might be available source for periodontal repair and regeneration. (Xiong et al., 2013)

1.4.3.2 Non-dental adult stem cells

Since the multipotency of adult stem cells relates to their origins, non-dental stem cells are not primary consideration for regenerative dentistry. However, bone marrow derived MSCs (BMSCs) were demonstrated to be able to respond to odontogenesis inductive signals sent from mouse E10 tooth germ epithelial cells and formed tooth when the recombination of the two group of cells transferred to mouse kidney capsule (Ohazama et al., 2004). Moreover, (Hu et al., 2006) showed that BMSCs can even be induced by embryonic dental epithelial cells to transdifferentiate into epithelial cell lineage: ameloblast-like cells.

1.4.4 Induced pluripotent stem (iPS) cells

Converting adult stem cells into embryonic-like status can combine the merits of both ES cells and adult stem cells: acquisition of easily scaled up patient-specific pluripotent stem cells without ethical problem and immune rejection and thus has been a research focus in stem cell-based regenerative medicine. (Takahashi and Yamanaka, 2006) demonstrated that pluripotent stem cells can be directly inducted from fibroblast cultures by the addition of four factors *Oct3/4, Sox2, c-Myc and Klf4*, and they named these cells “induced pluripotent stem (iPS) cells”.

In regenerative dentistry, iPS cells have been directed to differentiate into odontogenic lineage by using ameloblast serum-free conditioned medium (ASF-CM) supplement with bone morphogenetic protein 4 (BMP4) (ASF-BMP4) (Liu et al., 2013); and neural crest-like cells derived from iPS expressed the odontoblast maker dentin sialoprotein (DSP) when combined with E14.5 dental epithelium (Otsu et al., 2012).

However, iPS cells also have their drawbacks; the predominant one is the potential of tumorigenesis because of the retrovirus vectors, by which the factors are delivered to the aim cells can trigger oncogenes and mutations through genomic integration during the reprogramming procedure (Selvaraj et al., 2010, Ibarretxe et al., 2012). Thus, to overcome this obstacle, different substitutes have been added to mimic the factors to avoid genetic modification conducted by retrovirus. It has been reported that iPS cells can be generated completely without genetic alteration by just adding recombinant protein or chemicals to somatic cells, which are respectively named protein induced pluripotent stem cells (PiPSCs) and chemically induced pluripotent stem cells (CiPSCs) (Zhou et al., 2009, Hou et al., 2013)

These alternate methods for generating iPS cells suggest another way of thinking about application of iPS technique in tooth regeneration. Since odontogenic ability is the main property required from the cell source used in tooth regeneration, induced odontogenic stem (iOS) cells derived directly from adult dental stem cells by addition of factors expressed by embryonic dental stem cells that render them capable of inducing tooth that are not or not sufficiently expressed by adult dental stem cells may be a viable approach (Volponi et al., 2010).

1.5 Present obstacles in stem cell-based tooth regeneration aimed at clinical application

Ever since the landmark publication showed that embryonic tooth primordia can form teeth with normal structure after being transferred into the soft tissue of maxilla of the adult mouse (Ohazama et al., 2004), different stem cell sources had been used to produce bioengineered tooth primordia to achieve whole tooth regeneration: recombinations of mouse E10.5 inductive epithelial cells and cultured MSCs from bone marrow of adult mouse (Ohazama et al., 2004), separated mouse E14.5 tooth germ epithelial and inductive mesenchymal cells (Nakao et al., 2007) cultured human gingival epithelial cells and mouse E14.5 tooth germ inductive mesenchymal cells (Angelova Volponi et al., 2013) all succeeded in forming tooth primordia. It needs to be emphasized that in all the recombinations mentioned above, the inducing part, epithelial and/or mesenchymal cells, were uncultured embryonic cells. To date, no successful tooth formation has been reported in recombinations using *in vitro* expanded or adult source cells as the inducing cells.

Currently, there are two major challenges of utilizing adult dental MSCs in whole tooth regeneration. Firstly, adult dental MSCs lack the capacity to induce tooth formation that is present in embryonic tooth germ mesenchymal cells which are also derived from neural crest (Volponi et al., 2010); secondly, to achieve a "sustainable" usage of the limited amount of dental MSCs obtained from one patient, expansion *in vitro* is required. However, even embryonic dental mesenchymal cells lose their tooth forming capacity after being cultured *in vitro* (Keller et al., 2011).

In addition to the two challenges mentioned above, in the blueprint of whole tooth regeneration aimed at clinical use, more barriers need to be overcome. To name a few, risk of tumorigenesis must be under control; the time of formation of a new tooth in human needs to be dramatically shortened; precise control of the anatomy, occlusion and colour of the new tooth will be mostly concerned by dentists; patients with hypodontia due to gene defect won't benefit from this protocol unless we can alter the gene expression of collected stem cells (Abou Neel et al., 2014).

1.6 Aims of the research

The final goal is to generate tooth primordia entirely with proliferated adult cell populations. Towards this, experiments were carried out to

(1) determine if *in vitro* expanded embryonic/postnatal dental mesenchymal cells can contribute to tooth formation as inductive cells (Chapter III).
(2) establish a culture protocol to retain/restore odontogenic inductivity of proliferating cells (Chapter IV).
(3) identify the molecular signature of odontogenic inductivity (Chapter V).

Chapter II Material and Methods

Ethics statement: All animal experiments were carried out according to UK Home Office guidelines covered by Project and Personnel licenses to Professor Paul Sharpe.

2.1 Solutions and reagents

Table II-1. Dispase solution (10 ml)

Components	Volume
Dispase® II (Roche, 04942078001)	20 mg
Leibovitz's L-15 Medium (L-15) (Gibco®, 21083-027)	6 ml
Fetal bovine serum (FBS) (Gibco®, 10270-106)	4 ml
Usage: Heat inactivate FBS at 56°C for 30 mins before adding to the solution. Filter sterilize before use (MILLEX®GP, SLGP033RS) and store at 4°C.	

Table II-2. Collagenase and dispase solution (10ml)

Components	Volume
Collagenase D (Roche, 11088866001)	20 mg
Dispase® II (Roche, 04942078001)	15 mg
L-15 (Gibco®, 21083-027)	10 ml
Usage: Filter sterilize before use (MILLEX®GP, SLGP033RS) and only freshly made solution for use.	

Table II-3. L-ascorbic acid solution (0.1M, 30 aliquots)

Components	Volume
L-ascorbic acid (322.05 g/mol, Sigma®, 49752-10G)	0.57g
Double-distilled water (ddH_2O)	17.85 ml
Usage: Filter sterilize (MILLEX®GP, SLGP033RS) and make 30 aliquots of 595 µl. Store at -80°C and thaw when they will be used.	

Table II-4. Complete alpha minimal essential medium (α- MEM) (595 ml)

Components	Volume
α-MEM (BioWhittaker®, BE02-002F)	500 ml
FBS (Gibco®, 10270-106)	89.3 ml
Antibiotic-antimycotic (Gibco®, 15240-062)	5.95 ml
0.1M L-ascorbic acid (Sigma®, 49752-10G)	595 µl
Usage: Heat inactivate FBS at 56°C for 30 mins before adding to the medium. Filter sterilize before use (MILLEX®GP, SLGP033RS) and store at 4°C.	

Table II-5. Medium for u-bottomed plate 3D culture (50ml)

Components	Volume
Complete α-MEM	50 ml
Methyl cellulose (Sigma®, M7027)	0.125g
Usage: Filter sterilize before use (MILLEX®GP, SLGP033RS) and store at 4°C.	

Table II-6. Collagen gel matrix (157 µl)

Components	Volume
Reconstituted collagen solution*	125 µl
5X DMEM (Sigma®, D5648)	31.25 µl
1M NaOH (Made from powder of VWR BDH Prolabo®, 28244.262)	4-4.5µl
Storage: Neutralize the collagen solution with NaOH until the matrix turns purplish pink, keep on ice to maintain the liquid state and incubate at 37°C for 5 mins to produce gel scaffold.	

* Type I collagen was extracted from rat tail tendons and processed in acetic acid solution to obtain sterile soluble collagen followed the protocol of (Rajan et al., 2006).

Table II-7. Sodium borate (SB) buffer solution (52ml)

Components	Volume
HEPES buffer solution (Sigma®, H0887)	500 µl
FBS (Gibco®, 10270-106)	2ml
1X Dulbecco's phosphate-buffered saline (PBS, Sigma®, D8537)	50 ml
Usage: Heat inactivate FBS at 56°C for 30 mins before adding to the solution. Filter sterilize before use and only freshly made solution for use.	

2.2 Experimental mouse strains

In order to trace the origins of the cells contributing to the tooth primordia formation in epithelium-mesenchyme recombination experiments, three different strains of mouse embryos were used, respectively, wild-type mice (CD-1), transgenic mice expressing green fluorescent protein (GFP) and transgenic mice expressing membrane-targeted red fluorescent protein (tandem dimer Tomato, tdTomato) prior to Cre recombinase exposure (mTmG).

Origin of GFP mice: male homozygous B6.129P-Cx3cr1^{tm1Litt}/J mice with a C57BL/6J background (Jung et al., 2000) were purchased from the Jackson laboratory (Stock No. 005582) and crossed with CD-1 females to obtain F1 offspring.

Origin of mTmG mice: male homozygous B6.129(Cg)-Gt(ROSA)26Sor$^{tm4(ACTB-tdTomato,-EGFP)Luo}$/J mice with a C57BL/6J background (Muzumdar et al., 2007) were purchased from the Jackson laboratory (Stock No. 007676) and crossed with CD-1 females to obtain F1 offspring.

2.3 Isolation of embryonic dental epithelium and mesenchyme

Intact bilateral lower molar tooth germs were dissected from E14.5/E12.5 mouse embryos utilizing sterile fine needles in Leibovitz's L-15 medium (L-15, Gibco®, 21083-027). After being trimmed from the surrounding tissue, tooth germs were transferred into 1.2 U/ml Dispase and incubated at 37°C for 40 minutes. After being washed in L-15 medium, epithelium and mesenchyme of the tooth germs were mechanically separated with fine needles (Figure II-1).

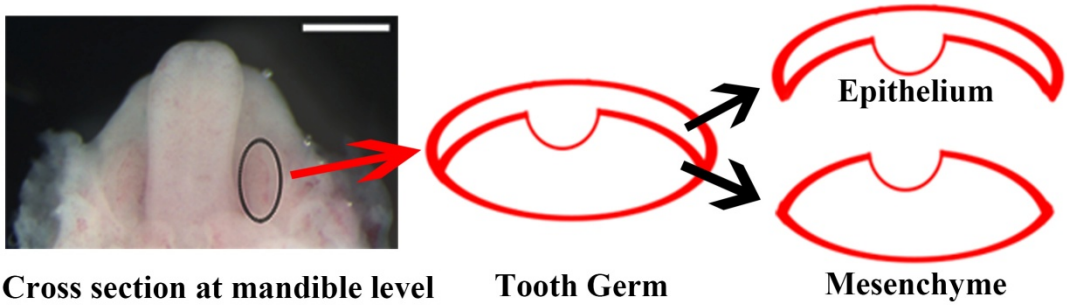

Figure II-1. Diagram of dissection of mouse E14.5/E12.5 lower molar germ.

(Scale bar: 1mm)

2.4 Standard cell culture

The embryonic dental mesenchyme was dissociated into single cells with Trypsin (TrypLE™ Express, 12604-039) and the trypsinization was blocked with trypsin inhibitor (Promocell, C-41120); dissociated cells then were re-suspended in complete α-MEM. Subsequently cells were plated in 6-well cell culture plates or 75cm^2 cell culture flasks (CELLSTAR®, 657160 or 658170) and then incubated at 37°C, 5% carbon dioxide (CO_2). Medium was changed every 2-3 days, and the culturing length varied from 24 hours to 5 weeks. Passage was performed at 1:2-3 ratio when the cells were 70% confluent.

2.5 Reassociation/recombination assays of epithelium and mesenchymal cells

4-10 pieces of E14.5/E12.5 tooth germ epithelial tissues were placed on a membrane cut from the cell culture insert (0.4 µm pore size, BD FalconTM, 353090). A 25 µl drop of collagen gel matrix was placed to wrap the epithelial tissues. 2-20×105 mesenchymal cells were centrifuged in a PCR tube (0.2 ml, STARLAB, I1402-8100) to form a pellet and then injected into the collagen gel on the top of the epithelial tissues using sharpened fine pipette tips (20µl, GELoader®, 022351656). 2ml Complete α-MEM was added into the culture dish where the recombination was cultured (diameter 35mm, CELLSTAR®, 627160) (Figure II-2). The recombinations were incubated at 37°C, 5% CO2 for 7-9 days. Medium was changed every 2-3 day.

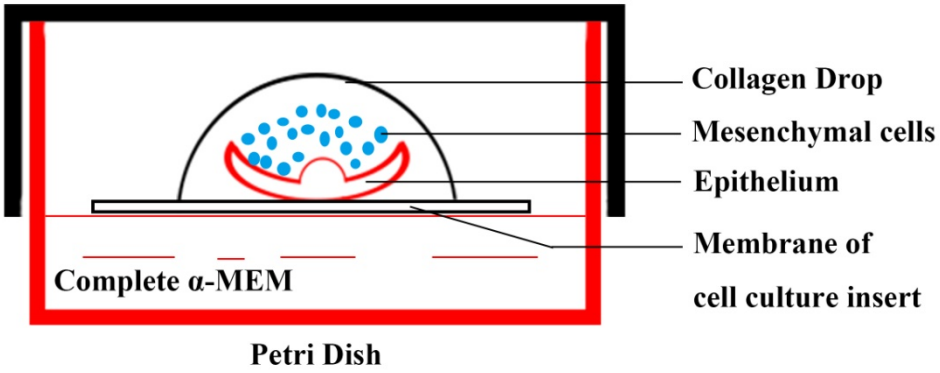

Figure II-2. Diagram of reassociation/recombination assays.

2.6 Methods for Chapter III

2.6.1 Dissection and culture of postnatal molar pulp cells

Upper and lower molar pulp pieces of PN7 mice were trimmed from the surrounding dental follicle tissues and digested in complex enzyme containing 2mg/ml Collagenase D and 120 unit/ml Dispase for 50 minutes, filtered through 70μm cell strainer (BD FalconTM 352350) to obtain a uniform single cell suspension. The pulp cells were cultured on 6-well plates at density of $1.2\text{-}1.5\times10^5$ cells/well. Medium was changed every 2-3 days. First passage was performed when P0 cells formed colonies and cells normally were used at P1 or above.

2.6.2 Histology and immunofluorescence

Recombination samples were fixed in PFA, washed in PBS, dehydrated in graded ethanol solution and then embedded in paraffin (Table II-8). 7 μm thick sections were mounted on slides in serial order and stained with Hematoxylin and Eosin (Table II-9).

For immunofluorescence (IF), sections were deparaffinized with Histoclear and rehydrated with decreasing ethanol series, following antigen being retrieved with 0.1 M Tris-HCl pH 9.0 or 9.5 solution; after the antigen retrieval, slides were washed in PBST solution (0.2% Tween20 in 1× PBS) and incubated in buffer (10% FBS and 1% BSA in 1× PBS) to block unspecific staining; Chicken anti-GFP antibody (Abcam®, ab13970) diluted 1:500 with blocking buffer was used as primary antibody for overnight at 4°C and second antibody: goat anti-chicken IgG (H+L) antibody (Alexa Fluor® 488, Invitrogen, A-11039) diluted 1:300 also with blocking buffer was used afterwards; PBST washed slides then were mounted using mounting medium with DAPI (VECTASHIELD®, H-1200) (Table II-10).

Table II-8. Tissue processing protocol

Steps	Reagents	Duration
Fixation	4% PFA	15min
	1× PBS	5min × 3 times
Dehydration	30% ethanol	15min
	50% ethanol	15min
	70% ethanol	15min
	80% ethanol	15min
	90% ethanol	15min
	100% ethanol	15min × 3 times
	100% ethanol: Histoclear = 1:1	15min
	Histoclear	5min × 5-6 times
	Histoclear: paraffin = 1:1	5min
	Paraffin	Minimum 30min × 6 times (with once overnight)
Embedment	Paraffin	Kept on cold plate until solid

Table II-9. H&E staining protocol

Reagents	Duration
Histoclear 1st	10min
Histoclear 2nd	10min
100% IMS 1st (Industrial Methylated Spirit)	2min
90% IMS 1st	2min
70% IMS 1st	2min
50% IMS 1st	2min
Deionised water 1st	2min
Ehrlich's Haematoxylin (Solmedia)	Dip for seconds
Running water	10min
Deionised water 2nd	Rinse
Acid alcohol (1% HCl in 95% IMS)	15s
Running water	10min
Deionised water 3rd	rinse
0.5% Eosin Y (Sigma) in 2 mM acetic acid	Dip for seconds
Deionised 4th	Rinse
Deionised 5th	Rinse
70% IMS 2nd	1min
90% IMS 2nd	2min
100% IMS 2nd	5min
100% IMS 3rd	5min
Histoclear 3rd	5min
Histoclear 4th	5min
Coverslip with Neo-Mount (Merck)	

Table II-10. Immunofluorescence protocol

Steps	Reagents/Process	Duration
Deparaffinization	Histoclear	15min × 2 times at room temperature
Rehydration	100% ethanol	5min × 3 times
	90% ethanol	5min
	70% ethanol	5min
	50% ethanol	5min
	1× PBS	5min
(Heat based) Antigen retrieval	Microwave at high heat	10min
	Cool down	10min
	0.1M Tris-HCl (pH 9.0 or 9.5)	10min
	PBST (1L PBS + 2 ml Tween20)	5min × 3 times
Blockage of unspecific staining	Blocking buffer (PBS with 1%BSA and 10%FBS)	1hr at room temperature
Primary antibody	Diluted primary antibody in blocking buffer to recommended concentration	Overnight at 4°
	PBST	5min × 3 times
Secondary antibody	Diluted second antibody in blocking buffer to recommended concentration	2hrs at room temperature
	PBST	5min × 3 times
Mounting	mounting medium with DAPI (VECTASHIELD)	

2.6.3 Confocal Fluorescence Tomography (Z-stack)

Recombination samples were fixed in 4% PFA for 20 minutes, washed 3 times in 1x PBS for 5 minutes, mounted on slides utilizing mounting medium with DAPI (VECTASHIELD® H-1200). Coverslips on top of specimen were sealed around perimeter with nail polish. Fluorescent tomography scans were performed on processed samples using z-stack imaging programme of confocal microscope (Leica TCS SP5).

2.6.4 *In vivo* culture of recombinations--subrenal capsule transplantations

Animal surgeries were performed by Prof. Paul Sharpe and Dr. Dhivya Chandrasekaran.

Recipient CD1 adult male mice were anesthetized, shaved, and cleaned. A small incision was made on the left flank of the mouse and the kidney was exposed. The tissue was kept moist with PBS throughout the surgery. A small nick was made on the rear side of the kidney. The end of a glass aspirator pipette was fused to a fine tip and inserted through the small nick to prepare the space for transplants between the capsula and kidney surface. Implants of 7 day *in vitro* cultured recombinations were washed in PBS, and placed under the renal capsule at the frond, middle and rear parts of the kidney with the fused fine tip (Figure II-3). The kidney was placed back into the cavity and the peritoneum and skin were sutured. The same operation was performed on the right kidney. Mice are immediately treated with Flunixin and Buprenorphine and placed in a cage on a heating pad. The host mice were sacrificed after 4 weeks, and the implants were dissected from kidney capsules and fixed in 4% paraformaldehyde (PFA) in PBS overnight at 4°C.

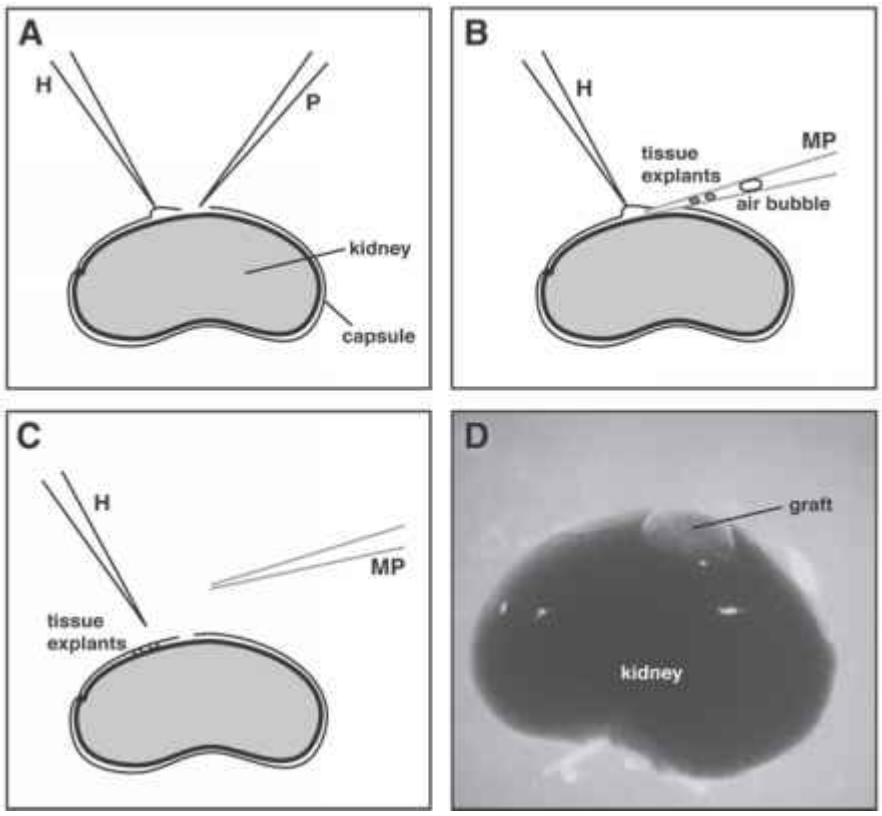

Figure II-3. Schematic representation of subrenal transplantation surgery procedure.

Reprinted from(Flick and Klug, 2006).

2.6.5 Micro computerized tomography (micro-CT)

Fixed specimens of *in vivo* cultured implants were washed in PBS and scanned by a microCT scanner (SkyScan 1272, Bruker microCT, UK) with an x-ray tube voltage of 80 kVp and a tube current of 125 µA operated by Dr. Christopher Healy. The specimens were characterized further by three-dimensional slice volumes, generated and measured with Microview software (GE).

2.7 Methods for Chapter IV

2.7.1 Hanging drops mediated 3D culture

2D cultured mesenchymal cells were re-suspended at the density of 300 cells/µl. Hanging drops were generated from the cell suspension on the inside surface of the lids of cell culture dishes (diameter 100mm, CELLSTAR®, 664160) with a volume of 10µL per drop. The lids were turned over and placed on the base of the dishes with 10ml Dulbecco's phosphate-buffered saline (DPBS, Sigma®, D8537) to maintain the humidity of the culture chambers (Figure II-4). Cell suspension hanging drops were incubated for 24-48 hours and harvested by flooding the drops with cell spheroids into a 50ml centrifuge tube.

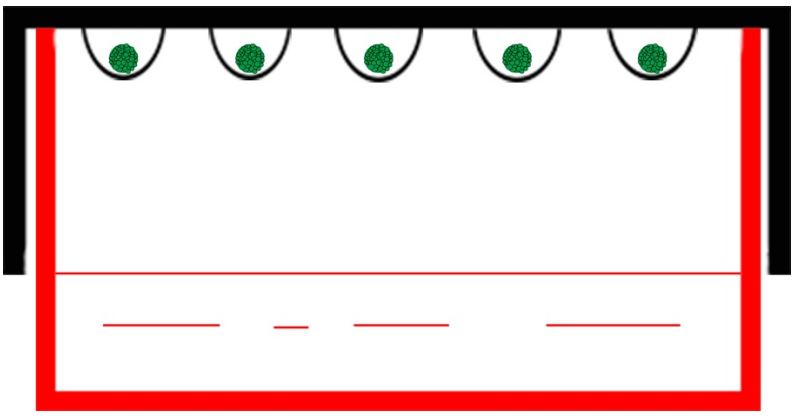

Figure II-4. Diagram of hanging drops mediated 3D culture.

2.7.2 Low cell binding surface plates mediated 3D culture

2D cultured mesenchymal cells were passaged at the density of 3×10^5 per well with 1ml medium onto 6-well low cell binding surface multidishes (NuncTM, 145383), which have been specially treated to prevent cell adhesion (Figure II-5).

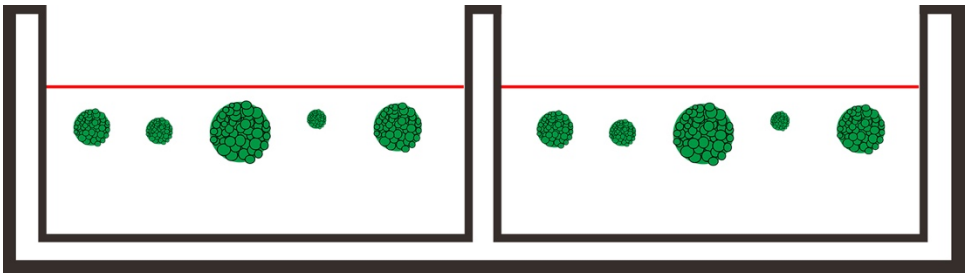

Figure II-5. Diagram of low cell binding surface plates mediated 3D culture.

2.7.3 U-bottomed plates mediated 3D culture

2D cultured mesenchymal cells were seeded onto u-bottomed 96-well culture plate at the density of 6×10^4 cells per well with 3D cultured media containing 0.25% methyl cellulose (Table II-5) and cultured for 2-7 days (Figure II-6). Media change was performed by careful pipetting rather than aspiration to avoid cell spheroid loss. Cell spheroids were disaggregated by incubation in Trypsin (TrypLE^{TM} Express, 12604-039) for 5 mins and vigorous pipetting.

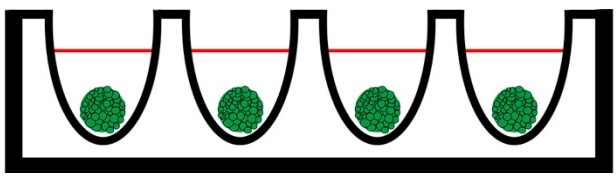

Figure II-6. Diagram of u-bottomed plates mediated 3D culture.

2.7.4 Treatment of drug induced autophagy

2D cultured cells were treated with media containing 100nM Rapamycin (Sigma®, R0395) for 24 hours and harvested for subsequent experiments.

2.7.5 Epithelium-mesenchyme Transwell co-culture system

Cell culture inserts (0.4 µm pore size, BD Falcon™, 353090) were introduced to the standard 2D culture plates to establish the epithelium-mesenchymal cell Transwell co-culture system. E14.5 epithelial explants were cultured on the cell inserts with progenitor cell targeted (PCT) oral epithelium defined medium (CELLnTEC, CnT-24). Mesenchymal cells were cultured on the culture plate bottom with complete α-MEM (Figure II-7). Media of mesenchymal cells and epithelium were changed separately every 2-3 days.

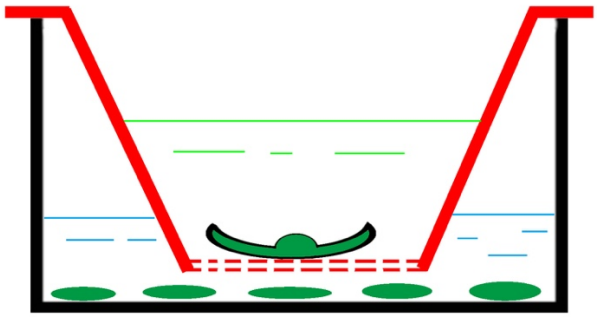

Figure II-7. Diagram of Transwell co-culture system.

2.7.6 Fresh-cultured mesenchymal cells 2D direct co-culture system

CD1 Freshly isolated and GFP 7-day-cultured E14.5 tooth germ mesenchymal cells were mixed in certain ratios and plated onto standard 2D culture plate/flask for direct co-culture (Figure II-8).

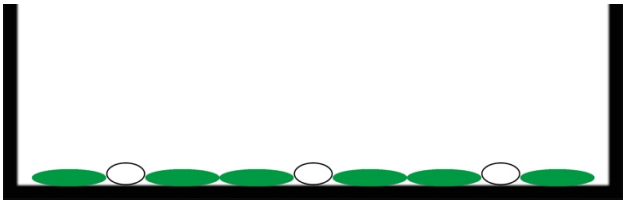

Figure II-8. Diagram of 2D direct co-culture system.

2.7.7 Flow Cytometry- Fluorescence- activated cell sorting (FACS)

Mixtures of CD1 and GFP cells were resuspended in 1 ml of SB buffer and passed through 70 µm cell strainer to obtain a uniform single-cell suspension.

1:1000 diluted DAPI (BioLegend, 422801) was applied to detect dead cells. CD1 cells, CD1 cells with 1:1000 DAPI and GFP cells in 200 µl SB buffer were used as the compensation controls. Samples were sent to the National Institute for Health Research (NIHR) Biomedical Research Centre. Cell sorting was performed through BD FACSAria™ II Cell Sorters monitored by FACSDIVA software. Separated CD1 and GFP cells were resuspended in complete α-MEM for subsequent experiments.

2.7.8 Quantitative real-time PCR (qPCR)

RNA extraction

RNA extraction of collected cells was performed using Micro Kit or Mini kit (RNeasy®, QIANGEN, 74004 or 74104) depending on the cell numbers (mini kit would be selected when cells were more than 5×10^5), following the protocols supplied by the manufacturer. RNA quality controls were performed by examination of OD ratios. The ratio of the readings at 260 nm and 280 nm (A260/A280) should be around 2, between 1.9-2.1 with an OD 260/230 of 1.8 or greater. Concentration and purity of extracted RNA samples were tested by spectrophotometers (NanoDrop™ 2000) following the protocol below (adapted from http://www.flychip.org.uk/protocols/):

1. Open the Nanodrop icon and select 'Nucleic Acid Measurements'.
2. Add 1 µl of solvent of RNA (RNA free water) to initialize the instrument.
3. After each and all subsequent measurements clean the pedestal by wiping with a dry lint-free tissue.
4. Add 1 µl of solvent and press 'Blank'.
5. Repeat the blanking until there is a stable baseline, close to zero.
6. Confirm that the baseline is correct by measuring 1 µl of solvent, as if it were your first sample by pressing 'Measure'.
7. Add 1 µl of the first sample making sure to add the sample ID (or name) to the 'Sample ID' field and then press 'Measure'
8. Repeat step 3 and then 7 for all samples.
9. Confirm that the baseline is correct after taking all measurements by measuring 1 µl of solvent, as if it were your last sample by pressing 'Measure'.
10. Each of the measurements is automatically saved by the instrument and these can then be calibrated using the in house script.

Complementary DNA (cDNA) synthesis

cDNA was generated from RNA samples via reverse transcription (RT) system (M-MLV Reverse Transcriptase, Promega, M1701) after the samples had been purified through deoxyribonuclease (DNase) system (RQ1 RNase-Free DNase, Promega, M6101). Components in a total reaction volume of 25 µl are as shown in Table II-11. Final concentration of cDNA was 40 ng/µl (1 µg/25 µl). Two negative controls were set up during the cDNA synthesis: one with no reverse transcriptase (M-MLV enzyme) added as RT negative control (RT-); one with just nuclease free water as no template control (NTC).

Table II-11. Components of cDNA synthesis reaction solution

Components	**Volume (V)**		
	RT+	**RT-**	**NTC**
RNA	**1 µg** (V depends on the concentration of RNA)		-
10x RQ1 RNase Free DNase buffer	1 µl		-
RQ1 RNase Free DNase	1 µl		-
RQ1 DNase Stop solution	1 µl		-
Random primer	2 µl		-
M-MLV 5x buffer	5 µl		-
dNTP	1.25 µl		-
M-MLV enzyme	1µl	-	-
Nuclease free water	12.75 µl - V_{RNA}	13.75 µl - V_{RNA}	25µl
Total Volume	**25µl**		

Table II-12. cDNA synthesis protocol

	Components	Volume (V)	Process
Mix 1st	RNA	1 µg	Incubate at 37°C for 30min
	10x RQ1 RNase Free DNase buffer	1 µl	
	RQ1 RNase Free DNase	1 µl	
	Nuclease free water	8 µl - V_{RNA}	
Mix 2nd	Mix 1st	10 µl	Incubate at 65°C for 10min; Spin down for 10s
	RQ1 DNase Stop solution	1 µl	
Mix 3rd	Mix 2nd	11µl	Incubate at 70°C for 5min; Kept on ice for 5min; Spin down for 10s
	Random primer	2 µl	
	Nuclease free water	2 µl	
Mix 4th	Mix 3rd	15µl	Incubate at RT for 10min; Incubate at 50°C for 50min; Spin down for 10s; Incubate at 70°C for 5min
	M-MLV 5x buffer	5 µl	
	dNTP	1.25µl	
	M-MLV enzyme	1 µl (0 for RT-)	
	Nuclease free water	2.75 µl (3.75µl for RT-)	
Final cDNA solution		25 µl	Kept at -20°C

qPCR

Glyceraldehyde 3-phosphate dehydrogenase (GAPDH) was chosen as the housekeeping gene. The information of GAPDH and all the selected dental development related genes including Paired Box 9 (Pax9), Msh Homeobox 1 (Msx1) were as listed in Table II-13.

Table II-13. Primer information

Primers		Sequence (5'-3')	Size (bp)	Tm (°C)
GAPDH	Forward	CCATGGAGAAGGCCGGGG	197	61.2
	Reverse	CAAAGTTGTCATGGATGACC		51.5
Pax9	Forward	CGCACGCAGTGAATGGATTG	120	57.3
	Reverse	GCTGGTGTAGGGTAAGGAGC		57.4
	Forward	ACCCATGATCCAGGGCTGTCTCG	92	62.9
Msx1	Reverse	CCGAGTGGCAAAGAAGTCATAGCAGC		61.6

Note: Tm-melting temperature

Relative standard curve method was used to analyze the qPCR results. cDNA of control group was diluted 1:10, 1:100, 1:1000, 1:10000 together with the original concentration solution (40 ng/µl) for setting the standard curves for both the gene of interest and endogenous control. qPCR reaction mix in a total volume of 20µl was prepared following Promega system (GoTaq® qPCR Mater Mix, Promega, A6001) as detailed in Table II-14. cDNA concentration in reaction mix was 2 ng/µl (40ng/20µl), while for the diluted ones were successively 0.2 ng/µl, 0.02 ng/µl, 0.002 ng/µl, 0.0002 ng/µl. qPCR was running by Real-time PCR cycler (Rotor-Gene Q) with the programme setting as in Table II-15.

Table II-14. Components of qPCR reaction mix

Components	Volume (µl)
DNA (RT+/ RT-/ NTC)	1
Primer (5mM, Forward : Reverse = 1:1)	2
Nuclease free water	7
GoTaq® Probe qPCR Master Mix (2×)	10
Total volume	**20**

Table II-15. qPCR programme settings

Cycle		Temperature (°C)	Duration
Deactivation		95	10 min
*Denaturation		95	15s
*Annealing	*Pax9/GAPDH*	53	30s
	Msx1/GAPDH	54	
*Extention		72**°C**	40s

Note: *step repeated in 40 cycles in order

2.8 Methods for Chapter V

2.8.1 Dissection of E10.5 1odontogenic and non-odontogenic branchial arch epithelium

The 1st (mandible process) and 2nd branchial arches were dissected from E10.5 mouse embryos, and further separated into oral cavity parts and non-dental parts by a cut-line illustrated in Figure II-9. Samples were incubated in 1.2 U/ml Dispase for separation of epithelium and mesenchyme. Epithelial tissues were collected for subsequent experiments.

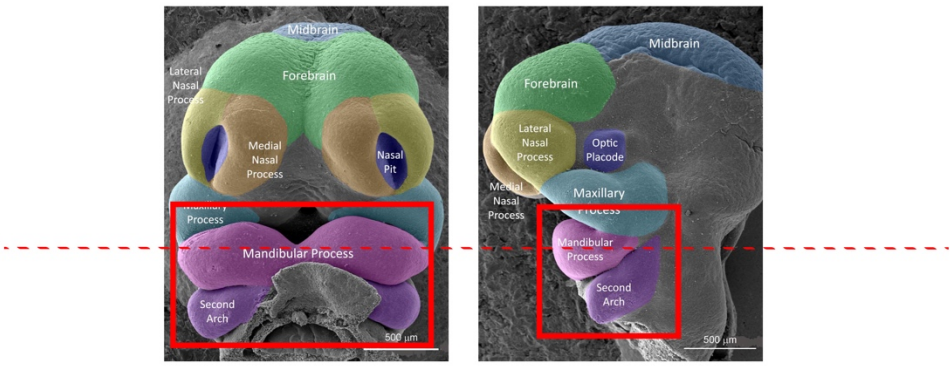

Figure II-9. Diagram of dissection of mouse E10.5 odontogenic and non-odontogenic epithelium.

Scanning electronic microscope image of front view of the head of E10.5 mouse embryo was adapted from FaceBase-Mouse Anatomy (Iwata et al.)

2.8.2 RNA sequencing

RNA extractions of the samples were performed using MicroPrep kit (Quick-RNA™, R1050), followed the protocols supplied by the manufacturer. Quantity and purity of RNA samples were tested by spectrophotometers (NanoDrop™ 2000). Samples were normalized according to the quality control guide provided by Oxford Genomics Centre and shipped in 96-well PCR plates (Thermo Scinetific™, AB0800). RNA sequencings were performed via platform of Illumina HiSeq4000.

Quality control of RNA sequencing raw reads was performed though FASTQC (Galaxy Version 0.69), and aligned to GRCm38/mm10 mouse genome reference using HISAT2 (Galaxy Version 2.0.5.2) (Kim et al., 2015a). Aligned read counts of each gene was generated by featureCounts (Galaxy Version 1.4.6.p5) (Liao et al., 2014) and differential expression analysis was performed via DEseq2 (Galaxy Version 2.11.39) (Love et al., 2014). A threshold of adjusted p value (Padj) <0.05 and fold change >2 were set to identify differentially expressed genes (DEGs). Visualizations of DEG results were performed using R studio (version 3.4.0), detailed file preparations, R packages and codes used are described in 2.8.3. Statistical overrepresentation tests of DEG sets were conducted through the PANTHER (Protein ANalysis THrough Evolutionary Relationships) classification system (Thomas et al., 2003) with a filter of Bonferroni correction adjusted *p*-Value <0.05. The up- and down-regulated DEGs were categorized by PANTHER protein class for identification of transcription factors, signalling molecules and receptors. Workflow is shown in Figure II-10.

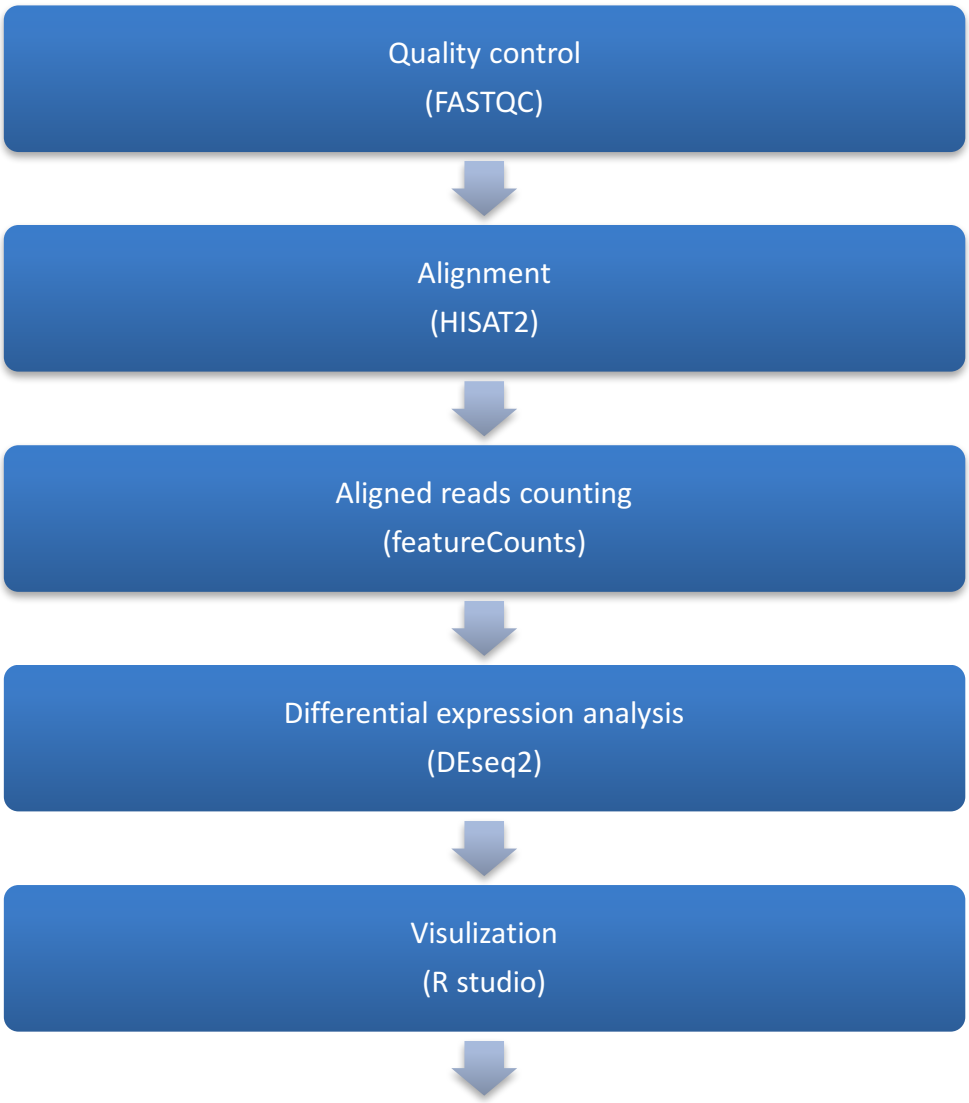

Figure II-10. Workflow of bioinformatics analysis of RNA seq data.

2.8.3 Visualizations of DEG results

Visualizations of DEG results were performed using R studio (version 3.4.0).

(1) Heatmaps

Data matrix preparation: DEG list and total normalized counts file (generated thought DEseq2) were put together in the same Excel work sheet. Via MATCH function, using DEG list as the look arrays, normalized counts of DEGs were selected. Data matrix should contain gene ID of DEGs and the corresponding normalized counts of the DEGs in each sample, saved as Comma-Separated Values (CSV) file ("heatmap.csv"). Example data matrix is as follow:

Gene ID	Sample 1	Sample 2	Sample 3	Sample 4	Smaple 5	Sample 6
DEG1	10	10	10	100	100	100
DEG2	20	20	20	200	200	200
DEG3	30	30	30	300	300	300
…	…	…	…	…	…	…

Main R packages: pheatmap

R codes:

```
# Draw Heatmap
> library(pheatmap)
> data<-read.csv("heatmap.csv", header = T, row.names = 1)
> pheatmap(data, scale = "row", clustering_distance_rows = "correlation",
show_rownames = F, color = colorRampPalette(c("green", "white", "red"))(50))


# k-means clustering for categorizing DEGs based on their expression patterns
across different samples. N is the set up number of categories/clusters.
```

```
> pheatmap(data, scale = "row", clustering_distance_rows = "correlation",
show_rownames = F, color = colorRampPalette(c("green", "white", "red"))(50),
kmeans_k = N, cluster_rows = F)

# Get cluster information. Here only focus on members of each cluster.
> obj<- pheatmap(data, scale = "row", clustering_distance_rows =
"correlation", show_rownames = F, color = colorRampPalette(c("green",
"white", "red"))(50), kmeans_k = N, cluster_rows = F)
> obj$kmeans$cluster

# Export cluster information as csv file
> write.table(obj$kmeans$cluster, file = "cluster info.csv", sep = " ",
row.names = T, col.names = T)
```

(2) Temporal expression profile plots

Based on the k-means clustering heatmap, colour coded expression levels can be roughly converted into numbers. For example, the following heatmap can be transformed into the matrix below according to the colour codes. Line charts generated from the matrix can show the general trend of expression patterns of different clusters of DEGs across different time points.

	0h	24h	48h	96h
Cluster 1	3	-1	-1	-1
Cluster 2	-2	-1	1	2
Cluster 3	-3	1	2	2
Cluster 4	2	-2	-1	2
Cluster 5	2	1	-1	-2
Cluster 6	-2	3	0	-1

(3) Volcano plots

Data matrix preparation: DEG lists containing gene ID, log2(Fold Change) and P-adj were saved as Tab-Delimited Text (txt) files ("volcano.txt"). Example data matrix as follow:

Gene ID	Log2 (FC)	P-adj
DEG1	4.697409689	0
DEG2	3.730776266	1.33E-248
DEG3	-2.478208709	2.54E-244
…	…	…

Main R packages: ggplot2

R codes:

```
> library(ggplot2)
> res<-read.table("volcano.txt", header = T, row.names = NULL)

# Set threshold values of fold change and p-value for significance
> threshold =as.factor (ifelse (res$P.adj<0.05 & abs(res$log2.FC.)>1,
ifelse(res$log2.FC.>1, 'Up', 'Down'), 'Not significant'))

# Draw volcano plots
> ggplot(data = res,aes(x=log2.FC.,y=-log10(P.adj),colour=threshold,
fill=threshold)) + scale_color_manual(values = c("green","grey","red"))
+ xlab("log2 Fold Change") + ylab("-log10 Padj")
+ geom_point(alpha=1, size=0.5) + ylim(c(0,100))+xlim(c(-3,3))
+ geom_hline(yintercept=1.3,linetype=4)
+ geom_vline(xintercept=c(-1,1),linetype=4)
+ theme(legend.position = "right")
```

(4) Venn diagrams (2 or 3 sets)

Data matrix preparation: 2 or 3 DEG sets were displayed in one work sheet with A, B (C) as the set names. Files saved as csv type ("Venn. csv"). Example data matrix as follow:

A	B	(C)
Set1 DEG1	Set2 DEG1	Set3 DEG1
Set1 DEG2	Set2 DEG2	Set3 DEG2
Set1 DEG3	Set2 DEG3	Set3 DEG3
…	…	…

Main R packages: VennDiagram

R codes:

```
> library(VennDiagram)
> Venn <- read_csv("~/Desktop/Venn.csv", na = "empty")


# Draw Venn diagram with 2 sets
> AB<-intersect(Venn$A,Venn$B)
> A_only<-setdiff(Venn$A,Venn$B)
> B_only<-setdiff(Venn$B,Venn$A)
> mx<-max(length(AB),length(A_only),length(B_only))
> AB<-c(AB,rep(NA,mx-length(AB)))
> A_only<-c(A_only,rep(NA,mx-length(A_only)))
> B_only<-c(B_only,rep(NA,mx-length(B_only)))
> res<-data.frame(AandB=AB,Aonly=A_only,Bonly=B_only)
> venn.diagram(x=list(A=Venn$A,B=Venn$B),filename = "Set1 vs. Set2.tiff",
category= c("Set 1","Set 2"),fill=c("red","green"),euler.d=TRUE, scaled=TRUE)
```

```
# Draw Venn diagram with 3 sets
> AB<-intersect(Venn$A,Venn$B)
> AC<-intersect(Venn$A,Venn$C)
> BC<-intersect(Venn$B,Venn$C)
> ABC<-intersect(intersect(Venn$A,Venn$B),Venn$C)
> A_only<-setdiff(Venn$A,union(Venn$B,Venn$C))
> B_only<-setdiff(Venn$B,union(Venn$A,Venn$C))
> C_only<-setdiff(Venn$C,union(Venn$A,Venn$B))
> mx<max(length(AB), length(AC), length(BC), length(A_only), length(B_only),
length(C_only))
> AB<-c(AB,rep(NA,mx-length(AB)))
> AC<-c(AC,rep(NA,mx-length(AC)))
> BC<-c(BC,rep(NA,mx-length(BC)))
> ABC<-c(ABC,rep(NA,mx-length(ABC)))
> A_only<-c(A_only,rep(NA,mx-length(A_only)))
> B_only<-c(B_only,rep(NA,mx-length(B_only)))
> C_only<-c(C_only,rep(NA,mx-length(C_only)))
> res<data.frame(AandB=AB, AandC=AC, BandC=BC, AandBandC=ABC,
Aonly=A_only, Bonly=B_only, Conly=C_only)
> venn.diagram(x=list(A=Venn$A,B=Venn$B,C=Venn$C),filename = "Set1 vs.
Set2 vs. Set3.tiff", category= c("Set1", "Set2", "Set3"), fill=c("red", "yellow",
"green"), euler.d=TRUE, scaled=TRUE)

# Explore overlap information as xls file
> write.table(res,"overlapper.xls",quote = F,row.names = F, sep = "\t",na=" ")
```

Chapter III Contribution of *In Vitro* Expanded Dental Mesenchymal Cells to Tooth Induction

3.1 Introduction

Ever since it was established in mice that embryonic tooth germs, when transplanted into adult mouths, can develop into teeth of normal size and structure (Ohazama et al., 2004), "whole tooth regeneration" is no longer just a concept, but has become a promising alternative treatment for missing teeth. In addition, bioengineered tooth primordia, rather than intact tooth germs, can be generated by reassociation of disassociated tooth germ epithelial and mesenchymal cells (Nakao et al., 2007, Ikeda et al., 2009, Kuchler-Bopp et al., 2016, Ono et al., 2017) and combination of either inductive dental epithelial cells and responsive mesenchymal cells (Ohazama et al., 2004) or inductive dental mesenchymal cells and responsive epithelial cells (Angelova Volponi et al., 2013). These biological implants of "artificial" tooth rudiments in prepared adult alveolar sockets can mimic the natural process of tooth development and lead to normal tooth formation, eruption and functioning (Ikeda et al., 2009, Oshima and Tsuji, 2014b, Ono et al., 2017). Based on these findings, theoretically, a novel treatment for missing teeth seems within reach.

However, practically, fresh embryonic tooth germs are apparently out of the question in the context of a dental clinical scenario. Cell lines generated from them are also unfeasible not only because of the ethical concerns for using human embryos and immune rejection problems of allogeneic transplantation, but also because the embryonic tooth cells lose their inducing ability after being expanded

in vitro (Keller et al., 2011). As the tooth develops, adult/postnatal dental stem cells can be harvested from various dental cell sources such as pulp, apical papilla, dental follicles, periodontal ligament, epithelial rests of Malassez of exfoliated deciduous teeth, extracted third molars/supernumerary teeth and etc. These adult dental stem cells have been widely studied due to their abundance and easy accessibility in clinic and their potential in dental and non-dental tissue regeneration. However, no adult dental stem cell source has been found to be capable of inducing *de novo* odontogenesis (Hu et al., 2014).

In vitro expanded embryonic and adult tooth cells can respond to the inducing signals from the inductive counterpart in recombinations and together generate tooth primordia through the interaction between epithelial and mesenchymal cells. However when recombined with non-inductive counterpart, they alone, do not have sufficient or any odontogenic capacity to initiate the process.

Patient specific dental stem cells can be easily obtained and scaled up by cell banking. Surgically implanting tooth primordia into the sites of missing tooth is no more difficult than dental implant surgery. Hence, how to bioengineer a tooth primordium using accessible cell sources is the biggest obstacle in the field of whole tooth bioengineering. Moreover, since adult dental mesenchymal stem cells are more readily accessible than adult dental epithelial stem cells, successful restoration of odontogenic induction capacity of adult dental mesenchymal stem cells could render industrialized whole tooth bioengineering realizable through standardized recombinations of inductive dental mesenchymal stem cells and any accessible and expandable oral epithelial cells such as gingival or oral mucosa epithelial cells. On the other hand, studying the odontogenic capacity of dental epithelial stem cells, and to engineer tooth primordia by combination of them and any accessible and expandable mesenchymal cells such as dental or bone marrow

mesenchymal stem cells, can yet be regarded as another strategy. This research will focus on the mesenchymal cell populations.

Some progress has been made concerning the rapid loss of odontogenic capacity of *in vitro* expanded embryonic tooth cells. Culturing embryonic dental mesenchymal cells in serum-free medium with knockout serum replacement (KSR) and growth factors (fibroblastic growth factor 2 and epidermal growth factor), Zheng et al. have prolonged their inductivity from 24 hours to 48 hours with tooth induction rates of 50% (Zheng et al., 2016a). As for cultured embryonic tooth cells that have already lost inducing ability, no successful recovery of their odontogenic capacity has been reported. Due to the limited number of cells that could be collected from one patient, massive proliferation and utilization of higher passage of dental stem cells are inevitable. It is of great importance to study the long term or permanent maintenance and restoration after loss of the odontogenic capacity of *in vitro* cultured embryonic dental mesenchymal cells.

To investigate if *in vitro* expanded dental mesenchymal cells have the potential to be inductive, the question to which this chapter aims to find an answer is: Can the failure of tooth induction be rescued by the presence of inductive fresh embryonic dental mesenchymal cells? In other words, can they take part in *de novo* odontogenesis as the inductive cells?

To answer the question, I established a series of epithelium-mesenchyme combination experiments for generating tooth primordia utilizing a novel cell-mixing approach. After cell counting, cultured embryonic/postnatal dental mesenchymal cells and fresh embryonic dental mesenchymal cells were mixed in different ratios, and combined with non-inductive epithelium. Fresh embryonic cells were from CD1 mouse E14.5 lower molar tooth germ mesenchyme. Cultured

cells were from genetically labelled mice (mostly GFP, sometimes mTmG) enabling the cell fates to be tracked, cultured embryonic cells were from the same source as fresh cells and postnatal cells were from mouse PN7 molar pulp. Non-inductive (E14.5/E12.5) molar germ epithelial tissues were genetically labelled, but differently from the cultured cells, to avoid contamination of fresh mesenchyme attached to epithelium that can occur during dissection. Based on the stages of epithelium, these experiments were divided into two parts: reassociations using E14.5 tooth germ epithelial tissues where epithelium was synchronic with the inductive mesenchymal cells and recombinations using E12.5 tooth germ epithelial tissues where heterochronic epithelium was more naïve in responding to inducing signals, requiring an extra induction from mesenchyme for synchronization (Figure III-1).

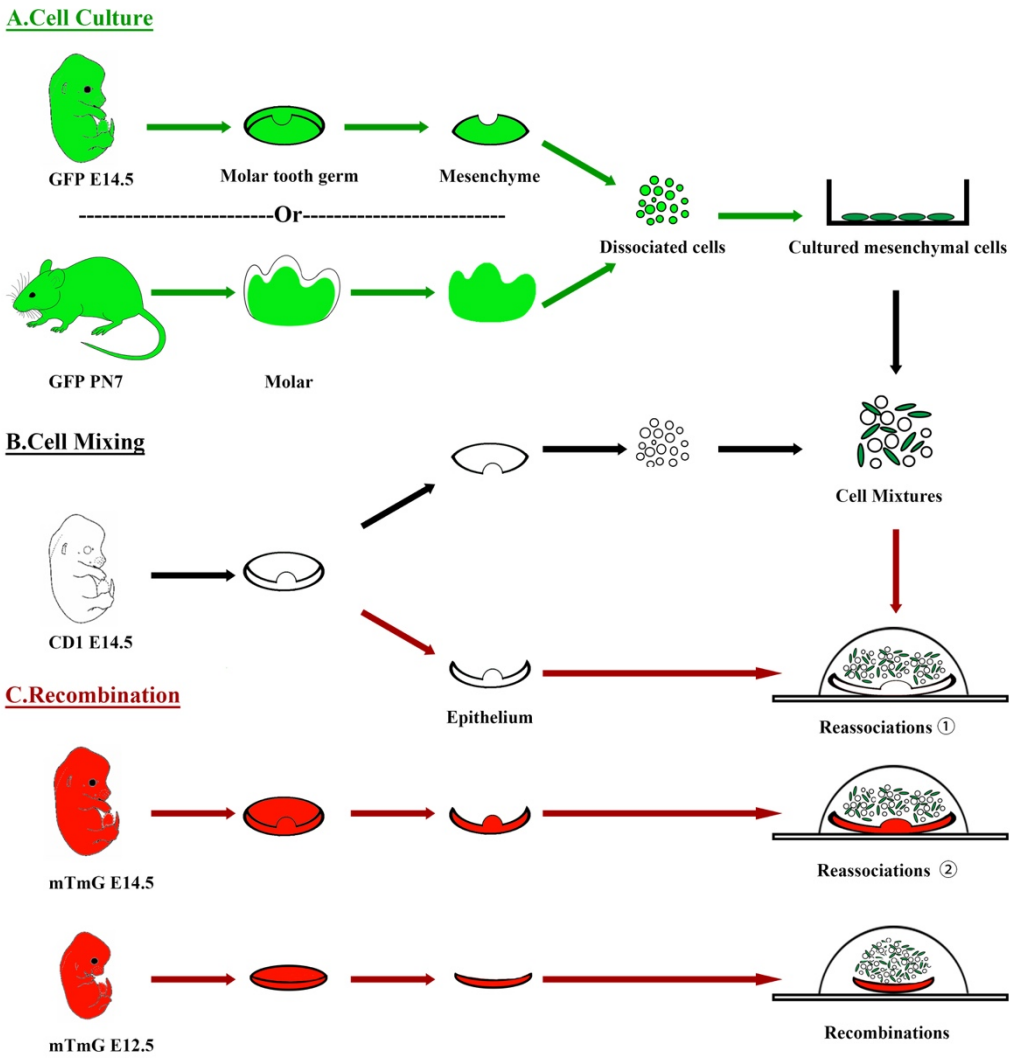

Figure III-1. Schematic representation of experimental design.

(A) Cell culture: *in vitro* expansion of green fluorescent protein (GFP) mouse E14.5 molar tooth germ mesenchymal cells or PN7 molar pulp cells. (B) Cell mixing: cultured GFP cells (either E14.5 mesenchymal cells or PN7 pulp cells) were mixed with noncultured (fresh) CD1 E14.5 molar tooth germ mesenchymal cells at different ratios (cultured:fresh = 1:9, 1:3, 1:1, 3:1, 9:1). (C) Combination: mixtures of cultured GFP cells and noncultured CD1 cells were combined with E14.5 (CD1/mTmG) E14.5 or E12.5 (mTmG) mouse molar tooth germ epithelial tissues, respectively in reassociations (①/②), and recombinations.

3.2 Results

3.2.1 Cultured embryonic (E14.5) dental mesenchymal cell behavior in mixed-cell reassociations

The cell-mixing approach was first tested in reassociations in which the responding epithelial tissues were from the same tooth germs as the fresh inductive mesenchymal cells (Figure III-1 (C) Reassociations ①). Pure fresh or cultured embryonic mesenchymal cells were combined with epithelium to serve as positive or negative controls. Reassociations were cultured *in vitro* for 7-9 days and then fixed for tissue processing and histological staining (H&E staining and immunofluorescence).

In the positive controls (GFP E14.5 fresh tooth germ mesenchymal cells combining with CD1 E14.5 tooth germ epithelial tissues), multiple cap stage tooth primordia could be observed after 3-4 days in culture, and continued developing to bell stage before fixation. Ameloblast-like and odontoblast-like cells were well-layered separately at the interface of each tooth primordium (Figure III-2.A). In the negative controls (GFP E14.5 cultured tooth germ mesenchymal cells combining with CD1 E14.5 tooth germ epithelial tissues), instead of tooth structures, epithelial cyst-like structures formed that were surrounded by cultured mesenchymal cells (Figure III-2.B).

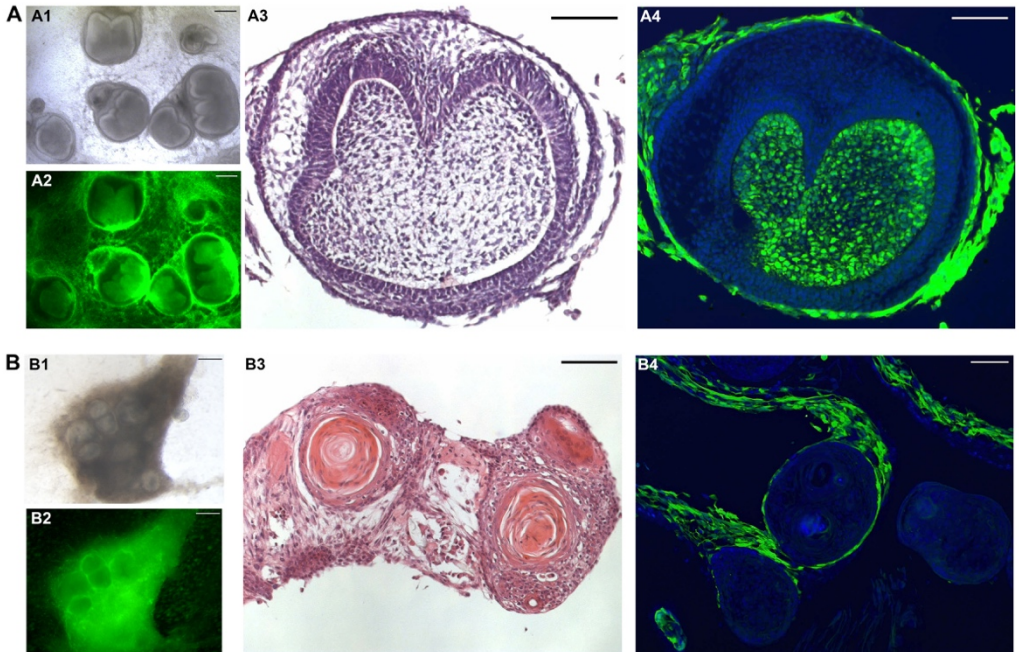

Figure III-2. Positive and negative controls for reassociations.

Combination of uncultured cells dissociated from GFP E14.5 tooth germ mesenchyme and fresh tissue of CD1 E14.5 tooth germ epithelium generated considerable well shaped and structured tooth primordia (A1-2). H&E staining (A3) and immunofluorescent image (A4) of the section of a primordium; Combination of GFP cultured E14.5 tooth germ mesenchymal cells and CD1 fresh E14.5 epithelial tissue formed cyst-like structures (A1-2). CD-1 epithelium "rolled up" into sphere shape and with negative GFP signals in fluorescent view. H&E staining (B3) and IF image (B4) of the cysts displayed that the cysts were composed of epithelial cells and surrounded by cultured mesenchymal cells. Scale bars: 250 µm (A1-2, B1-2); 100 µm (A3-4, B3-4).

In the experimental groups utilizing embryonic mesenchymal cell mixtures containing 10%, 25% and 50% cultured cells, tooth-like structures formed after 3-4 days in culture and became as defined as in the positive. During the process, it seemed that the mixed cell induced tooth development was slightly retarded than that induced by pure fresh cells. H&E staining results confirmed that ameloblast-like and odontoblast-like cells lined up respectively on the outside and inside of the junction between epithelium and mesenchyme (Figure III-3); while GFP immunofluorescent results revealed the origins of the mesenchymal cells contributing to the formation of the tooth primordia: cultured (GFP positive) cells were evenly scattered in the mesenchyme of the tooth primordia, some were at the epithelium-mesenchyme interface area with the typical columnar shape of odontoblasts (Figure III-3. C4). The different percentages of cultured cells in mixtures did not have a significant effect on the morphology and histology of the generated tooth primordia, but on the proportions of cultured cells among all the contributing mesenchymal cells. It is obvious that 50% cultured cell mixture induced tooth primordia have the most number of cultured cells, and the primordia formed in 10% cultured cell mixture reassociations have the fewest (Figure III-3. C4, A4).

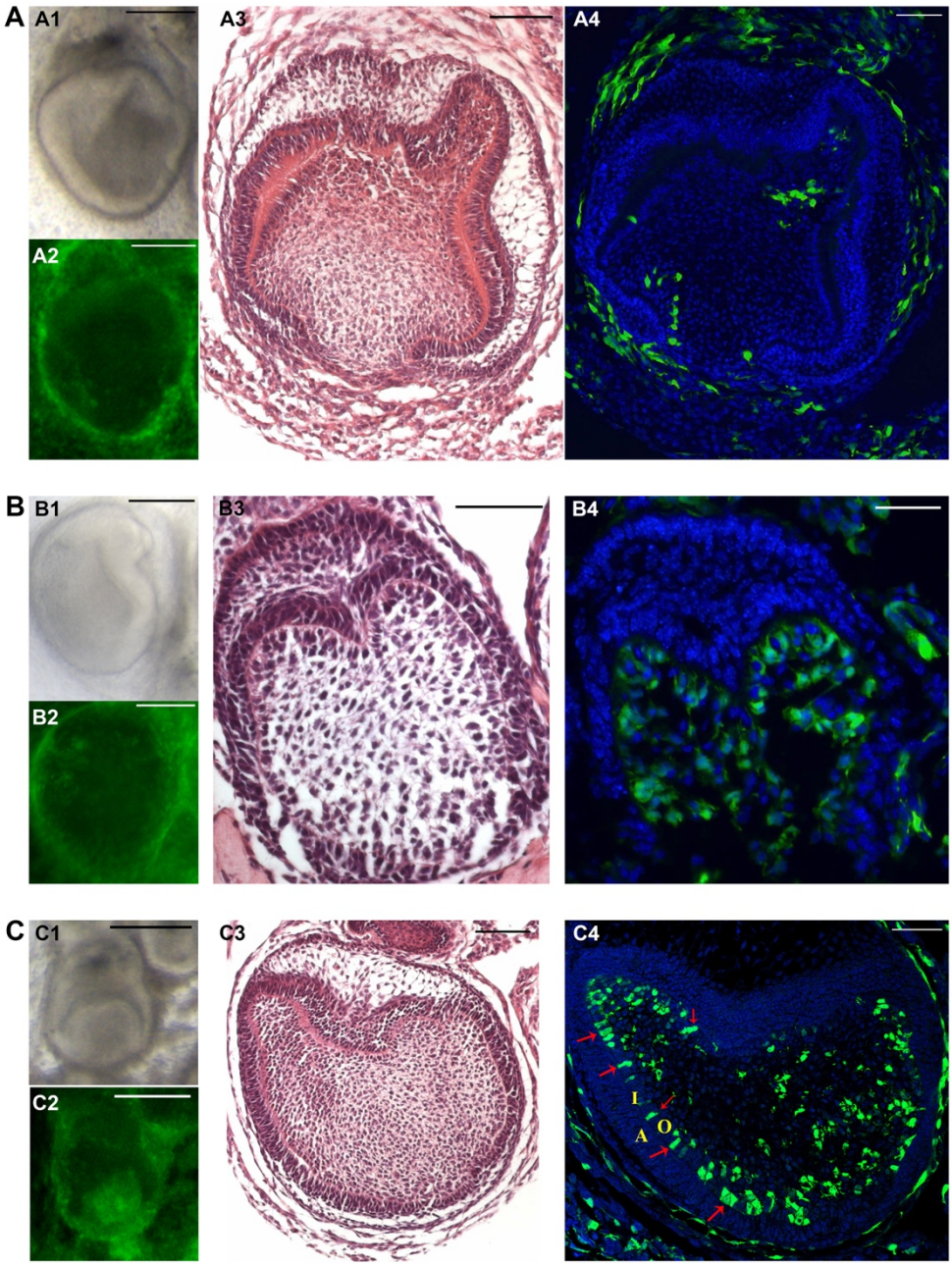

Figure III-3. Reassociations with mesenchymal cell mixtures of cultured embryonic cell percentage at 10%, 25% and 50%.

Mixed cell reassociations with 10% (A), 25% (B), 50% (C) cultured embryonic dental mesenchymal cells have induced tooth formation. H&E staining showed that they all have proper tooth primordium structures (A3, B3, C3). IF result revealed that cultured mesenchymal cells (green) were evenly scattered in tooth primordia, and considerable typical columnar odontoblast-like cells in the interface area were cultured cells (red arrow in C4). Comparing with teeth formed in 50% cultured cell

reassociations, 10% and 25% cultured cell reassociations formed teeth with lower proportion of cultured mesenchymal cells (green). Scale bars: 250 μm (A1-2, B1-2, C1-2); 50 μm (A3-4, B3-4, C3-4).

To rule out contamination of fresh mesenchyme attached to epithelium, trichrome reassociations utilising red, mTmG E14.5 tooth germ epithelial tissues were performed to test the upper limit of cultured cell percentages in mesenchymal cell mixtures for tooth induction (Figure III-1. (C) Trichrome Reassociations). Since the bichrome reassociation experiments have shown that the generated tooth-like structures are histologically identical to tooth primordia, the following experiments focused on the contribution of cultured cells to tooth formation. Bright-field microscopy was used to show whether teeth formed in the reassociations; fluorescence microscopy was used to detect contamination of fresh mesenchyme attached to epithelium: tomato red fluorescence for the epithelial tissues, and green fluorescence for the cultured cells. Fluorescent red and green views of the same position and magnification were merged through the layer blending mode “difference” in photo editing software (Adobe Photoshop CS6) in order to demonstrate the distribution of cultured cells inside the primordia.

The percentages of cultured cells in mesenchymal cell mixtures were increased from 50% to 75% and then 90%. Mixtures with up to 75% cultured cells succeeded in tooth induction: tooth rudiments were observed after 3-4 days in culture, and cultured cells have made a considerable contribution (Figure III-4. A, B). Confocal laser scanning fluorescent microscopy on 50% cultured cell trichrome reassociation has used to confirm that cultured cells were distributed evenly in primordium mesenchyme, a number of which differentiated into columnar odontoblasts lining the interface between epithelium and mesenchyme, which

was well-defined indicating no contamination of fresh mesenchyme attached to epithelium. The blue fluorescence of cells inside the primordium was much weaker than the cells outside, probably because of the compact structure and initiation of mineralization which might render penetration through primordia difficult for DAPI molecules (Figure III-4. A5, A6).

Mixtures with 90% cultured cells failed in tooth induction. As in the negative controls, cyst-like structures of “rolled up epithelial tissue balls surrounded by mesenchymal cells” were observed (Figure III-4. C).

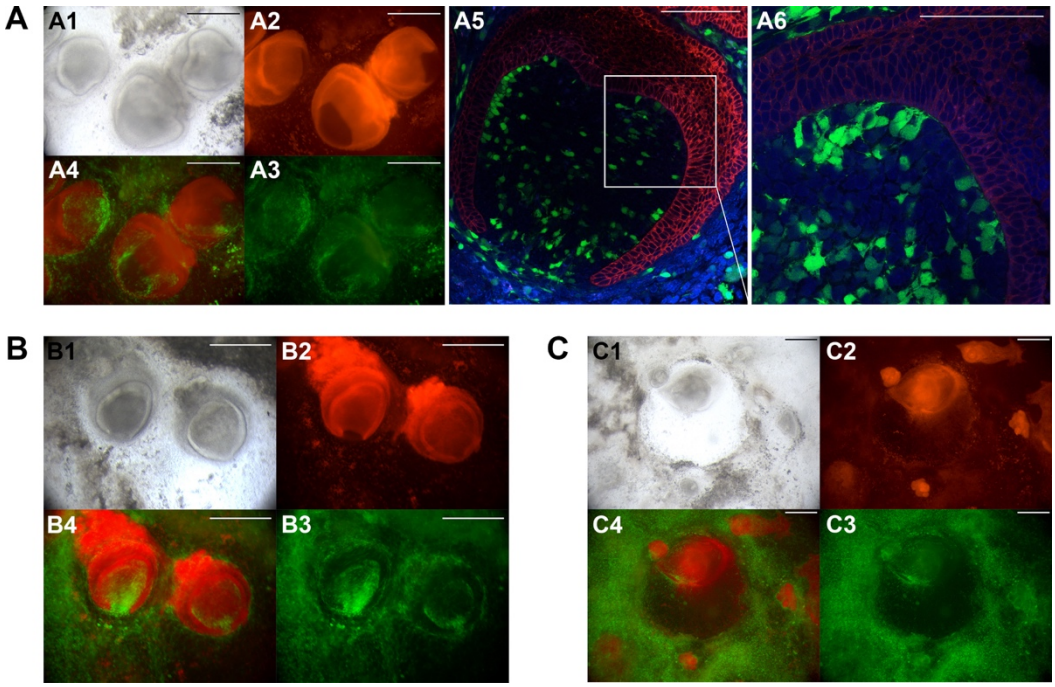

Figure III-4. Trichrome reassociations with mesenchymal cell mixtures of cultured embryonic cell percentage at 50%, 75% and 90%.

50% and 75% cultured E14.5 mesenchymal cell trichrome reassociations using mTmG E14.5 epithelium produced tooth primordia (A, B). Confocal scans of tooth formed in 50% cultured cell reassociation have shown that mTmG cell (red) was observed in the tooth primordium, the interface of epithelium and mesenchyme was well-defined. And again, cultured (green) and uncultured (blue) mesenchymal cells were distributed evenly in the primordium and odontoblast-like columnar

cultured cells can be observed in the interface area of epithelium and mesenchyme of the primordium (A5, A6). 90% cultured cell reassociations, however, failed in tooth formation, cysts formed instead (C). Scale bars: 100 μm (A5, A6); 250 μm (others).

3.2.2 Cultured postnatal (PN7) dental mesenchymal cell behavior in mixed-cell reassociations

Cell mixing approaches were applied with postnatal tooth cells in reassociation experiments. For practical reasons, GFP, rather than mTmG, epithelial tissues were utilized. Molar pulp cells were isolated from mTmG mouse pups at postnatal day 7 and expanded *in vitro*. Passage 1 postnatal dental mesenchymal cells were mixed with CD1 E14.5 fresh molar tooth germ mesenchymal cells at different ratios and then recombined with GFP E14.5 tooth germ epithelium.

In negative controls, as expected, pure cultured postnatal cells failed to induce tooth formation (Figure III-5.D). Mesenchymal cell mixtures containing 10% and 25% cultured postnatal cells successfully initiated tooth development, however, no contribution from postnatal cells could be detected (Figure III-5. A, B). When the percentage of postnatal cells increased to 50%, mesenchymal cell mixtures failed in tooth induction. (Figure III-5.C)

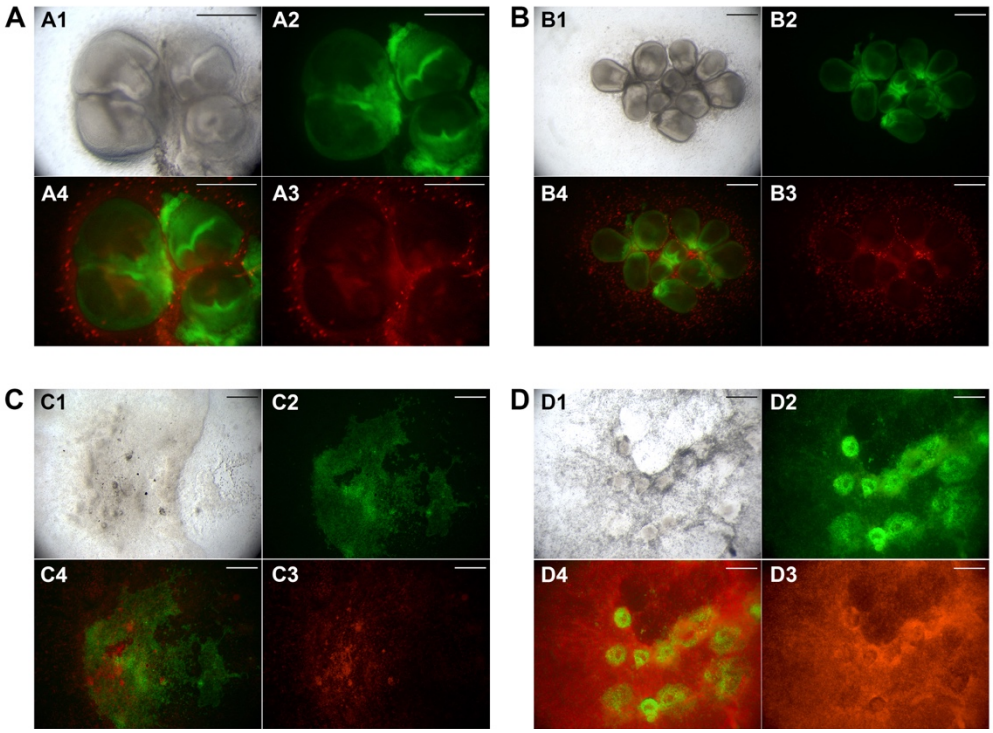

Figure III-5. Trichrome reassociations with mesenchymal cell mixtures of cultured postnatal cell percentages at 10%, 25%, 50% and 100%.

Tooth-like structures formed in reassociations of GFP E14.5 tooth germ epithelial tissue (green) and mesenchymal cell mixtures consisting of 10%, 25% cultured mTmG (red) postnatal (PN7) molar pulp cells (A, B). The majority of postnatal cells (red) were excluded from the tooth-like structures (A4, B4). 50% and 100% cultured postnatal cell reassociations failed in tooth induction (C, D). Scale bars: 500 μm.

3.2.3 Cultured embryonic (E14.5) dental mesenchymal cell behavior in mixed-cell recombinations

To further test the inductivity of mesenchymal cell mixtures, mTmG E14.5 mouse molar tooth germ epithelial tissues were replaced by mTmG E12.5 epithelium which is more naïve in responding to odontogenic signals (Figure III-1. (C) Recombinations ②).

In the positive controls with pure CD1 fresh E14.5 tooth germ mesenchymal cells, the appearance of tooth rudiments became defined after 4-5 days in culture, approximately 1-2 days longer than that in reassociations. Morphologically, these primordia were not distinct from those formed in reassociations (Figure III-6. A). In the negative controls with pure GFP cultured E14.5 dental mesenchymal cells, cysts formed as with E14.5 epithelium (Figure III-6. B).

In mixed cell recombination experiments, similar to the results of reassociations, mixtures with up to 75% cultured cells succeeded in tooth induction (Figure III-7. A-D) and failed when this percentage increased to 90% (Figure III-7. E). It was common to observe variations in morphology and cultured cell proportions in tooth primordia within the same recombination (Figure III-7. C). However, when compared among primordia formed in recombination groups with different percentages of cultured cells, there was a consistent general trend of increased contribution with increased percentage of cultured cells.

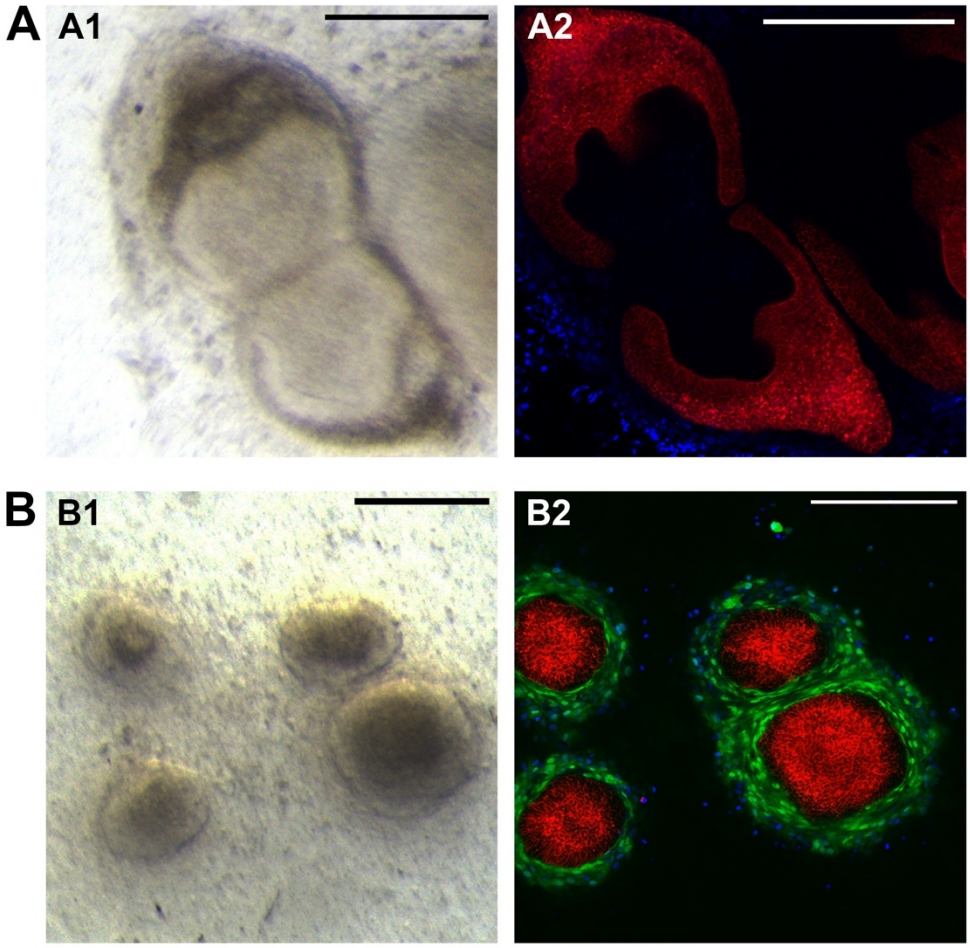

Figure III-6. Positive and negative controls for recombinations.

mTmG E12.5 tooth germ epithelial tissue (red) was recombined and cultured with: (A) non- cultured CD1 E14.5 tooth germ mesenchymal cells (non-labeled) where tooth-like structures formed (Positive control); (B) cultured GFP E14.5 molar germ mesenchymal cells (green) where cyst-like structures, "rolled-up" epithelium (red) surrounded by cultured mesenchymal cells (green), formed (Embryonic negative control). Scale bars: 250 µm.

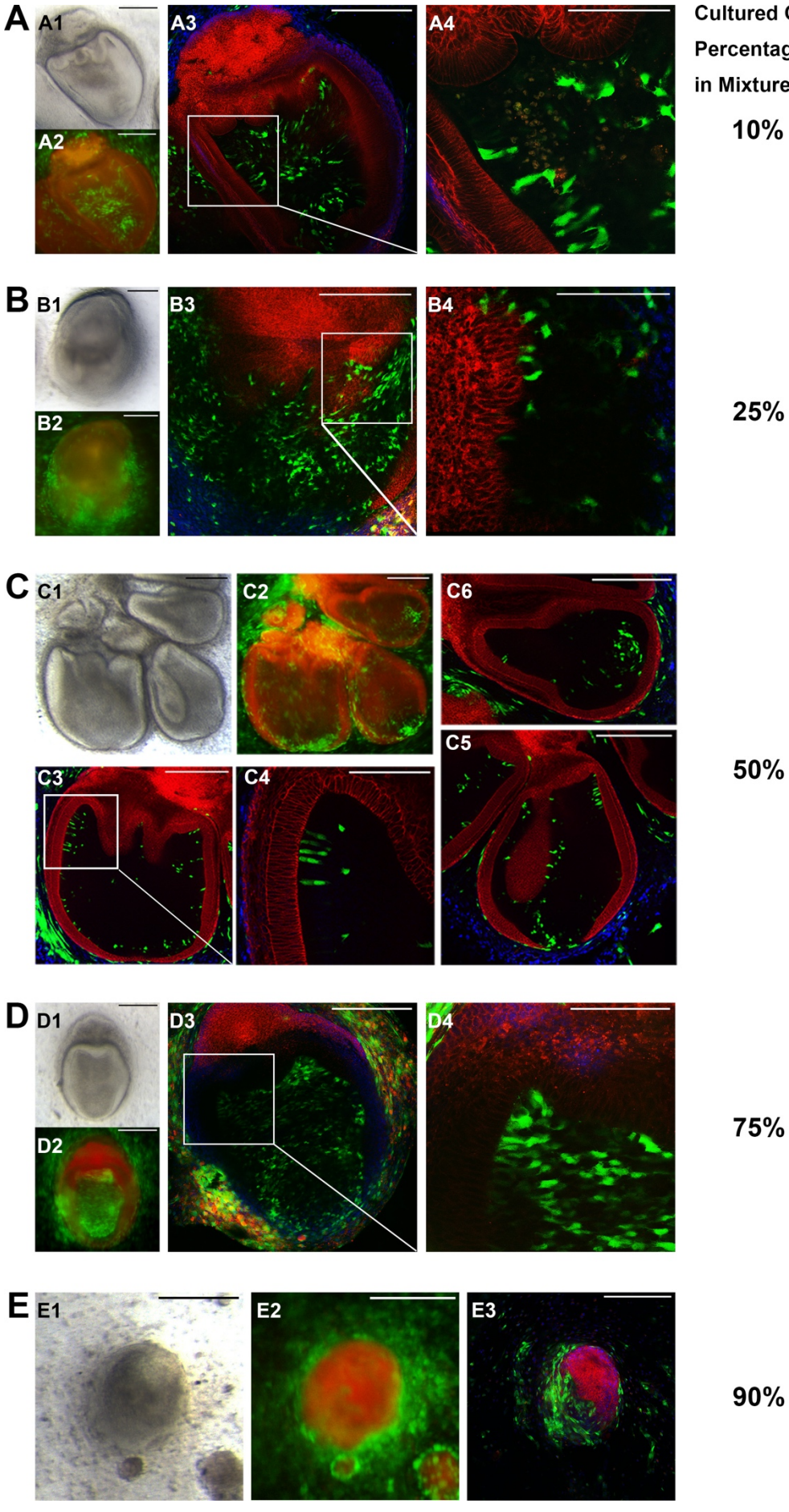
A
A1
A2
A3
A4
Cultured Cell
Percentage
in Mixtures
10%
B
B1
B2
B3
B4
25%
C
C1
C2
C6
C5
C3
C4
50%
D
D1
D2
D3
D4
75%
E
E1
E2
E3
90%

Figure III-7. Recombinations with mesenchymal cell mixtures of cultured embryonic cell percentage from 10% to 90%.

Recombinations of mTmG E12.5 molar germ epithelial tissue (red) and mixtures of cultured GFP E14.5 molar tooth germ mesenchymal cells (green) and CD1 wild-type E14.5 tooth germ dissociated cells (non-labeled): (A) 10% cultured and 90% fresh, (B) 25% cultured and 75% fresh, (C) 50% cultured and 50% fresh, (D) 75% cultured and 25% fresh, (E) 90% cultured and 10% fresh E14.5 molar germ mesenchymal cells. Tooth-like structures formed in recombinations with cell mixtures consisting of no more than 75% cultured E14.5 tooth germ mesenchymal cells (A1-2, B1-2, C1-2, D1-2). Green (GFP+) cells could be seen adjacent to the epithelium (A3, B3, C3, D3), exhibiting an elongated appearance (A4, B4, C4, D4). Cyst-like structures rather than teeth were formed in recombinations with cell mixtures consisting of 90% cultured cells (E). Scale bars: 100 μm (A4, B4, C4, D4); 250 μm (others).

To study if mixed-cell-induced tooth primordia could develop along normally and to examine cultured cell behavior in later stages of tooth development, *in vivo* culture of mixed-cell primordia was performed. Mixed-cell recombinations with 75% cultured cells were cultured *in vitro* until tooth primordia formed and then transplanted under kidney capsules of CD1 mouse hosts for 4-week *in vivo* culture (Figure III-8. A).

Bone-like structures with embedded teeth were observed in implants when collected from mouse subrenal capsules (Figure III-8. B). Micro-CT scan and 3D reconstructions showed that teeth with calcified crowns (enamel), a less calcified inside layer (dentine) and developing roots were present (Figure III-8. C, D). Confocal laser scanning fluorescent microscopy showed that cultured embryonic

tooth cells were evenly distributed in tooth pulp, both in the chamber and along the developing roots, some of which were at the edge of the pulp appearing to have elongated structures as odontoblast processes (Figure III-9).

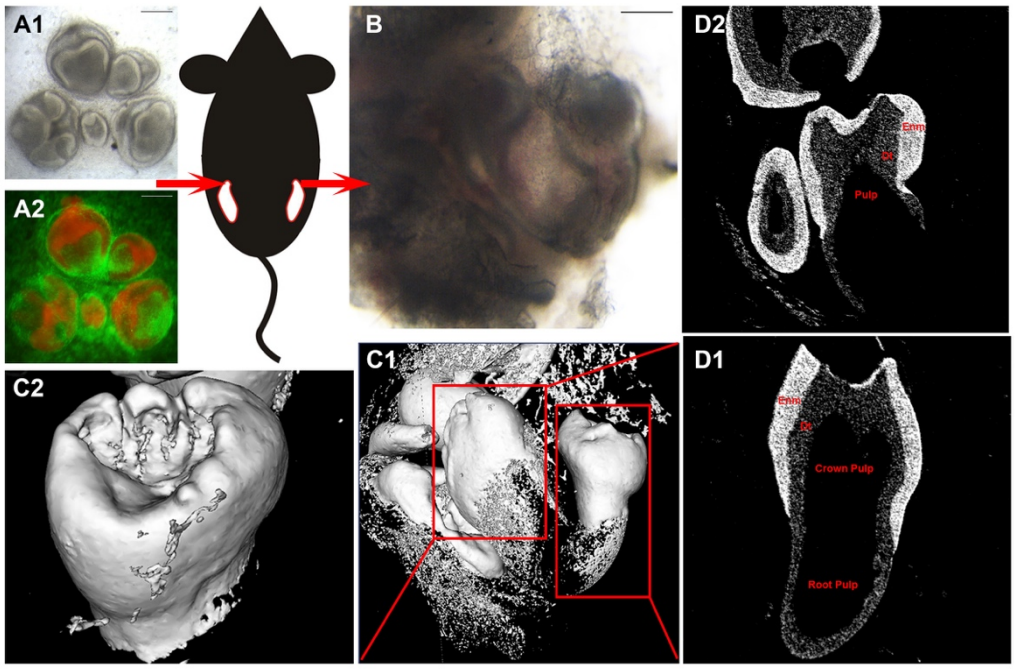

Figure III-8. Subcapsular transplantation of mixed cell recombination induced tooth primordia in mouse kidney and the micro-CT scans on collected implants. After 9 days of *in vitro* culture, tooth-like structures/tooth primordia formed in recombinations using cell mixtures consisting of 75% cultured GFP and 25% fresh CD1 E14.5 molar germ mesenchymal cells and mTmG E12.5 molar germ epithelial tissue (A1, A2) were transplanted under mouse renal capsules. Lumps of bone-like structures with embedded teeth were found after 4 weeks of *in vivo* culture (B). micro-CT scan (D1-2) and 3D reconstruction (C1-2) show that these teeth have calcified crowns (enamel), less calcified inside layer (dentine) and developing roots. Scale bar: 250 μm. (* Enm: Enamel; Dt: Dentine)

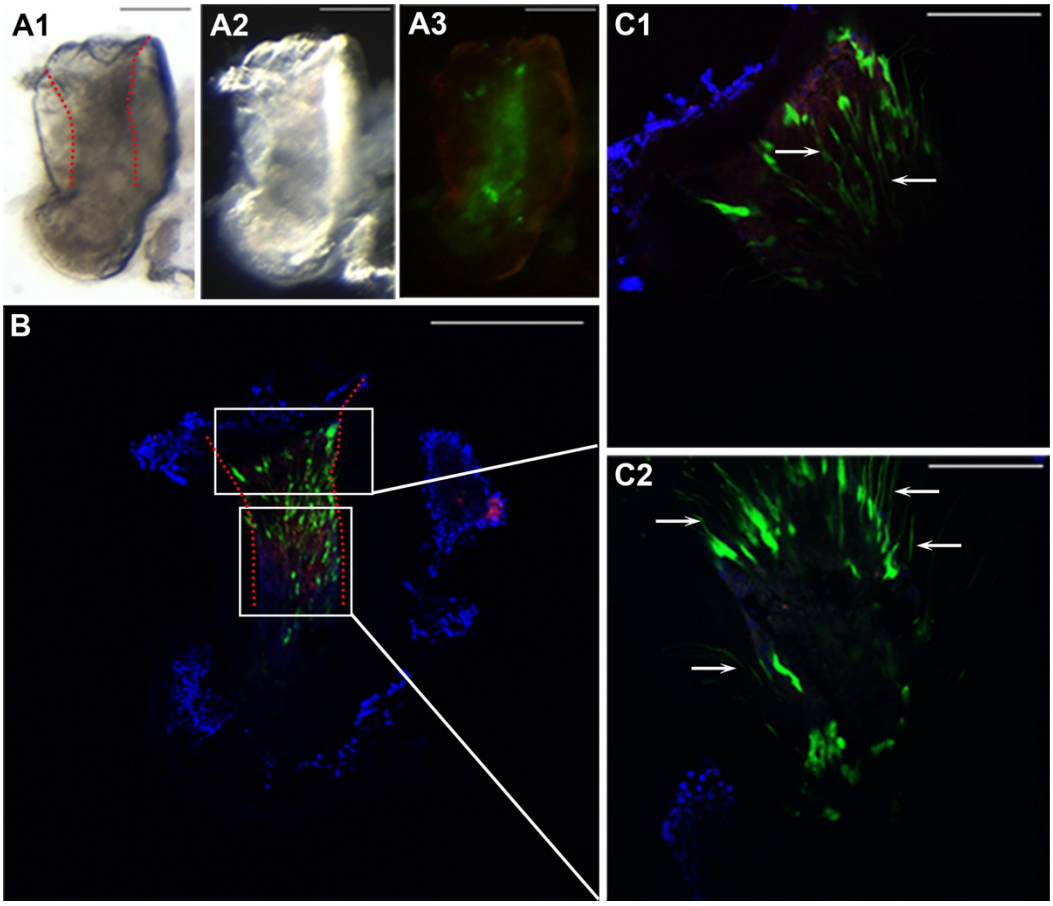

Figure III-9. Cultured cell contribution in tooth separated from subrenal capsular implants.

A single tooth was isolated from implant lumps which originate from recombinations using cell mixtures consisting of 75% cultured GFP and 25% fresh CD1 E14.5 molar germ mesenchymal cells and mTmG E12.5 molar germ epithelial tissue (A1: bright field; A2: black field. Red dot lines outline the pulp cavity). Fluorescent view (A3) and confocal scan (B) show that GFP+ cells (cultured cells) evenly distributed in tooth pulp, both in the chamber and along the developing root. Higher magnification confocal scans (C1-2) show that GFP+ cells at the edge of pulp appear to have elongated segments as odontoblast processes (white arrows). Scale bar: 250µm (A1-3), B; 100µm (C1-2).

3.2.4 Cultured postnatal (PN7) dental mesenchymal cell behavior in mixed-cell recombinations

E12.5 mTmG epithelium was utilized to examine the inducing ability of mixtures of GFP cultured postnatal (PN7) molar pulp cells and CD1 fresh E14.5 tooth germ mesenchymal cells.

Similar results to the reassociations where E14.5 epithelium was used, pure cultured postnatal cells (negative controls) and 50% postnatal cell mixtures did not induce tooth formation, while 25% did (Figure III-10. C). Although very few individual postnatal cells could be seen inside the tooth primordia (Figure III-10. C3), one cell seemed to have differentiated into an odontoblast at the epithelium-mesenchyme interface (Figure III-10. C5). The majority of postnatal cells however were excluded from tooth structures. Given the very low contribution from cultured postnatal cells, it was unnecessary to proceed to *in vivo* experiments for these recombinations.

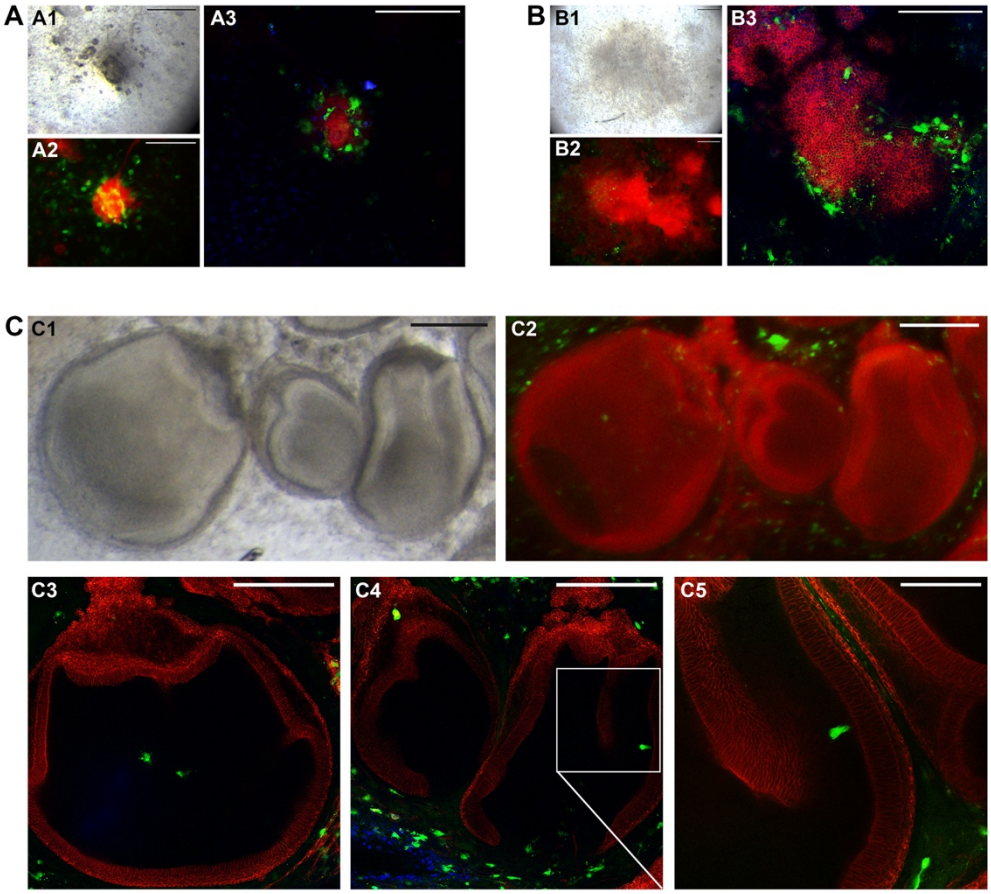

Figure III-10. Recombinations with mesenchymal cell mixtures of cultured postnatal cell percentage at 100%, 50% and 25%.

mTmG E12.5 tooth germ epithelial tissue (red) was recombined and cultured with 100% cultured GFP PN7 molar pulp cells (green) where no tooth formation was observed (Postnatal negative control) (A). 50% cultured GFP PN7 molar pulp cells (green) and 50% fresh CD1 E14.5 molar germ mesenchymal cells (nonlabeled) failed to form toothlike structures, shown in bright field (B1), fluorescent view (B2) and confocal scan (B3). Toothlike structures formed in recombinations with cell mixtures consisting of 25% cultured green fluorescent protein–positive (GFP+) postnatal (PN7) molar pulp cells(C1). The majority of postnatal cells (green) were excluded from the toothlike structures (C2). Few cultured GFP+ (green) cells could be seen inside the tooth primordia (C3-5). Scale bars: 100 µm (C5); 250 µm (others).

3.2.5 Summary

Since cultured mesenchymal cell populations behaved consistently in mixed cell reassociations and recombinations, a summary of tooth formation success rates and cultured cell contribution is presented in Table III-1.

Mouse E14.5 embryonic tooth germ mesenchymal cells have whole-tooth inducing ability which is lost after *in vitro* proliferation. Cultured embryonic cells mixed with fresh cells, can induce tooth formation when the cultured cell percentages in the mixture are below 75%, but cannot when above 90%. Cultured embryonic cells can make a significant contribution to tooth formation with an even distribution, differentiation into odontoblasts and continuous participation throughout later stages and root development.

Postnatal cultured dental pulp cells do not possess the capacity of *de novo* odontogenesis. Mixing with inductive fresh embryonic dental mesenchymal cells showed tooth induction can be initiated when postnatal cell percentages in the mixture are below 25%, but cannot when above 50%. Postnatal cultured cells barely contribute to the generated tooth primordia.

Table III-1. Tooth Formation Success Rate and Cultured Cell Contribution in All Experiments (including Reassociations and Recombinations).

Cultured Dental Mesenchymal Cell Origins (mixing with noncultured embryonic E14.5 molar tooth germ mesenchymal cells)		**Cultured Cell Percentage in Mesenchymal Cell Mixtures**						
		0 Positive Controls	**10%**	**25%**	**50%**	**75%**	**90%**	**100%** Negative Controls
Embryonic E14.5 Molar Tooth Germ Mesenchyme	**Tooth Formation Success Rate***	**100% (23/23)**	**100% (3/3)**	**100% (4/4)**	**100% (11/11)**	**90% (9/10)**	**0 (0/11)**	**0 (0/11)**
	Cultured Cell Contribution*	**-**	**√**	**√**	**√**	**√**	**-**	**-**
Postnatal PN7 Molar Pulp	**Tooth Formation Success Rate**	**100% (23/23)**	**100% (3/3)**	**85.7% (6/7)**	**0 (0/11)**	**Predicted -**	**Predicted -**	**0 (0/8)**
	Cultured Cell Contribution	**-**	**.**	**.**	**-**	**-**	**-**	**-**

* Experiment groups succeeded in tooth induction; Experiment groups failed in tooth induction

* Tooth Formation Success Rate= No. of experiments where tooth-like structures formed/No. of total experiments

* Cultured Cell Contribution: ”√“ meaning significant contribution to tooth primordia formed in experiments from cultured cell population; “.” meaning no (significant) contribution to tooth primordia formed in experiments from cultured cell population; “-“ meaning not applicable.

3.3 Discussion

3.3.1 Odontogenic Potential of *In vitro* Expanded Embryonic and Postnatal Tooth Cells

In stem cell based whole tooth bioengineering, either epithelial or mesenchymal cells are required to be inductive in order to initiate tooth formation mimicking the natural process of *de novo* odontogenesis. To date, only non-cultured embryonic dental cell populations possess this inducing ability which rapidly fades away during *in vitro* cell expansion. Adult dental stem cells can only participate in tooth formation as the recipients. Thus, to regain the lost odontogenic capacity in cultured embryonic tooth cells and to activate the inductivity in adult cells is a major goal in current research on tooth bioengineering.

Here, to explore the feasibility of this goal before any trials on specific methods, sets of combination experiments of non-inductive dental epithelium and mixed mesenchymal cells were performed to determine if cultured tooth cells, both embryonic and postnatal, can take part in tooth formation as the inducing cells.

From the results of mixed cell recombinations, it is obvious that the cultured embryonic cells can contribute to tooth formation when their percentage in the mixtures with inductive cells is less than 75%. They were evenly spread within the tooth primordia formed in recombinations and were able to differentiate into odontoblasts at the epithelium-mesenchyme interface. Moreover, they participated fully in root development of primordia transplanted under mouse renal capsule. All this evidence suggests an active role of cultured embryonic cells in tooth formation. However, postnatal cells have been shown to be capable of proliferation and differentiation when given the odontogenic culture environment (Soares et al., 2017, Kim et al., 2015b, Gronthos et al., 2000). Therefore, it is

reasonable to question whether the cultured cells contributing to tooth structures become inductive again, or they happened to be recruited and hence start to proliferate and differentiate in the odontogenic environment generated by interaction of inductive non-cultured embryonic mesenchymal cells and responsive dental epithelium.

Since mixtures of cultured postnatal cells and inductive cells succeeded in tooth formation at the ratios of 1:9 and 1:3 (respectively with postnatal cell percentage of 10% and 25%), if "recruitment" occurred, then cultured postnatal cells would be expected to show similar contributions to embryonic cultured cells in the tooth structures formed in recombinations with the same cultured-to-inductive cell ratios. However, postnatal cells were barely observed in the tooth primordia. Kökten et al. also found no contribution from postnatal bone marrow MSCs with a similar approach where bone marrow MSCs replaced postnatal dental cells (Kökten et al., 2014). On the contrary, bone marrow cells mixed with responding epithelial cells and reassociated with intact inductive mesenchyme did participate in tooth formation as an epithelial population and differentiate into ameloblasts and even odontoblasts (Hu et al., 2006). These results imply that although cultured embryonic, postnatal mesenchymal cells and bone marrow cells can fully participate in tooth formation as the recipients of inducing signals, they must become inductive to contribute to tooth formation induced by mesenchyme in the recombination experiments. In other words, odontogenic inductivity is strictly required from the contributing to participate in tooth induction.

Consistent with observations that a minimum of $13.5\pm0.5\times10^4$ inductive mesenchymal cells are required for successful tooth induction in cap stage tooth germ reassociation experiments (Nait Lechguer et al., 2008), recombinations of positive controls failed to induce tooth induction when inductive mesenchymal

cell numbers did not reach a threshold of approximately 1.5×10^5. A total mesenchymal cell number of 2×10^5 was used in each recombination. Mesenchymal cell mixtures with 50% and 75% cultured embryonic cells, respectively contained 1×10^5 and 5×10^4 fresh inductive cells which were not sufficient for tooth induction, indicating cultured embryonic cells must have become inductive to compensate the insufficiency of inductivity from the mesenchyme.

Meeting the threshold of inductive cell number is a necessary but not sufficient condition for mesenchymal cell mixtures to induce tooth formation. The total cell numbers of mixtures with 90% cultured embryonic cells were increased by 10 times to 2×10^6. Although with sufficient fresh inductive cells (2×10^5), mixtures failed in tooth formation. Similarly, failure to tooth formation occurred when the total cell number of mixtures with 50% cultured postnatal cells were increased by 4 times to 8×10^5 with 4×10^5 fresh inductive cells. These suggests a crucial role of the "relative percentage" in addition to the "absolute number" of inductive cells in mixtures.

To analyze how relative percentage of inductive cells can affect outcomes of recombination experiments, a simple mathematical model is employed to quantify the inducing ability. Assume that the inductivity of a single inductive, non-cultured embryonic tooth cell, is 1; and that of a non-inductive cell, either cultured embryonic or postnatal cell, is 0; The percentage of non-inductive cells in mixtures is x%, hence that of inductive cells is (100-x)%; Total cell number is N. Then the average tooth inducing ability of a cell mixture, or say the inductivity per cell (I)can be defined as a function as follow:

$$I = f(x) = \frac{N\times x\%\times0+N\times(100-x)\%\times1}{N} = 1\text{-}x\%$$

If the average inductivity simply results from the dilution effect generated by adding non-inductive cells, mixtures with the same percentage of embryonic cultured cells and postnatal cultured cells should have identical outcomes of tooth induction, which is in conflict with the findings observed in both reassociation and recombination experiments (see Table III-2). To adjust the gap between expectation and observation, the assumption of "cultured embryonic and postnatal cells share the same inductivity which is 0" might be in need of rectification.

Therefore, assume that the value of inductivity of cultured postnatal cells equals to "a". The modified function of average inductivity of cell mixtures containing postnatal cells, I (PN), can be defined as follow:

I (PN) = f(x) = $\frac{N\times x\%\times a+N\times(100-x)\%\times 1}{N}$ = 1- (1-a)•x%

Since mixtures containing 75% cultured embryonic cells, in which the average inductivity is 0.25, succeeded in tooth induction, while mixtures containing 90% cultured embryonic cells, in which the average inductivity is 0.1, failed, these show that the "tooth/no tooth formation" switch point falls into the average inductivity range of 0.1 to 0.25. Hence, to calculate backwards, mixtures containing 25% cultured postnatal cells succeeded, while those containing 50% cultured postnatal cells failed in tooth induction, the value of "a" can be narrowed down to the range of -2.6 to -0.5 as follow：

x	f(x)	Expected value of f(x)	Range of a
25	0.75+0.25a	> 0.1	> -2.6
50	0.5+0.5a	< 0.25	< -0.5

As shown in Table III-2, select **-1** from this range as it is easier to perform the calculation. With the adjusted average inductivity, the results now coincide with the scenario of "identical outcomes of tooth induction in mixtures with the same average inductivity". Having inductivity below 0 indicates that as these cultured postnatal cells were added to inductive cells, the total inductivity decreases rather than maintains as when cultured embryonic cells were added. The inhibiting effect of one postnatal cell can counteract the inducing ability of up to 2.6 inductive cells. In the sense of tooth inducing potential, these postnatal cells can be considered as not only "non-inductive" but also "anti-inductive".

Table III-2. Average inductivity calculation examples of differently componented cell mixtures based on assumption of all-or-nothing measurement of single cell inductivity.

Average Inductivity of Mixtures		**Cultured Cell Percentage of Mixtures (x%)**						
		0	**10**	**25**	**50**	**75**	**90**	**100**
Pure Cultured E14.5 Cells = 0		1	0.9	0.75	**0.5**	**0.25**	0.1	0
Pure Cultured PN7 Cells =	**0**	1	0.9	0.75	**0.5 ?**	**0.25 ?**	0.1	0
	-1	1	0.8	**0.5**	**0**	-0.5	-0.8	-1

Experiment groups succeeded in tooth induction

Experiment groups failed in tooth induction

? Unexplainable results in the sense of "identical outcomes of tooth induction in mixtures with the same average inductivity".

There is another possible mechanism that the inductivity of a cell is measured in a pattern of "spectrum" rather than "all-or-nothing". Adopting the same

mathematical model as above, the inductivity of fresh and cultured embryonic cells can be set to 1 and 0.5 respectively, signifying that cultured embryonic cells can possess partial inductivity and contribute to tooth induction only when they are with complete inductivity. Following the same formula, the inductivity of cultured postnatal cells can range from 0.25 to -0.8 as follow:

x	f(x)	Expected value of f(x)	Range of a
25	0.75+0.25a	> 0.55	> -0.8
50	0.5+0.5a	< 0.625	< 0.25

indicating that though they are more likely to be inhibitive due to the wider range below 0, the cultured postnatal cells might simply have much lower inductivity than that of cultured embryonic cells which leads to the requirement of higher percentage of inductive cells so as to raise the average inductivity of mixtures to the threshold (Table III-3).

Table III-3. Modified average inductivity calculation examples of differently componented cell mixtures based on assumption of spectral measurement of single cell inductivity.

Average Inductivity of Mixtures		Cultured Cell Percentage of Mixtures (x%)						
		0	**10**	**25**	**50**	**75**	**90**	**100**
Cultured E14.5 Cells = 0.5		1	0.95	0.875	0.75	**0.625**	**0.55**	0.5
Pure	**-0.5**	1	0.85	**0.625**	**0.25**	-0.125	-0.35	-0.5
Cultured	**0**	1	0.9	**0.75**	**0.5**	0.25	0.1	0
PN7 Cells =	**0.1**	1	0.91	**0.775**	**0.55**	0.325	0.19	0.1

Experiment groups succeeded in tooth induction

Experiment groups failed in tooth induction

Given the above, sufficient relative percentage of inductive cells in mixtures can contribute to creation of a micro-environment that is favourable to tooth induction. In addition, absolute numbers of inductive cells have to reach the threshold of 1.5×10^5 to trigger the induction process. It is also worth noting that, based on the experiments using mixtures of fresh and cultured embryonic cells, it is understandable that cultured cells were rescued from being incompetent to induce tooth formation to compensate the insufficiency of absolute number of inductive cells. However, the occurrence of this rescue effect is independent of the necessity for tooth induction. This can be proven by the considerable contribution from cultured cells to tooth structures formed in recombinations using mixtures containing 90% fresh cells where supplement of inductive cells is not necessary for tooth induction.

A process named “community effect” during animal embryonic development seems to have similar description as in the discussion above. It was first discovered by John Gurdon in the muscle precursor cells of *Xenopus* embryos, a phenomenon whereby “the ability of a cell to respond to induction by differentiating as muscle is enhanced by, or even dependent on, other neighboring cells differentiating in the same way at the same time.” (Gurdon, 1988). In other words, this “community effect” can act to allow heterogeneous cell populations to differentiate down a common pathway by cells interacting with their immediate neighbours. It is necessary for the cells to maintain tissue-specific gene expression and differentiate in a coordinated manner. Possible mechanisms for the community effect involve linear gene cascades and cell-cell interactions mediated by diffusible signaling factors. (Gurdon et al., 1993a, Gurdon et al., 1993b, Bolouri and Davidson, 2010, Saka et al., 2011) (Figure III-11).

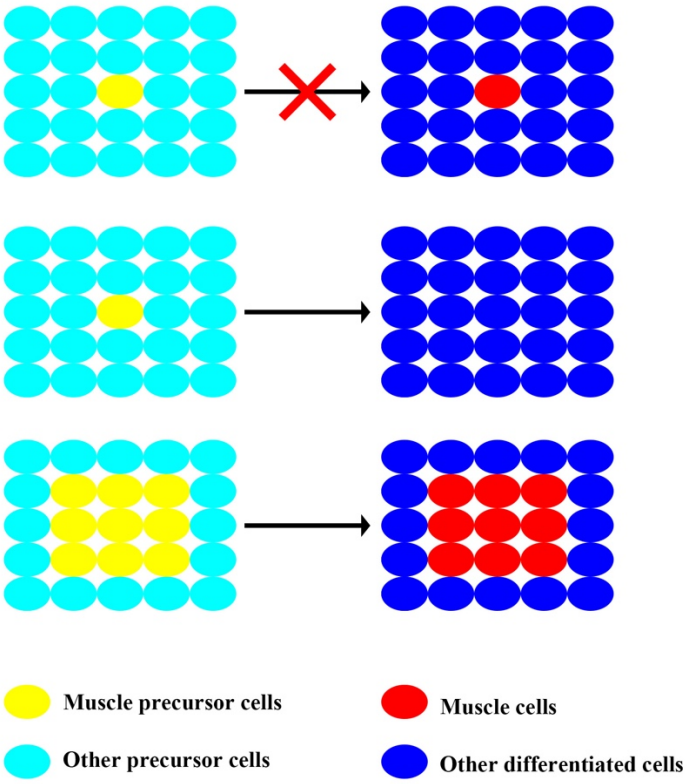

Figure III-11. Diagram illustrating the concept of the community effect in muscle embryonic development.

Adapted from (Saka et al., 2011)

In this study, cell mixing of cultured embryonic/postnatal dental cells with inductive non-cultured embryonic tooth cells can be considered as an artificially created odontogenic cell community. Though originally community effect refers to collective reaction of responding cells to inducing signals, while here the cultured cell populations are affected by fresh cells to become inducing cells in tooth formation, it is logically applicable to the situation. Hereby, piecing together the previous ratiocinations, the initiation process of tooth induction in mixed-cell recombinations can be summarized as follows: (Figure III-12).

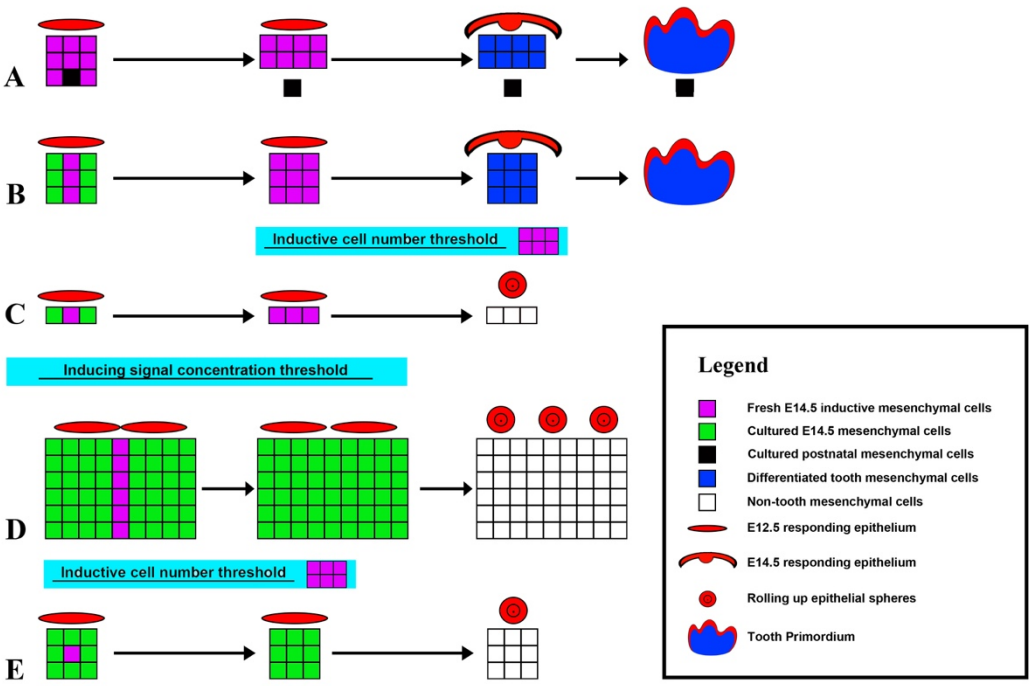

Figure III-12. Schematic representation of mechanism of community effect for tooth induction in mixed cell recombinations.

Table III-4. Recombination condition summary

Condition	Meeting thresholds of		Odontogenic community effect	Results	
	Inducing signal concentration	Inductive cell number		Tooth formation	Cultured cell contribution
A	√	√	·	√	·
B	√	√	√	√	√
C	√	·	√	·	-
D	·	√	·	·	-
E	·	·	·	·	-

Based on the capability of tooth induction, dental mesenchymal cells can be divided into inductive cells (non-cultured embryonic cells) and non-inductive cells (cultured embryonic and postnatal cells). Non-inductive cells can secrete partial tooth inducing signals yet not sufficient to induce tooth formation. In addition, cultured postnatal cells tend to have an inhibiting effect possibly due to secretion of signaling inhibitors which mathematically can counteract the inducing signals. Hence, mixtures with different proportions of inductive and non-inductive cell populations will result in different concentrations of inducing signals, which are required to reach a threshold for generating odontogenic mesenchymal cell community. Tooth induction will be initiated when the absolute number of inducing cells is above the minimum of 1.5×10^5. Otherwise, either the concentration of inducing signals or absolute inducing numbers does not meet the requirements, the mixture, as a whole, will fail to induce tooth formation, and inductive cells will become incompetent.

Cultured embryonic cells can be converted into inductive cells through a community effect when the concentration of inducing signals in the mixture is above the threshold, and together with originally inductive cells reach the minimum inducing cell number. Thus, the homogenized mesenchymal cell mixture will initiate tooth formation through interaction with the responding epithelium with contribution from originally cultured cells.

Cultured postnatal cells, on the other hand, seem to be immune to the community effect. Mixtures can accomplish tooth induction when both the signal concentration and inducing cell number meet their requirements, however, without a contribution from cultured postnatal cells. Since community effect is a phenomenon among embryonic cell populations, postnatal cells, though with common stemness, might have receptivity that is incompatible with embryonic

signaling patterns. This is possibly because of changes in expression and distribution of receptors in postnatal cells during development so that their odontogenic genes cannot be activated by embryonic inducing signals, which also tend to be weakened by probable secretion of inhibitors from postnatal cells. Supplement of special factors or even direct cell reprogramming might be required for such drastic switch of the odontogenic capacity in postnatal cells. Though showing capability of tooth tissue repair and regeneration, such incompetence to whole-tooth forming of postnatal dental cells is not entirely unexpected, since this could be a protection mechanism to prevent supernumerary teeth and odontoma in postnatal/adult individuals.

It is notable that sparse cultured postnatal cells can be observed in tooth structures formed in recombinations using 25% cultured postnatal cell mixtures where one cell differentiated into an odontoblast at the epithelial-mesenchymal junction. This little spark might ignite a hopeful possibility that postnatal cells can be activated to be inductive, only when the concentration of inducing signals is very high, as an extreme example, inductive to postnatal cell ratio up to 1.5×10^5:1. The other possibility is that these very few contributing postnatal cells are actually the desired stem cell population, since no specific selection procedure has been performed on cultured pulp cells which might result in massive dental fibroblasts with limited regenerative potency in the mixtures. As a tooth germ develops, inductive cell populations will gradually decrease (Keller et al., 2011). Therefore, it is highly possible that unselected postnatal pulp cells have very low proportion of whole-tooth inducing stem cells. If so, pure fresh inductive pulp stem cells above minimum inductive cell number, alone, can engage in tooth formation. However, the staining and high-pressure conditions involved in cell sorting procedure are not beneficial to cell survival, not to mention that there is no

standard selection protocol or reliable specific markers to separate whole-tooth-inductive cells from the other pulp cells.

Optimistically, if there were such whole-tooth-inductive stem cells in dental pulp, only very few in number, mass proliferation *in vitro* will be necessary for obtaining sufficient cells, which leads us back to the same problem cultured embryonic dental mesenchymal cells confront with. Since cultured embryonic tooth cells have been shown to be rescued from failure of tooth induction by a fresh inductive cell generated community effect, which possibly is mediated by certain diffusible tooth inducing signals, the next step of this research is focused on how to regain the lost inducing ability of cultured embryonic dental mesenchymal cells through artificially manipulable methodology such as special culturing conditions and cocktail of factors etc. Taking a step back, if such inductive postnatal pulp cells do not exist, further study on the tooth inducing signals can be conductive to promoting inductivity in postnatal cells. Additionally, studying on cultured embryonic tooth cells can directly benefit the strategy of establishing inductive cell lines derived from embryonic tooth cells, especially the third molar formation is initiated postnatally which can provide cell sources of postnatal tooth bud cells from adult individuals.

3.3.2 Considerations and Limitations in Experiment Design

In the reassociations where epithelial tissues and inductive mesenchymal cells are from the same molar tooth germs of CD1 mouse embryos at the stage of E14.5, contamination of fresh mesenchyme attached to the epithelium is visually undetectable, which can result in higher proportion of inductive cells that leads to false positive results, which can be avoided through introduction of differently labelled epithelium.

Since odontogenic potential shifts from epithelium to mesenchymal at stage E12 (Mina and Kollar, 1987), E12.5 dental epithelium is the most naïve responsive dental epithelium that requires additional induction from E14.5 mesenchyme for synchronization prior to tooth forming. This is probably the cause of the 1 day delay I observed in tooth structures beginning to appear in recombinations comparing with reassociations. Ideally, heterotypic epithelium should be utilized, since dental epithelium can, to some extent, weaken the convincingness of the inductivity of mesenchymal cells. However, for the purpose of this study, to test whether cultured cell populations can contribute to tooth induction, it is not necessary to advance recombinations to that level.

Variations of tooth morphology can be observed within single recombination. Outcomes did not differ much between the recombinations using mixed cells and complete inductive cells, except that mixed-cell-induced tooth development seemed slightly retarded than the teeth induced by the pure inductive cells. This possibly is because of the community effect process. On one hand, this can be a proof to support the previous inference that only inductive cells can participate in tooth induction which results in either teeth similar to those induced by pure inductive cells or complete failure. On the other hand, the experimental method applied for recombination in this study might not be sophisticated enough to offer

more information on detailed differences in tooth morphology which is currently far away from the research focus.

Variations can be also observed in the proportion of cultured embryonic cells contributing to the tooth structures formed in the same recombination (Figure III-7. C). The most likely possibility is that the homogeneity of collagen gel, cell mixture preparation including centrifuge, pipetting and injection can be affected by either environment (temperature and humidity etc. in the lab) or human factors that are not strictly under control which will lead to heterogeneous density in cell mixtures. The general trend of increased contribution with increased proportion of cultured embryonic cells is obvious which is more valuable than their performance in one specific primordium for the discussion about their odontogenic potential. Similarly, the setting of non-inductive to inductive cell ratios of 1:9,1:3,1:1,3:1,9:1, aims to conclude the general trend rather than a precise watershed ratio of tooth induction.

Chapter IV Microenvironmental Modification of Cultured Embryonic Dental Mesenchymal Cells

4.1 Introduction

The loss of odontogenic capacity in cultured embryonic dental mesenchymal cells can be attributed to two main aspects: spatial state change from three-dimensional (3D) to two-dimensional (2D) via standard monolayer culture and lack of responsive signals due to separation from the epithelium.

4.1.1 Three-dimensional Culture

2D monolayer culture is a conventional method for cell-based *in vitro* studies for efficient and reliable cell proliferation when large number of cells are required. However, the limitations of 2D culture have been increasingly recognized, since many results of *in vitro* experiments on 2D cultured cells cannot represent *in vivo* cell responses (Bhadriraju and Chen, 2002, Weaver et al., 1997, Birgersdotter et al., 2005). Unlike the aggregated spherical cells *in vivo*, cells in 2D culture flatten and expand along the culture surface. In addition to the morphological and physical changes, the adhering growth pattern of standard 2D culture selectively enhances the population of cells with higher expression of adhesion molecules and causes loss of polarity in cells that affects the intracellular signalling pathways. (Birgersdotter et al., 2005, Dr. Domokos Bartis, 2011, Zhou et al., 2017)

3D culture refers to *in vitro* cell culture systems that complement the 3rd dimension, mimicking the *in vivo* environment of cells. Cells can aggregate to form spheroids or clusters within a matrix, on a matrix or in suspension medium (Edmondson et al., 2014, Haycock, 2011). 3D cell cultures better preserve the

original cell characteristics including morphology, polarity, cell-cell and cell-ECM contacts. Moreover, the 3D-culture-mediated restoration of cell polarity can affect intracellular signalling independent of how long the cells have been cultured in 2D conditions (Birgersdotter et al., 2005).

Various 3D culture models have been applied in biomedical research such as drug discovery, cancer cell biology and stem cell based regenerative medicine (Zhou et al., 2017, Jakubikova et al., 2016, Godugu et al., 2013, Rimann and Graf-Hausner, 2012). 3D culture of human bone marrow mesenchymal stromal cells (MSCs) utilizing u-bottomed plates resulted in dedifferentiation of aged human MSCs to an early mesendoderm-like state, indicating a cell reprogramming potential of 3D culture which can maintain or restore the pluripotency of stem cells. Moreover, generation of these physically induced pluripotent stem cells can be inhibited by Bafilomycin A and enhanced by Rapamycin, respectively inhibitor and stimulator of autophagy (Pennock et al., 2015). Autophagy is a self-protection mechanism to promote cell survival under stress by removing unnecessary or dysfunctional components from the cell. Appropriate activation of autophagy can benefit stem cell protection in dental tissues (Zhuang et al., 2016). Human hair follicles share the similar development pattern with teeth. Hanging-drop-mediated 3D culture of *in vitro* expanded dermal papilla cells rescued them from failure of hair generation in combination with skin tissues and partially restored their expression of inductive transcriptional signature (Higgins et al., 2013).

In tooth formation, mesenchymal condensation is a crucial step. (Mammoto et al., 2011) demonstrated that physically compaction of early stage mesenchyme (E10) can induce expression of odontogenic transcription factors *Pax9* and *Msx1* and signal molecule BMP4, suggesting that physical alteration of cell culture environment is promising in restoration of tooth inducing ability of cultured cells.

4.1.2 Co-culture

Most biological events involve participation of multiple types of cells. Maintenance or activation of characteristics of some cell populations depends on presence of other cell populations (Goers et al., 2014). Typically, organ development such as odontogenesis is a process mediated by cross-talk between epithelium and mesenchyme (Thesleff and Sharpe, 1997). Separation from responsive epithelium can result in, although not immediate, rapid loss of tooth inducing ability in mesenchymal cells during standard monoculture.

Co-culture, or hetero-culture, can be defined as cell culture systems that enable heterotypic cells to communicate with or without direct contact. An immediate mode of co-culture is 2D direct co-culture system where mixtures of heterotypic cells are grown in traditional 2D culture conditions. In addition to the signalling molecules, the physical contact of different cells might also contribute to the cell-cell communication through actions of adhesion molecules. However, additional processes, such as cell sorting, are required to isolate the target cell population for further study. It also may compromise an appropriate environment for all cell types when they do not share the same requirements of culture conditions. To overcome these limitations, a non-contact Transwell co-culture system has been developed. Introduction of cell culture inserts divides the wells into top and bottom compartments where different cells can be easily separated. With porous membranes that permit penetration of small molecules, cells can be cultured in different conditions and maintain the communication without direct cell contact (Miki et al., 2012, Bogdanowicz and Lu, 2014, Arnold et al., 2001, Arrigoni et al., 2016, Goers et al., 2014).

Co-culture methods are favourable for research intensively based on study of cell-cell communication and interaction, such as organ engineering and cancer-host-

cell-interaction mediated cancer cell behavior (Bogdanowicz and Lu, 2014, Arrigoni et al., 2016, Miki et al., 2012, Zoumpopoulou et al., 2009, Du et al., 2015). Studies show that rat primary hepatocytes co-cultured with fibroblasts maintained viability and have demonstrated enhanced functionality (Bhandari et al., 2001); co-culture of endothelial and smooth muscle cells can mimic the structure of a vessel wall to create an improved model of the *in vivo* environment (Truskey, 2010).

Given the nature of reciprocal interaction between two cell populations during odontogenesis, Transwell co-culture of embryonic dental mesenchymal cells with responding epithelium is a promising approach to prevent them from loss of odontogenic inducing capacity during *in vitro* proliferation. With regard to the standard cultured cells that have already lost the induction ability, 2D direct co-culture of fresh and standard cultured embryonic tooth mesenchymal cells can be tested to recover the lost inducing ability, since fresh cells rescued cultured cells from odontogenic failure in mixed cell recombinations (Chapter III) due to a possible diffusible-factor-mediated community effect and they are homotypic cells requiring identical culture medium.

To sum up, it is interesting to apply microenvironment modification utilizing 3D culture and co-culture systems for maintenance and restoration of the odontogenic inductivity of *in vitro* expanded embryonic dental mesenchymal cells.

4.2 Results

4.2.1 Three-dimensional culture

To determine if 3D culture can recover the lost odontogenic capacity of cultured dental mesenchymal cells, 2D proliferated E14.5 dental mesenchymal cells were cultured in three different 3D culture systems: hanging drops, low cell binding surface 6-well plates and U-bottomed 96-well plates with seeding densities respectively 3000 cells/drop (10 µl), $3 \cdot 10^5$ cells/well (1ml) and $6 \cdot 10^4$ cells/well (200 µl), and then reassociated with responsive E14.5 tooth germ epithelium (Figure IV-1).

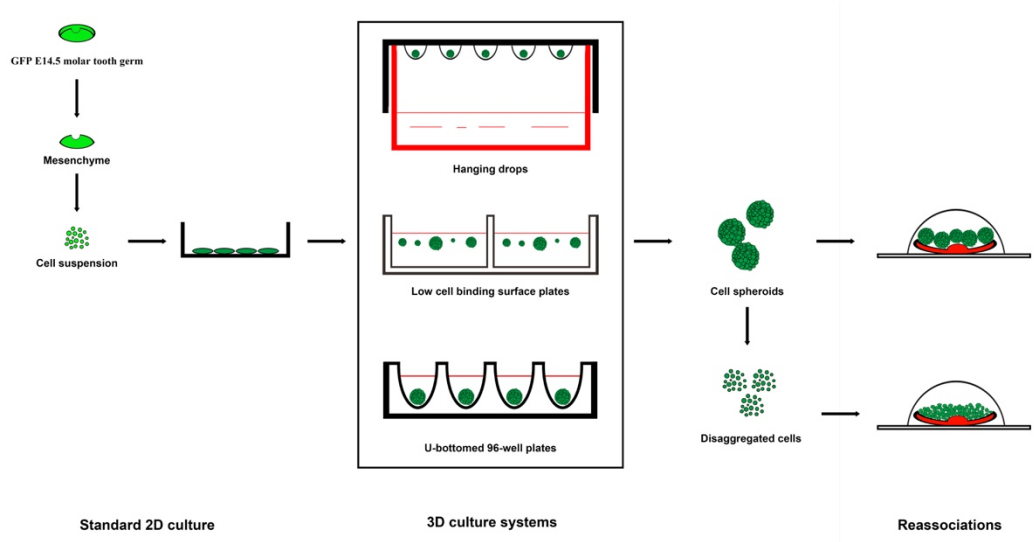

Figure IV-1. Schematic representation of experimental design of 3D culture of proliferating E14.5 tooth germ mesenchymal cells

GFP E14.5 molar tooth germ mesenchymal cells were proliferated through standard 2D culture, followed by 3D culture utilizing three different culture systems, respectively hanging drops, low cell binding surface plates and u-bottomed 96-well plates. Cell spheroids formed in 3D culture systems were either applied directly in reassociations with E14.5 mTmG molar tooth germ epithelial tissues, or disaggregated to cell suspension prior to reassociation assays.

Morphological alterations of 3D cultured mesenchymal cells

Morphological differences between 2D and 3D cultured cells can be observed within 24 hours after passage. Cells cultured in standard 2D conditions adhered to the surfaces of the culture plates and stretched into spindle shapes. Long culture duration rendered cells more flattened and elongated. 3D cultured cells, regardless of which method was applied, remained spherical as when they were plated, and aggregated to form cell clusters. In hanging drop and u-bottomed plate systems, cells tended to congregate into a single spheroid in each drop or well, while cells cultured in low cell binding plate system formed multiple cell clusters with various sizes the majority of which were close to the size of spheroids formed in hanging drops. Cell aggregates generated from u-bottomed plates with greater number of cells were significantly bigger in diameters. Prolonged culture of the aggregated cells resulted in smaller spheres and gradual loss of cell viability over a 7-day period (Figure IV-2).

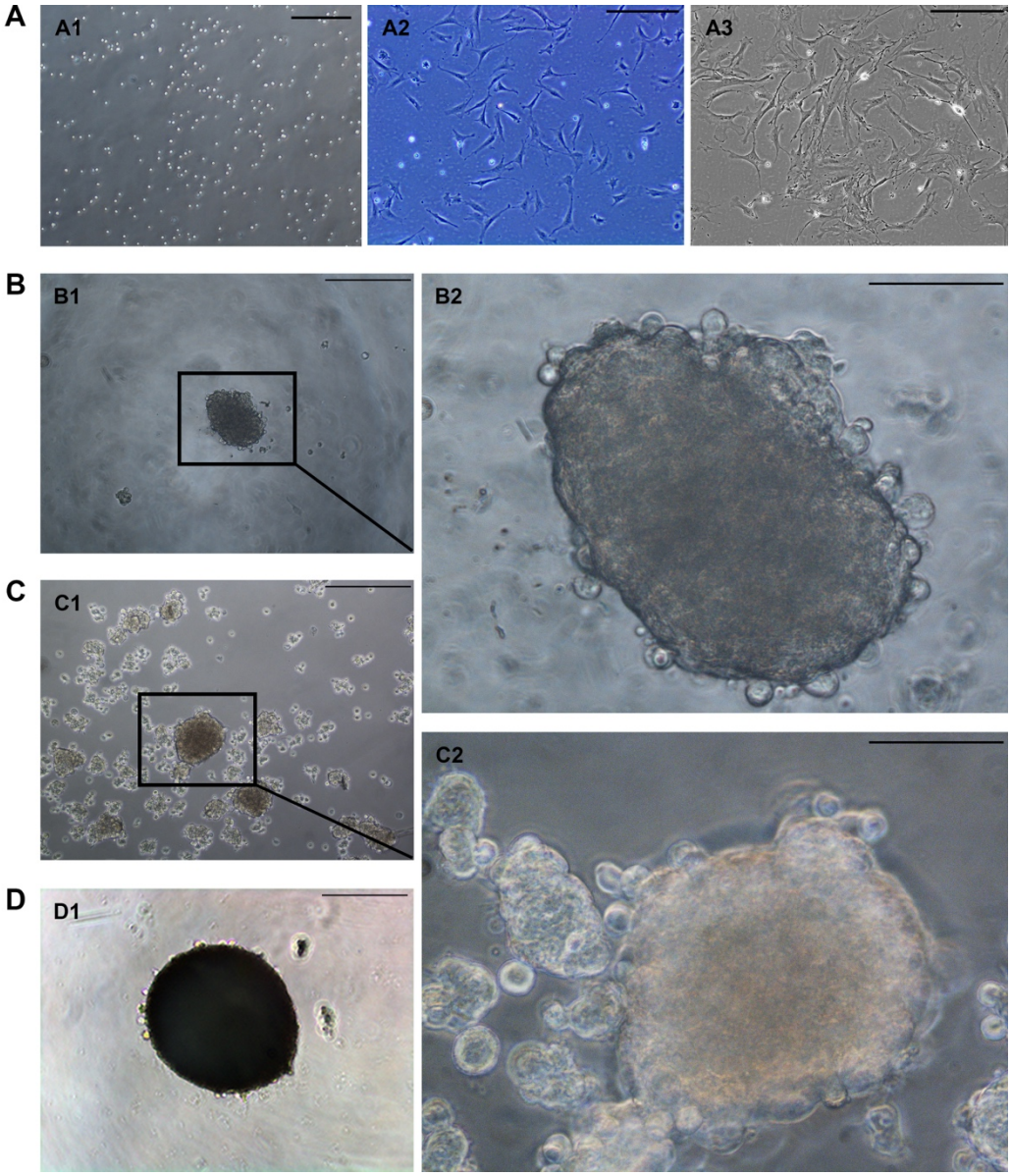

Figure IV-2. Cell aggregates in different 3D culture systems.

Proliferating E14.5 dental mesenchymal cells (P0 cultured for 7 days) were disassociated (A1) and passaged to standard 2D culture plates (A2), hanging drops (B), low cell binding surface 6-well plates (C) and u-bottomed 96-well plates (D). After 24-hour incubation, cell condensates formed in 3D culture systems (B1, C1, D1), while cells in normal 2D culture plates attached to the plate surface appearing the typical spindle shape (A2) and further stretched and expanded when culture duration prolonged to 96 hours (A3). Scale bars: 50 μm (B2, C2); 400 μm (D1;)200 μm (others).

Odontogenic gene expression of 3D cultured mesenchymal cells

Preliminary gene expression comparisons were carried out between mesenchymal cells cultured on low cell binding plates (3D culture) and in standard 2D conditions. Odontogenic genes *Pax9* and *Msx1* are transcription factors expressed in tooth germ mesenchyme that are required for tooth formation (Peters et al., 1998, Chen et al., 1996). These genes appeared to be up-regulated in 3D cultured cells in comparison with their standard 2D cultured controls (Figure IV-3).

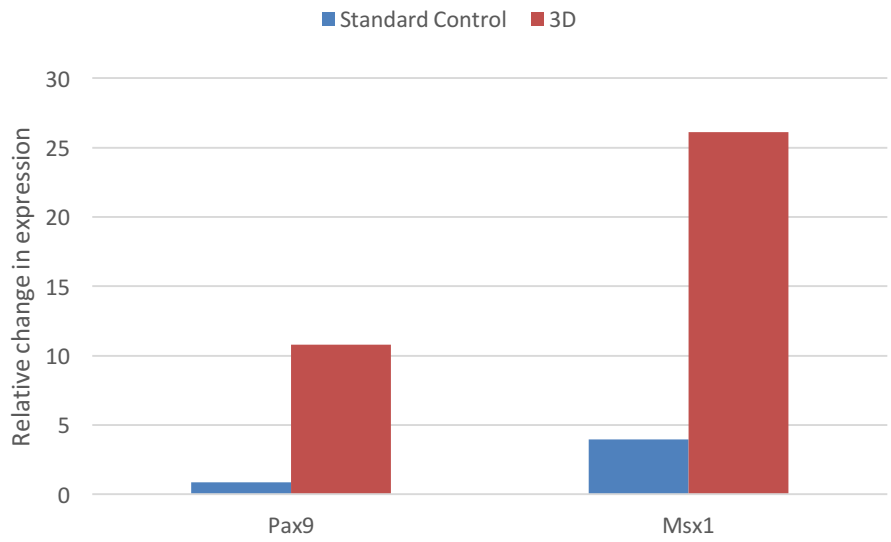

Figure IV-3. Gene expression differences between 3D cultured dental mesenchymal cells and their standard 2D cultured controls.

E14.5 dental mesenchymal cells (P1) were passaged onto low cell binding surface dish (**3D**) and 2D culture plates (standard control) for 36 hours. qPCR of 2 different target genes: *Pax9* and *Msx1* was performed on the two groups of 36h cultured P2 cells. n=1.

3D cultured mesenchymal cells in reassociation experiments

The odontogenic induction capacity of aggregated cultured embryonic dental mesenchymal cells was tested in reassociation experiments with E14.5 tooth germ epithelial tissues. Cell aggregates from none of the three culture systems succeeded in odontogenesis initiation (Figure IV-4,Figure IV-5,Figure IV-6).

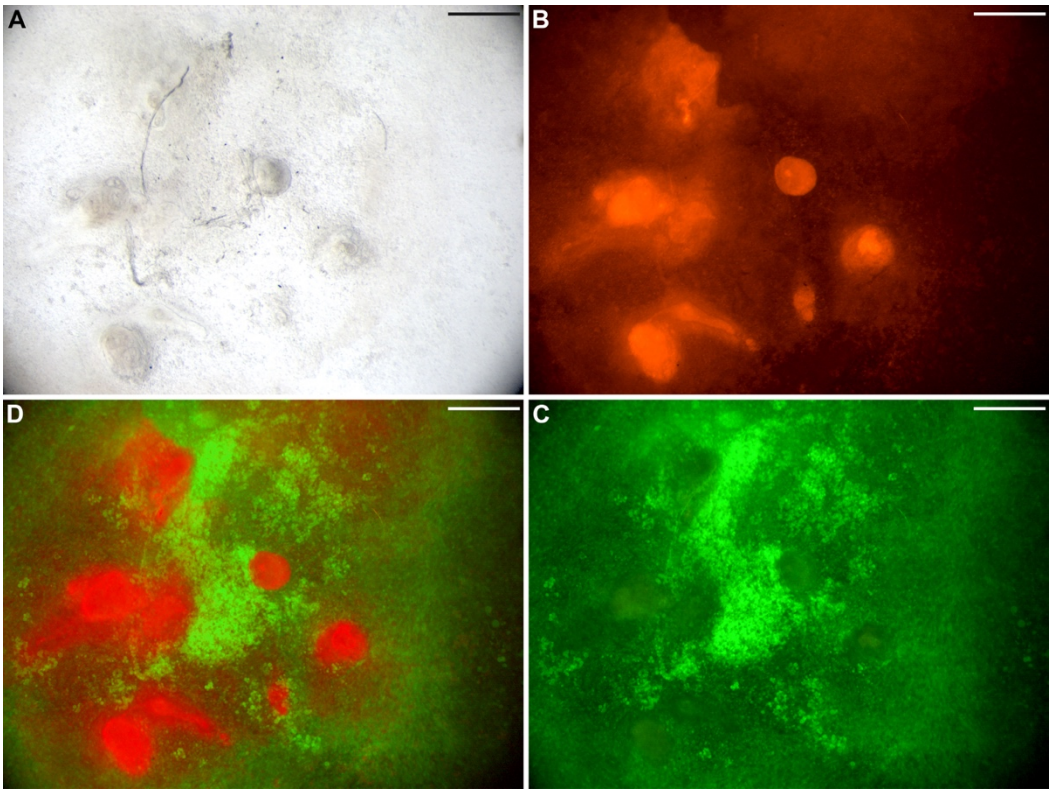

Figure IV-4. Reassociation experiments with *in vitro* expanded embryonic dental mesenchymal cells that had been 3D cultured in hanging drops.

GFP proliferated embryonic tooth germ mesenchymal cells were cultured in hanging drops for 36h prior to reassociations with mTmG E14.5 tooth germ epithelium. No tooth-like structures were observed in the reassociations after 7 days in culture. Scale bars: 500 μm.

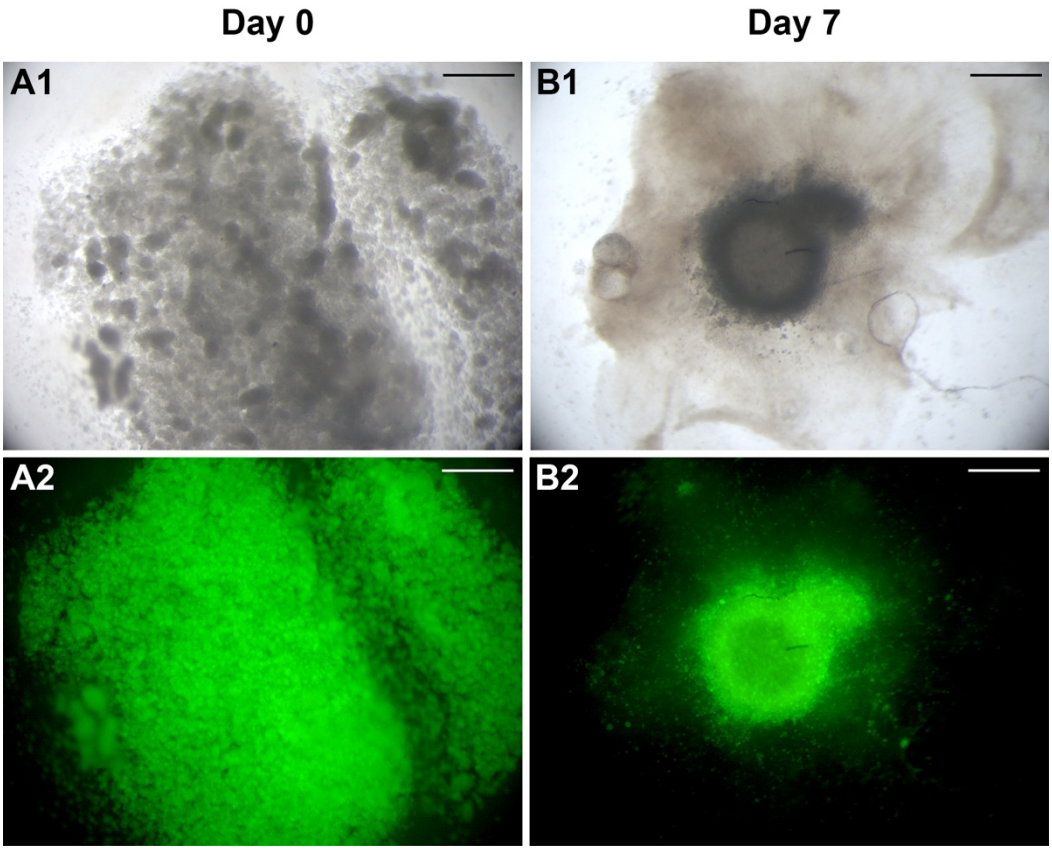

Figure IV-5. Reassociation experiments with *in vitro* expanded embryonic dental mesenchymal cells that had been 3D cultured on low cell binding surface plates. GFP cultured E14.5 tooth germ mesenchymal cells were passaged onto low cell binding surface plates for 36h, and then recombined with CD1 E14.5 tooth germ epithelial tissue. (A) Without dissociation, these 3D cultured mesenchymal cells (green) stayed aggregated as spheres in the reassociations; (B) After 7 days in culture, the GFP cell clusters appeared to be more condensed; however, no evident structures were observed. Scale bars: 500 μm.

Cell spheroids created in u-bottomed plates were mechanically disaggregated prior to reassociation experiments, whereas neither cell condensates nor scattered cells were capable of tooth induction (Figure IV-6). Vigorous agitation

was insufficient for a thorough disaggregation of cell spheroids, cells still tended to remain clustered.

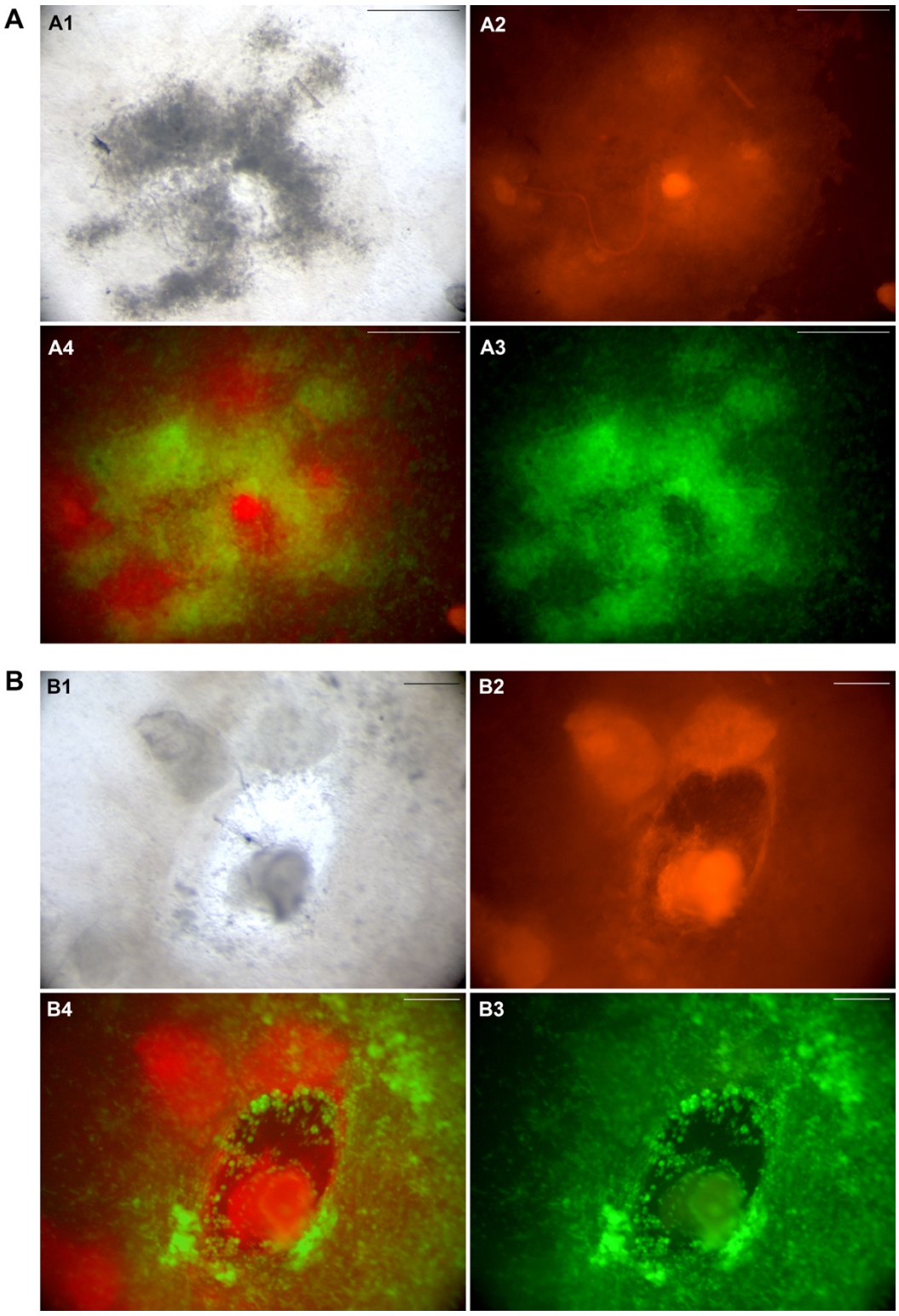

Figure IV-6. Reassociation experiments with *in vitro* expanded embryonic dental mesenchymal cells that had been 3D cultured on U-bottomed 96-well plates.

GFP proliferated embryonic tooth germ mesenchymal cells were cultured in u-bottomed wells for 5 days, cell spheroids (A) and disaggregated cells (B) were recombined with mTmG E14.5 tooth germ epithelium. No tooth-like structures were observed in the reassociations after 7 days in culture. Scale bars: 500 µm.

Additionally, since 3D-culture-associated expression of dedifferentiation markers could be induced by simulation of autophagy (Pennock et al., 2015), 2D cultured cells were treated with rapamycin (100nM), an exogenous autophagy stimulator for 24 hours prior to reassociations, which failed to induce tooth formation (Figure IV-7).

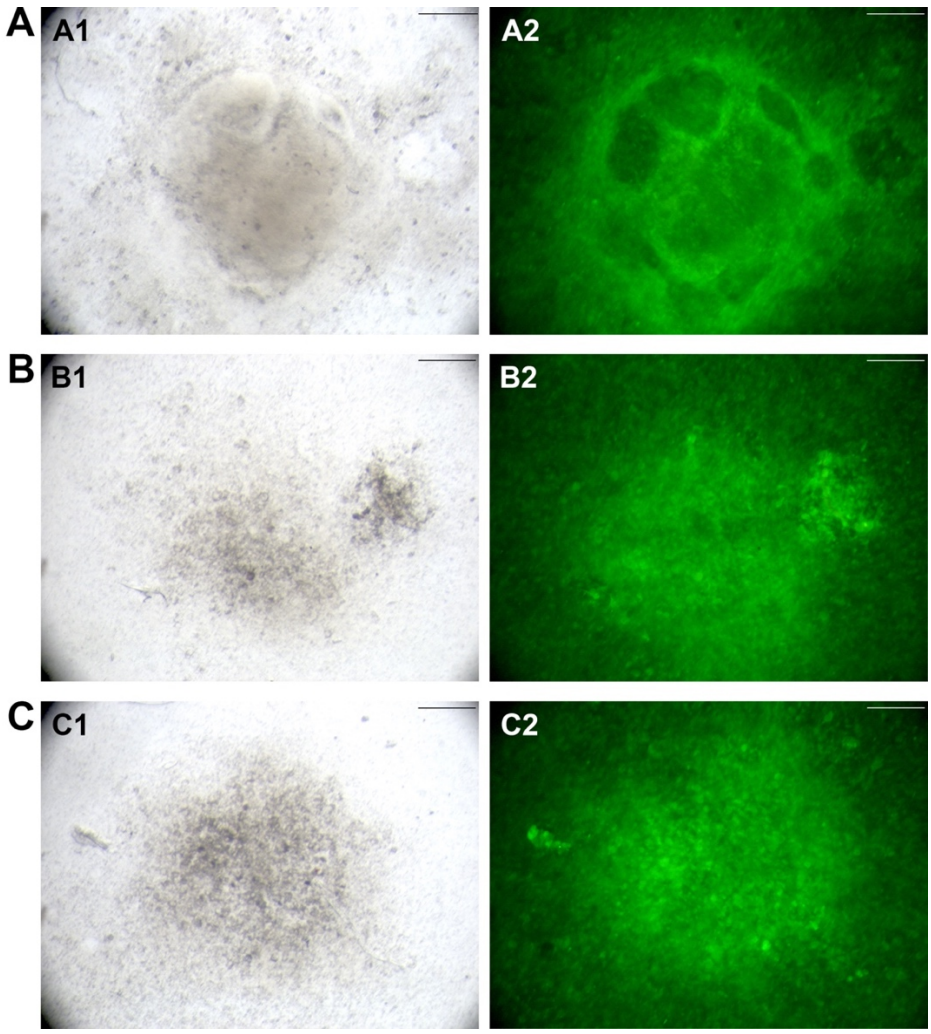

Figure IV-7. Reassociation experiments with *in vitro* expanded embryonic dental mesenchymal cells that had been treated with Rapamycin

GFP cultured E14.5 tooth germ mesenchymal cells were treated with 100 nM rapamycin (dissolved in DMSO) for 24 hours prior to reassociations with CD1 E14.5 epithelium whereas no teeth formed (A). Cells cultured with media with same concentrations of DMSO as the Rapamycin treated cells served as the solvent controls (B). Controls with cells cultured in normal media. Scale bars: 250 µm.

4.2.2 Co-culture

4.2.2.1 Epithelial-mesenchymal cell Transwell co-culture

To determine if a co-culture system can retain the odontogenic capacity of cultured dental mesenchymal cells, noncultured E14.5 tooth germ mesenchymal cells were co-cultured with E14.5 tooth germ epithelial tissues in a Transwell system for 7 days. E14.5 tooth germ mesenchymal cells cultured for 7 days in standard 2D culture conditions served as negative controls (Figure IV-8).

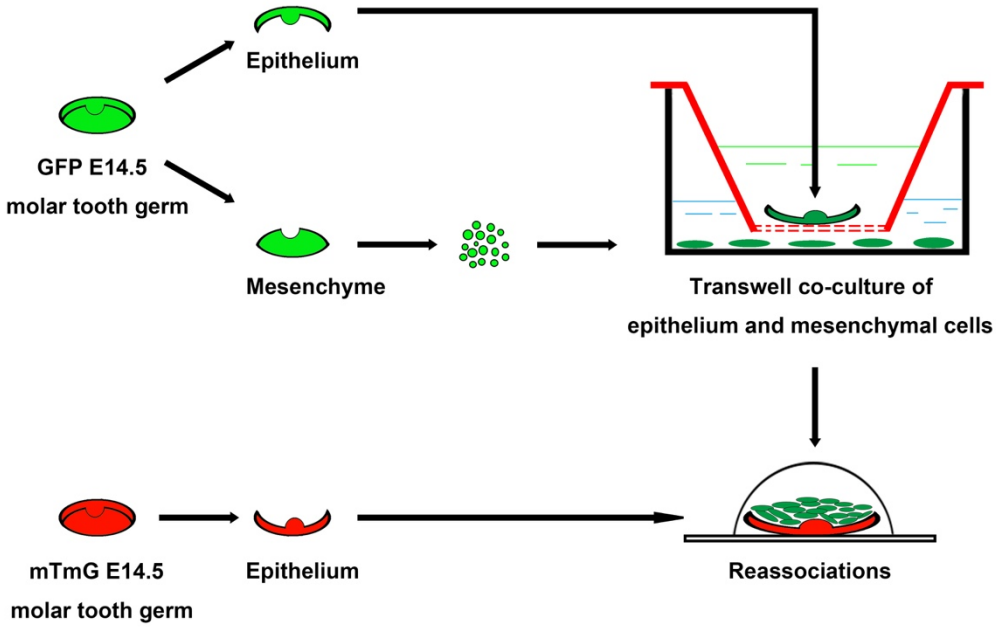

Figure IV-8. Schematic representation of experimental design of Transwell co-culture of E14.5 tooth germ epithelium and mesenchymal cells

GFP E14.5 molar tooth germs were separated into epithelial tissues and mesenchymal cells and co-cultured in a Transwell culture system where the mesenchymal cells were grown on the culture plate wells and epithelial tissues were cultured as explants on the membranes of the cell culture inserts. Co-cultured mesenchymal cells were collected after 7 days and reassociated with E14.5 mTmG tooth germ epithelium.

Morphological appearance of co-cultured mesenchymal cells

No evident gross morphological differences were observed in co-cultured mesenchymal cells compared with their controls (Figure IV-9)

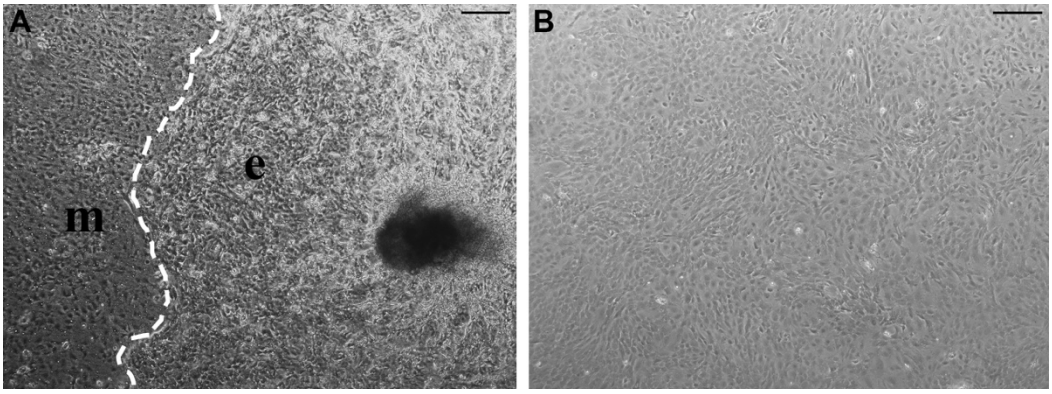

Figure IV-9. Morphological appearance of mesenchymal cells co-cultured with epithelium explants.

(*A*) m: mesenchymal cells; e: epithelium explants; dotted line: border of epithelium explants. Uncultured E14.5 mesenchymal cells co-cultured with E14.5 epithelium for 7 days did not show evident difference with their control; (*B*) Control group: confluent 7 days cultured mesenchymal cells. Scale bars: 200 μm.

Odontogenic gene expression of co-cultured mesenchymal cells

Preliminarily, embryonic dental mesenchymal cells Transwell co-cultured with responding epithelium had higher levels of *Pax9* and *Msx1* expression than those mono-cultured cells in the absence of epithelium (Figure IV-10), suggesting that the presence of epithelial tissue does influence odontogenic gene expression in cultured dental mesenchymal cells.

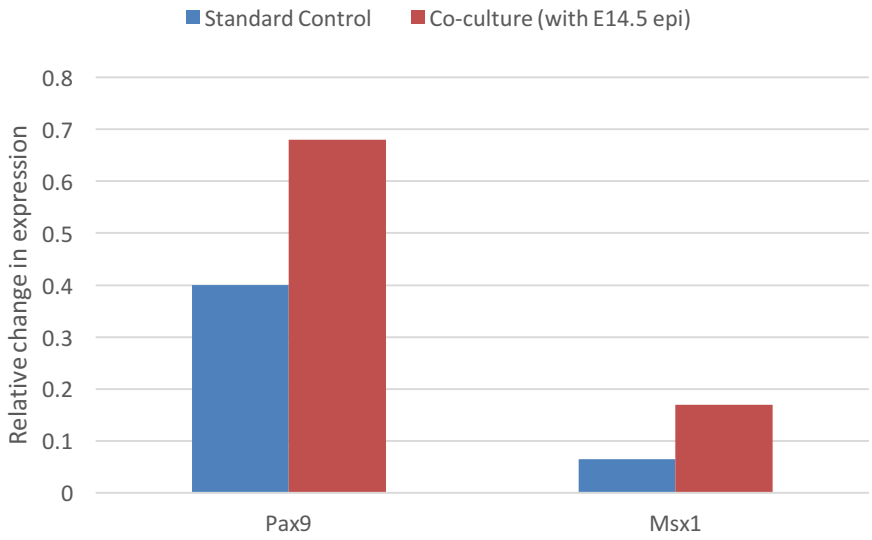

Figure IV-10. Gene expression differences between dental mesenchymal cells co-cultured with E14.5 epithelium and their standard 2D cultured controls.

E14.5 tooth germ mesenchymal cells were Transwell co-culutred with E14.5 tooth germ epithelial tissues for 7 days. The 2D controls are E14.5 tooth germ mesenchymal cells cultured in standard 2D conditions for 7 days. n=1.

Reassociations with mesenchymal cells Transwell co-cultured with epithelium

Reassociation experiments were applied to determine if the presence of epithelium in the culture of mesenchymal cells was sufficient to maintain their tooth forming capacity. Teeth were not observed in the reassociation experiments utilizing mesenchymal cells that Transwell co-cultured with epithelium (Figure IV-11).

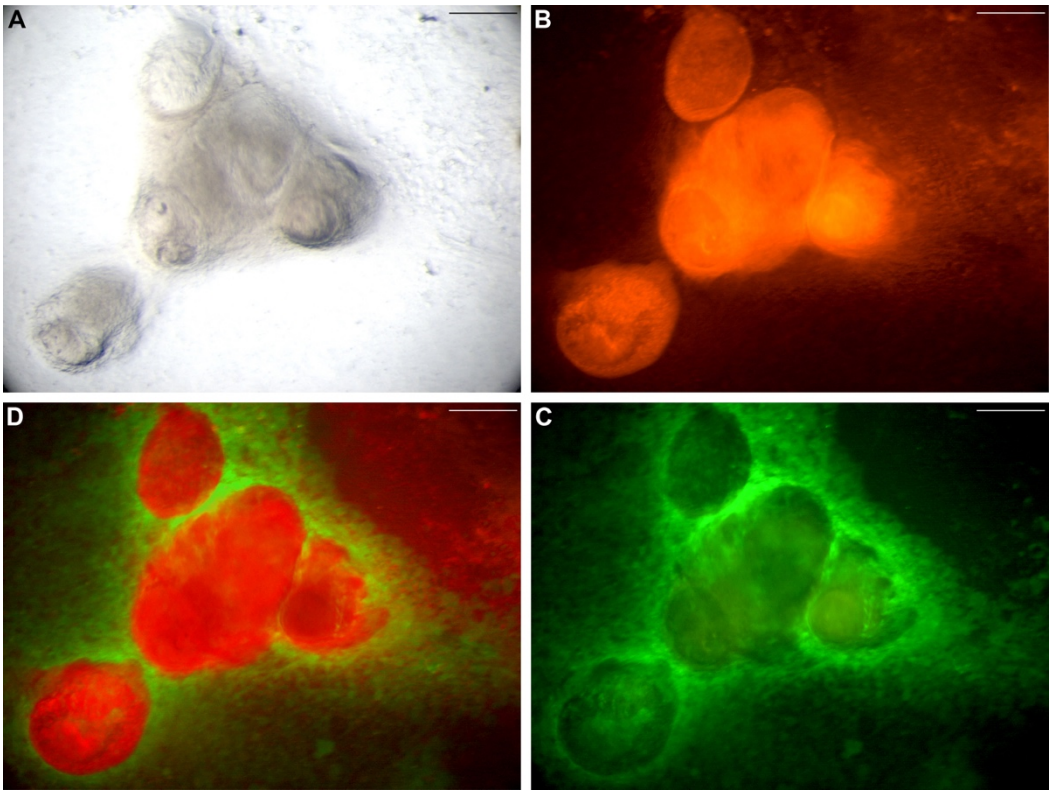

Figure IV-11. Reassociation experiments with *in vitro* expanded embryonic dental mesenchymal cells that had been Transwell co-cultured with epithelium. GFP proliferating embryonic tooth germ mesenchymal cells were co-cultured with E14.5 tooth germ epithelium for 7 days prior to reassociations with mTmG E14.5 tooth germ epithelium. No tooth-like structures were observed in the reassociations after 7 days in culture. Scale bars: 250 μm.

4.2.2.2 Fresh-cultured mesenchymal cell 2D direct co-culture

To examine if cell-mixing induced odontogenic ability rescue/community effect of fresh cells on cultured cells in mixed cell recombinations can occur under 2D conditions, GFP cultured tooth germ mesenchymal cells were mixed with noncultured CD1 cells at the ratio of 2:1 and co-cultured in normal 2D conditions for 12h. GFP and CD1 cells were then separated through fluorescence-activated cell sorting (FACS) and used in reassociations respectively. Reassociations with 12h mono-cultured GFP passage cells and CD1 fresh cells served as the experimental controls (Figure IV-12).

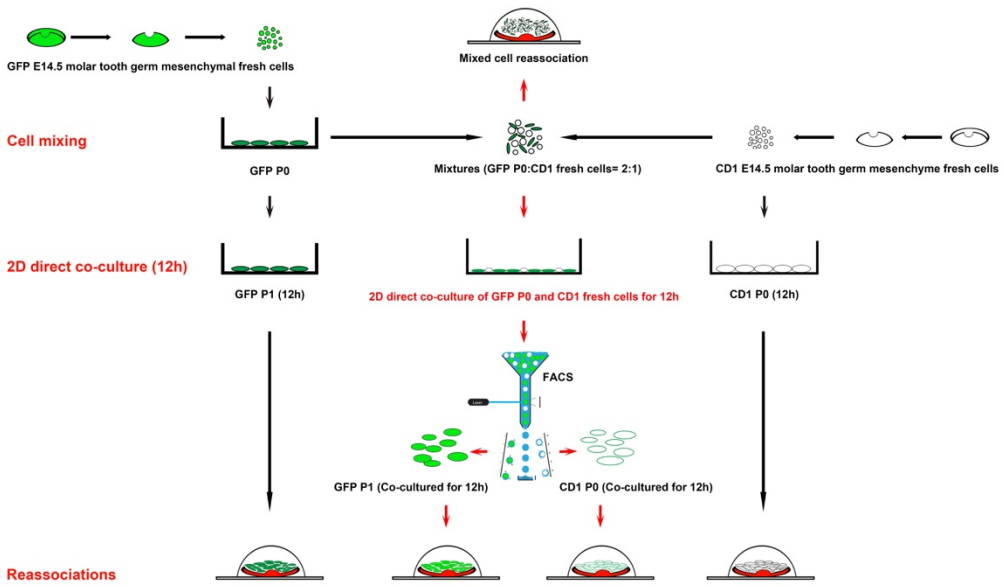

Figure IV-12. Schematic representation of experimental design of 2D direct co-culture of fresh and cultured E14.5 tooth germ mesenchymal cells

GFP cultured (P0) and CD1 fresh E14.5 tooth germ mesenchymal cells were mixed at the ratio of 2:1. Partial of the mixtures were tested in the reassociation assays. The rest of the mixtures were seeded onto standard 2D culture plates/flasks. After 12h incubation, the co-cultured cell mixtures were collected and separated through FACS. 12-hour co-cultured and mono-cultured GFP P1 cells and CD1 P0 cells were reassociated with mTmG E14.5 tooth germ epithelial tissues separately.

Part of the mixtures with cultured/fresh cell ratio of 2:1 were reassociated with mTmG E14.5 tooth germ epithelium whereas multiple cap stage tooth primordia formed with a considerable contribution from cultured cells, which confirmed the rescue effect of fresh cells on the lost odontogenic capacity of cultured cells (Figure IV-13).

2D direct co-culture of GFP proliferated cells and CD1 fresh cells did not rescue the cultured cells from failure of tooth induction--cysts formed in the reassociations with co-culture treated GFP expanded cells (Figure IV-14 B). Fresh CD1 cells cultured in 2D conditions for 12h, with or without presence of GFP cultured cells, successfully induced tooth development (Figure IV-14 A, Figure IV-15 A). These suggest that the community effect in mixed-cell reassociations did not occur under 2D conditions.

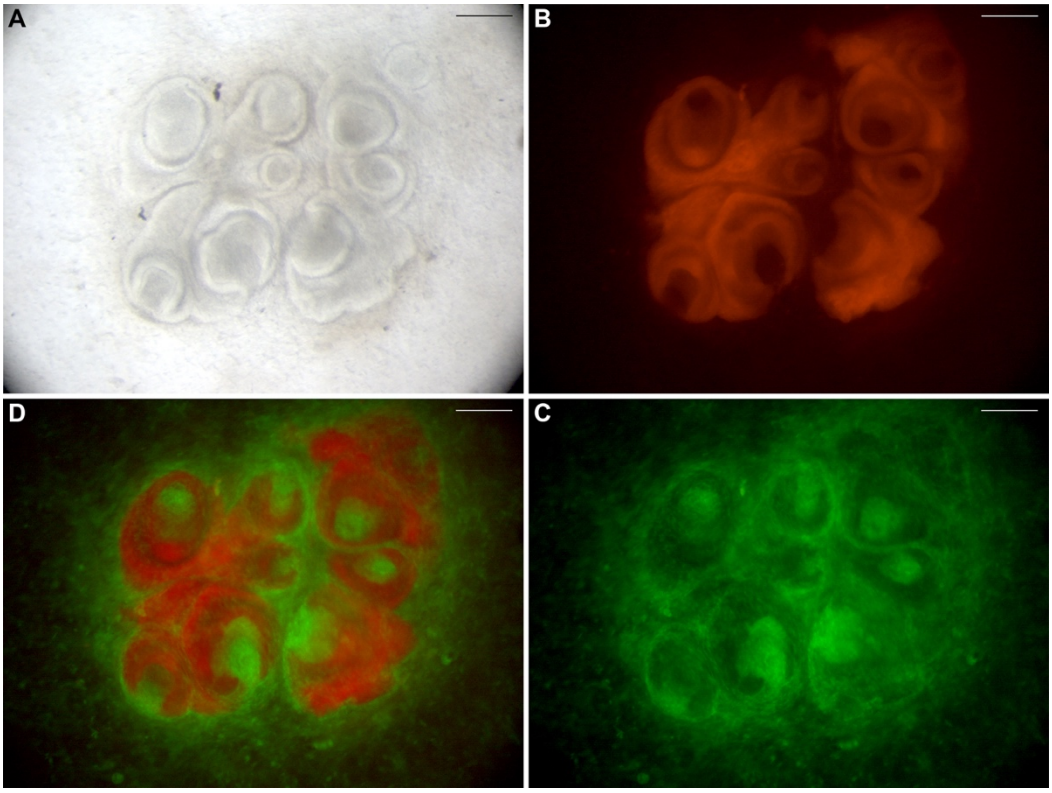

Figure IV-13. Reassociation experiments with embryonic dental mesenchymal cell mixtures with the fresh : cultured cell ratio of 1:2.

GFP cultured and CD1 fresh E14.5 tooth germ mesenchymal cells were mixed at the ratio of 2:1 and reassociated with mTmG E14.5 tooth germ epithelium. Well-structured tooth primordia formed with considerable contributions from cultured (green) cells. Scale bars: 250 µm.

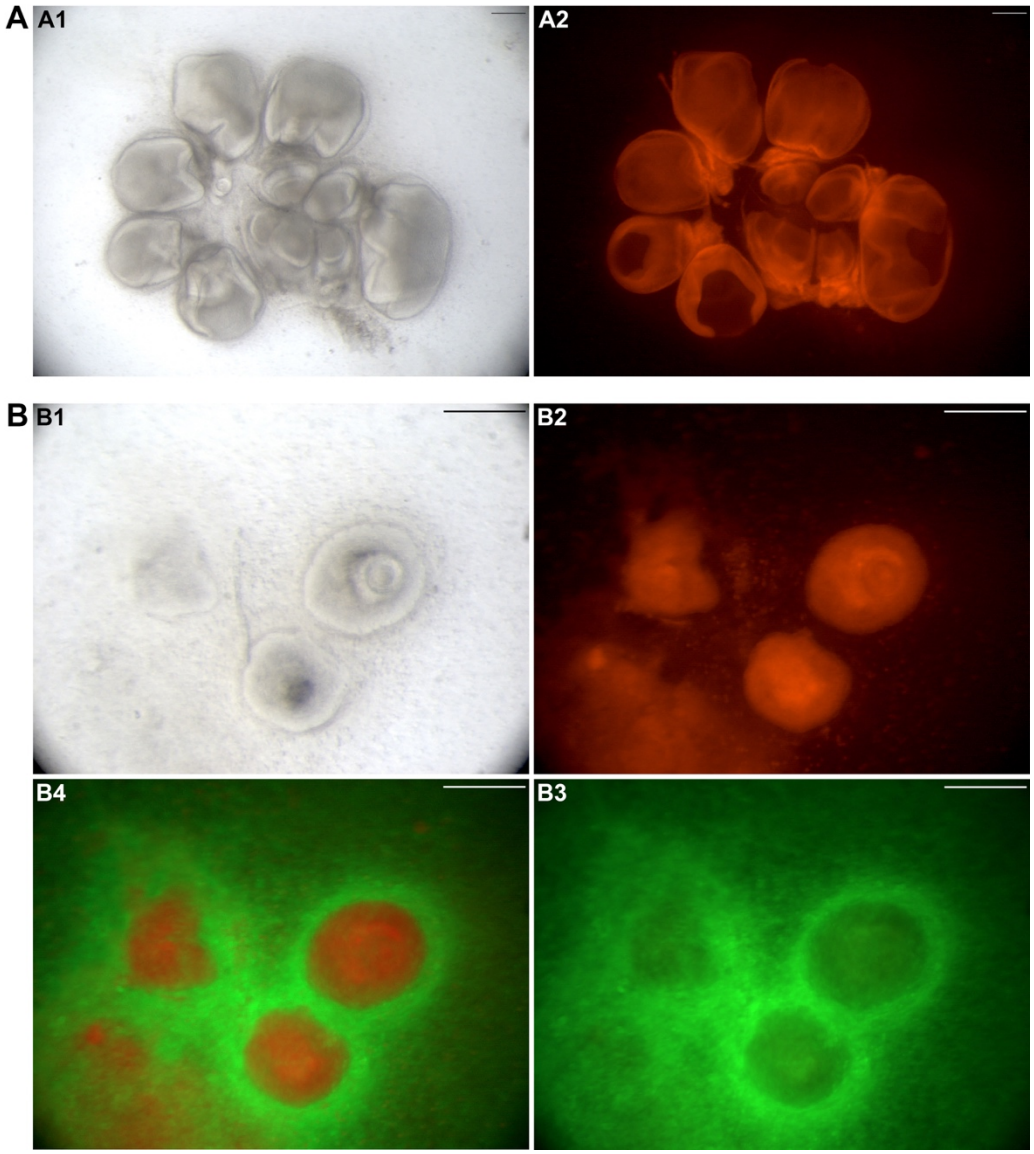

Figure IV-14. Reassociation experiments with FACS separated inductive and non-inductive embryonic dental mesenchymal cells that had been 2D direct co-cultured at the fresh: cultured cell ratio of 1:2 for 12h.

GFP cultured and CD1 fresh E14.5 tooth germ mesenchymal cells were mixed at the ratio of 2:1 and co-cultured under 2D conditions for 12 hours. GFP and CD1 cells then were separated through FACS and recombined with mTmG E14.5 tooth germ epithelium respectively. Sorted CD1 cells successfully induced tooth development (A) while sorted GFP cells formed cysts (B). Scale bars: 250 μm.

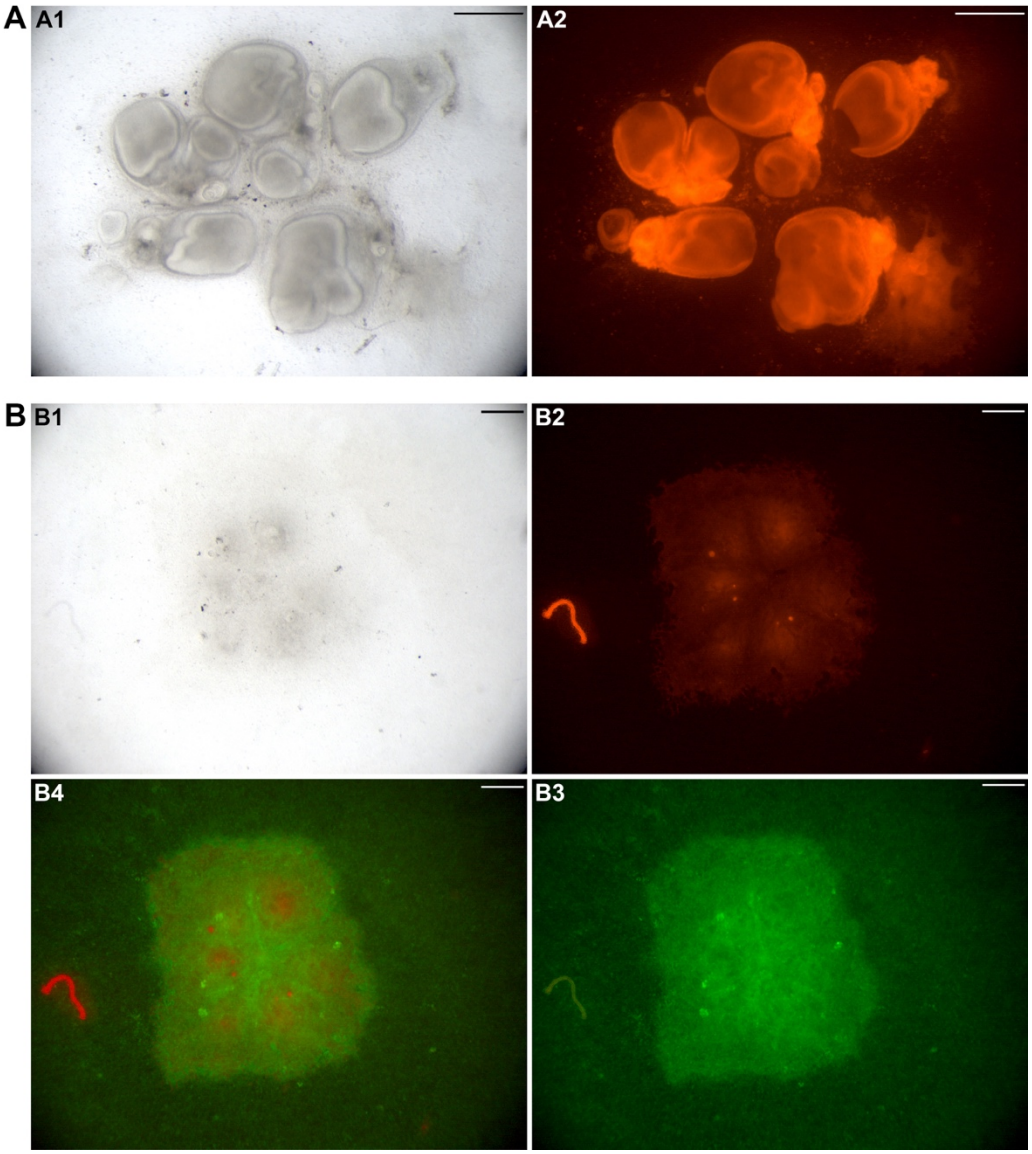

Figure IV-15. Reassociation experiments with 12h mono-cultured inductive and non-inductive embryonic dental mesenchymal cells.

CD1 fresh embryonic tooth germ mesenchymal cells were cultured for 12 hours prior to reassociations with mTmG E14.5 tooth germ epithelium and succeeded in initiation of odontogenesis (A). Whereas proliferated GFP cells which had been passaged and cultured for 12 hours failed (B). Scale bars: 500 µm.

4.2.3 Summary

3D culture and epithelium-mesenchyme Transwell co-culture of proliferating embryonic E14.5 tooth germ mesenchymal cells increased their expression of odontogenic genes *Pax9* and *Msx1* compared with standard monolayer mono-culture controls, however, her failed to restore the lost capacity of *de novo* odontogenesis in reassociation experiments.

The community effect of fresh tooth germ mesenchymal cells rescuing cultured cells from failure of tooth induction in mixed-cell recombinations did not occur under 2D direct co-culture conditions. Fresh inductive cells that had undergone 12 hours of standard 2D mono-culture or co-culture with proliferated cells maintained the odontogenic induction ability.

4.3 Discussion

4.3.1 Three-dimensional culture

3D culture showed the potential to drive specialized cells toward pluripotency (Pennock et al., 2015, Higgins et al., 2013, Volkmer et al., 2008, Zhou et al., 2017). Aggregated, rather than monolayer, muscle precursor cells maintained the specific tissue-inducing ability, and differentiated into muscle cells when cultured between two pieces of vegetal regions of blastula in the first study on community effect (Gurdon, 1988). These results suggest an important role of 3D cell aggregation on restoration or maintenance of stem cell stemness.

From the results presented here, regardless of the culture system applied, 3D culture enabled morphological alteration of the *in vitro* expanded embryonic tooth germ mesenchymal cells from spindle to spherical, which is similar to freshly isolated cells. They aggregated to form cell spheroids within 24 hours. Difficulties in mechanical disaggregation of cell spheroids for preparation of single cell suspension indicated a tissue-like tight cell-cell connection.

Synergic expression of transcription factors encoded by Paired domain gene *Pax9* and homeobox gene *Msx1* is crucial for the expression of *Bmp4* in dental mesenchyme which is required in the progression of the molar rudiment from the bud stage to the cap stage (Ogawa et al., 2006). In both *Pax9*-deficient and *Msx1*-deficient mice, tooth development is arrested at the bud stage (Peters et al., 1998, Chen et al., 1996). The preliminary qPCR data showed that 3D cultured embryonic tooth germ mesenchymal cells had higher expression of odontogenic genes *Pax9* and *Msx1* compared with standard 2D cultured mesenchymal cells, suggesting that physical alterations can affect dental inductivity of tooth cells and 3D culture might, to some extent, restore the odontogenic capacity of cultured mesenchymal

cells. *Pax9* and *Msx1* expression of 3D cultured cells were assessed merely with the cells cultured on low cell binding plates. Given the different spheroid sizes and culture conditions, it is of interest to compare expression level of odontogenic genes of spheroids generated in different 3D culture systems.

Oxygen tension in culture conditions shows correlations with maintenance of stem cell stemness (Azevedo et al., 2015). Comparing with cells cultured in normal 20% O_2, human tendon stem cells cultured in a hypoxic condition with 5% O_2 had higher proliferation and expression of stem cell marker genes *Nanog* and *Oct-4*, and generated more tendon-like structures in *ex vivo* experiments (Zhang and Wang, 2013). One possible mechanism is that hypoxia mimics the *in vivo* conditions where oxygenation is restricted, especially in embryos. Unlike the homogenous and sufficient supply in 2D culture, oxygen delivery in cell spheroids formed in 3D culture is in a gradient fashion (Figure IV-16). A drop to 0% of the oxygen tension in the centre of the cell spheroids was observed after 5 days in a scaffold based 3D culture (Volkmer et al., 2008), which in combination with limitation of nutrition, accumulation of CO_2 and poor removal of cell waste results in necrosis in the core zone (Edmondson et al., 2014). Similar to 2D culture conditions, with sufficient exposure to oxygen and supplement and effective clearance of toxin, the periphery zone of cell spheroids has normal proliferation. In the layer between necrotic core and proliferation zone where oxygen tension is approximately 4-5% (Volkmer et al., 2008), consistent with the value that is proven to be favourable to stemness maintenance (Zhang and Wang, 2013), cells show maximum dedifferentiation and quiescence (Lv et al., 2016).

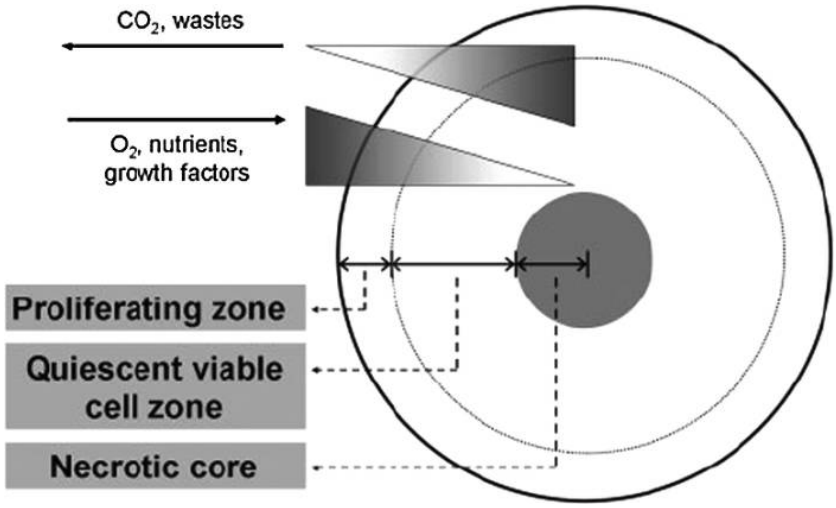

Figure IV-16. The schematic diagram of typical zones of cell proliferation in a 3D spheroid.

Reprinted from (Lin and Chang, 2008)

In order to create maximum contact between the responding dental epithelium and the most odontogenic cell population in the heterogeneous cell aggregates, cells reside in the “quiescent zone” according to the gradient hypoxia model of 3D generated cell spheroids, cell spheres were replaced by disassociated cells, which also resulted in failure of tooth induction. One possibility is that the disassociated cells were used without screening out the necrotic cell population, which can impede the contact of inductive cells with epithelium. However, the dead cell percentage of 3D cultured human MSCs within 5 days were shown to be below 5% (Pennock et al., 2015). Based on the observations of mixed cell recombinations in Chapter III, fresh embryonic tooth cells mixed with 25% non-contributing cultured postnatal cells can still induce tooth formation, indicating incompetency of 3D cultured cells in tooth induction, including the cell population in quiescent layer. Cell death in spheres is related to their sizes. A necrotic core can be observed in a cell sphere with a size of above 500 μm in diameter due to the limitation of diffusion of molecules, especially oxygen, and accumulation of metabolic waste

(Lin and Chang, 2008). U-bottomed plate-mediated 3D cultured human mesenchymal stromal cell spheroids with 60,000 cells per spheroid experienced a decrease in diameters from 1000 μm to 600 μm during the 3D culture day 1- to day 7 (Pennock et al., 2015). **Figure IV-2** shows that, typically, in this research, the diameters of mouse embryonic dental mesenchymal cell spheroids generated from u-bottomed plates and hanging drops were respectively 600-650 μm and 100-150 μm, low cell binding surface plate-mediated cell spheroids had more variations in size up to 100-150 μm. Therefore, cell death might affect more or merely in u-bottomed plate-mediated spheroids due to the larger sizes. In addition, 3D-culture-associated expression of dedifferentiation markers could be induced by simulation of autophagy (Pennock et al., 2015). However, Rapamycin treated 2D cultured cells failed in tooth induction, indicating stimulation of autophagy in cultured cells may not be sufficient to rescue their odontogenic induction ability.

3D cultured dermal papilla passage cells induced *de novo* hair follicle regeneration with 22% of transcripts differentially expressed between intact papillae and passage cells restored (Higgins et al., 2013). On one hand, this suggests that inductive cells are not necessarily genetically identical to fresh cells, which supports the assumption discussed in Chapter III that the inductivity of a cell is measured in a “spectrum” rather than “all-or-nothing” fashion. On the other hand, it indicates that fractional restoration of inductive transcript expression cannot initiate organogenesis when below a certain threshold, which probably explains why 3D cultured embryonic tooth germ passage cells failed in tooth induction although with some up-regulated odontogenic genes compared with 2D cultured controls. Although sharing similar development patterns of sequential and reciprocal interactions between epithelium and mesenchyme, hairs naturally grow in a regenerative manner in cycles of growth, rest, shedding, and regrowth; whereas teeth are not only more complex structures, but also restricted in

replacement throughout lifetime, none in mice, none to once in humans. 3D culture may partially restore the tooth inducing capacity which may favour dental tissue regeneration, yet inadequate to induce *de novo* odontogenesis. Based on the "inductivity threshold" assumption mentioned in Chapter III (**Table III-3**), to see if there is partial restoration of odontogenic inductivity in proliferated cells after 3D culture, mix-cell recombination experiments can be performed with cell mixtures of 3D cultured cells and fresh cells, examining if 3D cultured cells require fewer fresh cells than standard cultured cells to induce tooth formation. For instance, if the inductivity of a cultured cell increased from 0.5 to 0.6 after being cultured in 3D conditions, then the average inductivity of the mixtures of 90% 3D cultured cells and 10% fresh cells will correspondingly increase from 0.55 to o.64 which will pass the threshold of tooth induction.

Cell density and culture duration in different 3D culture systems were determined according to published conditions (Higgins et al., 2013, Pennock et al., 2015). Given the different research subjects, ideally, the culture conditions should be systematically optimized and tested in recombinations. U-bottomed 96 well plates may be the optimal approach to serve this purpose, since they can generate cell spheroids of uniform sizes in wide range, and they can conveniently be applied in combination with other methods such as different factor supplement in media and co-culture with epithelium using 96-well cell culture inserts. Hanging drops are limited in volume of media per drop and fragile to external force; low cell binding surface plates form cell spheroids with irregular size and require centrifuge for changing media.

It has not been examined in this research whether the outer layers of cell spheroids proliferated. However, RNA yield difference of 3D and 2D cultured cells with the same initial cell numbers can be circumstantial evidence for higher

efficiency in cell expansion of 2D culture than 3D culture. Identical initial numbers of cultured embryonic tooth mesenchymal cells were passaged onto standard and low cell binding surface 6-well plates with the same seeding density, 2D cultured passage cells had approximately twice the amount of RNA yield as the 3D cultured cells when collected for RNA extraction after 36 hours. 2D cultured cells showed increased expression of genes that promote cell proliferation and repressed those limiting cell growth comparing with their corresponding tissue origins (Birgersdotter et al., 2005). 3D culture allows proliferation of cells at a rate close to *in vivo* levels, which is not efficient to obtain large number of cells within a short period. Moreover, as illustrated above, cell aggregates cannot survive long term static culture due to the expanding necrotic cores. Therefore, the practical application of future optimized 3D culture system for obtaining tooth inducing cells will be short term 3D culture for restoration of odontogenic capacity following standard 2D culture for rapid cell expansion.

4.3.2. Co-Culture

Adult pluripotent cells can be induced through additional supplement of small molecule compounds or recombinant proteins without introduction of direct genetic modifications (Zhou et al., 2009, Hou et al., 2013). Odontogenic differentiation of stem cells can be induced by replacement of normal culture media with tooth-cell-conditioned media (Liu et al., 2013, Ning et al., 2010, Li et al., 2013a). These findings suggest that chemical alterations of culture microenvironment play a crucial role in cell fate determination.

Transwell co-culture of tooth germ epithelium and mesenchymal cells can be considered as a chemical approach for microenvironmental alteration. Increased expression of odontogenic genes *Pax9* and *Msx1* in embryonic dental mesenchymal cells Transwell co-cultured with responding epithelium indicates that manipulation of signal interactions might be productive in maintenance of odontogenic induction capacity in cultured mesenchymal cells. However, failure of tooth induction in reassociation assays implied incompetency of the Transwell co-cultured mesenchymal cells in *de novo* odontogenesis.

The concentration of paracrine factors in the microenvironment of recipient cells rapidly decayed with the increasing distance from the secreting cells in both contact and non-contact co-culture models (Lai et al., 2013) (Figure IV-17).

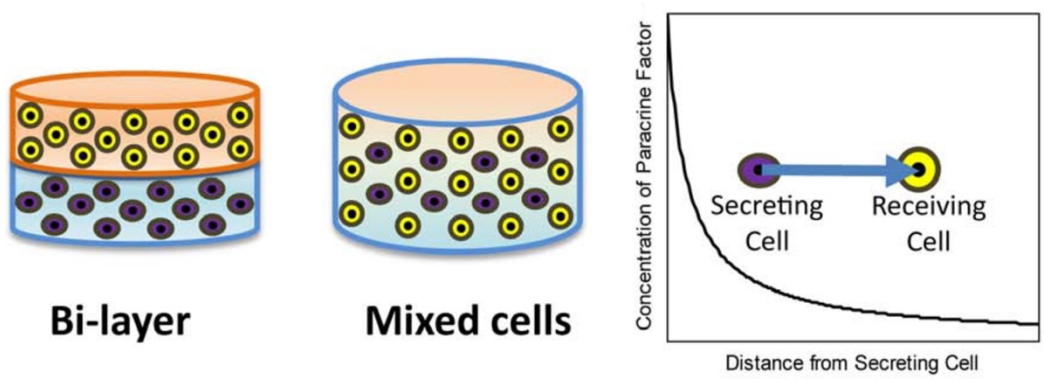

Figure IV-17. Schematic diagram of rapidly decayed paracrine factor concentration with distance from a secreting cell to receiving cell.

Reprinted from (Lai et al., 2013)

In the Transwell co-culture system, the cross-talk between embryonic tooth germ epithelium and mesenchymal cells is assumed to be mediated by semipermeable membrane permitted exchange of diffusible factors. The distance from a cell insert membrane to the bottom surface of a well of a culture plate is 0.9mm, which is high comparing with the normal size of a cell (10-30 μm). The 0.4 μm pore size of the membrane can allow free penetration of small molecules, but may limit the diffusion of large molecules. Effective growth area of the membrane and the plate well are 4.2 cm^2 and 9.6 cm^2 respectively, which may cause more than a 2-fold reduction in epithelium secreted factors than mesenchymal factors in the environment. In addition, the dilution effect of medium on diffusible factors may also contribute to inadequacy of epithelial responding signals which may be the reason of ineffectiveness of co-cultured mesenchymal cells in whole tooth induction.

Non-dental epithelium can be induced to become odontogenic responding epithelium when combined with inductive mesenchymal cells (Angelova Volponi et al., 2013), suggesting that the odontogenic response of epithelium is not independent of the inducing signals from inductive mesenchymal cells. In the Transwell co-culture systems, epithelium and mesenchymal cells were cultured separately in 2D conditions, which can affect their gene expression pattern and thus may alter the cell secretion of both cell populations. Further study is required to determine if the signalling environment in Transwell co-culture system mimics the *in vivo* odontogenic epithelial-mesenchymal interactions.

Mechanisms of the community effect which enabled cultured embryonic dental mesenchymal cells rescued from failure of odontogenesis by presence of fresh cells may include paracrine diffusible factors mediating heterotypic cell-cell interactions. Theoretically, the 2D direct co-culture of fresh and *in vitro* expanded cell populations can create a signalling environment for occurrence of the community effect.

Cell mixtures with cultured/fresh cell ratio of up to 3:1 can induce tooth formation. Here a lower cultured/fresh cell ratio of 2:1 was applied to secure sufficient odontogenic inductivity from the fresh cells to the whole cell mixtures. Successful tooth formation with a considerable contribution from cultured cell population of the mixtures in reassociation assays confirmed the occurrence of the community effect. Cultured cells alone, after being 2D direct co-cultured with inductive cells for 12 hours, failed to induce tooth development in reassociation assays. Whereas the inductive cells co-cultured with non-inductive cells for 12h were still able to initiate *de novo* odontogenesis. On one hand, these results suggest that the loss of odontogenic induction capacity of embryonic dental mesenchymal cells is not

an immediate occurrence when 2D proliferation is initiated, but a culture duration related event. On the other hand, the attempts to create community effect in 2D conditions failed.

Prolonged duration of 2D direct co-culture should not be necessary, since the community effect is a transient process where cell fates are determined rapidly after establishment of cell community (Saka et al., 2011). Additionally, prolonged 2D culture of fresh cells will render them incompetent to induce odontogenesis. To reduce the dilution effect of media on concentration of diffusible factors in the cell community, cell mixtures were resuspended in 100µl media in an Eppendorf tube where the loose cell pellet could be submerged by restricted, 100µl, rather than millilitres of media as in plate or flask based cell culture. Loose cell pellet was incubated for 3 hours. GFP cultured cells FACS sorted from these mixtures did not succeed in tooth induction. It was observed during FACS that the GFP cultured cells were evidently greater in size than the 12h co-cultured inductive cells, indicating that 2D culture-stimulated alterations were not eliminated through co-culture which may impede the restoration of odontogenic induction capacity.

Regardless of 3D culture models or co-culture systems, the aim is to reproduce *in vivo* conditions that are favourable to the maintenance or restoration of odontogenic induction capacity of proliferating cells via *in vitro* manipulable approaches. Here the experimental designs oversimplified the variables during odontogenesis, assuming that single factor could determine cell fates. However, it is more likely that more than one determining factors are involved in tooth inducing ability restoration of cultured dental cells. Therefore, in addition to optimization of each specific approach, a combination of 3D culture and co-culture (Figure IV-18) with considerations of factor supplements and additional physicochemical conditions such as adjustment of oxygen tension, may be

required to restore the odontogenic induction ability of cultured embryonic dental mesenchymal cells.

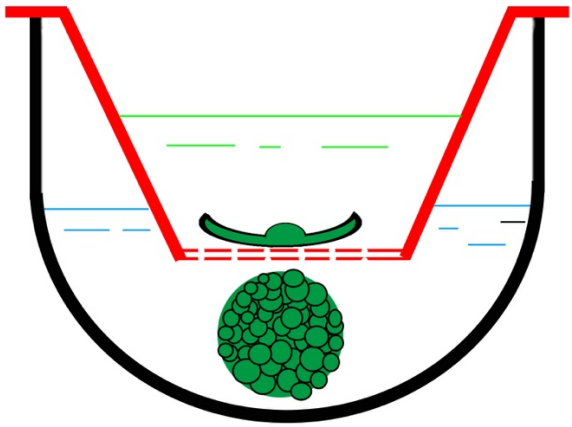

Figure IV-18. Schematic representation of an example of a culture system combining 3D culture and co-culture.

Chapter V Gene Expression Profiling of Dental Cells with Odontogenic Induction Capacity

5.1 Introduction

Cells with identical genomes can present heterogeneity of phenotypes due to different gene expression patterns that can pass on to their daughter cells. In embryonic development, embryonic stem cells derived from inner cell mass of blastocyst are pluripotent. Progressive gene expression alterations in cells result in differentiation to specialized cell linages with decreasing potential to generate other cell types (O'Neill, 2015).

Stem cell based regenerative biology aims to revert differentiated cells into embryonic-like state with pluripotency. The best-known example is induced pluripotent stem (iPS) cells that result from direct cell reprogramming of somatic cells by the introduction of 4 exogenous factors (*Oct3/Oct4, Sox2*, *c-Myc* and *Klf4*) (Takahashi and Yamanaka, 2006). Dedifferentiation of mature cells to a less-differentiated stage within the lineage is observed in natural process, such as heart regeneration due to dedifferentiation of cardiomyocytes in Zebrafish(Poss et al., 2002). In mammals, FGF1 stimulation and p38 MAPK inhibition can induce cardiomyocytes to dedifferentiate (Engel et al., 2005). Transdifferentiation is to convert mature cells to a different cell linage without reverting to embryonic state, which also naturally exist and can be experimentally induced (Jopling et al., 2011). Along with the development in databases and analysis of regulatory networks, key transcription factors for a certain transdifferentiation can be predicted by computing programmes (Rackham et al., 2016).

In tooth regeneration, with transfection of well-established odontogenic genes *Pax9* and *Bmp4*, mouse iPS cells differentiated into odontoblast-like cells, rather than tooth inducing cells (Seki et al., 2015), suggesting additional gene regulations are required to induce odontogenic inductivity in cells.

Mechanism of the loss of odontogenic induction capacity in cultured embryonic tooth germ mesenchymal cells may be revealed by examination of gene expression changes induced by *in vitro* culture. However, drastic gene dysregulation can occur during cell culture (Zheng et al., 2016b). Since the hair inducing ability of cultured dermal papilla was rescued by 3D culture with restoration of 22% of transcripts differentially expressed between intact papillae and passage cells (Higgins et al., 2013), it is reasonable to assume that the acquisition of tooth inducing cells does not necessarily mean reversion of cultured cells to uncultured state, but inductive state, which may remain some features induced by *in vitro* culture.

To narrow down the range of key genes of tooth inducing ability, ideally, odontogenic inductivity needs to be recovered in cultured cells by culture condition manipulations such as 3D culture or co-culture to allow an informative comparison between inductive, non-inductive and re-inductive cell populations. Unfortunately, attempts to obtain a re-inductive cell population failed (Chapter IV). However, in the experiment of 2D direct co-culture of fresh and cultured mesenchymal cells, 12 hour-cultured cells were found to remain the odontogenic inductivity. Alternatively, instead of re-inductive cells, retain-inductive cells can also provide information about cultured cells with inductivity.

Additionally, during tooth development, odontogenic inductivity initially lies in epithelium and then transfers to mesenchyme (Mina and Kollar, 1987). Theoretically, epithelial inductive signals can induce odontogenic inductivity in mesenchymal cells.

The branchial arches are a series of externally visible anterior tissue bands lying under the early brain that form different structures of head and neck. The 1st arch is also named the mandibular process, where odontogenesis begins between embryonic day 10 to 11 in mice. The 2nd arch mainly develops into the hyoid. Epithelium of 1st and 2nd arches share the same origin from oral ectoderm, yet give rise to different facial structures (Hill, 2017). Comparisons of the gene expressions between these two types of epithelial tissues at the stage of E10.5 when the 1st arch epithelium starts to show odontogenic inductivity can be beneficial to dissect the molecular basis of the odontogenic inductivity of inducing dental epithelium.

5.2 Results

5.2.1 Global gene expression profiling of inductive embryonic DMCs

To explore the maximum culture duration embryonic dental mesenchymal cells can maintain tooth inducing ability, CD1 E14.5 tooth germ mesenchymal cells were collected at 24, 48 and 96 hours after being plated on standard 2D culture plates. Fresh cells and the 24, 48, 96 hour-cultured P0 cells were tested for odontogenic induction capacity in reassociation assays with mTmG E14.5 tooth germ epithelial tissues. Part of the cells from each group were preserved for RNA extraction and prepared to be submitted for RNA sequencing (Figure V-1).

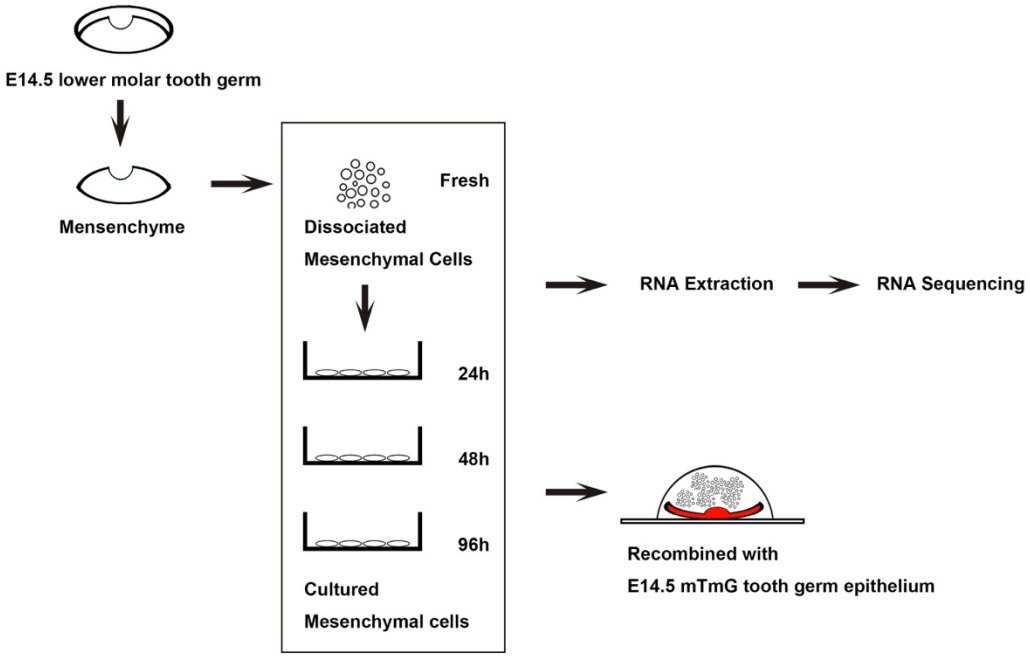

Figure V-1. Schematic representation of experimental design.

CD1 E14.5 molar tooth germ mesenchymal cells were cultured *in vitro* for 0h (fresh cells), 24h, 48h and 96h, followed by RNA extraction and preparation for RNA sequencing. Cells collected at different time points were tested in reassociation assays with mTmG E14.5 tooth germ epithelial tissues for odontogenic induction capacity.

Maximum of 48 hours of *in vitro* expansion of mesenchymal cells maintained the odontogenic induction ability.

Mesenchymal cells adhered to and further stretched along the culture plate surface with increasing culture period. Cells cultured for 24 and 48 hours succeeded in inducing tooth formation, where tooth primordia were well structured as the teeth formed in reassociations with fresh cells. 96h cultured P0 cells, did not initiate tooth development (Figure V-2)

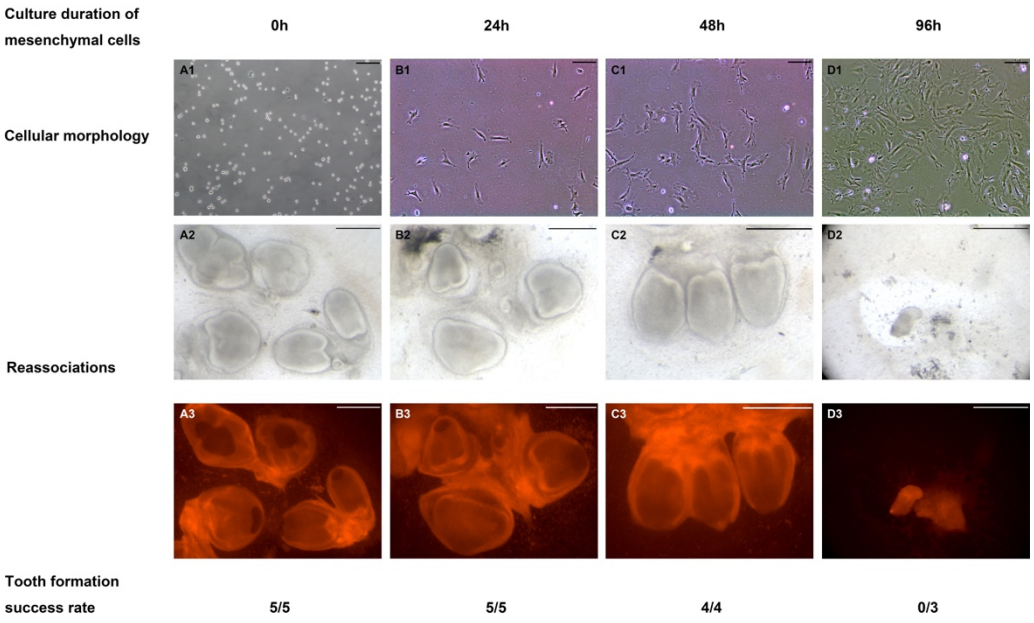

Figure V-2. Cytomorphology and tooth induction results of reassociation assays. A1-D1 show the adhering growing pattern of *in vitro* cultured mesenchymal cells. Cells morphologically transformed from spherical to flat and became more stretched as culture duration increased. Fresh, 24h and 48h cultured cells were able to induce tooth formation in reassociation assays with mTmG E14.5 tooth germ epithelial tissues with a success rate of 100% (A, B, C 2-3). 96h cultured cells failed to initiate tooth development (D2-3). Scale bars: 500 µm.

Change of transcriptomic profiling of dental mesenchymal cells correlated with *in vitro* culture.

To understand the genetic basis of the impact of *in vitro* culture on odontogenic inductivity, short term cultured cells that retained inductive are convenient study subjects to reveal the key gene or genes for maintenance and restoration of tooth inducing ability of cultured cells.

Global gene expression profiles of fresh and 24h, 48h, 96h cultured embryonic dental mesenchymal cells were obtained from RNA sequencing data with 3 replicates. From the sample-to-sample hierarchical cluster analysis (Figure V-3), all the samples clustered into two main subsets: fresh (0h cultured) cells and cultured cells. In the cultured cell subsets, 48h and 96h cultured cells shared a higher correlation than that with 24h cultured cells. These results can be further analyzed by the principle component analysis (Figure V-4). Projected points of fresh cell and cultured cell samples evidently mapped into two directions on the axis of PC1. Projected points of 48h and 96h cultured cells were separated from 24h cultured cell points on the axis of PC2. In addition, all the replicates were clustered together showing a good reproducibility, except for the 96h cultured cell samples, which were slightly dispersed. This implies that prolonged *in vitro* culture may introduce more variations to originally identical cell populations.

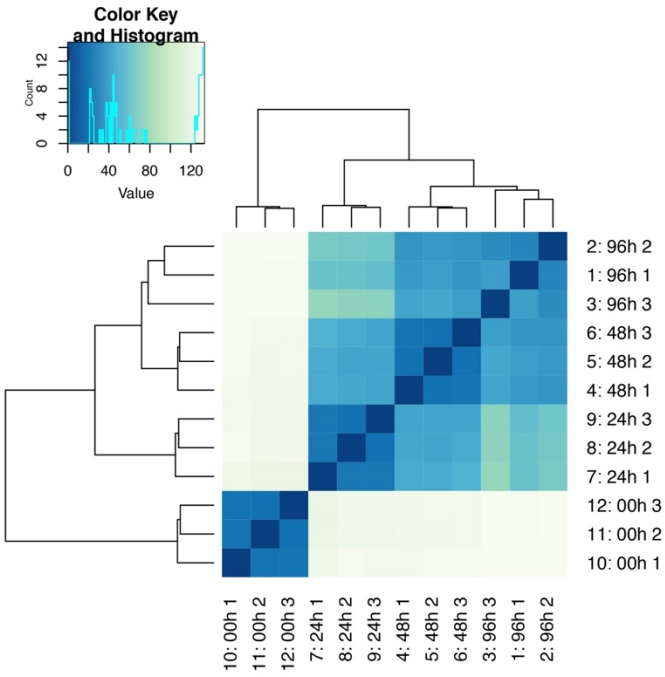

Figure V-3. Heat map of sample-sample correlation distances of mesenchymal cells collected at different time points with biological replicates.

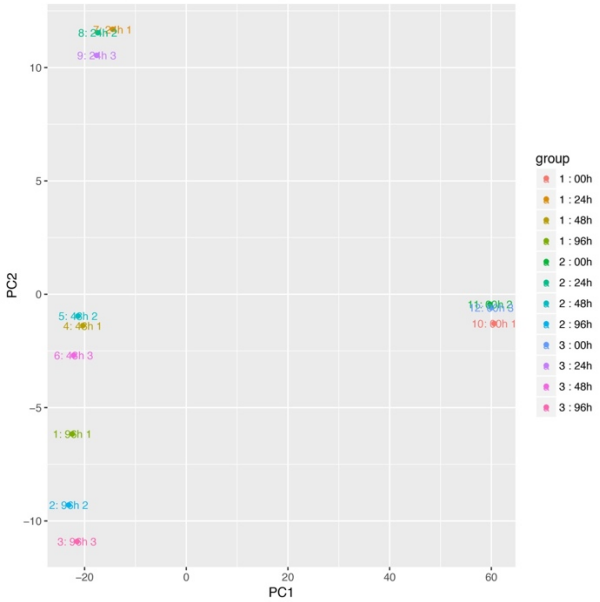

Figure V-4. Principle component analysis (PCA) of mesenchymal cells collected at different time points with biological replicates.

With the threshold of adjusted *p* value≤0.05 and fold change≥2, lists of differentially expressed genes (DEGs) were generated between each pair of conditions (0h vs. 24h, 0h vs. 48h, 0h vs. 96h, 24h vs. 48h, 24h vs. 96h and 48 vs. 96h). Numbers of DEGs are presented in Table V-1. As shown in the stacked histogram of DEG numbers during different phases of cell culture (Figure V-5), major changes of gene expression occurred within 24 hours in culture, as culture duration increased, the scale of gene expression change was decreased.

Venn diagram of DEG sets of different phase of cell culture (**Figure V-6**) shows that a majority (4937) of the DEGs were found only in the category of "0h vs. 24h". In the subsets of "24h vs. 48h" and "48h vs. 96h", most of the DEGs overlapped with the subset "0h vs. 24h" (respectively 614+124 and 318+124), with 124 DEGs included in all 3 subsets. Some DEGs were exclusively in "24h vs. 48h" (336) or "48h vs. 96h" (93). Venn diagram between DEG sets of fresh mesenchymal cells and cultured cells with different culture durations (**Figure V-7**) shows that comparing with fresh cells, cultured cells with different culture durations have shared a similar gene expression dysregulation, given the majority of DEGs (4056) were found in the overlap of all 3 sets ("0h vs. 24h", "0h vs. 48h" and "0h vs. 96h"). However, some culture duration specific features can be observed as well: 1098 DEGs only in "0h vs. 24h", 283 DEGs only in "0h vs. 48h" and 693 DEGs in "0h vs. 96h".

These results imply that the impact of *in vitro* culture on embryonic dental mesenchymal cells mainly occurred immediately within 24 hours. Some of the impact existed throughout the culture periods. Prolonged culture induced additional gene expression alterations on a smaller scale than the changes occurred at the beginning of cell culture.

Table V-1. Numbers of differentially expressed genes (DEGs) of mesenchymal cells collected at different time points.

	24h		48h		96h	
0h vs.	**3996**	**2033**	**3746**	**2118**	**3589**	**2242**
24h vs.	-		**374**	**751**	**781**	**1696**
48h vs.	-		-		**140**	**446**

*A vs. B: number in red box refers to up-regulated genes in A; number in green box refers to down-regulated genes in A.

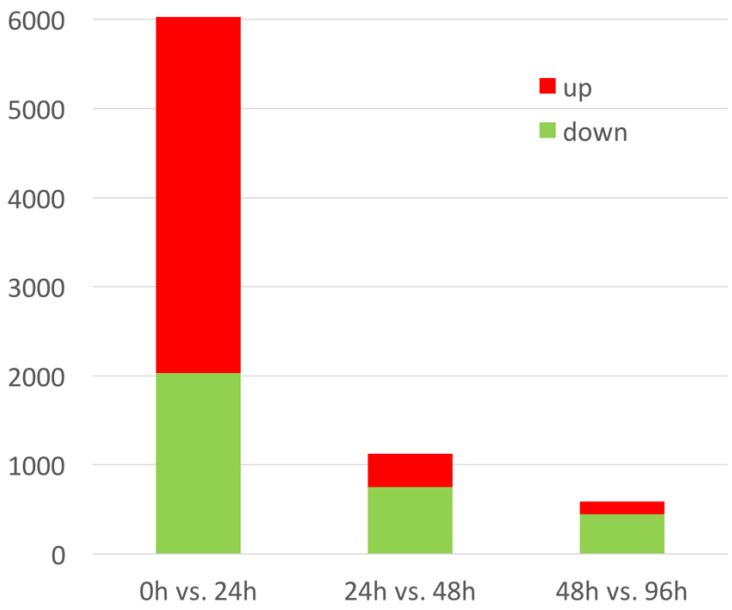

Figure V-5. Stacked histogram of DEG numbers during different phases of cell culture.

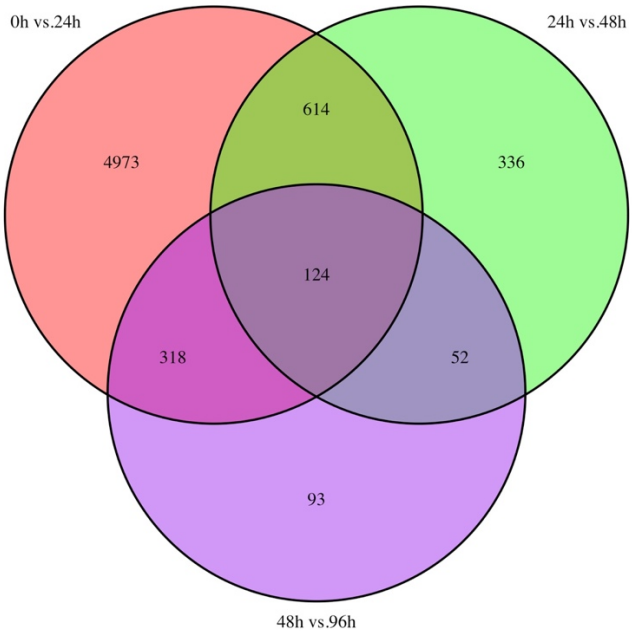

Figure V-6. Venn diagram of DEGs between DEG sets of mesenchymal cell populations from different phases of *in vitro* expansion.

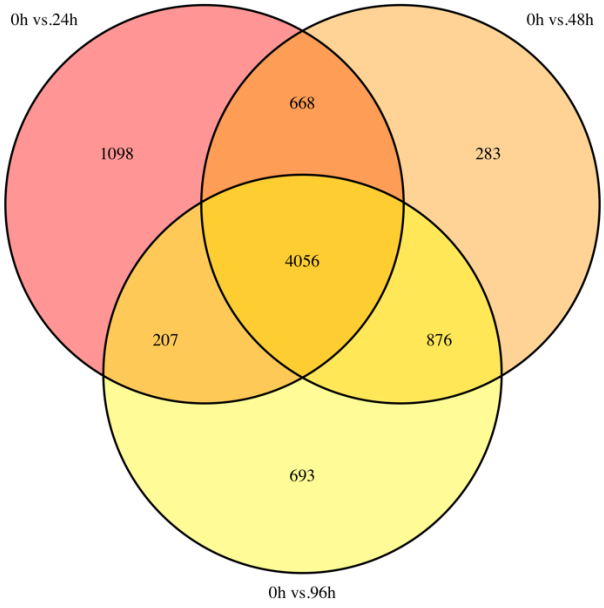

Figure V-7. Venn diagram between DEG sets of fresh mesenchymal cells and cultured cells with different culture durations.

Normalized counts of a total number of 8286 DEGs from all the pairwise comparisons were selected to generate the gene expression heat map (Figure V-8). Overall, the cultured cell samples shared a similar pattern of gene expression.

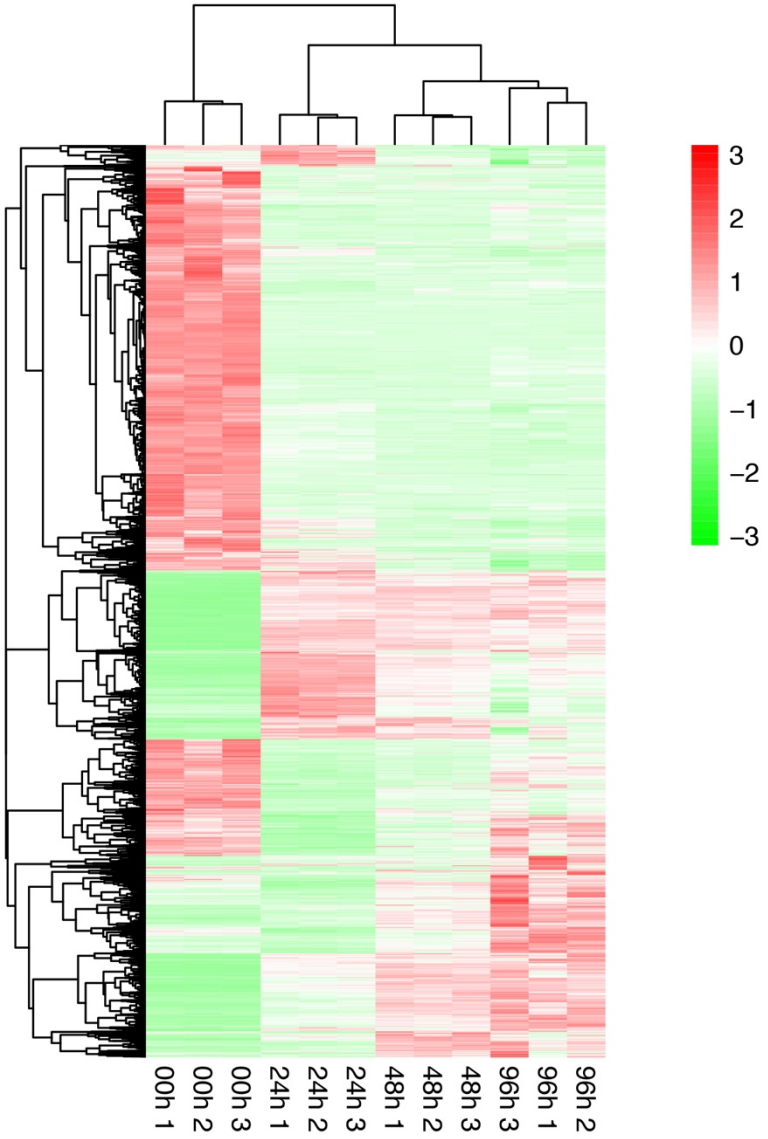

Figure V-8. Heat map of relative expression of DEGs of mesenchymal cells collected at different time points with biological replicates.

The DEGs were clustered into 6 groups based on the expression patterns during different phases of cell culture (Figure V-9), namely the “rapid decrease” (cluster 1), “slow decrease” (cluster 5), “rapid increase” (cluster 3), “slow increase” (cluster 2), “decrease then increase” (cluster 4), and “increase then decrease” (cluster 6) groups. The gene expression change patterns of the clusters are shown with line charts (Figure V-10, separately in Figure V-11, Figure V-12, Figure V-13). Gene lists of each cluster can be found in appendix.

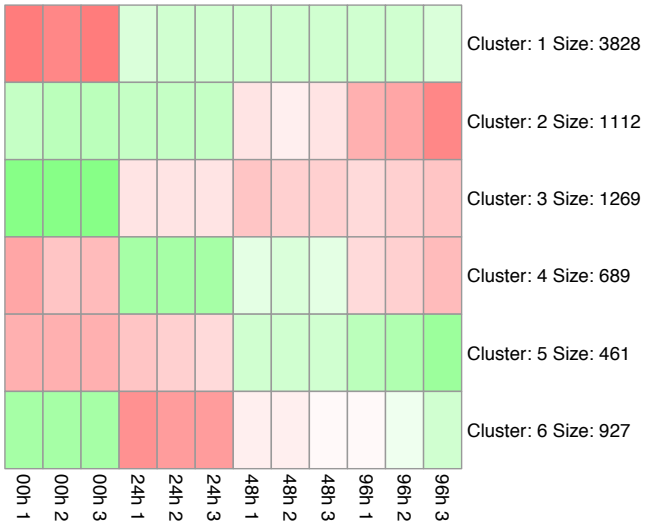

Figure V-9. Clustered heat map of relative expression of DEGs of mesenchymal cells collected at different time points with biological replicates.

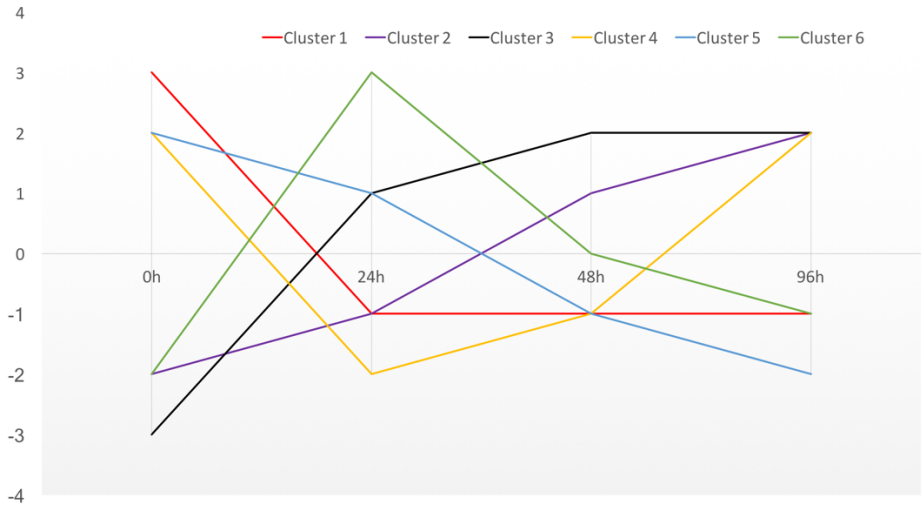

Figure V-10. Line chart of expression level change during cell culture of DEGs in different cluster.

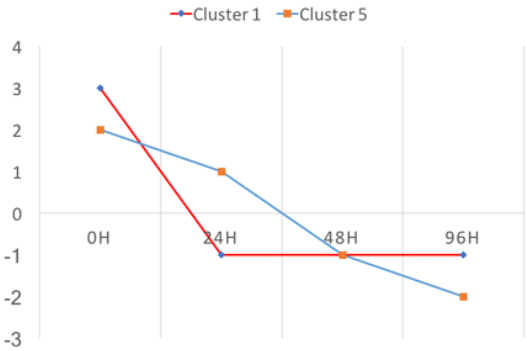

Figure V-11. Expression pattern of DEGs in cluster 1 and 5.

The majority of DEGs (3828/8286) followed a "rapid decrease" pattern where gene expression dropped sharply within 24 hours in culture and stayed low at later stages. While in the cluster with the smallest size, cluster 5, DEGs also showed a downward trend but in a gradient pattern throughout cell culture.

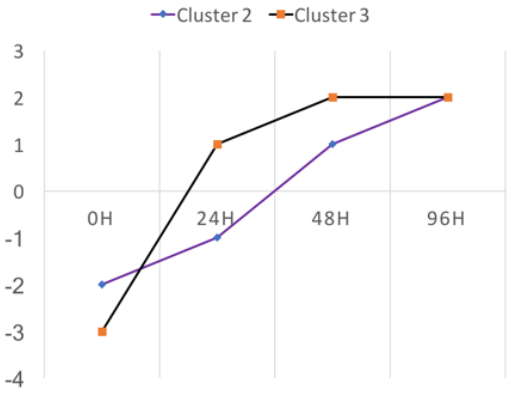

Figure V-12. Expression pattern of DEGs in cluster 2 and 3.

Cluster 2 and 3 were similar in size, genes in these clusters increased during cell culture. The expression level of DEGs in cluster 3 increased rapidly within 24 hours and progressively during later stages. While cluster 2 DEGs showed a gradual growth during culture.

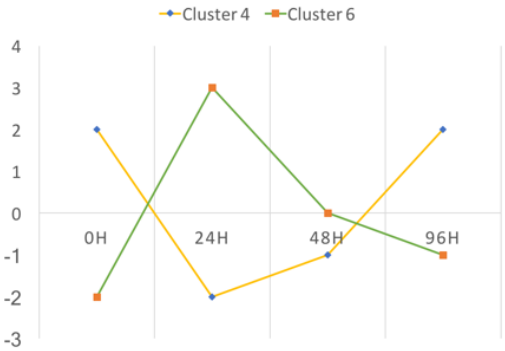

Figure V-13. Expression pattern of DEGs in cluster 4 and 6.

Cluster 4 and 6 DEGs shared a similar change pattern that gene expression drastically changed at the beginning of culture, followed by slow return to the original status. In cluster 4, the pattern can be summarized as "rapid decrease followed by slow increase", and "rapid increase followed by slow decrease" for cluster 6.

Since in reassociation assays, mesenchymal cells cultured for up to 48 hours succeeded in tooth induction, despite drastic changes in gene expression occurring within 24 hours, these alterations did not impair the tooth inducing ability of cells. Therefore, genes with significant changes at later stages are the key to unlock the molecular mechanism for maintenance or restoration of odontogenic induction capacity, such as DEGs in cluster 5,3,4,6. The simplest way to conduct this is to compare gene expression changes between cultured inductive (24h,48h cultured) cells and cultured non-inductive (96h-cultured) cells, especially between 48h and 96h cultured cells due to the occurrence of the turnover point of odontogenic inductivity.

Signalling pathway molecules and transcription factors are of great interest to provide the basis for direct restoration of tooth inducing ability of cultured cells. Statistical overrepresentation test of pathways was performed on DEGs between 24h and 96h cultured cells through the PANTHER (Protein ANalysis THrough Evolutionary Relationships) classification system. With a filter of Bonferroni correction adjusted *p*-Value <0.05, 4 pathways were screened out from a total number of 166 PANTHER pathways: Wnt signalling, Integrin signalling, Cadherin signalling and Alzheimer disease-presenilin pathways (Table V-2).

The up- and down-regulated DEGs of 24h/48h vs. 96h cultured cells were categorized by PANTHER protein class. The identified transcription factors, signalling molecules and receptors were presented in Table V-3 and Table V-4.

Table V-2. PANTHER overrepresentation test of pathways on DEGs between 24h and 96h-cultured cells.

PANTHER Pathways	Ref List (22221)	DEGs (2322)	DEGs (expected)	Over/ Under	Fold Enrichment	P-value*
Wnt signaling pathway (P00057)	306	56	31.98	+	1.75	1.05E-02
Integrin signalling pathway (P00034)	191	39	19.96	+	1.95	1.52E-02
Cadherin signaling pathway (P00012)	154	36	16.09	+	2.24	1.92E-03
Alzheimer disease-presenilin pathway (P00004)	124	28	12.96	+	2.16	2.92E-02

*p-value adjusted by Bonferroni correction for multiple testing

Table V-3. DEGs encoding transcription factors, signalling molecules and receptors from DEG set of 24h vs. 96h-cultured cells.

	Up-regulated in 24h cultured cells	Down-regulated in 24h cultured cells
Transcription factors	(37) Cbx5, Cited1, Dlx2, Dlx3, Dmp1, E2f7, Foxd1, Hif3a, Hivep3, Hmgb1, Hmgb2, Hmgb3, Irf5, Klf14, Klhl6, Mybl2, Myc, Mycl, Mycn, Myod1, Nlrp3, Npas3, Nr1h5, Nr5a2, Onecut1, Pgr, Ppargc1b, Prdm16, Sall3, Samd1, Sp7, Spi1, Spib, Spry1, St18, Tal1, Tead4	(66) Alx4, Ar, Arntl2, Btbd11, Cebpb, Crip2, Dach2, Dbp, Emx2, Epas1, Fli1, Foxc1, Foxj1, Foxs1, Gata2, Gata3, Grhl3, Hlx, Ifi35, Irf7, Irf8, Irx3, Junb, Ldb3, Lhx9, Lrrc73, Mdfic, Mxd4, Myf5, Myf6, Myog, Nacad, Nkx2-9, Nlrp10, Nlrx1, Nod1, Nr1d1, Nr1h3, Nr4a1, Onecut2, Pdlim2, Per3, Pir, Ppara, Ppargc1a, Prox1, Rarb, Runx1, Sall1, Sox13, Sox21, Sox21, Sp9, Stat3, Stat4, Stat5a, Tbx18, Tbx20, Tcea3, Tec, Nr4a3, Tfec, Tle6, Tox, Vdr, Zfp219, Zfp385a
Signalling molecules	(58) Angptl7, Apln, Arhgdig, Bcl2, Bmp2, Bmp3, Bmp8b, C3, C4b, Calca, Calcb, Cd37, Cd53, Cd84, Clec12a, Clec2l, Cnih2, Cntf, Cort, Csf3, Dlk1, Edn2, Efna2, Efnb3, Esm1, Fgf3, Frzb, Hbegf, Hmgb1, Hmgb2, Hmgb3, Il16, Il31ra, Lcp2, Lgals7, Mapk8ip2, Nog, Nppb, Nrg2, Nxph3, Pdgfb,	(92) Angpt1, Angpt2, Angpt4, Angptl4, App, Ar, Artn, Btbd11, Btc, Ccbe1, Ccl7, Cd274, Cd59a, Cd59b, Cd81, Cd82, Clec2d, Cnp, Ddt, Ecm2,Sparcl1, Efna3, Fgf11, Fgf12, Fgf14, Fgf16, Fgf18, Fgf9, Fli1, Fzd8, Gdf15, Gdf9, Gpnmb, Icam1, Icam2, Icam4, Il13ra2, Il27ra, Il2rg, Il3ra, Il6ra, Inhbb, Kitl, Klrg2, Lefty1, Lgals2, Lif, Mcf2l, Mfap4, Mgp, Nts, Osmr, Otor, Pdgfa, Pdgfd, Pgf, Pkdrej, Plcd1, Plcd3, Plcg2, Psen2, Rcan1, Rcan3, Rln1,

	Penk, Plcb2, Ppp1r1a, Pthlh, S100a7a, Scg2, Siglec15, Spi1, Spib, Spry1, Tenm2, Tmem130, Tspan13, Tspan33, Vav1, Vav3, Wnt7a	Rom1, S100a1, S100a13, Scg5, Sema3b, Sema3c, Sema3d, Sema4f, Shc4, Siglecg, Sncg, Sparc, Stc1, Tgfbi, Tnc, Tnxb, Tox, Trf, Tspan11, Tspan12, Tspan17, Unc93b1, Vegfd, Vip, Wisp1, Wisp2, Wnt16, Wnt2, Wnt9a
Receptors	(45) Acvr1b, Adgrb2, Adgrb3, Baiap2l2, C3ar1, Cckar, Cd36, Cd37, Cd5, Cd53, Celsr1, Csf2rb, Csf2rb2, Dlk1, Ednrb, Frzb, Gabbr2, Gldn, Gpr27, Grm7, Il1rapl2, Itgb2, Lamb3, Lbr, Lingo1, Lingo2, Lrfn2, Ngfr, Nrcam, Ntng1, Olfm2, Omd, P2ry1, Paqr9, Pim3, Ptafr, Ptch1, Ptch2, Ptger3, Ramp2, Scarf1, Sstr2, Tenm2, Tspan13, Tspan33	(99) Acvrl1, Adgrg2, Adgrl4, Adra1d, Adra2a, Adrb2, Adrb3, Agtr1a, Agtr1b, Agtr2, Antxr1, Bdkrb2, Ccdc28a, Cd40, Cd81, Cd82, Chl1, Cnr1, Disp1, Disp2, Ecm2, Eng, Eva1c, F3, Fas, Fmod, Fzd8, Gpr135, Gpr3, Gpr37, Gpr39, Gpr85, Grina, Htr1d, Htr2a, Htr7, Igf2r, Il1rap, Il1rl2, Il4ra, Islr, Itgb4, Itgb5, Itgbl1, Lama1, Lama2, Lama5, Lamb2, Lmbr1, Loxl2, Loxl3, Loxl4, Lpar3, Lrrc55, Lrrn4cl, Ltb4r1, Ltb4r2, Ltbr, Lum, Mc5r, Mrgpre, Mrgprf, Ms4a4d, Ntng2, Ogn, P2ry14, Paqr7, Pink1, Pla2r1, Prelp, Procr, Prss12, Ptger1, Ramp1, Reep2, Rom1, Slit1, Slitrk3, Slitrk5, Sorcs1, Spred3, Ssc5d, Sstr4, Tbxa2r, Tcp11l2, Tmem176a, Tnfrsf14, Tnfrsf18, Tnfrsf1b, Tnfrsf26, Tpbgl, Tshr, Tspan11, Tspan12, Tspan17, Tspo, Unc5b, Unc5c, Vipr2

Table V-4. DEGs encoding transcription factors, signalling molecules and receptors from DEG set of 48h vs. 96h-cultured cells.

	Up-regulated in 48h cultured cells	Down-regulated in 48h cultured cells
Transcription factors	(6) Cited1, Klhl6, Mycn, Nr5a2, Smyd1, Sp7	(14) Ar, Crip1, Dach2, Dbp Ifi204, Irf7, Nr1d1, Pir, Rfx8, Sp9, Tbx20, Tcea3, Tfec, Tle6
Signalling molecules	(14) Bmp2, Bmp3, Bmp8b, Dlk1, Esm1, Il31ra, Nog, Nov, Pdgfb, Pthlh, S100a7a, Tnmd, Tspan33, Wnt4	(22) Angpt1, Angptl4, Ar, Ccbe1, Cd59a, Clec2d, Fgf1, Fgf14, Gpnmb, Icam1, Il13ra2, Psen2, S100a1, Scg5, Sema3b, Sema4f, Sparcl1, Stc1, Trf, Tspan17, Unc93b1, Wisp2
Receptors	(13) Adgrb3, Adgrf2, Avpr1a, Cckar, Csf2rb, Dlk1, Gprc6a, Ngfr, Olfml1, P2ry1, Paqr9, Sstr1, Tspan33	(30) Adgrg2, Adgrl4, Agtr1b, Agtr2, Bdkrb2, Cd40, Evi2a, Htr7, Itgb4, Itgbl1, Lama1, Lamc3, Loxl4, Lrrc55, Lum, Mrgprf, Ms4a4d, Ntng2, Pla2r1, Prelp, Procr, Prss12, Ramp3, Slc52a3, Sorcs1, Ssc5d, Tnfrsf1b, Trpm3, Tspan17, Unc5d

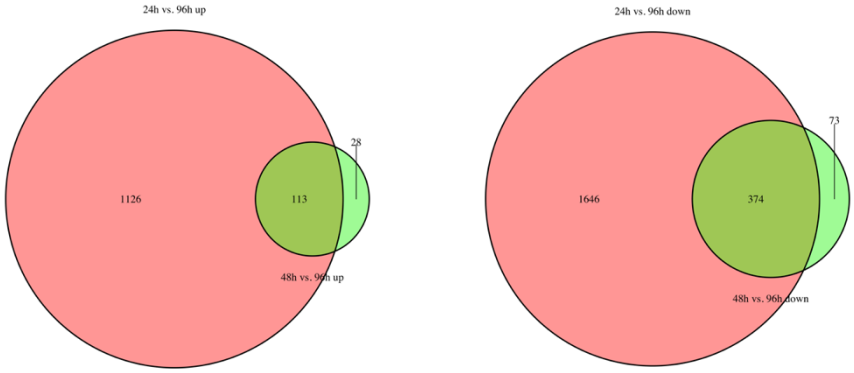

Figure V-14. Venn diagram of DEGs between up and down regulated DEG sets of "24h vs. 96h" and "48h vs. 96h" cultured cells.

Table V-5. Common DEGs encoding transcription factors, signalling molecules and receptors from DEG sets of 24h vs. 96h and 48h vs. 96h-cultured cells.

	Up-regulated in 24/48h cultured cells	**Down-regulated in 24/48h cultured cells**
Transcription factors	(5) Cited1, Klhl6, Mycn, Nr5a2, Sp7	(11) Ar, Dach2, Dbp, Irf7, Nr1d1, Pir, Sp9, Tbx20, Tcea3, Tfec, Tle6
Signalling molecules	(11) Bmp2, Bmp3, Bmp8b, Dlk1, Esm1, Il31ra, Nog, Pdgfb, Pthlh, S100a7a, Tspan33	(20) Angpt1, Angptl4, Ar, Ccbe1, Cd59a, Clec2d, Fgf14, Gpnmb, Icam1, Il13ra2, Psen2, S100a1, Scg5, Sema3b, Sema4f, Stc1, Trf, Tspan17, Unc93b1, Wisp2
Receptors	(8) Adgrb3, Cckar, Csf2rb, Dlk1, Ngfr, P2ry1, Paqr9, Tspan33	(24) Adgrg2, Adgrl4, Agtr1b, Agtr2, Bdkrb2, Cd40, Htr7, Itgb4, Itgbl1, Lama1, Loxl4, Lrrc55, Lum, Mrgprf, Ms4a4d, Ntng2, Pla2r1, Prelp, Procr, Prss12, Sorcs1, Ssc5d, Tnfrsf1b, Tspan17

5.2.2 Global gene expression profiling of inductive embryonic dental epithelial cells

To identify the gene expression signatures of inductive odontogenic epithelium, global gene expression profiles of mouse E10.5 1st and 2nd branchial arches were established from RNA sequencing data with 4 replicates. To further restrict the differences of the two groups of epithelium to odontogenic and non-odontogenic potentials, epithelium of the 1st branchial arches (mandibular processes), was dissected from the dental areas which are in the developing oral cavities (Figure V-15). The rest of the 1st arch epithelium, which does not have tooth inducing potential, was collected with the 2nd arch epithelium as the non-odontogenic epithelium. For convenience, the odontogenic and non-odontogenic epithelium are respectively referred to as 1st and 2nd arch epithelium.

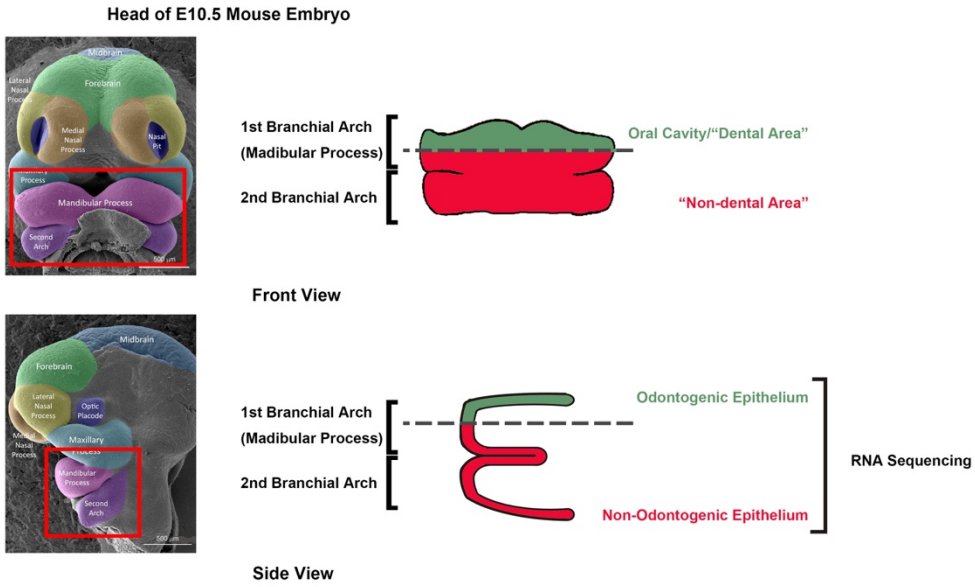

Figure V-15. Schematic representation of dissection of odontogenic and non-odontogenic branchial arch epithelium.

Scanning electronic microscope images of front and side views of the head of E10.5 mouse embryo are adapted from FaceBase-Mouse Anatomy (Iwata et al.).

The sample-to-sample hierarchical cluster analysis showed that two main clusters were generated respectively consisting of the 1st and 2nd branchial arch epithelial samples (Figure V-16). Principle component analysis showed that the 1st and 2nd branchial arch epithelial samples were divided into two domains on the axis of PC1 (Figure V-17). These results demonstrated that the gene expression patterns were evidently different between the odontogenic and non-odontogenic epithelial tissues.

Differentially expressed genes (DEGs) were selected with the threshold of adjusted *p* value≤0.05 and fold change≥2 (Figure V-18). The generated DEG list contains 253 genes with higher expression and 439 genes with lower expression in 1st than in 2nd branchial arch epithelium (Figure V-19).

DEGs were analyzed through PANTHER classification system for statistical overrepresentation test of pathways. 5 pathways were screened out with the threshold of Bonferroni correction adjusted *p*-value <0.05: Wnt signaling pathway, Cadherin signaling pathway, Heterotrimeric G-protein signaling pathway-Gi alpha and Gs alpha mediated pathway, Heterotrimeric G-protein signaling pathway-Gq alpha and Go alpha mediated pathway and Ionotropic glutamate receptor pathway (Table V-6). The up- and down-regulated DEGs were categorized by PANTHER protein class and the identified transcription factors, signalling molecules and receptors were presented in Table V-7.

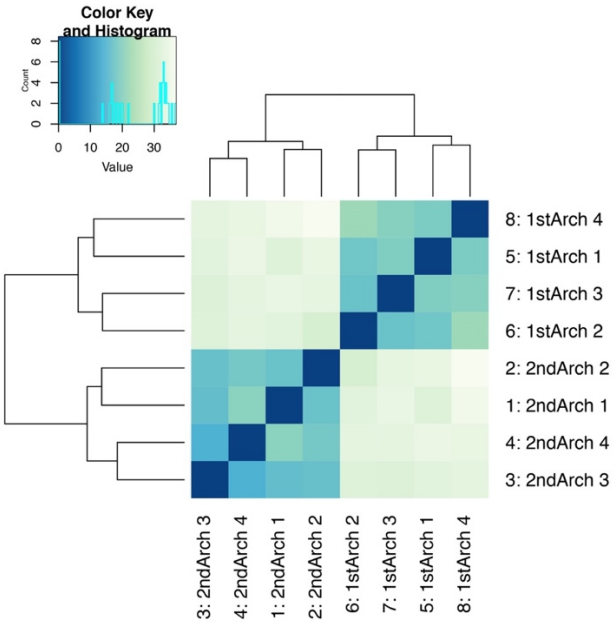

Figure V-16. Heat map of sample-sample correlation distances of E10.5 1st (odontogenic) and 2nd (non-odontogenic) branchial arch epithelium with biological replicates.

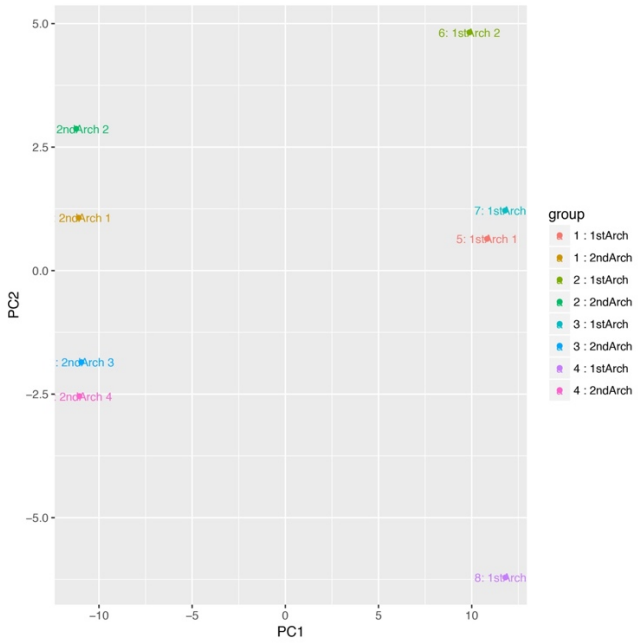

Figure V-17. Principle component analysis (PCA) of E10.5 1st (odontogenic) and 2nd (non-odontogenic) branchial arch epithelium with biological replicates.

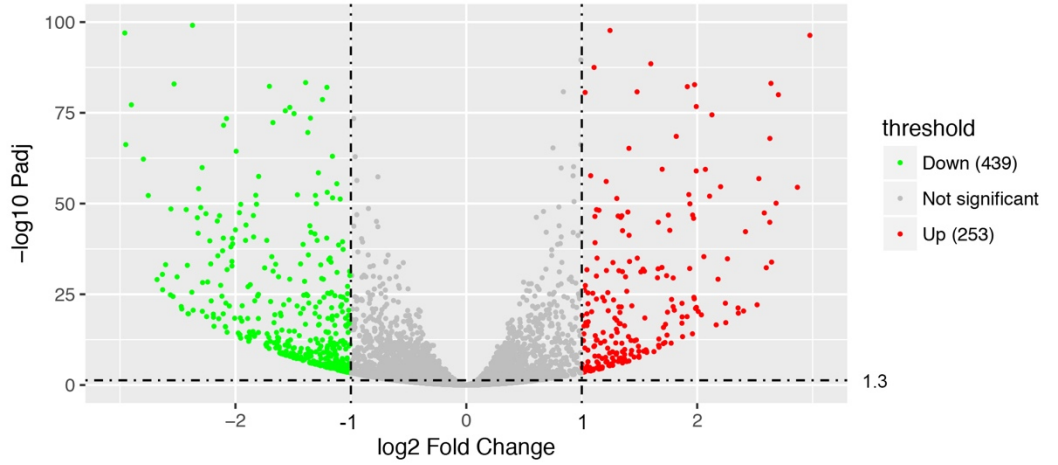

Figure V-18. Volcano Plot of relative gene expressions between E10.5 1st (odontogenic) and 2nd (non-odontogenic) branchial arch epithelium.

Threshold of DEG identification: adjusted *p*-Value <0.05 and |log2 Fold change|>1.

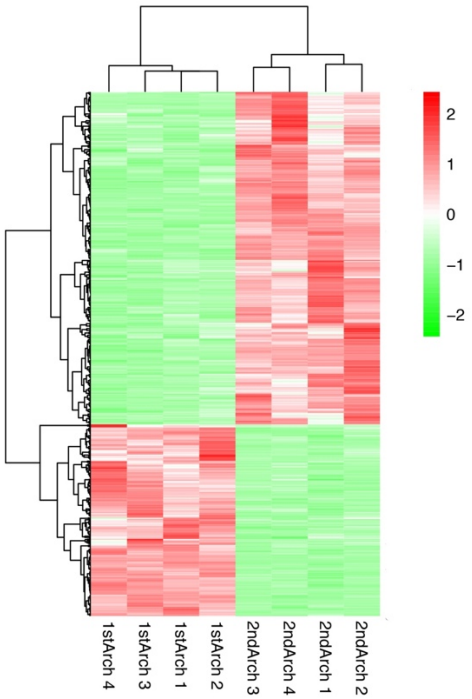

Figure V-19. Heat map of relative expression of DEGs of E10.5 1st (odontogenic) and 2nd (non-odontogenic) branchial arch epithelium with biological replicates.

Table V-6. PANTHER overrepresentation test of pathways on DEGs between 1st and 2nd branchial arch epithelium.

PANTHER Pathways	Ref List (22221)	DEGs (665)	DEGs (expected)	Over/ Under	Fold Enrichment	P-value*
Wnt signaling pathway (P00057)	306	28	9.16	+	3.06	5.18E-05
Cadherin signaling pathway (P00012)	154	20	4.61	+	4.34	1.30E-05
Heterotrimeric G-protein signaling pathway-Gi alpha and Gs alpha mediated pathway (P00026)	156	15	4.67	+	3.21	1.60E-02
Heterotrimeric G-protein signaling pathway-Gq alpha and Go alpha mediated pathway (P00027)	119	14	3.56	+	3.93	3.28E-03
Ionotropic glutamate receptor pathway (P00037)	50	8	1.5	+	5.35	2.56E-02

*p-value adjusted by Bonferroni correction for multiple testing

Table V-7. DEGs encoding transcription factors, signalling molecules and receptors from DEG set of 1st vs. 2nd E10.5 branchial arch epithelium.

	Up-regulated in 1st branchial arch epithelium	Down-regulated in 1st branchial arch epithelium
Transcription factors	(32) Ascl5, Barx1, Dlx1, Dlx2, Dlx3, Dmbx1, Erg, Esrrg, Evx1, Foxi3, Foxo1, Irx1, Lhx6, Lmo1, Lmo2, Msx1, Msx2, Nkx2-3, Otx1, Pitx1, Pitx2, Rorb, Runx1, Runx2, Sox14, Sp5, Sp7, Tbx3, Vgll2, Zbtb7c, Zfp385c, Zfp536	(47) Barx2, Bhlhe22, Ehf, Emx2, En2, Esr1, Ets1, Foxa1, Foxb2, Foxc1, Foxc2, Foxd1, Foxi2, Foxq1, Hcls1, Hoxa1, Hoxa2, Hoxa3, Hoxb1, Hoxb2, Hoxc5, Ikzf1, Ikzf3, Irf1, Irf5, Irx2, Irx4, Mitf, Nfkbiz, Nkx2-5, Nkx2-6, Nkx6-1, Nr2f1, Otx2, Pax1, Pax9, Ppargc1a, Prdm16, Sim2, Six1, Six2, Sox10, Sox21, Sox21, Sox9, Spry4, Tcerg1l, Tshz3
Signalling molecules	(23) Arhgdig, Bdnf, Bmp2, Bmp4, Bok, Cd59a, Dlk1, Elmod1, Erg, Fgf10, Fgf15, Fgf17, Fgf8, Fgf9, Gdf6, Ltbp2, Nog, Nxph3, Pdgfd, Pnoc, Ppp1r1a, Tspan18, Wnt5a	(32) Arhgdib, Cx3cl1, Cxcl15, Ehf, Epgn, Ets1, Fgf14, Gdnf, Gpnmb, Hbegf, Iapp, Icam1, Il2rg, Lgals7, Lgals9, Lif, Lifr, Mitf, Mstn, Nell1, Pdzd2, Plce1, Pmel, Sfrp1, Sparcl1, Spry4, Tgfb3, Tgfbi, Trf, Upk1b, Wnt10b, Wnt2
Receptors	(14) Aatk, Cd5, Chl1, Cnr1, Dlk1, Kera, Ntng2, Oprd1, Oprk1, Oxtr, Ptch2, Slitrk6, Tspan18, Unc5c	(29) Adgre1, Adora2b, Adra2b, Adrb1, Adrb2, Alcam, Bmpr1b, Cd36, Eng, Glp2r, Gpr3, Gpr37, Gprc5a, Islr, Islr2, Lrrn2, Mrc1, Ngfr, Ntsr1, Olfm1, Olfml2a, Pex5l, Rxfp3, Sfrp1, Sstr4, Tgfbr3, Trpm3, Unc5a, Upk1b

5.2.3 Integration of gene profiles of inductive dental mesenchyme and epithelium

The two sets of gene expression profiles were generated from different cell types, mesenchymal and epithelial cells. However, the comparisons were both performed between inductive and non-inductive cell populations. Mutual gene expression differences between the two sets of profiles may provide some information on the odontogenic inductivity.

214 DEGs from the DEG set of 24h vs. 96 h cultured cells were found to be included in the epithelial DEG set (Figure V-20). Overlapped DEGs dropped to 63 when the mesenchymal 0h vs. 96h cultured cell DEG set was replaced with 48h vs. 96h subset (Figure V-21), and *Dlk1* was the only gene of interest remained in the mutual DEG list. The mutual DEGs between DEG sets of 1st vs. 2nd branchial arch epithelium and 24h/48h vs. 96h cultured mesenchymal cells were further categorized by PANTHER protein class with the identified transcription factors, signalling molecules and receptors presented respectively in Table V-8 and Table V-9.

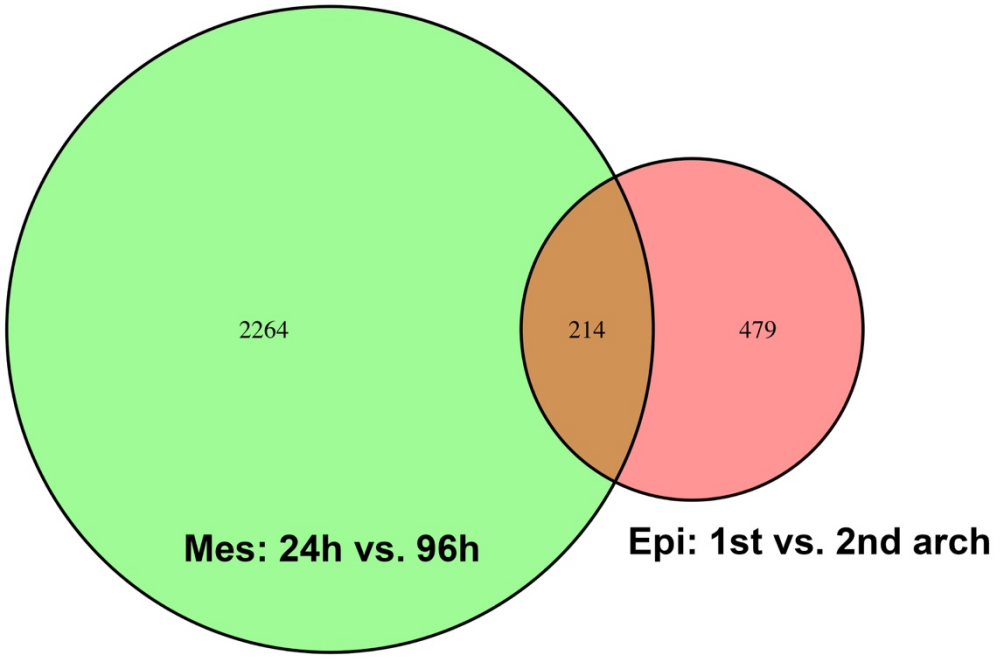

Figure V-20. Venn diagram of DEGs between DEG sets of epithelial and mesenchymal (wide range of) inductive vs. non-inductive cell populations.

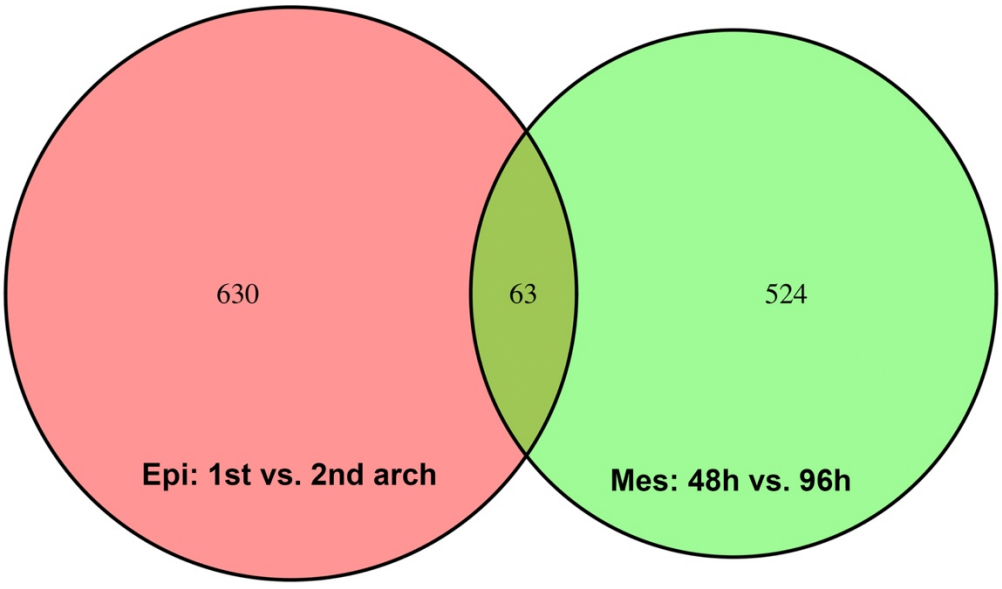

Figure V-21. Venn diagram of DEGs between DEG sets of epithelial and mesenchymal (restricted range of) inductive vs. non-inductive cell populations.

Table V-8. DEGs encoding transcription factors, signalling molecules and receptors from the mutual DEGs between DEG sets of 1st vs. 2nd branchial arch epithelium and 24h vs. 96h cultured mesenchymal cells.

	Up in inductive cells	Down in inductive cells
Transcription factors	(3) Dlx2, Dlx3, Sp7	(6) Bhlhe40, Cavin2, Emx2, Foxc1, Ppargc1a, Sox21
Signalling molecules	(5) Arhgdig, Bmp2, Dlk1, Nxph3, Ppp1r1a	(7) Fgf14, Gpnmb, Il2rg, Lif, Sparcl1, Tgfbi, Wnt2
Receptors	(1) Dlk1	(5) Fgf14, Gpnmb, Il2rg, Lif, Sparcl1, Tgfbi, Wnt2

Table V-9. DEGs encoding transcription factors, signalling molecules and receptors from the mutual DEGs between DEG sets of 1st vs. 2nd branchial arch epithelium and 48h vs. 96h cultured mesenchymal cells.

	Up in inductive cells	Down in inductive cells
Transcription factors	(1) Sp7	(1) Bhlhe40
Signalling molecules	(2) Bmp2, Dlk1	(3) Fgf14, Gpnmb, Sparcl1
Receptors	(1) Dlk1	(1) Trpm3

From a preliminary microarray result comparing human fresh and cultured tooth germ mesenchymal cells, 14 genes were found to have higher expression in fresh cells, *Col14a1, Dach1, Dcc, Dlk1, Efnb2, Fat3, Itga9, Jag1, Mmp1, Pcdhb3, Ptch1, Sostdc1 Tbx22* and *Wif1*. In combination with some well-established odontogenic genes such as *Bmp4, Pax9, Msx1, Lhx6, Lef1, Dlx1, Dlx2, Dlx3* and some tooth development related genes *Pitx2, p21, Edar, Axin2, Barx1, Dix1, Dix2, Gli1, Gli2, Glis3* (Tucker and Sharpe, 2004), a list of genes of interest was generated and matched with DEG subsets of 0h vs. 96 h cultured cells and 1st vs. 2nd branchial arch epithelium.

Most of the well-established odontogenic genes were found in both DEG sets including *Bmp4, Dlk1, Dlx1, Dlx2, Dlx3, Fat3, Lhx6, Msx1, Pax9, Pitx2, Runx2, Wif1.* The rest were mainly included only in the mesenchymal DEG sets, such as *Lef1, Sostdc1, Dcc, Edar, Axin2, Gli1, Jag1, Dach1* etc. The expression patterns of genes of interest in mesenchymal and epithelial cells are shown in Figure V-22. Most of the genes showed the expression pattern of “rapid decrease” in cultured mesenchymal cells and with higher expression in odontogenic epithelium. While *Dlk1, Dlx2* and *Lhx6* showed a progressive decrease in cultured mesenchymal cells*. Jag1, Bmp4* and *Efnb2* showed higher expression in cultured mesenchymal cells, and Pax9 was with lower expression in odontogenic epithelium.

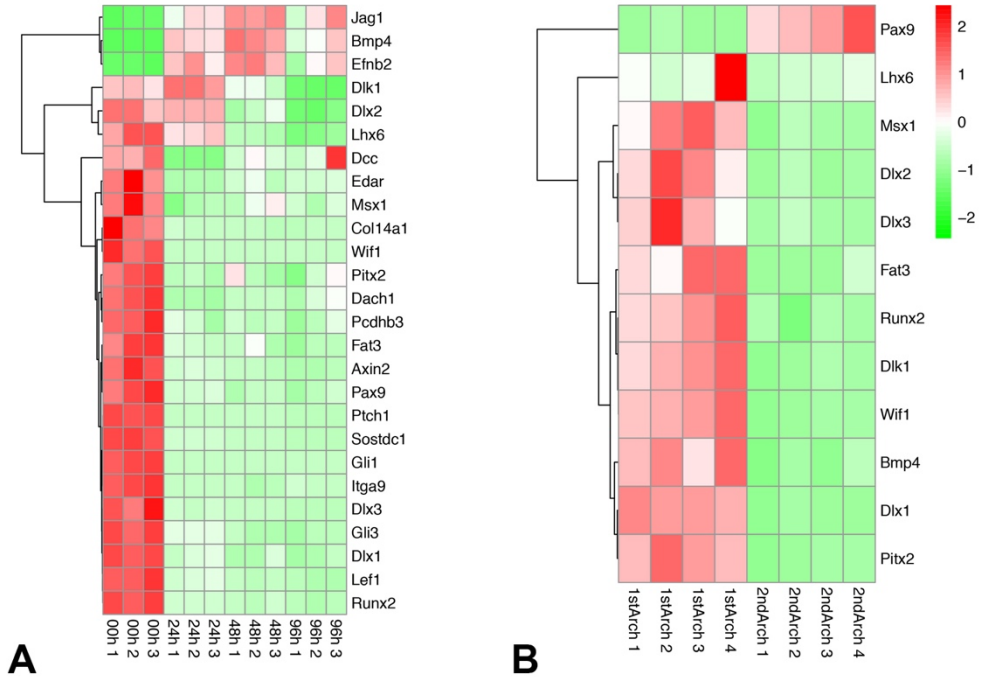

Figure V-22. Heat map of relative expression of genes of interest.

(A) in mesenchymal cells collected at different time points with biological replicates. (B) in E10.5 1st (odontogenic) and 2nd (non-odontogenic) branchial arch epithelium with biological replicates.

5.2.4 Summary

Impairment of the odontogenic inductivity of *in vitro* cultured embryonic dental mesenchymal cells occurred 48-96 hours after the cells were plated.

Major impact of *in vitro* culture on the gene expression pattern of dental mesenchymal cells occurred within 24 hours, some of which continued to exist throughout the culture period. Prolonged culture induced additional gene expression alterations with smaller scale than the changes occurred at the beginning of culture.

Mesenchymal and epithelial inductive vs. non-inductive cell comparisons shared some identical differentially expressed genes (DEGs) including most of the well-established odontogenic genes. Both comparisons revealed high correlation of odontogenic induction ability with Wnt signalling pathway.

Narrowed-down comparison range of culture period to 48h to 96 h, when the odontogenic inductivity turnover occurred, reduced the number of overlapped DEGs with epithelial comparisons between odontogenic and non-odontogenic cell populations. *Dlk1* remained in the mutual DEG list.

5.3 Discussion

5.3.1 Key gene/genes of odontogenic inductivity

In vitro expansion induced differential expression of approximately 6000 genes (**Figure V-7**), which made it difficult to identify one gene or gene sets that played a key role in the maintenance of odontogenic induction capacity. However, from the reassociation assays, up to 48 hour cultured mesenchymal cells succeeded in tooth induction. Furthermore, gene expression profiling revealed that the majority of differentially expression genes (DEGs) fell into the beginning phase of culture within 24 hours. These results suggest that the short-term culture induced drastic gene expression changes that did not impair the tooth inducing ability of mesenchymal cells. In other words, in addition to the initial drastic alterations, genes continued or started to become dysregulated at latter stages, especially where turnover of odontogenic inductivity occurred, may be of crucial importance, which greatly reduced the scope of key gene pool.

From the distribution of genes of interest in DEG sets comparing cells in different stages of culture (**Figure V-23**), most of the genes were only expressed differentially at the stage of 0h to 24h (*Msx1, Pax9, Bmp4, Dlx1, Dlx3, Fat3, Pax9, Runx2, Lef1, Col14a1, Dach1, Itga9, Jag1, Pcdhb3, Ptch1*); Some were found in both 0h vs.24h and 24h vs.48h (*Wif1, Dcc, Edar*). Some were included in subsets of 0h vs. 24h and 48h vs. 96h (*Sostdca1, Axin2, Gli1, Gli3*). The gene that showed differential expression only in stage of 48h to 96h was *Dlk1.*

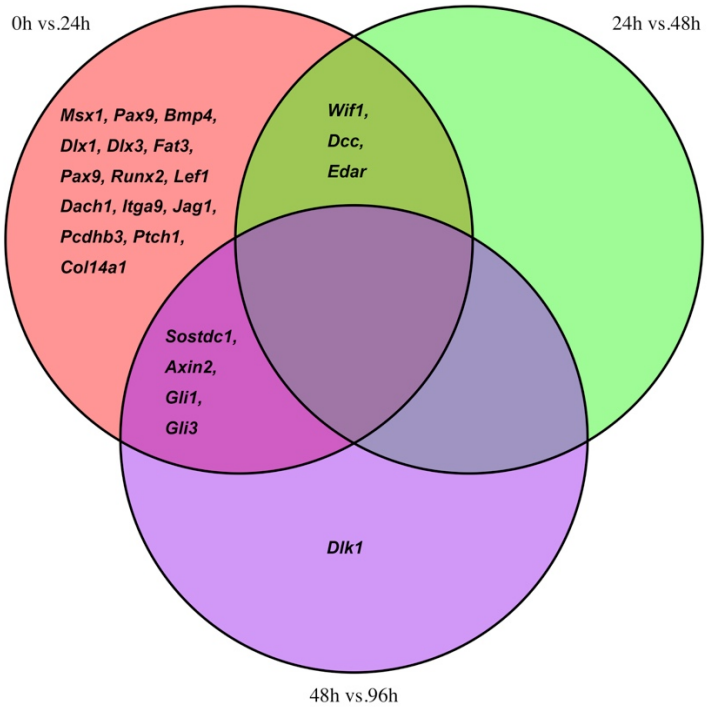

Figure V-23. Venn diagram of genes of interest between DEG sets of fresh mesenchymal cells and cultured cells with different culture durations.

Simplified models of variation trends of genes of interest during cell culture can be summarized as “rapid decrease at the early stage” represented by *Msx1*, “progressive decrease mainly before the middle stage” represented by *Wif1*, “progressive decrease with plateau at the middle stage” represented by *Sostdc1* and “rapid decrease only at the late stage” represented by *Dlk1* (Figure V-24).

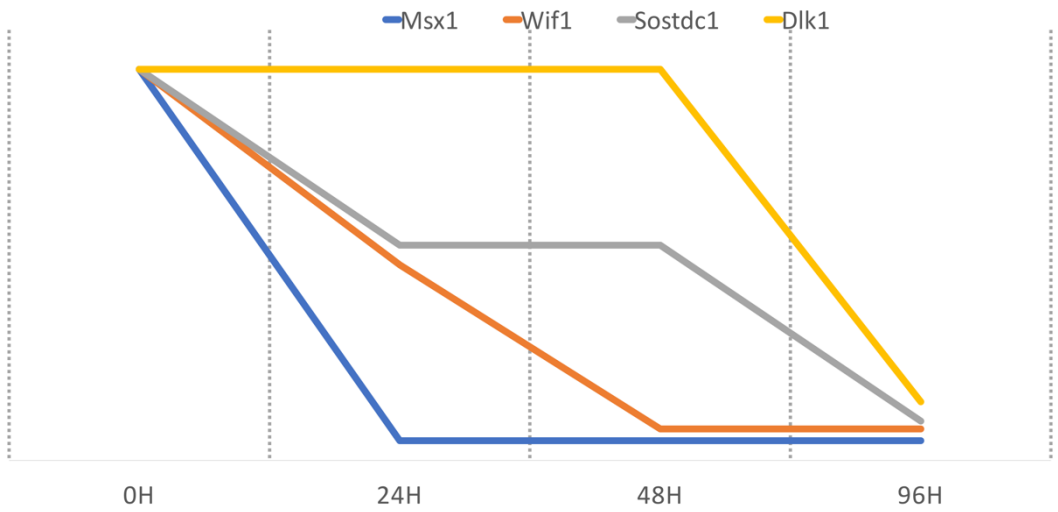

Figure V-24. Simplified models of variation trends of genes of interest during cell culture.

As discussed above that genes expressed differently at latter stages are of crucial importance. Here genes with *Msx1*-type variation trend showed expression changes only at the beginning phase of culture, indicating that they are probably not the determining genes for odontogenic inductivity. *Dlk1* showed expression alterations only at the latter stage where cells lost tooth inducing ability, implying a direct correlation with odontogenic inductivity in a possible "toggle switch" fashion. *Wif1*- and *Sostdc1*-type variation trends both showed continued changes after the alterations at the early stage. The progressive change pattern of these genes may suggest an accumulating impact on odontogenic inductivity. Additionally, Sostdc1-type genes showed significant changes specifically at the inductivity turnover stage (48h-96h), which may indicate a stronger correlation with tooth inducing ability than *Wif1*-type genes.

5.3.2 Correlations of Wnt signalling pathway and odontogenic inductivity

From the results of statistical overrepresentation test of pathways on DEG sets of fresh vs. cultured mesenchymal cells, odontogenic vs. non-odontogenic epithelium, Wnt signalling pathway showed significant overrepresentation.

Wnt (Wingless-related integration site) signalling is a highly conserved pathway that induces cell responses through activation of gene transduction via paracrine or autocrine Wnt ligands binding with Frizzled receptors. It plays a crucial role in embryonic development and organogenesis including odontogenesis by regulating diverse processes such as axis patterning, cell proliferation, migration and fate specification (Sarkar and Sharpe, 1999, Tamura and Nemoto, 2016, Logan and Nusse, 2004, Sarkar et al., 2000). The variable combinations of ligands and receptors render the pathway functions complex under different circumstances (Jansson et al., 2015). Wnt ligand protein WNT3a maintained the hair inducing ability of cultured dermal papilla (DP) cells (Kishimoto et al., 2000), but impeded the maintenance of stemness of neural stem cells in culture, rather, WNT3a treatment promoted differentiation of neural stem cells into neuronal cells (Muroyama et al., 2004). GSK3-specific inhibitor mediated activation of Wnt pathway maintained the pluripotency of human and mouse embryonic stem cells (Sato et al., 2004) and promoted dental tissue regeneration (Neves et al., 2017).

Here, 10 out 19 mouse Wnt genes were identified as DEGs between fresh and cultured embryonic dental mesenchymal cells. The distributions of these differentially expressed Wnt genes in DEG sets comparing cells in different stages of culture are shown in Figure V-25. Consistent to the general trend of all the DEGs, most of the Wnt DEGs (*Wnt5a, 6, 7a, 7b, 10a,11*) showed expression changes at the beginning of cell culture. *Wnt2, 4, 16* showed continued significant alterations at later stages. Wnt9a expression changes occurred only at the middle stage. Expression pattern of each differentially expressed Wnt gene was presented in Figure V-26.

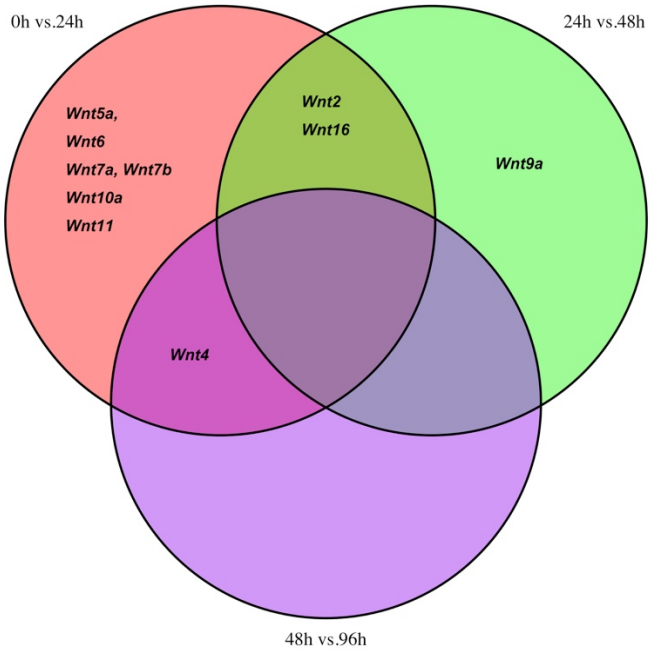

Figure V-25. Venn diagram of genes encoding Wnt proteins between DEG sets of fresh mesenchymal cells and cultured cells with different culture durations.

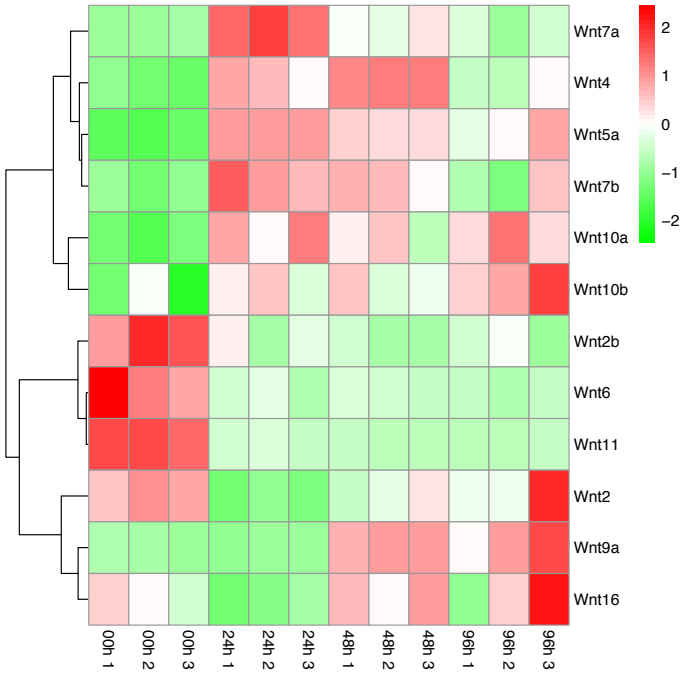

Figure V-26. Heat map of relative expression of genes encoding Wnt proteins in mesenchymal cells collected at different time points with biological replicates.

5.3.3 Considerations and limitations of current analysis

A similar study was performed by Zheng et al.(Zheng et al., 2016a) where up to 24 hours in culture E14.5 tooth germ mesenchymal cells maintained tooth inducing ability, whereas 48 hour-cultured cells formed cysts in subrenal *in vivo* culture. The differences in findings might due to different culture conditions, however, the general trend of short term culture maintained and prolonged culture impaired the odontogenic induction capacity of cultured mesenchymal cells was identical with the observations in this research. To avoid loss of important bioinformation, analysis on inductive and non-inductive cultured mesenchymal cells was mainly performed between 24h and 96h cultured cells, while the comparisons between 48h vs. 96h, when odontogenic inductivity turnover occurred in this study, were considered as a representation of strong correlation with odontogenic inductivity.

Since there were multiple time points, combinations of different comparison strategies were necessary for optimization of DEG selections. For instance, normalized counts of *Lhx6* in each time point were presented below (Table V-10). With the threshold of fold change>2, *Lhx6* would be considered to show no dysregulation throughout the culture since the fold changes of *Lhx6* between 0h vs. 24h, 24h vs. 48h and 48h vs. 96h were around 1.5. However, when compare 0h vs. 96h, *Lhx6* can be selected as DEG with fold change of 2.4. DEGs with such accumulating impact might be omitted if comparisons simply conducted between neighbouring time points.

Table V-10. Normalized counts of *Lhx6* in each time point of mesenchymal cell culture.

	0h	24h	48h	96h
Replicate 1	8314.9	6874.5	5023.0	3630.4
Replicate 2	10030.9	7222.7	5052.1	3932.3
Replicate 3	10143.3	7684.3	4801.4	4198.4
Mean	9496.4	7260.5	4958.8	3920.4
Fold change	0h vs. 24h	24h vs.48h	48h vs. 96h	0h vs. 96h
	1.3	1.5	1.3	2.4

More downstream analysis of DEGs has not been organized and presented here due to the limited time, such as enrichment analysis of gene ontology of biological process and cellular component. Interaction network of transcription factors and DEGs is of great interest as well.

Chapter VI General Discussion and Future Directions

6.1 Discussion

Biological autologous tissues or organs are preferable to artificial replacements. In dental clinics, artificial implants are not recommended when preservation of autologous tooth roots is possible even if complex surgeries such as root resections or separations were required. Stem cell based tooth bioengineering aims to generate biological teeth through activation of odontogenic induction potential of dental stem cells.

Ever since it was proved that a shift of odontogenic inductivity from dental epithelium to mesenchyme occurs during tooth development (Mina and Kollar, 1987) (Figure VI-1), many cell sources were found to be capable of responding to either epithelial or mesenchymal tooth inducing signals to initiate odontogenesis (Svandova et al., 2014). However, to date, the cell sources providing inducing signals can only be obtained from freshly isolated embryonic tooth germs, which impedes the process of clinical application of stem cell based tooth bioengineering.

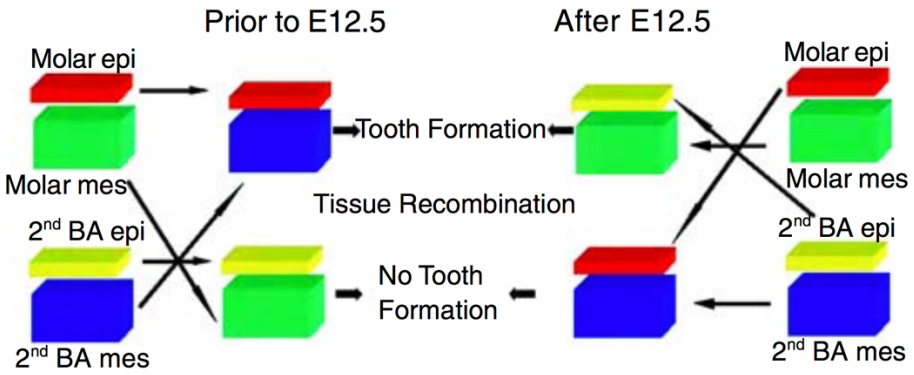

Figure VI-1. Shift of odontogenic inductivity from embryonic dental epithelium to mesenchyme.

During development of mouse molar tooth germs, prior to E12.5, the molar epithelium recombined with non-dental mesenchyme, 2nd branchial arch mesenchyme can induce tooth formation, while the dental mesenchyme cannot. After E12.5, molar mesenchyme, rather than epithelium, can induce tooth formation when recombined with non-dental counterparts. (epi: epithelium; mes: mesenchyme; BA: branchial arch). Reprinted from (Zhang et al., 2005).

It is the first time to be proved in this research that *in vitro* expanded embryonic dental mesenchymal cells can contribute to *de novo* odontogenesis as inductive cells. In reassociations/recombinations with responding dental epithelium, with presence of fresh tooth germ mesenchymal cells, cultured cells participated in tooth formation and made considerable contributions (Chapter III). Microenvironmental modification of cultured mesenchymal cells utilizing 3D culture and co-culture systems were attempted to restore their odontogenic induction capacity, however failed in tooth induction with the established experimental conditions from literature (Chapter IV). Short term cultured (within 48 hours) mesenchymal cells were found to be a natural *in vitro* proliferating cell

population that maintained odontogenic inductivity. Global gene expression profiling of fresh mesenchymal cells and cells cultured for increasing durations (24h, 48h, 96h) showed that drastic gene expression alterations occurred at the beginning of cell culture with 24 hours. In combination with gene expression comparisons between odontogenic and non-odontogenic epithelium, the *Wnt* signalling pathway including *Dlk1* showed strong correlations with maintenance of odontogenic induction capacity (Chapter V).

In reassociation assays with 24h/48h-cultured mesenchymal cells, no evident differences in tooth morphology were observed comparing with fresh cell induced tooth primordia, despite the drastic gene expression changes between short term cultured and fresh mesenchymal cells, indicating cells with full odontogenic inductivity are not necessarily noncultured cell populations, a 24h/48h-cultured-cell-like gene expression pattern will be sufficient to restore odontogenic inductivity in cells cultured for prolonged durations. In reassociation/recombination assays with mixtures of fresh and cultured mesenchymal cells, generated tooth structures were similar to the pure fresh cell induced teeth, suggesting activation of full odontogenic inductivity in long cultured cells.

Additionally, even for the standard culture, different culture protocols including whether perform heat inactivation of FBS, various culture medium recipes etc. may affect the decreasing rate of the odontogenic inductivity of standard cultured cells. As mentioned in Chapter V (5.3.3): A similar study was performed by Zheng et al. (Zheng et al., 2016a) where up to 24 hours in culture E14.5 tooth germ mesenchymal cells maintained tooth inducing ability, whereas 48 hour-cultured cells can induce tooth formation in this research. Moreover, there are several concerns about FBS safety in the production of human therapeutic products

including immune rejection and transmissible spongiform encephalopathies which can cause treatment failures and adverse reactions (Escobar and Chaparro, 2016).

6.2 Future Work

6.2.1 Short-range research plans

To understand the molecular basis of maintenance of odontogenic inductivity during *in vitro* cell proliferation, further analysis including optimization of comparison strategies and construction of transcription-factor-DEG interaction networks are required to identify the gene expression signature of cultured cells remained odontogenic inductivity.

With regard to the restoration of cultured cells that lost tooth inducing ability, in addition to optimization of experimental conditions of 3D culture and co-culture systems, since in mixed cell recombinations, cultured cells become inductive due to a possible community effect of fresh inductive cells, theoretically, a re-inductive cell population can be obtained by isolation of the cultured cells from the recombinations prior to initiation of odontogenesis (Figure VI-2). RNA sequencing raw reads of 3 replicates of the samples in this experiment are received, analysis will be performed when data preparation accomplished.

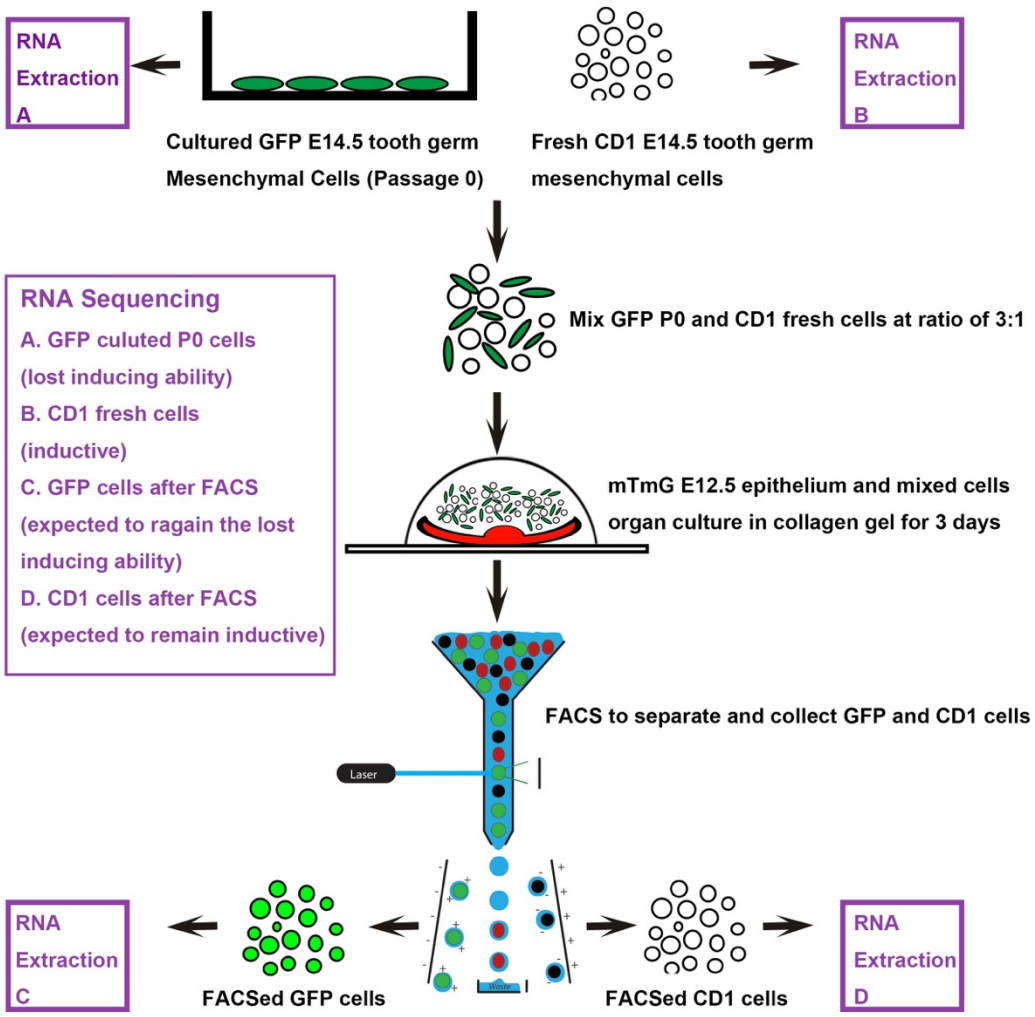

Figure VI-2. Schematic representation of experimental design.

Mixed cell recombinations were performed as described in Chapter III. Prior to tooth formation, recombinations were collected and collagen gel matrices were digested in complex enzyme containing Collagenase A and Dispase to release the cells. Mixtures of GFP and CD1 mesenchymal cells and mTmG epithelial cells were separated through FACS. Cell populations of cultured GFP and fresh CD1 before and after recombinations were prepared for RNA extraction. RNA samples with 3 replicates were sent for sequencing analysis.

The gene expression analysis will be used to provide the basis for direct restoration of inductive capacity in cultured mesenchymal cells. Signalling pathways identified including Wnt/β- catenin, will be manipulated by treating monolayer cultures of embryonic mesenchymal cells with proteins and/or small molecule agonists or antagonists. Successful up or down regulation of signalling will be assayed by using qPCR for pathway downstream genes. Inductive ability will be assayed by recombination of cells with non-inductive embryonic epithelial tissues. To test transcription factors, appropriate expression vectors will be constructed and transfected into cultured mesenchymal cells and stable lines generated. Expression levels will be established by qPCR and inductive ability assayed by recombination of cells with non-inductive embryonic epithelial cells.

6.2.2 Long-range research plans

Protocols established by embryonic cell experiments will be applied to promote tooth inducing capacity in adult mesenchymal cells. Hypothesis is that tooth inducing capacity in dental pulp mesenchyme cells can be restored by manipulating the same processes as those used in cultured embryonic mesenchymal cells. This will involve testing all the conditions and manipulations that have been found to restore inductive capacity in cultured embryonic cells in adult dental pulp cells from both mice and humans, including cultured condition alterations (3D culture, co-culture ect.), signalling pathway manipulations and transcription factor study ect. Inductive capacity will be assayed in recombinations with mouse non-inductive embryonic dental epithelial tissues and further tested with mouse/human adult non-dental epithelial cells, such as gingival epithelial cells. Finally, tooth primordia bioengineered entirely from human adult cell populations will be transplanted into the oral cavities of immune-compromised mice.

Bibliography

ABOU NEEL, E. A., CHRZANOWSKI, W., SALIH, V. M., KIM, H. W. & KNOWLES, J. C. 2014. Tissue engineering in dentistry. *J Dent,* 42**,** 915-28.

AN, Z., SABALIC, M., BLOOMQUIST, R. F., FOWLER, T. E., STREELMAN, T. & SHARPE, P. T. 2018. A quiescent cell population replenishes mesenchymal stem cells to drive accelerated growth in mouse incisors. *Nature Communications,* 9**,** 378.

ANGELOVA VOLPONI, A., KAWASAKI, M. & SHARPE, P. T. 2013. Adult human gingival epithelial cells as a source for whole-tooth bioengineering. *J Dent Res,* 92**,** 329-34.

ARNOLD, J. T., KAUFMAN, D. G., SEPPALA, M. & LESSEY, B. A. 2001. Endometrial stromal cells regulate epithelial cell growth in vitro: a new co-culture model. *Hum Reprod,* 16**,** 836-45.

ARRIGONI, C., BERSINI, S., GILARDI, M. & MORETTI, M. 2016. In Vitro Co-Culture Models of Breast Cancer Metastatic Progression towards Bone. *Int J Mol Sci,* 17.

AZEVEDO, M. M., TSIGKOU, O., NAIR, R., JONES, J. R., JELL, G. & STEVENS, M. M. 2015. Hypoxia inducible factor-stabilizing bioactive glasses for directing mesenchymal stem cell behavior. *Tissue Eng Part A,* 21**,** 382-9.

BHADRIRAJU, K. & CHEN, C. S. 2002. Engineering cellular microenvironments to improve cell-based drug testing. *Drug Discov Today,* 7**,** 612-20.

BHANDARI, R. N., RICCALTON, L. A., LEWIS, A. L., FRY, J. R., HAMMOND, A. H., TENDLER, S. J. & SHAKESHEFF, K. M. 2001. Liver tissue engineering: a role for co-culture systems in modifying hepatocyte function and viability. *Tissue Eng,* 7**,** 345-57.

BIRGERSDOTTER, A., SANDBERG, R. & ERNBERG, I. 2005. Gene expression perturbation in vitro--a growing case for three-dimensional (3D) culture systems. *Semin Cancer Biol,* 15**,** 405-12.

BOGDANOWICZ, D. R. & LU, H. H. 2014. Multifunction co-culture model for evaluating cell-cell interactions. *Methods Mol Biol,* 1202**,** 29-36.

BOLOURI, H. & DAVIDSON, E. H. 2010. The gene regulatory network basis of the "community effect," and analysis of a sea urchin embryo example. *Dev Biol,* 340**,** 170-8.

CAPLAN, A. I. 1994. The mesengenic process. *Clin Plast Surg,* 21**,** 429-35.

CARLSON, B. M. 2013. *Human Embryology and Developmental Biology*, Elsevier/Saunders.

CHAI, Y., JIANG, X., ITO, Y., BRINGAS, P., JR., HAN, J., ROWITCH, D. H., SORIANO, P., MCMAHON, A. P. & SUCOV, H. M. 2000. Fate of the mammalian cranial

neural crest during tooth and mandibular morphogenesis. *Development,* 127**,** 1671-9.

CHEN, Y., BEI, M., WOO, I., SATOKATA, I. & MAAS, R. 1996. Msx1 controls inductive signaling in mammalian tooth morphogenesis. *Development,* 122**,** 3035-44.

CORDEIRO, M. M., DONG, Z., KANEKO, T., ZHANG, Z., MIYAZAWA, M., SHI, S., SMITH, A. J. & NOR, J. E. 2008. Dental pulp tissue engineering with stem cells from exfoliated deciduous teeth. *J Endod,* 34**,** 962-9.

D'AQUINO, R., GRAZIANO, A., SAMPAOLESI, M., LAINO, G., PIROZZI, G., DE ROSA, A. & PAPACCIO, G. 2007. Human postnatal dental pulp cells co-differentiate into osteoblasts and endotheliocytes: a pivotal synergy leading to adult bone tissue formation. *Cell Death Differ,* 14**,** 1162-71.

DOMINICI, M., LE BLANC, K., MUELLER, I., SLAPER-CORTENBACH, I., MARINI, F., KRAUSE, D., DEANS, R., KEATING, A., PROCKOP, D. & HORWITZ, E. 2006. Minimal criteria for defining multipotent mesenchymal stromal cells. The International Society for Cellular Therapy position statement. *Cytotherapy,* 8**,** 315-7.

DR. DOMOKOS BARTIS, D. J. P. 2011. Three dimensional tissue cultures and tissue engineering. *In:* PÉCS, U. O. (ed.).

DU, H., SHI, H., CHEN, D., ZHOU, Y. & CHE, G. 2015. Cross-talk between endothelial and tumor cells via basic fibroblast growth factor and vascular endothelial growth factor signaling promotes lung cancer growth and angiogenesis. *Oncol Lett,* 9**,** 1089-1094.

EDMONDSON, R., BROGLIE, J. J., ADCOCK, A. F. & YANG, L. 2014. Three-dimensional cell culture systems and their applications in drug discovery and cell-based biosensors. *Assay Drug Dev Technol,* 12**,** 207-18.

EGUSA, H., SONOYAMA, W., NISHIMURA, M., ATSUTA, I. & AKIYAMA, K. 2012. Stem cells in dentistry--part I: stem cell sources. *J Prosthodont Res,* 56**,** 151-65.

ENGEL, F. B., SCHEBESTA, M., DUONG, M. T., LU, G., REN, S., MADWED, J. B., JIANG, H., WANG, Y. & KEATING, M. T. 2005. p38 MAP kinase inhibition enables proliferation of adult mammalian cardiomyocytes. *Genes Dev,* 19**,** 1175-87.

ESCOBAR, C. H. & CHAPARRO, O. 2016. Xeno-Free Extraction, Culture, and Cryopreservation of Human Adipose-Derived Mesenchymal Stem Cells. *Stem Cells Translational Medicine,* 5**,** 358-365.

FLICK, B. & KLUG, S. 2006. Whole embryo culture: an important tool in developmental toxicology today. *Curr Pharm Des,* 12**,** 1467-88.

FUKUMOTO, S. & YAMADA, Y. 2005. Review: extracellular matrix regulates tooth morphogenesis. *Connect Tissue Res,* 46**,** 220-6.

GODUGU, C., PATEL, A. R., DESAI, U., ANDEY, T., SAMS, A. & SINGH, M. 2013. AlgiMatrix™ Based 3D Cell Culture System as an In-Vitro Tumor Model for Anticancer Studies. *PLoS ONE,* 8**,** e53708.

GOERS, L., FREEMONT, P. & POLIZZI, K. M. 2014. Co-culture systems and technologies: taking synthetic biology to the next level. *J R Soc Interface,* 11.

GRAZIANO, A., D'AQUINO, R., LAINO, G. & PAPACCIO, G. 2008. Dental pulp stem cells: a promising tool for bone regeneration. *Stem Cell Rev,* 4**,** 21-6.

GRONTHOS, S., MANKANI, M., BRAHIM, J., ROBEY, P. G. & SHI, S. 2000. Postnatal human dental pulp stem cells (DPSCs) in vitro and in vivo. *Proc Natl Acad Sci U S A,* 97**,** 13625-30.

GURDON, J., TILLER, E., ROBERTS, J. & KATO, K. 1993a. A community effect in muscle development. *Current biology,* 3**,** 1-11.

GURDON, J. B. 1988. A community effect in animal development. *Nature,* 336**,** 772-4.

GURDON, J. B., LEMAIRE, P. & KATO, K. 1993b. Community effects and related phenomena in development. *Cell,* 75**,** 831-4.

HARADA, H., KETTUNEN, P., JUNG, H. S., MUSTONEN, T., WANG, Y. A. & THESLEFF, I. 1999. Localization of putative stem cells in dental epithelium and their association with Notch and FGF signaling. *J Cell Biol,* 147**,** 105-20.

HAYCOCK, J. W. 2011. 3D cell culture: a review of current approaches and techniques. *Methods Mol Biol,* 695**,** 1-15.

HIGGINS, C. A., CHEN, J. C., CERISE, J. E., JAHODA, C. A. & CHRISTIANO, A. M. 2013. Microenvironmental reprogramming by three-dimensional culture enables dermal papilla cells to induce de novo human hair-follicle growth. *Proc Natl Acad Sci U S A,* 110**,** 19679-88.

HILL, M. A. 2017. *Embryology Pharyngeal arches.* [Online]. Available: https://embryology.med.unsw.edu.au/embryology/index.php/Pharyngeal_arches [Accessed].

HONDA, M. J., IMAIZUMI, M., TSUCHIYA, S. & MORSCZECK, C. 2010. Dental follicle stem cells and tissue engineering. *J Oral Sci,* 52**,** 541-52.

HOU, P., LI, Y., ZHANG, X., LIU, C., GUAN, J., LI, H., ZHAO, T., YE, J., YANG, W., LIU, K., GE, J., XU, J., ZHANG, Q., ZHAO, Y. & DENG, H. 2013. Pluripotent stem cells induced from mouse somatic cells by small-molecule compounds. *Science,* 341**,** 651-4.

HU, B., UNDA, F., BOPP-KUCHLER, S., JIMENEZ, L., WANG, X. J., HAIKEL, Y., WANG, S. L. & LESOT, H. 2006. Bone marrow cells can give rise to ameloblast-like cells. *J Dent Res,* 85**,** 416-21.

HU, X., LIN, C., SHEN, B., RUAN, N., GUAN, Z., CHEN, Y. & ZHANG, Y. 2014. Conserved odontogenic potential in embryonic dental tissues. *J Dent Res,* 93**,** 490-5.

IBARRETXE, G., ALVAREZ, A., CANAVATE, M. L., HILARIO, E., AURREKOETXEA, M. & UNDA, F. 2012. Cell Reprogramming, IPS Limitations, and Overcoming Strategies in Dental Bioengineering. *Stem Cells Int,* 2012**,** 365932.

IKEDA, E., MORITA, R., NAKAO, K., ISHIDA, K., NAKAMURA, T., TAKANO-YAMAMOTO, T., OGAWA, M., MIZUNO, M., KASUGAI, S. & TSUJI, T. 2009. Fully functional bioengineered tooth replacement as an organ replacement therapy. *Proc Natl Acad Sci U S A,* 106**,** 13475-80.

IKEDA, E., YAGI, K., KOJIMA, M., YAGYUU, T., OHSHIMA, A., SOBAJIMA, S., TADOKORO, M., KATSUBE, Y., ISODA, K., KONDOH, M., KAWASE, M., GO, M. J., ADACHI, H., YOKOTA, Y., KIRITA, T. & OHGUSHI, H. 2008. Multipotent cells from the human third molar: feasibility of cell-based therapy for liver disease. *Differentiation,* 76**,** 495-505.

INANC, B., ELCIN, A. E. & ELCIN, Y. M. 2009. In vitro differentiation and attachment of human embryonic stem cells on periodontal tooth root surfaces. *Tissue Eng Part A,* 15**,** 3427-35.

IWATA, J., BRINGAS, P. & CHAI, Y.: University of Southern California. Available: https://www.facebase.org/mouseanatomy [Accessed 2014].

JAKUBIKOVA, J., CHOLUJOVA, D., HIDESHIMA, T., GRONESOVA, P., SOLTYSOVA, A., HARADA, T., JOO, J., KONG, S.-Y., SZALAT, R. E., RICHARDSON, P. G., MUNSHI, N. C., DORFMAN, D. M. & ANDERSON, K. C. 2016. A novel 3D mesenchymal stem cell model of the multiple myeloma bone marrow niche: biologic and clinical applications. *Oncotarget,* 7**,** 77326-77341.

JANSSON, L., KIM, G. S. & CHENG, A. G. 2015. Making sense of Wnt signaling-linking hair cell regeneration to development. *Front Cell Neurosci,* 9**,** 66.

JOPLING, C., BOUE, S. & IZPISUA BELMONTE, J. C. 2011. Dedifferentiation, transdifferentiation and reprogramming: three routes to regeneration. *Nat Rev Mol Cell Biol,* 12**,** 79-89.

JUNG, S., ALIBERTI, J., GRAEMMEL, P., SUNSHINE, M. J., KREUTZBERG, G. W., SHER, A. & LITTMAN, D. R. 2000. Analysis of fractalkine receptor CX(3)CR1 function by targeted deletion and green fluorescent protein reporter gene insertion. *Mol Cell Biol,* 20**,** 4106-14.

JUSSILA, M. & THESLEFF, I. 2012. Signaling networks regulating tooth organogenesis and regeneration, and the specification of dental mesenchymal and epithelial cell lineages. *Cold Spring Harb Perspect Biol,* 4**,** a008425.

KANG, H. K., ROH, S., LEE, G., HONG, S. D., KANG, H. & MIN, B. M. 2008. Osteogenic potential of embryonic stem cells in tooth sockets. *Int J Mol Med,* 21**,** 539-44.

KELLER, L., KUCHLER-BOPP, S., MENDOZA, S. A., POLIARD, A. & LESOT, H. 2011. Tooth engineering: searching for dental mesenchymal cells sources. *Front Physiol,* 2**,** 7.

KIM, D., LANGMEAD, B. & SALZBERG, S. L. 2015a. HISAT: a fast spliced aligner with low memory requirements. *Nat Meth,* 12**,** 357-360.

KIM, S., SHIN, S. J., SONG, Y. & KIM, E. 2015b. In Vivo Experiments with Dental Pulp Stem Cells for Pulp-Dentin Complex Regeneration. *Mediators Inflamm,* 2015**,** 409347.

KISHIMOTO, J., BURGESON, R. E. & MORGAN, B. A. 2000. Wnt signaling maintains the hair-inducing activity of the dermal papilla. *Genes Dev,* 14**,** 1181-5.

KOYAMA, N., OKUBO, Y., NAKAO, K. & BESSHO, K. 2009. Evaluation of pluripotency in human dental pulp cells. *J Oral Maxillofac Surg,* 67**,** 501-6.

KUCHLER-BOPP, S., BECAVIN, T., KOKTEN, T., WEICKERT, J. L., KELLER, L., LESOT, H., DEVEAUX, E. & BENKIRANE-JESSEL, N. 2016. Three-dimensional Micro-culture System for Tooth Tissue Engineering. *J Dent Res,* 95**,** 657-64.

KÖKTEN, T., LESOT, H. & KUCHLER-BOPP, S. 2014. Experimental Design for the Innervation of Tooth Forming from Implanted Cell Re-associations. 360-363.

LAI, J. H., KAJIYAMA, G., SMITH, R. L., MALONEY, W. & YANG, F. 2013. Stem cells catalyze cartilage formation by neonatal articular chondrocytes in 3D biomimetic hydrogels. *Sci Rep,* 3**,** 3553.

LI, T. X., YUAN, J., CHEN, Y., PAN, L. J., SONG, C., BI, L. J. & JIAO, X. H. 2013a. Differentiation of mesenchymal stem cells from human umbilical cord tissue into odontoblast-like cells using the conditioned medium of tooth germ cells in vitro. *Biomed Res Int,* 2013**,** 218543.

LI, Z., YU, M. & TIAN, W. 2013b. An inductive signalling network regulates mammalian tooth morphogenesis with implications for tooth regeneration. *Cell Prolif,* 46**,** 501-8.

LIAO, Y., SMYTH, G. K. & SHI, W. 2014. featureCounts: an efficient general purpose program for assigning sequence reads to genomic features. *Bioinformatics,* 30**,** 923-30.

LIN, D., HUANG, Y., HE, F., GU, S., ZHANG, G., CHEN, Y. & ZHANG, Y. 2007. Expression survey of genes critical for tooth development in the human embryonic tooth germ. *Dev Dyn,* 236**,** 1307-12.

LIN, R. Z. & CHANG, H. Y. 2008. Recent advances in three-dimensional multicellular spheroid culture for biomedical research. *Biotechnol J,* 3**,** 1172-84.

LIU, L., LIU, Y. F., ZHANG, J., DUAN, Y. Z. & JIN, Y. 2013. Ameloblasts serum-free conditioned medium: bone morphogenic protein 4-induced odontogenic differentiation of mouse induced pluripotent stem cells. *J Tissue Eng Regen Med*.

LIU, W., SELEVER, J., LU, M. F. & MARTIN, J. F. 2003. Genetic dissection of Pitx2 in craniofacial development uncovers new functions in branchial arch morphogenesis, late aspects of tooth morphogenesis and cell migration. *Development,* 130**,** 6375-85.

LOGAN, C. Y. & NUSSE, R. 2004. The Wnt signaling pathway in development and disease. *Annu Rev Cell Dev Biol,* 20**,** 781-810.

LOVE, M. I., HUBER, W. & ANDERS, S. 2014. Moderated estimation of fold change and dispersion for RNA-seq data with DESeq2. *Genome Biology,* 15**,** 550.

LV, D., YU, S.-C., PING, Y.-F., WU, H., ZHAO, X., ZHANG, H., CUI, Y., CHEN, B., ZHANG, X., DAI, J., BIAN, X.-W. & YAO, X.-H. 2016. A three-dimensional collagen scaffold cell culture system for screening anti-glioma therapeutics. *Oncotarget,* 7**,** 56904-56914.

MAMMOTO, T., MAMMOTO, A., TORISAWA, Y. S., TAT, T., GIBBS, A., DERDA, R., MANNIX, R., DE BRUIJN, M., YUNG, C. W., HUH, D. & INGBER, D. E. 2011. Mechanochemical control of mesenchymal condensation and embryonic tooth organ formation. *Dev Cell,* 21**,** 758-69.

MIKI, Y., ONO, K., HATA, S., SUZUKI, T., KUMAMOTO, H. & SASANO, H. 2012. The advantages of co-culture over mono cell culture in simulating in vivo environment. *J Steroid Biochem Mol Biol,* 131**,** 68-75.

MINA, M. & KOLLAR, E. J. 1987. The induction of odontogenesis in non-dental mesenchyme combined with early murine mandibular arch epithelium. *Arch Oral Biol,* 32**,** 123-7.

MIURA, M., GRONTHOS, S., ZHAO, M., LU, B., FISHER, L. W., ROBEY, P. G. & SHI, S. 2003. SHED: stem cells from human exfoliated deciduous teeth. *Proc Natl Acad Sci U S A,* 100**,** 5807-12.

MORSCZECK, C., GOTZ, W., SCHIERHOLZ, J., ZEILHOFER, F., KUHN, U., MOHL, C., SIPPEL, C. & HOFFMANN, K. H. 2005. Isolation of precursor cells (PCs) from human dental follicle of wisdom teeth. *Matrix Biol,* 24**,** 155-65.

MUROYAMA, Y., KONDOH, H. & TAKADA, S. 2004. Wnt proteins promote neuronal differentiation in neural stem cell culture. *Biochemical and Biophysical Research Communications,* 313**,** 915-921.

MUZUMDAR, M. D., TASIC, B., MIYAMICHI, K., LI, L. & LUO, L. 2007. A global double-fluorescent Cre reporter mouse. *Genesis,* 45**,** 593-605.

NAIT LECHGUER, A., KUCHLER-BOPP, S., HU, B., HAÏKEL, Y. & LESOT, H. 2008. Vascularization of Engineered Teeth. *Journal of Dental Research,* 87**,** 1138-1143.

NAKAMURA, S., YAMADA, Y., KATAGIRI, W., SUGITO, T., ITO, K. & UEDA, M. 2009. Stem cell proliferation pathways comparison between human exfoliated deciduous teeth and dental pulp stem cells by gene expression profile from promising dental pulp. *J Endod,* 35**,** 1536-42.

NAKAO, K., MORITA, R., SAJI, Y., ISHIDA, K., TOMITA, Y., OGAWA, M., SAITOH, M., TOMOOKA, Y. & TSUJI, T. 2007. The development of a bioengineered organ germ method. *Nat Methods,* 4**,** 227-30.

NEVES, V. C., BABB, R., CHANDRASEKARAN, D. & SHARPE, P. T. 2017. Promotion of natural tooth repair by small molecule GSK3 antagonists. *Sci Rep,* 7**,** 39654.

NING, F., GUO, Y., TANG, J., ZHOU, J., ZHANG, H., LU, W., GAO, Y., WANG, L., PEI, D., DUAN, Y. & JIN, Y. 2010. Differentiation of mouse embryonic stem cells into dental epithelial-like cells induced by ameloblasts serum-free conditioned medium. *Biochem Biophys Res Commun,* 394**,** 342-7.

O'DONOGHUE, K. & FISK, N. M. 2004. Fetal stem cells. *Best Pract Res Clin Obstet Gynaecol,* 18**,** 853-75.

O'NEILL, C. 2015. The epigenetics of embryo development. *Animal Frontiers,* 5**,** 42-49.

OGAWA, T., KAPADIA, H., FENG, J. Q., RAGHOW, R., PETERS, H. & D'SOUZA, R. N. 2006. Functional consequences of interactions between Pax9 and Msx1 genes in normal and abnormal tooth development. *J Biol Chem,* 281**,** 18363-9.

OHAZAMA, A., MODINO, S. A., MILETICH, I. & SHARPE, P. T. 2004. Stem-cell-based tissue engineering of murine teeth. *J Dent Res,* 83**,** 518-22.

ONO, M., OSHIMA, M., OGAWA, M., SONOYAMA, W., HARA, E. S., OIDA, Y., SHINKAWA, S., NAKAJIMA, R., MINE, A., HAYANO, S., FUKUMOTO, S., KASUGAI, S., YAMAGUCHI, A., TSUJI, T. & KUBOKI, T. 2017. Practical whole-tooth restoration utilizing autologous bioengineered tooth germ transplantation in a postnatal canine model. *Sci Rep,* 7**,** 44522.

OSHIMA, M., MIZUNO, M., IMAMURA, A., OGAWA, M., YASUKAWA, M., YAMAZAKI, H., MORITA, R., IKEDA, E., NAKAO, K., TAKANO-YAMAMOTO, T., KASUGAI, S., SAITO, M. & TSUJI, T. 2011. Functional tooth regeneration using a bioengineered tooth unit as a mature organ replacement regenerative therapy. *PLoS One,* 6**,** e21531.

OSHIMA, M. & TSUJI, T. 2014a. Functional tooth regenerative therapy: tooth tissue regeneration and whole-tooth replacement. *Odontology,* 102**,** 123-36.

OSHIMA, M. & TSUJI, T. 2014b. *Whole Tooth Regeneration Using a Bioengineered Tooth*.

OTSU, K., KISHIGAMI, R., OIKAWA-SASAKI, A., FUKUMOTO, S., YAMADA, A., FUJIWARA, N., ISHIZEKI, K. & HARADA, H. 2012. Differentiation of induced pluripotent stem cells into dental mesenchymal cells. *Stem Cells Dev,* 21**,** 1156-64.

OTSU, K., KUMAKAMI-SAKANO, M., FUJIWARA, N., KIKUCHI, K., KELLER, L., LESOT, H. & HARADA, H. 2014. Stem cell sources for tooth regeneration: current status and future prospects. *Front Physiol,* 5**,** 36.

PAPPA, K. I. & ANAGNOU, N. P. 2009. Novel sources of fetal stem cells: where do they fit on the developmental continuum? *Regen Med,* 4**,** 423-33.

PENNOCK, R., BRAY, E., PRYOR, P., JAMES, S., MCKEEGAN, P., STURMEY, R. & GENEVER, P. 2015. Human cell dedifferentiation in mesenchymal condensates through controlled autophagy. *Sci Rep,* 5**,** 13113.

PETERS, H., NEUBUSER, A., KRATOCHWIL, K. & BALLING, R. 1998. Pax9-deficient mice lack pharyngeal pouch derivatives and teeth and exhibit craniofacial and limb abnormalities. *Genes Dev,* 12**,** 2735-47.

PHINNEY, D. G. & PROCKOP, D. J. 2007. Concise review: mesenchymal stem/multipotent stromal cells: the state of transdifferentiation and modes of tissue repair--current views. *Stem Cells,* 25**,** 2896-902.

POSS, K. D., WILSON, L. G. & KEATING, M. T. 2002. Heart regeneration in zebrafish. *Science,* 298**,** 2188-90.

RACKHAM, O. J., FIRAS, J., FANG, H., OATES, M. E., HOLMES, M. L., KNAUPP, A. S., SUZUKI, H., NEFZGER, C. M., DAUB, C. O., SHIN, J. W., PETRETTO, E., FORREST, A. R., HAYASHIZAKI, Y., POLO, J. M. & GOUGH, J. 2016. A predictive computational framework for direct reprogramming between human cell types. *Nat Genet,* 48**,** 331-5.

RAJAN, N., HABERMEHL, J., COTE, M. F., DOILLON, C. J. & MANTOVANI, D. 2006. Preparation of ready-to-use, storable and reconstituted type I collagen from rat tail tendon for tissue engineering applications. *Nat Protoc,* 1**,** 2753-8.

RIMANN, M. & GRAF-HAUSNER, U. 2012. Synthetic 3D multicellular systems for drug development. *Curr Opin Biotechnol,* 23**,** 803-9.

SAKA, Y., LHOUSSAINE, C., KUTTLER, C., ULLNER, E. & THIEL, M. 2011. Theoretical basis of the community effect in development. *BMC Systems Biology,* 5**,** 1-14.

SALAS-ALANIS, J. C., WOZNIAK, E., MEIN, C. A., DURAN MCKINSTER, C. C., OCAMPO-CANDIANI, J., KELSELL, D. P., HUA, R., GARZA-RODRIGUEZ, M. L., CHOATE, K. A. & BARRERA SALDAÑA, H. A. 2015. Mutations in EDA and EDAR Genes in a Large Mexican Hispanic Cohort with Hypohidrotic Ectodermal Dysplasia. *Annals of Dermatology,* 27**,** 474-477.

SARKAR, L., COBOURNE, M., NAYLOR, S., SMALLEY, M., DALE, T. & SHARPE, P. T. 2000. Wnt/Shh interactions regulate ectodermal boundary formation during mammalian tooth development. *Proc Natl Acad Sci U S A,* 97**,** 4520-4.

SARKAR, L. & SHARPE, P. T. 1999. Expression of Wnt signalling pathway genes during tooth development. *Mech Dev,* 85**,** 197-200.

SATO, N., MEIJER, L., SKALTSOUNIS, L., GREENGARD, P. & BRIVANLOU, A. H. 2004. Maintenance of pluripotency in human and mouse embryonic stem cells through activation of Wnt signaling by a pharmacological GSK-3-specific inhibitor. *Nat Med,* 10**,** 55-63.

SEKI, D., TAKESHITA, N., OYANAGI, T., SASAKI, S., TAKANO, I., HASEGAWA, M. & TAKANO-YAMAMOTO, T. 2015. Differentiation of Odontoblast-Like Cells From Mouse Induced Pluripotent Stem Cells by Pax9 and Bmp4 Transfection. *Stem Cells Transl Med,* 4**,** 993-7.

SELVARAJ, V., PLANE, J. M., WILLIAMS, A. J. & DENG, W. 2010. Switching cell fate: the remarkable rise of induced pluripotent stem cells and lineage reprogramming technologies. *Trends Biotechnol,* 28**,** 214-23.

SEO, B. M., MIURA, M., GRONTHOS, S., BARTOLD, P. M., BATOULI, S., BRAHIM, J., YOUNG, M., ROBEY, P. G., WANG, C. Y. & SHI, S. 2004. Investigation of multipotent postnatal stem cells from human periodontal ligament. *Lancet,* 364**,** 149-55.

SHARPE, P. T. 2016. Dental mesenchymal stem cells. *Development,* 143**,** 2273-2280.

SHINMURA, Y., TSUCHIYA, S., HATA, K. & HONDA, M. J. 2008. Quiescent epithelial cell rests of Malassez can differentiate into ameloblast-like cells. *J Cell Physiol,* 217**,** 728-38.

SMITH, C. E. & WARSHAWSKY, H. 1977. Quantitative analysis of cell turnover in the enamel organ of the rat incisor. Evidence for ameloblast death immediately after enamel matrix secretion. *Anat Rec,* 187**,** 63-98.

SOARES, D. G., ROSSETO, H. L., SCHEFFEL, D. S., BASSO, F. G., HUCK, C., HEBLING, J. & DE SOUZA COSTA, C. A. 2017. Odontogenic differentiation potential of human dental pulp cells cultured on a calcium-aluminate enriched chitosan-collagen scaffold. *Clin Oral Investig*.

SONOYAMA, W., LIU, Y., FANG, D., YAMAZA, T., SEO, B. M., ZHANG, C., LIU, H., GRONTHOS, S., WANG, C. Y., WANG, S. & SHI, S. 2006. Mesenchymal stem cell-mediated functional tooth regeneration in swine. *PLoS One,* 1**,** e79.

SVANDOVA, E., VESELA, B., KRIVANEK, J., HAMPL, A. & MATALOVA, E. 2014. Recent approaches in tooth engineering research. *Folia Biol (Praha),* 60 Suppl 1**,** 21-9.

TAKAHASHI, K. & YAMANAKA, S. 2006. Induction of pluripotent stem cells from mouse embryonic and adult fibroblast cultures by defined factors. *Cell,* 126**,** 663-76.

TAMURA, M. & NEMOTO, E. 2016. Role of the Wnt signaling molecules in the tooth. *Jpn Dent Sci Rev,* 52**,** 75-83.

THESLEFF, I. 2003. Epithelial-mesenchymal signalling regulating tooth morphogenesis. *J Cell Sci,* 116**,** 1647-8.

THESLEFF, I. & SHARPE, P. 1997. Signalling networks regulating dental development. *Mech Dev,* 67**,** 111-23.

THOMAS, P. D., CAMPBELL, M. J., KEJARIWAL, A., MI, H., KARLAK, B., DAVERMAN, R., DIEMER, K., MURUGANUJAN, A. & NARECHANIA, A. 2003. PANTHER: A Library of Protein Families and Subfamilies Indexed by Function. *Genome Research,* 13**,** 2129-2141.

THOMSON, J. A., ITSKOVITZ-ELDOR, J., SHAPIRO, S. S., WAKNITZ, M. A., SWIERGIEL, J. J., MARSHALL, V. S. & JONES, J. M. 1998. Embryonic Stem Cell Lines Derived from Human Blastocysts. *Science,* 282**,** 1145-1147.

TRUSKEY, G. A. 2010. Endothelial Cell Vascular Smooth Muscle Cell Co-Culture Assay For High Throughput Screening Assays For Discovery of Anti-Angiogenesis Agents and Other Therapeutic Molecules. *Int J High Throughput Screen,* 2010**,** 171-181.

TUCKER, A. & SHARPE, P. 2004. The cutting-edge of mammalian development; how the embryo makes teeth. *Nat Rev Genet,* 5**,** 499-508.

TUMMERS, M. & THESLEFF, I. 2009. The importance of signal pathway modulation in all aspects of tooth development. *J Exp Zool B Mol Dev Evol,* 312B**,** 309-19.

VOLKMER, E., DROSSE, I., OTTO, S., STANGELMAYER, A., STENGELE, M., KALLUKALAM, B. C., MUTSCHLER, W. & SCHIEKER, M. 2008. Hypoxia in static and dynamic 3D culture systems for tissue engineering of bone. *Tissue Eng Part A,* 14**,** 1331-40.

VOLPONI, A. A., PANG, Y. & SHARPE, P. T. 2010. Stem cell-based biological tooth repair and regeneration. *Trends Cell Biol,* 20**,** 715-22.

VOLPONI, A. A. & SHARPE, P. T. 2013. The tooth -- a treasure chest of stem cells. *Br Dent J,* 215**,** 353-8.

WANG, L., SHEN, H., ZHENG, W., TANG, L., YANG, Z., GAO, Y., YANG, Q., WANG, C., DUAN, Y. & JIN, Y. 2011. Characterization of stem cells from alveolar periodontal ligament. *Tissue Eng Part A,* 17**,** 1015-26.

WEAVER, V. M., PETERSEN, O. W., WANG, F., LARABELL, C. A., BRIAND, P., DAMSKY, C. & BISSELL, M. J. 1997. Reversion of the malignant phenotype of human breast cells in three-dimensional culture and in vivo by integrin blocking antibodies. *J Cell Biol,* 137**,** 231-45.

WEISSMAN, I. L. 2000. Stem cells: units of development, units of regeneration, and units in evolution. *Cell,* 100**,** 157-68.

XIONG, J., GRONTHOS, S. & BARTOLD, P. M. 2013. Role of the epithelial cell rests of Malassez in the development, maintenance and regeneration of periodontal ligament tissues. *Periodontol 2000,* 63**,** 217-33.

YALVAC, M. E., RIZVANOV, A. A., KILIC, E., SAHIN, F., MUKHAMEDYAROV, M. A., ISLAMOV, R. R. & PALOTAS, A. 2009. Potential role of dental stem cells in the cellular therapy of cerebral ischemia. *Curr Pharm Des,* 15**,** 3908-16.

YAO, S., PAN, F., PRPIC, V. & WISE, G. E. 2008. Differentiation of Stem Cells in the Dental Follicle. *Journal of Dental Research,* 87**,** 767-771.

YOUNG, H. E. & BLACK, A. C. 2004. Adult stem cells. *The Anatomical Record Part A: Discoveries in Molecular, Cellular, and Evolutionary Biology,* 276A**,** 75-102.

YU, J., HE, H., TANG, C., ZHANG, G., LI, Y., WANG, R., SHI, J. & JIN, Y. 2010. Differentiation potential of STRO-1+ dental pulp stem cells changes during cell passaging. *BMC Cell Biol,* 11**,** 32.

YU, J. & THOMSON, J. A. 2010. *Embryonic Stem Cells.* [Online]. Bethesda, MD: National Institutes of Health, U.S. Department of Health and Human

Services. Available: http://stemcells.nih.gov/info/Regenerative_Medicine/Pages/2006Chapter1.aspx [Accessed 2014].

ZHANG, J. & WANG, J. H. 2013. Human tendon stem cells better maintain their stemness in hypoxic culture conditions. *PLoS One,* 8**,** e61424.

ZHANG, L., MORSI, Y., WANG, Y., LI, Y. & RAMAKRISHNA, S. 2013. Review scaffold design and stem cells for tooth regeneration. *Japanese Dental Science Review,* 49**,** 14-26.

ZHANG, Y. D., CHEN, Z., SONG, Y. Q., LIU, C. & CHEN, Y. P. 2005. Making a tooth: growth factors, transcription factors, and stem cells. *Cell Res,* 15**,** 301-16.

ZHENG, Y., CAI, J., HUTCHINS, A. P., JIA, L., LIU, P., YANG, D., CHEN, S., GE, L., PEI, D. & WEI, S. 2016a. Remission for Loss of Odontogenic Potential in a New Micromilieu In Vitro. *PLoS One,* 11**,** e0152893.

ZHENG, Y., JIA, L., LIU, P., YANG, D., HU, W., CHEN, S., ZHAO, Y., CAI, J., PEI, D., GE, L. & WEI, S. 2016b. Insight into the maintenance of odontogenic potential in mouse dental mesenchymal cells based on transcriptomic analysis. *PeerJ,* 4**,** e1684.

ZHOU, H., WU, S., JOO, J. Y., ZHU, S., HAN, D. W., LIN, T., TRAUGER, S., BIEN, G., YAO, S., ZHU, Y., SIUZDAK, G., SCHOLER, H. R., DUAN, L. & DING, S. 2009. Generation of induced pluripotent stem cells using recombinant proteins. *Cell Stem Cell,* 4**,** 381-4.

ZHOU, Y., CHEN, H., LI, H. & WU, Y. 2017. 3D culture increases pluripotent gene expression in mesenchymal stem cells through relaxation of cytoskeleton tension. *Journal of Cellular and Molecular Medicine,* 21**,** 1073-1084.

ZHUANG, H., ALI, K., ARDU, S., TREDWIN, C. & HU, B. 2016. Autophagy in dental tissues: a double-edged sword. *Cell Death Dis,* 7**,** e2192.

ZOUMPOPOULOU, G., TSAKALIDOU, E., DEWULF, J., POT, B. & GRANGETTE, C. 2009. Differential crosstalk between epithelial cells, dendritic cells and bacteria in a co-culture model. *Int J Food Microbiol,* 131**,** 40-51.

Appendix

Gene lists of clusters

Listed below are the members of DEG clusters which were generated according to different dysregulation pattern during culture of E14.5 mouse molar tooth bud mesenchymal cells (**Figure V-9**).

Publication

YANG, L., ANGELOVA VOLPONI, A., PANG, Y. & SHARPE, P. T. 2017. Mesenchymal Cell Community Effect in Whole Tooth Bioengineering. J Dent Res, 96, 186-191.

Gene lists of clusters

Cluster 1 (3828)

37135	2610307P16Rik	4930581F22Rik	A430046D13Rik	Actr3b	Ager	Ankrd6	Asb14
37865	2610316D01Rik	4930587E11Rik	A630001G21Rik	Acvr2a	Agmo	Ankrd63	Asb4
38961	2610507I01Rik	4931403E22Rik	A730017C20Rik	Acvr2b	Ago4	Ano1	Ascc1
39873	2610524H06Rik	4931403G20Rik	A730020E08Rik	Acy1	Agrn	Ano5	Ascl2
40057	2700046A07Rik	4931440P22Rik	A730063M14Rik	Adad1	Agt	Anp32a	Asgr1
0610009L18Rik	2700069I18Rik	4933406C10Rik	A830010M20Rik	Adal	Agtr2	Anpep	Aspa
0610039K10Rik	2700081O15Rik	4933406I18Rik	A930001A20Rik	Adam11	AI182371	Anxa9	Aspdh
0610043K17Rik	2810001G20Rik	4933408B17Rik	A930006K02Rik	Adam22	AI450353	Aoah	Aspg
1110002J07Rik	2810013P06Rik	4933409K07Rik	A930013F10Rik	Adam30	AI467606	Aoc3	Aspn
1110020A21Rik	2810029C07Rik	4933413J09Rik	A930033H14Rik	Adam33	AI504432	Ap1m2	Asprv1
1110032A03Rik	2810403D21Rik	4933417E11Rik	A930041C12Rik	Adam5	AI661453	Ap1s3	Astn1
1110032F04Rik	2810408A11Rik	4933430I17Rik	AA387883	Adamdec1	AI662270	Ap4m1	Asxl3
1190002N15Rik	2810410L24Rik	4933431E20Rik	AA465934	Adamts10	AI854703	Apba2	Atat1
1300017J02Rik	2810429I04Rik	4933439C10Rik	Aadat	Adamts13	Aif1	Apcdd1	Atf3
1500015O10Rik	2810433D01Rik	4933439K11Rik	Aaed1	Adamts14	Aim2	Aph1c	Atf7ip2
1500026H17Rik	2810442N19Rik	5031426D15Rik	Aamdc	Adamts15	Airn	Aplnr	Atp1a2
1600020E01Rik	2810454H06Rik	5031434O11Rik	Aard	Adamts16	Ajap1	Apoc1	Atp1a3
1700001L05Rik	2810459M11Rik	5330417C22Rik	Aatk	Adamts17	Ak8	Apod	Atp1b2
1700001L19Rik	2810468N07Rik	5430402O13Rik	AB124611	Adamts19	Akap5	Apoe	Atp2a3
1700001O22Rik	2900011O08Rik	5430416N02Rik	Abat	Adamts2	Akap8l	Apold1	Atp2b3
1700001P01Rik	2900041M22Rik	5430421F17Rik	Abca1	Adamts20	Akna	Appl2	Atp2b4
1700003E16Rik	2900055J20Rik	5430427O19Rik	Abca13	Adamts3	Aknad1	Aqp4	Atp4a
1700003F12Rik	2900076A07Rik	5530601H04Rik	Abca14	Adamts4	Akr1c14	Aqp9	Atp6v0d2
1700008O03Rik	2900092D14Rik	5730508B09Rik	Abca2	Adamts8	Alas2	Arap3	Atp7b
1700010K23Rik	2900097C17Rik	5730522E02Rik	Abca4	Adamtsl2	Alb	Arc	Atp8a1
1700012D01Rik	3010001F23Rik	5730559C18Rik	Abca6	Adap1	Alcam	Arfgef3	Atp8a2
1700017G19Rik	3100003L05Rik	5830454E08Rik	Abca8a	Adap2	Aldh1a2	Arg1	Atp8b5
1700018A04Rik	3110035E14Rik	5830473C10Rik	Abca8b	Adarb2	Aldh1a3	Arg2	Atp9a
1700018L02Rik	3110045C21Rik	5930412G12Rik	Abca9	Adck2	Aldh3a1	Arhgap15	Atxn7l1
1700019D03Rik	3110056K07Rik	6030408B16Rik	Abcb8	Adcy2	Aldh5a1	Arhgap18	Atxn7l1os2
1700023F06Rik	3300002I08Rik	6330403K07Rik	Abcc12	Adcy4	Aldh9a1	Arhgap20	Atxn7l2
1700027H10Rik	3830408C21Rik	6430531B16Rik	Abcc9	Adcy7	Aldoc	Arhgap25	AU021092
1700028E10Rik	4430402I18Rik	6430573F11Rik	Abcd2	Adcy8	Alkal2	Arhgap30	Auts2
1700028K03Rik	4632427E13Rik	6820431F20Rik	Abcg1	Adcy9	Alkbh6	Arhgap33	AV051173
1700029J03Rik	4632428C04Rik	8430408G22Rik	Abcg3	Add2	Alox12	Arhgap33os	Avil
1700029J07Rik	4732471J01Rik	9030612E09Rik	Abcg4	Add3	Alox5ap	Arhgap4	AW046200
1700061G19Rik	4831440E17Rik	9130019P16Rik	Abcg5	Adgra3	Alpl	Arhgap6	AW549542
1700065D16Rik	4833411C07Rik	9130024F11Rik	Abcg8	Adgrb1	Alx1	Arhgap8	Awat2
1700086L19Rik	4833417C18Rik	9230102K24Rik	Abhd14b	Adgrb2	Alx4	Arhgap9	Axin2
1700086O06Rik	4833418N02Rik	9230110C19Rik	Abhd3	Adgrb3	Amacr	Arhgef15	B130034C11Rik
1700108F19Rik	4833422C13Rik	9330020H09Rik	Abi2	Adgrd1	Ambn	Arhgef16	B230118H07Rik
1700109K24Rik	4833422M21Rik	9330151L19Rik	Abi3	Adgre1	Amer2	Arhgef26	B230119M05Rik
1700113A16Rik	4921507P07Rik	9330158H04Rik	Abi3bp	Adgre4	Amigo1	Arhgef3	B230216N24Rik
1700125H03Rik	4930412C18Rik	9330159F19Rik	Ablim2	Adgrf5	Amn	Arhgef4	B230217C12Rik
1810006J02Rik	4930413G21Rik	9330162O12Rik	Ablim3	Adgrg1	Ampd1	Arhgef9	B230311B06Rik
1810011O10Rik	4930432K21Rik	9330175E14Rik	Acacb	Adgrg3	Amph	Arid4b	B330016D10Rik
1810014B01Rik	4930447C04Rik	9330179D12Rik	Acap1	Adgrl4	Amt	Arid5a	B3galt2
1810026B05Rik	4930447M23Rik	9430038I01Rik	Acat1	Adgrv1	Amy1	Arl11	B3galt5
1810041H14Rik	4930451G09Rik	9430078K24Rik	Acat3	Adi1	Angpt1	Arl4c	B3gat1
1810041L15Rik	4930455G09Rik	9430083A17Rik	Accs	Adora2a	Angptl1	Arl5b	B3gat2
1810062O18Rik	4930470H14Rik	9530026P05Rik	Ace	Adra1a	Angptl4	Armc2	B3glct
2010107G23Rik	4930478L05Rik	9530077C05Rik	Ace2	Adrb1	Angptl6	Armc3	B3gnt7
2210039B01Rik	4930480K23Rik	9530091C08Rik	Acer2	Adssl1	Ank1	Armcx6	B3gnt8
2310010J17Rik	4930486L24Rik	9930021J03Rik	Ache	AF357355	Ank2	Arnt2	B430010I23Rik
2310015A10Rik	4930502E18Rik	a	Ackr1	AF357399	Ankef1	Arrb1	B4galnt3
2410004I01Rik	4930521E06Rik	A130077B15Rik	Acod1	AF357425	Ankmy1	Arrb2	B4galnt4
2500002B13Rik	4930539E08Rik	A230050P20Rik	Acot1	AF529169	Ankrd10	Arrdc3	B830017H08Rik
2500004C02Rik	4930549G23Rik	A230057D06Rik	Acr	Afap1l1	Ankrd24	Arrdc4	B9d2
2610005L07Rik	4930557K07Rik	A230072C01Rik	Acrbp	Afp	Ankrd33b	Arsb	Bach1
2610020C07Rik	4930562C15Rik	A330009N23Rik	Acsf2	Agap1	Ankrd37	Arsj	Baiap2l2
2610027K06Rik	4930563D23Rik	A330074K22Rik	Acss1	Agap2	Ankrd44	Art3	Baiap3
2610035D17Rik	4930563E22Rik	A330076H08Rik	Acss3	Agbl3	Ankrd45	Art5	Bank1
2610203C22Rik	4930570G19Rik	A330093E20Rik	Actn3	Agbl5	Ankrd53	Asb1	Barx2

Batf	C130060C02Rik	Caskin1	Ccrl2	Cep19	Clec4a2	Cp	Cxxc5
Batf3	C130074G19Rik	Casp1	Ccser1	Cep70	Clec4a3	Cpa1	Cyb561
Bbof1	C1qa	Casp3	Cct6b	Cep83os	Clec4e	Cpa2	Cyb561d1
Bbox1	C1qb	Casp4	Cd14	Cep85l	Clec5a	Cpa4	Cybb
Bbs2	C1qc	Casp6	Cd163	Cep95	Clec7a	Cped1	Cybrd1
Bbs7	C1ql1	Casp9	Cd164l2	Cerkl	Clic5	Cplx2	Cygb
Bbs9	C1qtnf3	Casq1	Cd180	Cetn4	Clic6	Cpm	Cyp11a1
BC005561	C1qtnf4	Catsperd	Cd1d1	Cfap20	Clip4	Cpne5	Cyp26a1
BC025920	C1qtnf7	Catsperz	Cd1d2	Cfap44	Clk1	Cpne7	Cyp26b1
BC026585	C1qtnf9	Cbfa2t3	Cd200	Cfap46	Clk4	Cpne8	Cyp27a1
BC035044	C1s1	Cblb	Cd24a	Cfap57	Clmn	Cps1	Cyp2d22
BC037032	C1s2	Cbln1	Cd27	Cfap73	Clmp	Cpvl	Cyp2r1
BC039771	C230004F18Rik	Cbln2	Cd274	Cfap77	Cln3	Cpxm1	Cyp2s1
BC049730	C230035I16Rik	Cbln4	Cd300a	Cfh	Clrn1	Cr2	Cyp2t4
BC051142	C2cd3	Cbr1	Cd300c2	Cfp	Clstn3	Cracr2a	Cyp39a1
BC051226	C2cd4a	Cbs	Cd300lg	Cgn	Clu	Cradd	Cyp46a1
BC064078	C2cd4c	Ccbe1	Cd302	Cgnl1	Cluap1	Creb3l3	Cyp7b1
BC065397	C2cd5	Ccdc106	Cd33	Ch25h	Cma1	Creb3l4	Cys1
Bche	C3ar1	Ccdc113	Cd36	Chad	Cmc4	Crebrf	Cysltr1
Bckdha	C430049B03Rik	Ccdc117	Cd37	Chadl	Cmpk2	Crebzf	Cyth1
Bckdhb	C5ar1	Ccdc120	Cd38	Chd1l	Cmtm8	Creg2	Cyth4
Bcl11a	C630043F03Rik	Ccdc125	Cd40	Chd3	Cmya5	Crem	Cytip
Bcl11b	C730036E19Rik	Ccdc136	Cd46	Chd5	Cnih2	Crip3	Cyyr1
Bcl2a1a	C77080	Ccdc138	Cd48	Chdh	Cnksr2	Crispld1	D030045P18Rik
Bcl2a1b	C77370	Ccdc148	Cd52	Chgb	Cnmd	Crnde	D030068K23Rik
Bcl2a1d	C8g	Ccdc151	Cd53	Chic1	Cnnm1	Crocc	D130020L05Rik
Bcl2l11	C920021L13Rik	Ccdc155	Cd59b	Chn2	Cnr2	Crocc2	D130040H23Rik
Bcl6b	Cachd1	Ccdc157	Cd68	Chodl	Cntd1	Crtac1	D16Ertd472e
Bcl7c	Cacna1d	Ccdc158	Cd72	Chp2	Cntln	Crtc1	D330041H03Rik
Bdh2	Cacna1e	Ccdc159	Cd74	Chrd	Cntn1	Cry2	D330045A20Rik
Bdkrb2	Cacna1g	Ccdc166	Cd79a	Chrdl1	Cntn3	Crybb3	D330050G23Rik
Becn2	Cacna1h	Ccdc171	Cd79b	Chrdl2	Cntn4	Cryl1	D3Ertd751e
Begain	Cacna2d2	Ccdc173	Cd83	Chrm2	Cntn6	Crym	D430019H16Rik
Bend5	Cacna2d3	Ccdc177	Cd86	Chrna5	Cntnap1	Cryz	D430041D05Rik
Best1	Cacnb1	Ccdc190	Cd93	Chrna7	Cntnap2	Csad	D630003M21Rik
Bfsp1	Cacng4	Ccdc191	Cdadc1	Chrnb2	Cntnap4	Csf1r	D630010B17Rik
Bhlha15	Cacng7	Ccdc27	Cdc14a	Chst1	Cntnap5b	Csf2ra	D630033O11Rik
Bhlhe40	Cacng8	Ccdc28b	Cdc26	Chst10	Col11a2	Csf2rb	D630045J12Rik
Bik	Cadm2	Ccdc3	Cdc42ep4	Chst2	Col13a1	Csf2rb2	D6Ertd527e
Bin2	Cadm3	Ccdc30	Cdca7l	Chst3	Col14a1	Csf3r	D830030K20Rik
Birc2	Cadm4	Ccdc36	Cdcp1	Chst5	Col15a1	Csgalnact1	D930016D06Rik
Birc3	Cadps2	Ccdc39	Cdh1	Chst8	Col16a1	Csmd1	D930048N14Rik
Blnk	Cahm	Ccdc40	Cdh12	Ciart	Col17a1	Csmd2	Daam2
Blvrb	Calb2	Ccdc60	Cdh17	Cib2	Col18a1	Cspg5	Dab1
Bmf	Calca	Ccdc62	Cdh19	Cilp	Col22a1	Csrnp1	Dach1
Bmp3	Calcb	Ccdc85c	Cdh22	Cilp2	Col23a1	Csrnp3	Dapk2
Bmp5	Calcr	Ccdc88b	Cdh24	Cir1	Col24a1	Cst7	Dazl
Bmp6	Calcrl	Ccdc88c	Cdh5	Cirbp	Col25a1	Ctdsp2	Dbndd1
Bmp7	Calml4	Ccdc91	Cdh6	Cish	Col26a1	Ctf1	Dbpht2
Bmx	Caln1	Ccl12	Cdh8	Cited1	Col27a1	Ctf2	Dbx2
Bnc1	Camk1g	Ccl27a	Cdh9	Ckmt1	Col28a1	Ctla2a	Dcaf12l1
Bnc2	Camkv	Ccl28	Cdk19	Clca2	Col3a1	Ctla2b	Dcaf12l2
Bnip3l	Camp	Ccl3	Cdk20	Clca3a1	Col6a1	Ctrb1	Dcaf8
Brdt	Camta1	Ccl4	Cdk5r1	Clcn2	Col6a2	Ctsc	Dcdc2a
Brinp3	Cand2	Ccl6	Cdkn1b	Cldn1	Col6a5	Ctsk	Dclk2
Brwd3	Capn3	Ccl9	Cdkn1c	Cldn11	Col6a6	Ctss	Dclk3
Bsdc1	Capn6	Ccna1	Cdo1	Cldn15	Col8a2	Cttnbp2	Dcn
Btbd2	Caprin2	Ccng2	Cdr1	Cldn2	Col9a2	Cux2	Dcstamp
Btbd3	Caps2	Ccnjl	Cebpa	Cldn34c1	Col9a3	Cwc22	Dcx
Btd	Car11	Ccnl1	Cecr2	Cldn4	Colec10	Cx3cr1	Ddb2
Btg1	Car14	Ccnl2	Cecr6	Cldn7	Colgalt2	Cxcl1	Ddc
Btk	Car15	Ccp110	Cel	Clec10a	Copg2	Cxcl10	Ddx25
Btla	Car2	Ccr1	Celf2	Clec11a	Coq8a	Cxcl13	Ddx4
Btn2a2	Car7	Ccr10	Celrr	Clec12a	Corin	Cxcl16	Ddx43
Btnl9	Car8	Ccr2	Celsr1	Clec12b	Coro1a	Cxcl2	Ddx50
C030034L19Rik	Card9	Ccr3	Celsr2	Clec14a	Coro2a	Cxcl5	Ddx59
C030037D09Rik	Carf	Ccr5	Cenpv	Clec2i	Coro2b	Cxcr4	Ddx60
C130036L24Rik	Carmil3	Ccr7	Cep112	Clec2l	Cox20	Cxx1c	Deaf1
C130046K22Rik	Casd1	Ccr8	Cep131	Clec4a1	Cox4i2	Cxxc4	Dedd2

Defb36	Drc3	Egr1	F13a1	Fbxo43	Frrs1l	Gfra2	Gm19522
Dennd1c	Drp2	Egr2	F2rl2	Fbxw10	Frzb	Gfra3	Gm1966
Dennd3	Dsc3	Egr3	F2rl3	Fcer1g	Fscn3	Gfra4	Gm20199
Dennd6b	Dsel	Egr4	F730043M19Rik	Fcgbp	Fsd1l	Ggnbp1	Gm20219
Derl3	Dsg1a	Ehf	F8	Fcgr1	Ftcd	Gimap3	Gm2061
Dffb	Dsg2	Eid1	Faah	Fcgr2b	Fth1	Gimap4	Gm20751
Dgkb	Dsg3	Eid2b	Fam102a	Fcgr3	Fundc1	Gimap6	Gm2518
Dgki	Dsp	Eif4a2	Fam105a	Fcho1	Fut10	Gja4	Gm266
Dgkk	Dtd1	Elfn2	Fam107a	Fcna	Fut2	Gja5	Gm31520
Dguok	Dtl	Elmo1	Fam117a	Fcrls	Fut4	Gjc2	Gm32168
Dhdh	Dtwd2	Eln	Fam120aos	Fendrr	Fut9	Gjc3	Gm35612
Dhx58	Dtx1	Elovl2	Fam122b	Fermt1	Fuz	Gk5	Gm3704
Dio3os	Dtx3	Elovl4	Fam124b	Fermt3	Fxyd1	Gkn3	Gm38426
Diras2	Dtx3l	Emb	Fam135b	Fgd2	Fxyd2	Glb1l2	Gm4013
Dis3l2	Dupd1	Emcn	Fam13a	Fgd5	Fxyd6	Glcci1	Gm4285
Disc1	Dusp1	Emid1	Fam155a	Fgf1	Fxyd7	Gldn	Gm4349
Dixdc1	Dusp13	Emilin1	Fam161a	Fgf11	Fyb	Gli1	Gm4425
Dkk1	Dusp2	Emilin3	Fam167a	Fgf12	Fzd1	Gli3	Gm4787
Dkkl1	Dusp22	Enam	Fam171a2	Fgf14	Fzd10	Glod4	Gm4890
Dlec1	Dusp26	Endou	Fam171b	Fgf15	Fzd3	Glp2r	Gm5083
Dleu2	Dusp28	Enho	Fam178b	Fgf17	Fzd9	Glt1d1	Gm5084
Dlg2	Dusp6	Enox1	Fam180a	Fgf18	G0s2	Glt8d2	Gm5127
Dlgap3	Dync1i1	Enpep	Fam184a	Fgf21	G630025P09Rik	Glul	Gm527
Dll1	Dync2h1	Enpp1	Fam189a1	Fgf3	Gab1	Gm10046	Gm5483
Dll3	Dynlt1f	Enpp2	Fam196b	Fgfr1	Gab3	Gm10190	Gm5577
Dll4	Dyx1c1	Enpp3	Fam198a	Fgfr3	Gabra1	Gm10364	Gm5617
Dlx1	Dzank1	Entpd1	Fam19a1	Fgl2	Gabra2	Gm10432	Gm5820
Dlx3	Dzip1	Entpd3	Fam19a3	Fhit	Gabra4	Gm10549	Gm5868
Dlx4	E130008D07Rik	Epb41	Fam19a4	Fhod3	Gabrb2	Gm10658	Gm6225
Dlx4os	E130018N17Rik	Epb41l4aos	Fam209	Fibcd1	Gabrb3	Gm10677	Gm6297
Dlx6os1	E130102H24Rik	Epb41l4b	Fam213a	Fign	Gabre	Gm10789	Gm6377
Dmc1	E130114P18Rik	Epb42	Fam217a	Fignl2	Gabrg3	Gm10941	Gm6566
Dmrta1	E130307A14Rik	Epc2	Fam221a	Filip1	Gabrr1	Gm11110	Gm7008
Dmrtb1	E130308A19Rik	Epcam	Fam222a	Firre	Gad1os	Gm11266	Gm715
Dmrtc1a	E230016M11Rik	Epha3	Fam227a	Fkbp1b	Gadl1	Gm11541	Gm7173
Dmxl2	E2f2	Epha5	Fam228a	Fli1	Gal	Gm11627	Gm826
Dnaaf3	Eaf2	Epha7	Fam228b	Flrt1	Gal3st3	Gm11733	Gm867
Dnah1	Ebf1	Ephb1	Fam229b	Flt4	Galnt12	Gm11837	Gm9899
Dnah11	Ebf2	Ephb6	Fam26d	Flywch2	Galnt13	Gm11992	Gm996
Dnah17	Ebf3	Ephx3	Fam35a	Fmn2	Galnt16	Gm12522	Gmfg
Dnah2	Ebf4	Ephx4	Fam43a	Fmnl2	Galnt5	Gm12657	Gna14
Dnah7a	Echdc2	Epm2a	Fam46a	Fmo1	Galnt6	Gm12992	Gnao1
Dnah7b	Eci2	Epn3	Fam46c	Fmo2	Gap43	Gm13178	Gnaz
Dnah7c	Eci3	Epop	Fam49a	Fn3k	Gapdhs	Gm13212	Gng11
Dnah9	Ecm2	Epor	Fam69a	Fnbp4	Gas1	Gm13375	Gng2
Dnaic1	Edar	Epsti1	Fam69b	Fndc5	Gas2	Gm13547	Gng3
Dnajb13	Edaradd	Erbb3	Fam69c	Fos	Gata1	Gm13807	Gng4
Dnajb9	Edn3	Ercc6l2	Fam71a	Fosb	Gata6	Gm13889	Gng8
Dnajc22	Ednra	Erdr1	Fam71e1	Foxd1	Gatd1	Gm14207	Gngt2
Dnajc6	Ednrb	Erg	Fam78a	Foxd2os	Gatm	Gm14634	Gon7
Dnm1	Eepd1	Erich2	Fam78b	Foxd3	Gbp10	Gm15408	Got1l1
Dnm3os	Efcab1	Ermap	Fam83b	Foxf1	Gbp7	Gm15506	Gpa33
Dnmt3a	Efcab2	Ermn	Fam89a	Foxj1	Gbp9	Gm15612	Gpat2
Doc2b	Efhb	Ermp1	Fancc	Foxl1	Gbx2	Gm15631	Gpbp1l1
Doc2g	Efhc1	Esam	Fank1	Foxn3	Gcc1	Gm15706	Gpc2
Dock10	Efhc2	Esr1	Fap	Foxo6	Gcgr	Gm15708	Gpc3
Dock2	Efhd1	Esrrb	Far2	Foxp2	Gch1	Gm16070	Gpc6
Dock3	Efna1	Esrrg	Fat2	Foxred2	Gck	Gm16386	Gpd1
Dock6	Efna2	Ets2	Fat3	Fpr2	Gdap10	Gm1653	Gpm6a
Dok2	Efna3	Etv1	Fbln1	Fras1	Gdap1l1	Gm1661	Gpr132
Dok3	Efna4	Evc	Fbln7	Frat1	Gdf10	Gm16702	Gpr137c
Dpf3	Efnb3	Evi2a	Fbxl13	Frat2	Gdf5	Gm1673	Gpr146
Dpp6	Efr3b	Evl	Fbxl16	Frem1	Gdf7	Gm16740	Gpr155
Dpyd	Efs	Evpl	Fbxl19	Frg2f1	Gdpd2	Gm16845	Gpr162
Dpysl4	Egfem1	Exoc3l	Fbxl22	Frk	Gdpd3	Gm16853	Gpr165
DQ267100	Egfl6	Exph5	Fbxo10	Frmd5	Gem	Gm16973	Gpr171
DQ267101	Egfl7	Eya2	Fbxo27	Frmpd1	Gfap	Gm16982	Gpr173
DQ267102	Egfl8	Eya4	Fbxo33	Frmpd3	Gfpt2	Gm17066	Gpr182
Draxin	Egflam	F11r	Fbxo41	Frmpd4	Gfra1	Gm19461	Gpr183

Gpr21	H3f3a	Hspa12b	Ing4	Kazald1	Klf14	Lincred1	Lyve1
Gpr22	H3f3b	Hspa1a	Inha	Kazn	Klf2	Lingo1	Lyz2
Gpr25	Haghl	Hspa1b	Inmt	Kbtbd11	Klf4	Lingo3	Lztfl1
Gpr27	Hap1	Htr1a	Ino80dos	Kbtbd13	Klhdc8b	Lipc	Lzts3
Gpr3	Hapln3	Htr1f	Inpp4b	Kbtbd7	Klhl10	Lipe	Macrod2
Gpr34	Has1	Htr2b	Inpp5d	Kcna1	Klhl15	Lix1	Madcam1
Gpr37	Has3	Htr5b	Inpp5j	Kcna2	Klhl17	Lix1l	Madd
Gpr4	Hbp1	Htra3	Insig1	Kcna3	Klhl23	Lmntd2	Maf
Gpr55	Hcar2	Hvcn1	Ints6l	Kcna4	Klhl24	Lmo1	Maf1
Gpr65	Hcls1	Hyal3	Ip6k2	Kcna6	Klhl3	Lmo2	Mafb
Gpr84	Hcn1	Hymai	Iqcb1	Kcnab2	Klhl32	Lmo3	Maged2
Gpr88	Hcn3	Ibsp	Iqcd	Kcnb1	Klhl34	Lmx1a	Magee2
Gprasp1	Hcn4	Ica1	Iqcg	Kcnc2	Klhl36	Lnx1	Magef1
Gprasp2	Hcrtr2	Icam1	Iqsec2	Kcnd3	Klhl4	LOC101056073	Magel2
Gprc5c	Hdac11	Icam2	Irf1	Kcne1l	Klhl40	LOC102640359	Mak
Gprin1	Hdac5	Icos	Irf2bp2	Kcne4	Klhl6	LOC105246056	Malt1
Gprin2	Hdac8	Icosl	Irf2bpl	Kcng1	Klhl7	LOC106557447	Maml3
Gpsm3	Hdac9	Id1	Irf4	Kcng3	Klrb1a	LOC106740	Mamstr
Gpt	Hdc	Id2	Irf5	Kcng4	Klrb1c	Lockd	Maneal
Gramd1a	Hddc2	Ier2	Irf6	Kcnh1	Kmt5c	Lonrf2	Mansc4
Gramd1b	Hddc3	Ifi203	Irf8	Kcnh3	Kremen2	Lonrf3	Maob
Gramd1c	Hecw2	Ifi207	Irf9	Kcnh5	Krt1	Lpar1	Map1b
Grap	Heph	Ifi27	Irgm2	Kcnip2	Krt10	Lpar3	Map2
Grasp	Hes5	Ifi27l2a	Irx2	Kcnip3	Krt14	Lpl	Map2k6
Grb7	Hes7	Ifi44	Isl1	Kcnip4	Krt15	Lppos	Map3k13
Greb1	Hexdc	Ifit3	Islr	Kcnj11	Krt17	Lpxn	Map3k5
Grhl2	Hexim1	Ifitm1	Islr2	Kcnj2	Krt222	Lrfn1	Map3k8
Gria1	Hexim2	Ifitm2	Ism1	Kcnj3	Krt5	Lrfn2	Map4k1
Gria2	Hey1	Ifitm5	Ism2	Kcnj8	Krt6a	Lrfn5	Map4k2
Gria4	Heyl	Ifnlr1	Isoc1	Kcnma1	Ksr1	Lrguk	Map7d2
Grid1	Hfe	Ift140	Isoc2a	Kcnmb4	Ky	Lrmp	Mapk10
Grid2ip	Hfm1	Ift80	Ispd	Kcnn2	L3mbtl3	Lrp1b	Mapk13
Grik1	Hgf	Ift88	Isyna1	Kcnn3	Lag3	Lrp3	Mapk15
Grik4	Hhatl	Igdcc3	Itga2	Kcnq1	Lair1	Lrp4	Mapk4
Grik5	Hhex	Igdcc4	Itga9	Kcnq1ot1	Lama3	Lrrc17	Mapk8
Grin2a	Hhip	Igfbp3	Itgal	Kcnq4	Lamc3	Lrrc23	Mapk8ip1
Grin2c	Hhipl2	Igfbp4	Itgb1bp2	Kcnrg	Laptm5	Lrrc25	Mapk8ip2
Grin3a	Hic2	Igflr1	Itgb2	Kcns1	Large2	Lrrc34	Marveld2
Grm3	Hid1	Igll1	Itgb3	Kcns3	Lat	Lrrc3b	Mas1
Grm4	Hif3a	Iglon5	Itgb3bp	Kcnt2	Lat2	Lrrc4	Matk
Grtp1	Hist1h2ae	Igsf10	Itgb8	Kcnu1	Lax1	Lrrc49	Matn2
Gsc	Hist1h2ai	Igsf11	Itgbl1	Kcp	Lbp	Lrrc4b	Matn4
Gsg1l	Hist2h2be	Igsf3	Itih5	Kctd12	Lck	Lrrc55	Mb21d2
Gsta3	Hist3h2ba	Igsf6	Itk	Kctd12b	Lcn2	Lrrc56	Mbnl3
Gstk1	Hk3	Igtp	Itm2a	Kctd14	Lcorl	Lrrc63	Mbtd1
Gstm5	Hkdc1	Ihh	Itpk1	Kctd16	Lcp1	Lrrc7	Mbtps1
Gstm6	Hlcs	Iigp1	Itpka	Kdf1	Lcp2	Lrrn1	Mc2r
Gstm7	Hlf	Ikzf1	Itpkb	Kdm5b	Ldb2	Lrrn2	Mc5r
Gstt1	Hmgb3	Ikzf4	Ivd	Kdm6a	Ldlrad3	Lrrn3	Mccc1os
Gtdc1	Hmgcs2	Il10	Iyd	Kdm7a	Lef1	Lrrtm1	Mccc2
Gtf2i	Hoga1	Il10ra	Jag2	Kdr	Letm2	Lrrtm2	Mcf2
Gucy1b2	Hook1	Il11ra1	Jak3	Kera	Lgals4	Lrrtm3	Mchr1
Gucy2e	Hopx	Il13	Jakmip2	Khdrbs2	Lgals7	Lrrtm4	Mcl1
Gucy2f	Hoxd8	Il16	Jarid2	Kif16b	Lgi1	Lsamp	Mcm9
Guf1	Hp	Il17rb	Jmjd1c	Kif17	Lgi2	Lst1	Mcmdc2
Gxylt2	Hpca	Il17rd	Jmy	Kif19a	Lgi3	Ltb	Mcoln2
Gypa	Hpcal4	Il18	Josd1	Kif21a	Lgi4	Ltbp4	Mctp1
H1f0	Hpgd	Il1b	Jph3	Kif21b	Lgr4	Luc7l3	Mdfi
H1foo	Hpgds	Il1r2	Jph4	Kif26a	Lgr5	Lum	Mdga1
H1fx	Hpse	Il1rapl1	Jpx	Kif26b	Lhfpl2	Lvrn	Mdga2
H2-Aa	Hpse2	Il1rapl2	Jsrp1	Kif27	Lhfpl4	Ly6h	Mdk
H2-Ab1	Hrc	Il20ra	Jun	Kif3a	Lhpp	Ly86	Mdm1
H2-DMb1	Hs3st4	Il21r	Junb	Kif5a	Lifr	Ly9	Me3
H2-DMb2	Hs3st5	Il22ra1	Jund	Kifc2	Lilr4b	Lyl1	Meaf6
H2-Ke6	Hs3st6	Il33	Kank3	Kit	Lilra6	Lypd1	Mecom
H2-M3	Hsd11b2	Il6	Kank4	Kiz	Lilrb4a	Lypd3	Med12l
H2-Oa	Hsd17b14	Impg2	Kansl1l	Klf10	Lin28b	Lypd6b	Med31
H2-T23	Hsd3b7	Ing2	Kantr	Klf11	Lin7a	Lyplal1	Mef2c
H2afv	Hsf3	Ing3	Kat6b	Klf12	Lin7b	Lysmd3	Megf11

Megf6	Mmp15	Myo15	Ngp	Ntrk3	Pald1	Pcsk1n	Pkd1l3
Mei4	Mmp25	Myo16	Nhs	Nudt13	Palmd	Pcsk5	Pkdcc
Meiob	Mmp9	Myo1f	Nhsl1	Nudt14	Pan2	Pcyt1b	Pkhd1
Meioc	Mmrn1	Myo1g	Nhsl2	Nudt17	Pantr1	Pdcd4	Pkhd1l1
Meltf	Mmrn2	Myo5b	Nim1k	Nup210	Panx2	Pde11a	Pkia
Meox1	Mndal	Myo6	Nipal2	Nupr1l	Panx3	Pde1a	Pkib
Mesp2	Mnt	Myo7a	Nipsnap1	Nwd2	Papln	Pde1b	Pknox2
Mest	Mob3b	Myom2	Nkain3	Nxf2	Paqr3	Pde1c	Pkp3
Metap1d	Mog	Myom3	Nkd1	Nxnl2	Paqr5	Pde2a	Pla2g3
Mettl15	Morc1	Myoz3	Nkx2-3	Nxpe2	Paqr6	Pde3a	Pla2g4c
Mettl23	Morn1	Myrf	Nlgn1	Nxpe4	Pard3b	Pde3b	Pla2g4e
Mettl24	Mos	Myrip	Nlgn2	Nxph1	Park2	Pde4c	Pla2g5
Mettl27	Moxd1	Myzap	Nlgn3	Nyx	Parp14	Pde5a	Plac1
Mex3a	Mpeg1	Mzb1	Nlrp1b	Oas1a	Parp16	Pde7b	Plag1
Mex3b	Mpo	N4bp2	Nlrp3	Oas1b	Parp9	Pde9a	Plagl1
Mfap2	Mpp2	N4bp2l1	Nlrp5-ps	Oas2	Particl	Pdgfra	Plbd1
Mfap4	Mpp3	N4bp3	Nlrp6	Oasl1	Parvb	Pdk1	Plcb1
Mfng	Mpped2	Naalad2	Nmbr	Oasl2	Parvg	Pdk2	Plcb2
Mfsd13a	Mpst	Nadk2	Nme3	Oaz2	Pax9	Pdlim4	Plcg1
Mfsd2b	Mpzl1	Naip2	Nmi	Oaz3	Paxbp1	Pdp1	Plch1
Mfsd4a	Mpzl2	Nalcn	Nmnat2	Obscn	Pbx2	Pdxp	Plch2
Mfsd4b5	Mrc1	Nanos3	Nmral1	Obsl1	Pcbd1	Pdzd2	Plcl2
Mfsd7a	Mrnip	Nap1l5	Nnat	Ocln	Pccb	Pdzk1ip1	Plcxd3
Mgarp	Mro	Napb	Nod2	Ocstamp	Pcdh1	Pdzrn3	Pld4
Mgat4a	Mroh6	Napsa	Nos1	Ogt	Pcdh10	Pdzrn4	Pld5
Mgat5	Ms4a2	Narf	Nos3	Oit3	Pcdh11x	Pecam1	Plek
Mgat5b	Ms4a4a	Nat8l	Notch3	Olfm1	Pcdh12	Peg10	Plekha5
Mgp	Ms4a4c	Nav3	Notch4	Olfm4	Pcdh15	Peg3	Plekha6
Mia	Ms4a6b	Ncald	Notum	Olfml1	Pcdh17	Peli1	Plekhg1
Mib2	Ms4a6c	Ncam2	Nova2	Olfml2a	Pcdh20	Penk	Plekhg5
Milr1	Ms4a6d	Ncan	Noxo1	Olfml3	Pcdh8	Per1	Plekhs1
Mindy4	Ms4a7	Ncf1	Npas2	Olfr1372-ps1	Pcdhac1	Per2	Pllp
Mir186	Msantd1	Ncf2	Nphp3	Olfr876	Pcdhb10	Pf4	Plp1
Mir1938	Msh2	Ncf4	Npl	Olfr920	Pcdhb11	Pfkm	Plppr1
Mir212	Msh5	Nckap1l	Npm2	Omd	Pcdhb12	Pfn2	Plppr3
Mir23a	Msi1	Nckap5	Nppc	Omp	Pcdhb13	Pfn4	Plppr4
Mir24-2	Msi2	Ncoa1	Npr1	Ooep	Pcdhb14	Pgghg	Plppr5
Mir27a	Msr1	Ncoa7	Nptx1	Ophn1	Pcdhb15	Pglyrp1	Pls1
Mir3058	Msrb2	Ndp	Nr3c2	Oplah	Pcdhb16	Pgm2l1	Plscr1
Mir3061	Mst1r	Ndrg2	Nr4a1	Opn1sw	Pcdhb17	Pgm5	Plscr4
Mir3064	Mstn	Ndst3	Nr4a2	Oprd1	Pcdhb18	Phactr2	Plvap
Mir335	Msx1	Ndufa4l2	Nr4a3	Osbp2	Pcdhb19	Phactr3	Plxdc1
Mir467c	Msx1os	Necab1	Nr5a2	Osgep	Pcdhb2	Phex	Plxna4
Mir6386	Mtcl1	Necab3	Nrap	Osm	Pcdhb20	Phf1	Plxnb3
Mir677	Mtfp1	Nefl	Nrarp	Osr2	Pcdhb21	Phf21a	Plxnd1
Mir6907	Mthfs	Negr1	Nrbp2	Ostn	Pcdhb22	Phf21b	Pm20d2
Mir6935	Mthfsl	Neil2	Nrep	Otof	Pcdhb3	Phf24	Pnisr
Mir6976	Mtmr7	Neil3	Nrg3	Otogl	Pcdhb4	Phip	Pnkd
Mir6992	Mtss1	Nek1	Nrg4	Otor	Pcdhb5	Phkb	Pnldc1
Mir7-1	Mturn	Nell1	Nrgn	Oxtr	Pcdhb6	Phlda2	Pnmal2
Mir7036	Mtx3	Nemp2	Nrk	P2rx3	Pcdhb7	Phospho1	Pnpla3
Mir704	Muc1	Neo1	Nrn1	P2ry1	Pcdhb8	Phyh	Pnrc1
Mir7673	Muc13	Net1	Nrp2	P2ry10	Pcdhb9	Phyhip	Podxl
Mir92b	Mx1	Neto2	Nrros	P2ry12	Pcdhga1	Pi15	Podxl2
Mir99ahg	Mx2	Neurl1a	Nrsn1	P2ry13	Pcdhga2	Pi16	Pof1b
Mirlet7d	Mxd1	Neurl1b	Nrsn2	P2ry14	Pcdhga3	Pianp	Pogk
Mirlet7f-1	Mxd3	Neurl3	Nrtn	P2ry6	Pcdhga4	Pigp	Poli
Misp	Mxi1	Nfam1	Nrxn1	P3h2	Pcdhga6	Pik3ap1	Polr3gl
Mitf	Myb	Nfasc	Nrxn2	P3h3	Pcdhga9	Pik3c2g	Postn
Mkrn1	Mybpc2	Nfatc1	Nrxn3	P4htm	Pcdhgb1	Pik3cd	Pou3f1
Mkrn2os	Mybpc3	Nfatc2	Nsmf	Pabpc4l	Pcdhgb6	Pik3r6	Pou3f2
Mkrn3	Mycbpap	Nfatc4	Nt5e	Pacrg	Pcdhgb7	Pim1	Pou3f3
Mkx	Mycn	Nfe2	Ntf5	Pacsin1	Pcdhgc4	Pink1	Pou6f1
Mlf1	Myef2	Nfe2l3	Ntm	Padi3	Pced1a	Pipox	Ppdpf
Mllt3	Myh7b	Nfia	Ntn1	Padi4	Pcf11	Pirb	Ppef1
Mllt6	Myh8	Nfib	Ntn3	Pafah1b3	Pclo	Pitpnc1	Ppfia2
Mlph	Myl4	Nfkbid	Ntn5	Paip2	Pcmtd2	Pitpnm3	Ppfia4
Mlxipl	Mylip	Nfkbiz	Ntng1	Pak1	Pcnx	Pitx2	Ppfibp2
Mme	Mylk3	Ngfr	Ntrk2	Pak6	Pcsk1	Piwil1	Ppl

Ppm1e	Psma8	Rasd1	Rhox5	Rxfp3	Sema6a	Slc15a2	Smim24
Ppm1j	Psmb8	Rasgef1b	Rhpn1	Rxra	Sema6b	Slc15a3	Smim3
Ppm1k	Psmb9	Rasgrf2	Rhpn2	Rxrg	Sema6c	Slc16a10	Smkr-ps
Ppp1r13b	Pstpip1	Rasgrp4	Ribc2	Rybp	Sema6d	Slc16a2	Smoc1
Ppp1r14c	Ptafr	Rasip1	Rilpl2	Ryr1	Sema7a	Slc16a8	Smoc2
Ppp1r15a	Ptch1	Rasl10a	Rimbp2	Ryr2	Senp7	Slc16a9	Smox
Ppp1r16b	Ptch2	Rasl10b	Rimkla	Ryr3	Serf1	Slc18a1	Smpd3
Ppp1r26	Ptgdr	Rasl12	Rimklb	S100a1	Serinc2	Slc18b1	Smpd5
Ppp1r36	Ptger3	Rasl2-9	Rims1	S100a14	Serinc4	Slc1a2	Smpx
Ppp1r3b	Ptger4	Rassf10	Rin2	S100a16	Serpina3f	Slc22a17	Smtnl2
Ppp1r3c	Ptgfr	Rassf2	Rinl	S100a8	Serpina3n	Slc22a23	Smyd3
Ppp1r3f	Ptgis	Rassf4	Ripor3	S100a9	Serpinb12	Slc22a3	Snap25
Ppp1r3g	Pth1r	Rassf9	Ripply3	S100b	Serpinb5	Slc22a5	Snca
Ppp1r9a	Pth2r	Raver2	Rmnd5a	S1pr3	Serpinb6b	Slc23a1	Sned1
Ppp1r9b	Pthlh	Rbfox1	Rmst	S1pr4	Serpind1	Slc25a23	Snhg10
Ppp2r2b	Ptn	Rbm11	Rnasel	Sall3	Sertad3	Slc25a27	Snhg11
Ppp2r3d	Ptov1	Rbm24	Rnf112	Sall4	Sertm1	Slc25a31	Snhg18
Ppp3cc	Ptpdc1	Rbm39	Rnf122	Samd14	Sesn1	Slc25a36	Snhg8
Ppp3r2	Ptpn18	Rbm3os	Rnf125	Samd15	Sesn3	Slc25a53	Snora21
Ppp4r1l-ps	Ptpn20	Rbm46	Rnf130	Samd9l	Sez6l	Slc26a10	Snora28
Ppp4r4	Ptpn4	Rbm47	Rnf138rt1	Sapcd1	Sez6l2	Slc26a11	Snora31
Ppp6r2	Ptpn6	Rbm4b	Rnf144a	Sardh	Sfrp1	Slc27a3	Snora44
Pqlc1	Ptprc	Rbmx	Rnf152	Sarm1	Sfrp2	Slc27a6	Snora81
Prag1	Ptprcap	Rbp1	Rnf157	Sash3	Sfrp4	Slc2a12	Snord104
Pram1	Ptprd	Rbp7	Rnf167	Sat2	Sfrp5	Slc2a13	Snord123
Prcd	Ptpro	Rcbtb2	Rnf17	Satb1	Sfxn4	Slc30a10	Snord23
Prdm1	Ptprr	Rcor2	Rnf180	Satb2	Sfxn5	Slc35d3	Snord32a
Prdm11	Ptprs	Rcsd1	Rnf182	Saxo2	Sgcz	Slc37a2	Snord37
Prdx2	Ptprt	Rd3	Rnf207	Sbk1	Sgtb	Slc38a3	Snord55
Prelid2	Ptpru	Rdm1	Rnf208	Sbk2	Sh2d4b	Slc39a8	Sntb1
Prelid3a	Pts	Rec8	Rnf225	Scai	Sh2d5	Slc40a1	Sntg2
Prex1	Pycard	Reck	Rnf32	Scaper	Sh2d7	Slc41a1	Snx29
Prex2	Pygl	Redrum	Rnft2	Scara5	Sh3bgrl2	Slc43a3	Sobp
Prickle2	Pygm	Reep1	Rnu73b	Scarf1	Sh3bp2	Slc44a1	Socs1
Primpol	Pygo1	Rem2	Robo1	Scarna13	Sh3bp5	Slc44a5	Socs2
Prkcb	Pyroxd2	Reps2	Ror1	Scd2	Sh3gl2	Slc45a2	Socs3
Prkch	Qprt	Rerg	Rora	Scg2	Sh3gl3	Slc4a11	Soga3
Prkcq	Qrich2	Ret	Rorb	Scg3	Sh3rf2	Slc4a3	Sorcs3
Prkra	R74862	Retreg1	Rorc	Scin	Sh3tc1	Slc4a5	Sorl1
Prmt8	Rab11fip4	Rev3l	Rp9	Scml2	Shank1	Slc52a3	Sort1
Prob1	Rab15	Rflna	Rpgrip1	Scml4	Shank3	Slc5a7	Sostdc1
Proca1	Rab20	Rftn2	Rpl39l	Scn1a	Shc2	Slc6a13	Sowaha
Prokr1	Rab26	Rfx2	Rprd1a	Scn2b	Shcbp1l	Slc6a17	Sox10
Prokr2	Rab26os	Rfx3	Rprml	Scn3a	Shd	Slc6a3	Sox12
Prom1	Rab33a	Rfx8	Rps27	Scn4a	She	Slc6a4	Sox13
Proser3	Rab36	Rgag1	Rragd	Scn4b	Shf	Slc7a10	Sox17
Prph	Rab37	Rgcc	Rsad2	Scn7a	Shisa2	Slc7a8	Sox18
Prr15	Rab38	Rgmb	Rsbn1l	Scn8a	Shroom2	Slc8a2	Sox2
Prr16	Rab3d	Rgn	Rsf1	Scn9a	Siae	Slc8a3	Sox21
Prr18	Rab3il1	Rgs1	Rsph4a	Scnn1a	Siah3	Slc9a2	Sox2ot
Prr19	Rab40b	Rgs11	Rspo1	Scube1	Sigirr	Slc9a5	Sox5
Prr3	Rab6b	Rgs14	Rspo2	Sdc1	Siglece	Slc9a7	Sox6
Prr36	Rabgap1l	Rgs18	Rspo3	Sdcbp2	Sik1	Slco2b1	Sox7
Prr7	Rabl2	Rgs2	Rspo4	Sdk1	Sim2	Slfn4	Sox8
Prrg1	Rac2	Rgs22	Rsrc2	Sdk2	Sirpa	Slfn5	Sox9
Prrt1	Rac3	Rgs5	Rsrp1	Sec1	Sirt3	Slfn8	Sp100
Prrt2	Rad51b	Rgs7bp	Rtkn	Sele	Sirt4	Slitrk1	Sp110
Prrt3	Rad51c	Rgs9	Rtl1	Selenbp1	Six2	Slitrk2	Sp3os
Prrt4	Rad9b	Rgs9bp	Rtn1	Selenbp2	Six4	Slitrk4	Sp4
Prrxl1	Ralgds	Rhbdl1	Rtn4rl1	Selenop	Six5	Slitrk6	Spa17
Prss22	Ralgps2	Rhbdl2	Rtn4rl2	Selp	Skida1	Smad3	Spaca1
Prss30	Ramp2	Rhbdl3	Rttn	Selplg	Skor1	Smagp	Spag16
Prss36	Ranbp6	Rhd	Rubcnl	Sema3g	Sla	Smarca1	Sparcl1
Prss41	Rapgef4	Rho	Rubie	Sema4a	Slain1	Smarca2	Spata1
Prss50	Rapgef5	Rhobtb1	Rufy4	Sema4c	Slc10a4	Smarcal1	Spats2l
Prtg	Rapgefl1	Rhobtb2	Rundc3b	Sema4d	Slc10a6	Smarce1	Spdef
Prtn3	Rarb	Rhof	Runx2	Sema4g	Slc12a1	Smc2os	Spdya
Psd2	Rarres2	Rhoh	Rwdd2a	Sema5a	Slc12a5	Smco3	Spef1
Psd4	Rasal3	Rhov	Rxfp2	Sema5b	Slc13a3	Smim10l2a	Spef2

Spem1	Sugct	Tdrd1	Tmem170b	Tppp3	Ttpa	Vwa2	Zdhhc1
Sphkap	Sult1a1	Tdrd3	Tmem178	Tpst1	Ttyh3	Vwa5b2	Zdhhc15
Spi1	Sult5a1	Tdrd9	Tmem178b	Trabd2b	Tub	Vwc2	Zdhhc23
Spin2c	Sult6b2	Tecrl	Tmem191c	Traf3ip3	Tubb1	Vwce	Zeb2os
Spin4	Susd1	Teddm2	Tmem2	Trem1	Tulp1	Vwde	Zfand1
Spint1	Susd4	Tek	Tmem200b	Trem2	Tulp2	Vwf	Zfand4
Spn	Sv2a	Tekt1	Tmem204	Treml2	Tunar	Was	Zfas1
Spns2	Sv2b	Tekt2	Tmem215	Trerf1	Twist1	Wbp1	Zfhx4
Spock1	Svip	Tenm1	Tmem218	Trf	Twist2	Wdfy4	Zfp114
Spock2	Svopl	Tenm2	Tmem229a	Trib1	Twsg1	Wdpcp	Zfp184
Spon1	Syce2	Tenm4	Tmem229b	Tril	Txnip	Wdr31	Zfp185
Spon2	Sycp3	Tesc	Tmem231	Trim14	Tyrobp	Wdr34	Zfp280d
Spred1	Syn2	Tesmin	Tmem240	Trim29	Uba7	Wdr60	Zfp286
Sprn	Syn3	Tet1	Tmem241	Trim30a	Ubap1l	Wdr72	Zfp292
Spry1	Syndig1	Tet2	Tmem25	Trim33	Ubash3b	Wdr78	Zfp354c
Spry3	Syne4	Tet3	Tmem252	Trim34b	Ube2e2	Wdr86	Zfp36
Spta1	Syngap1	Tex11	Tmem255a	Trim5	Ube2l6	Wdr93	Zfp362
Sptb	Syngr3	Tex14	Tmem26	Trim6	Ubtd2	Wfikkn1	Zfp36l1
Sptbn2	Synpr	Tex9	Tmem260	Trim62	Ubxn11	Wfikkn2	Zfp383
Sptbn4	Syp	Tfap2b	Tmem262	Trim63	Ulk4	Whrn	Zfp385b
Spty2d1	Sypl2	Tfap2c	Tmem266	Trim67	Unc119	Wif1	Zfp385c
Srcin1	Syt14	Tfdp2	Tmem269	Trim71	Unc13c	Wipf1	Zfp395
Srgn	Syt15	Tgfbr3	Tmem28	Trim72	Unc13d	Wipf3	Zfp422
Srl	Syt16	Tgfbr3l	Tmem30b	Trim9	Unc45b	Wisp3	Zfp423
Srpk3	Syt2	Tgm1	Tmem39b	Triqk	Unc5cl	Wnk2	Zfp428
Srr	Syt3	Th	Tmem40	Tro	Unc5d	Wnk3	Zfp454
Srsf12	Syt6	Thbs2	Tmem42	Trp53i11	Unc80	Wnk4	Zfp467
Ssbp2	Syt9	Thbs4	Tmem44	Trp53i13	Upp1	Wnt11	Zfp473
Ssbp4	Sytl4	Themis2	Tmem51	Trp63	Use1	Wnt2b	Zfp488
Ssc4d	T	Thpo	Tmem59l	Trp73	Ush1c	Wnt6	Zfp521
Sspo	Tac1	Thra	Tmem71	Trpc3	Ushbp1	Wscd1	Zfp523
Sstr1	Tacr1	Thrb	Tmem74b	Trpc4	Usp11	Xkr4	Zfp532
Ssu2	Tacr3	Thsd1	Tmem8	Trpc5	Usp2	Xkr6	Zfp534
St18	Taf7	Thsd7a	Tmem8b	Trpm1	Usp21	Xkrx	Zfp536
St6gal1	Taf7l	Thsd7b	Tmem91	Trpm2	Usp22	Xlr	Zfp551
St6gal2	Tagln3	Tia1	Tmem94	Trpm3	Usp27x	Xlr3a	Zfp558
St6galnac2	Tal1	Tiam1	Tmie	Trpm5	Usp29	Xlr3b	Zfp575
St6galnac3	Tbc1d10c	Ticam2	Tmigd1	Trpm6	Usp3	Xlr3c	Zfp606
St6galnac5	Tbc1d16	Tie1	Tmprss15	Trps1	Usp43	Xlr4b	Zfp618
St7	Tbc1d24	Tifa	Tmprss3	Trpv6	Usp51	Xndc1	Zfp619
St8sia1	Tbc1d2b	Tigd3	Tmprss6	Tsc22d1	Usp53	Xpnpep2	Zfp641
St8sia2	Tbc1d30	Timp4	Tmprss7	Tsc22d3	Utp14b	Xrcc5	Zfp667
St8sia4	Tbc1d32	Tinag	Tmsb15b1	Tsga10	Vamp2	Xylt1	Zfp69
St8sia6	Tbc1d4	Tjp3	Tmsb15b2	Tshz1	Vangl2	Ybx2	Zfp704
Stab1	Tbc1d8	Tlcd1	Tmtc2	Tshz2	Vash1	Yod1	Zfp711
Stac	Tbkbp1	Tlcd2	Tmx4	Tshz3	Vash2	Ypel1	Zfp772
Stac3	Tbl1xr1	Tle2	Tnf	Tspan13	Vav1	Ypel2	Zfp773
Stag3	Tbr1	Tle3	Tnfaip6	Tspan14	Vcan	Ypel4	Zfp783
Stap2	Tbx1	Tle4	Tnfaip8l1	Tspan15	Vegfa	Zan	Zfp804b
Star	Tbx2	Tlr12	Tnfaip8l2	Tspan18	Vegfd	Zap70	Zfp808
Stard10	Tbx21	Tlr13	Tnfaip8l3	Tspan32	Vgll4	Zar1	Zfp810
Stat2	Tbx4	Tlr7	Tnfrsf14	Tspan6	Vhl	Zbp1	Zfp811
Stc1	Tbx6	Tlr8	Tnfrsf19	Tspan8	Vill	Zbtb10	Zfp819
Steap4	Tc2n	Tm6sf1	Tnfrsf25	Tspear	Vip	Zbtb11	Zfp820
Stfa2	Tcam1	Tmc3	Tnfrsf9	Tspyl1	Vipr1	Zbtb12	Zfp831
Stfa2l1	Tcea2	Tmc7	Tnfsf10	Tssk6	Vit	Zbtb16	Zfp85os
Stfa3	Tceal3	Tmc8	Tnfsf11	Tst	Vldlr	Zbtb44	Zfp879
Stk11ip	Tceal5	Tmem100	Tnfsf13	Tsx	Vmn2r29	Zbtb7c	Zfp92
Stk26	Tceal6	Tmem132a	Tnfsf9	Ttc21a	Vmn2r57	Zc2hc1c	Zfp945
Stk3	Tcf12	Tmem132b	Tnip3	Ttc22	Vpreb3	Zc3h12b	Zfp946
Stk32b	Tcf15	Tmem132c	Tnk1	Ttc23	Vps13b	Zc3h12d	Zfp950
Stk32c	Tcf24	Tmem132d	Tnni3	Ttc23l	Vps37d	Zc3h6	Zfp951
Stk38l	Tcf4	Tmem132e	Tnnt1	Ttc25	Vsig2	Zc4h2	Zfp956
Stmn1	Tcf7	Tmem145	Tnrc6b	Ttc26	Vsig8	Zcchc12	Zfp982
Stox1	Tcf7l1	Tmem150c	Tns2	Ttc3	Vsnl1	Zcchc16	Zfp992
Stra6	Tcp11	Tmem151b	Tns4	Ttc39a	Vstm2a	Zcchc18	Zfpm2
Strip2	Tcp11l2	Tmem158	Tox2	Ttc39aos1	Vstm2b	Zcchc5	Zfr2
Stx1b	Tctex1d1	Tmem163	Tox3	Ttc41	Vstm4	Zcwpw1	Zhx3
Stxbp6	Tctn3	Tmem169	Tpgs2	Ttc6	Vwa1	Zdbf2	Zim1

Zkscan16	Zmat4	Zmym3	Zmynd15	Zranb3	Zswim5
Zkscan2	Zmiz1	Zmym6	Zpbp	Zscan18	Zyg11a

Cluster 2 (1112)

36951	6530402F18Rik	Adamts5	Ang2	Atf5	Camk1	Cdkn2b	Col4a1
0610040J01Rik	8430436N08Rik	Adamts9	Angpt2	Atp6v0a4	Cap2	Cdnf	Col4a2
1110012L19Rik	9030617O03Rik	Adamtsl4	Ank3	Atp6v0b	Capg	Cdsn	Col4a3
1110019D14Rik	9230114K14Rik	Adamtsl5	Ankk1	Atp6v0e2	Capn1	Cebpb	Col4a4
1110046J04Rik	9330159M07Rik	Adgre5	Ankrd34a	Avpi1	Car5b	Cemip	Col4a5
1500011K16Rik	9530053A07Rik	Adra1d	Ankrd55	AY512931	Car9	Cend1	Col4a6
1600014C10Rik	9930111J21Rik1	Adra2a	Ano10	Azin2	Card6	Cep295nl	Col5a1
1600019K03Rik	9930111J21Rik2	Adrb2	Ano3	B230307C23Rik	Casp12	Cercam	Col5a3
1600027J07Rik	A330033J07Rik	Adrb3	Antxr1	B2m	Casq2	Cers4	Colca2
1700003M07Rik	A430105I19Rik	Aebp1	Anxa11	B3galt4	Catip	Ces2g	Comtd1
1700007K13Rik	A930001C03Rik	Afap1	Aox1	B4galnt1	Cavin2	Cfap100	Coro6
1700010I14Rik	AA536875	Afap1l2	Aox4	Bace2	Cbarp	Chac1	Cox6a2
1810034E14Rik	Abca12	Aga	Ap3m2	Bbc3	Cbr2	Chl1	Cox6b2
1810062G17Rik	Abca3	Agbl2	Ap5s1	BC017643	Ccdc162	Chmp4c	Cpb1
2010315B03Rik	Abcb1a	Agtr1a	Apba1	BC022687	Ccdc65	Chpf	Cpe
2210408F21Rik	Abcb9	Agtr1b	Apobec1	BC029722	Ccdc68	Chpf2	Cpeb1
2310008N11Rik	Abcc4	Agtrap	Apobec3	Bcl2l15	Ccdc80	Chrnb1	Cpne2
2310030G06Rik	Abhd2	AI413582	Apobr	Best3	Ccdc85a	Chst12	Cpq
2900026A02Rik	Abhd4	AI429214	Apol9a	Bglap2	Cd248	Cisd3	Cpt1a
3300005D01Rik	Acaa1b	AI464131	App	Bgn	Cd80	Clec2d	Cpt1c
3425401B19Rik	Acad10	AI593442	Aqp5	Bicdl1	Cd81	Clgn	Cpxm2
3830417A13Rik	Acad11	AI987944	Arap2	Bid	Cdc42bpg	Clstn2	Cpz
4732491K20Rik	Acbd4	Ak1	Arhgap22	Bloc1s3	Cdc42ep1	Cltb	Cracr2b
4833419F23Rik	Acot11	Akap6	Arhgap23	Bst2	Cdc42ep2	Clvs1	Crct1
4833427G06Rik	Acot13	Akr1b10	Arhgap24	Btc	Cdc42ep5	Cmah	Creb3
4921504A21Rik	Acot6	Akr1b8	Arhgap44	C030006K11Rik	Cdh10	Cnga3	Creb5
4930429B21Rik	Acox1	Akr1c19	Arhgdib	C130083M11Rik	Cdh2	Cnn1	Crebl2
4930523C07Rik	Acox3	Aldh1l2	Arhgef19	C1ql3	Cdhr1	Cnppd1	Creld1
4930550C14Rik	Acsbg1	Aldh4a1	Arhgef2	C1qtnf2	Cdk18	Col10a1	Crip2
4933412E12Rik	Acvrl1	Alkal1	Arpp21	C2	Cdk2ap2	Col12a1	Crisp2
5430403N17Rik	Acy3	Alox5	Asah1	C230024C17Rik	Cdkl1	Col19a1	Crlf2
5830418P13Rik	Acyp2	Alpk1	Asb2	C330024D21Rik	Cdkl2	Col1a1	Cryab
5830432E09Rik	Adam15	Ampd3	Asic3	C430002N11Rik	Cdkn1a	Col1a2	Csn3
5930430L01Rik	Adam23	Ang	Asl	Calhm2	Cdkn2a	Col2a1	Cspg4

Cst3	Dhrs7	Emx2os	Fbn1	Gas6	Gm4262	Hexb	Igf2r
Cst6	Dhx32	Eng	Fbxl2	Gata2	Gm5124	Hhipl1	Igfbp2
Cstb	Dio2	Eno3	Fbxl8	Gata3	Gm5144	Hist1h1c	Igfbp7
Ctnna2	Disp1	Eogt	Fbxo16	Gatsl3	Gnb5	Hist1h1d	Igsf9b
Ctnnd2	Disp2	Ephx1	Fbxo2	Gba	Gns	Hist1h2al	Ikbip
Ctsa	Dkk3	Eps8l2	Fbxo25	Gbp2	Gpbar1	Hist1h2bc	Il11
Ctsb	Dmd	Ercc5	Fbxo32	Gbp3	Gpc4	Hist1h2be	Il13ra2
Ctsd	Dmpk	Erfe	Fbxo36	Gda	Gpm6b	Hist1h3b	Il15
Ctsl	Dnah10	Espn	Fbxo6	Gdf15	Gpnmb	Hist2h2bb	Il17ra
Ctsz	Dnajb5	Esrp2	Fbxw26	Gdnf	Gpr149	Hist3h2a	Il17rc
Cxcl14	Dnajc28	Eva1c	Fbxw9	Ggact	Gpr39	Hk1	Il18rap
Cxcr6	Dner	Exd1	Fes	Ggt7	Gpr75	Hmox1	Il1r1
Cyb561d2	Dok5	Exoc3l4	Fgf16	Ghdc	Gpx3	Homer3	Il1rap
Cyba	Dpp7	Exoc4	Fgf9	Gjb3	Grem1	Hotairm1	Il34
Cyp1b1	Dram1	F3	Ficd	Gjb5	Grhl3	Hoxa1	Il3ra
Cyp2u1	Dsc2	Fabp3	Flot1	Glipr1	Gria3	Hoxc13	Il4ra
Cyp4f16	Dusp27	Fabp4	Flt3l	Glis2	Grn	Hpcal1	Il6ra
Cyp4f17	Dusp3	Fads3	Fmod	Glis3	Gsn	Hrct1	Il7
Cystm1	Dusp8	Fah	Fndc3b	Glmp	Gyg	Hrh1	Inhbb
D5Ertd605e	Dynlt3	Fam110c	Folr1	Glrp1	Gzmb	Hs1bp3	Inpp1
D730005E14Rik	Dyrk3	Fam114a1	Foxc1	Glrx	Gzmc	Hsd17b1	Irak2
Dact1	Dysf	Fam124a	Foxl2	Gm10635	Gzme	Hspa12a	Irak3
Dagla	E030011O05Rik	Fam129a	Foxq1	Gm12185	H2-D1	Hspb2	Irak4
Daglb	E130310I04Rik	Fam131c	Foxs1	Gm12295	H2-K1	Hspb3	Irgm1
Dapp1	E2f6	Fam149a	Frem2	Gm12610	H2afj	Hspb8	Irs3
Dbndd2	Ecm1	Fam160a1	Frrs1	Gm13490	H6pd	Hspg2	Isg20
Dcst1	Eda2r	Fam169b	Fstl3	Gm13986	Hapln4	Htatip2	Itga1
Dcxr	Efemp1	Fam189a2	Ftl1	Gm15417	Has2	Htr2a	Itgb1bp1
Ddit3	Ehd3	Fam20a	Fuca1	Gm15908	Hcar1	Htra1	Itgb4
Ddit4l	Ehhadh	Fam212b	Fzd8	Gm15987	Hcn2	Hyal1	Kank1
Ddx58	Elavl2	Fam214b	G630071F17Rik	Gm16062	Hdhd3	Ica1l	Kcnab1
Def6	Elfn1	Fam219a	Gabarap	Gm16793	Hebp2	Iffo1	Kcnj4
Defb1	Elovl7	Fam219aos	Galns	Gm19710	Helz2	Ifi204	Kcnmb1
Defb48	Emc9	Fam26e	Galnt18	Gm26705	Herc6	Ifi35	Kctd17
Dgkg	Emp2	Fam83h	Garem2	Gm2694	Hes1	Ifi47	Kctd21
Dhrs3	Emx2	Fas	Gas2l1	Gm3716	Hexa	Ifitm3	Kctd4

Kdelr3	Lrrc73	Mgmt	Nacc2	Oas1c	Pctp	Plpp2	Pstpip2
Kif1a	Lrrc75b	Mgst2	Nagk	Odam	Pcx	Plpp6	Pter
Klc3	Ltb4r1	Micall2	Naglu	Ofcc1	Pde4dip	Pltp	Ptger1
Klf15	Ltb4r2	Mien1	Naif1	Ogfod2	Pde6h	Plxdc2	Ptgr2
Klhdc7a	Ltbr	Mir377	Nap1l2	Olfml2b	Pdgfa	Plxnb2	Ptgs1
Klhl13	Luzp2	Mlkl	Nat14	Olfr1314	Pdgfd	Plxnc1	Ptgs2os2
Klhl26	Lxn	Mmp14	Nat2	Olfr1317	Pdk4	Pm20d1	Ptk2b
Klhl30	Ly6a	Mmp19	Nat6	Olfr1318	Pdlim2	Pmaip1	Ptp4a3
Klhl38	Ly6e	Mmp23	Ndrg4	Olfr456	Pef1	Pml	Ptprb
Klrg2	Ly6f	Mn1	Neat1	Olfr78	Perp	Pmm1	Ptprq
Krt20	Lynx1	Mocos	Nell2	Onecut2	Pex5l	Pnp	Ptprv
Lama5	M1ap	Mogat2	Neu3	Optc	Pfkp	Pnp2	Pwwp2b
Lamb1	Maats1	Mpp1	Neurl2	Osgin1	Pgpep1	Pnpla2	Qpct
Lamb2	Mab21l3	Mrgpre	Nid1	Osmr	Pgpep1l	Pold4	Rab27a
Lamp1	Macc1	Mrgprf	Nid2	Ostf1	Phactr1	Popdc2	Rab30
Lamp2	Malrd1	Mroh1	Nipal1	Ostm1	Phf19	Pou3f4	Rab32
Layn	Mamdc2	Mrvi1	Nkd2	P2rx1	Phkg1	Ppard	Rab3b
Lce1g	Man2b1	Ms4a4d	Nkx2-9	P2rx4	Phldb3	Ppbp	Rab3c
Lce1h	Man2b2	Msrb1	Nlrc3	P2rx5	Phospho2	Ppp1r12b	Rab42
Ldb3	Manea	Mt1	Nlrp10	P2ry2	Phyhd1	Ppp1r14a	Rab7b
Lefty1	Mansc1	Mtm1	Nmrk1	P4ha3	Pidd1	Ppp2r2c	Rai2
Lgals2	Map1a	Mtus2	Nnmt	Pafah2	Pisd	Pqlc2	Ramp3
Lgals8	Map3k15	Mustn1	Nod1	Pamr1	Pitpnm1	Prdx5	Rap1gap2
Lhx9	Map3k6	Mvp	Npdc1	Papss2	Pla1a	Prelp	Rarres1
Lif	Map3k7cl	Mxra7	Npr3	Parm1	Pla2g16	Prkaa2	Rb1
Lncenc1	Map7	Mxra8	Npy1r	Parp3	Pla2r1	Prkcd	Rbks
Loxl1	Mapkapk3	Myf5	Nr1d1	Parp4	Plau	Prkcg	Rcan1
Loxl2	Mc4r	Myf6	Nrip3	Pbx4	Plcd1	Prl3a1	Rdh5
Loxl3	Mcub	Myh1	Nts	Pbxip1	Plcd3	Prnp	Reep2
Loxl4	Mdfic	Myh2	Nucb1	Pcdha10	Pld2	Prr13	Rem1
Lpcat2	Mdm2	Myl6b	Nudt16	Pcdha12	Pld3	Prr32	Renbp
Lrp1	Medag	Mylk	Nudt18	Pcdhga11	Plekha2	Prrg4	Rftn1
Lrp10	Mettl21b	Myog	Nudt22	Pcdhgb8	Plekha7	Prss35	Rgl3
Lrp11	Mfap3l	Myom1	Nup62cl	Pcdhgc5	Plekhb2	Psen2	Rgs21
Lrrc27	Mfap5	Nabp1	Nupr1	Pck2	Plin4	Psph	Rgs4
Lrrc28	Mfsd1	Nacad	Oacyl	Pcolce	Plod2	Psrc1	Rhbdd1

Rhbdf2	Serinc3	Slc2a10	Spsb4	Sytl1	Tmem108	Trim65	Vps13c
Rhoj	Serpina3g	Slc2a4	Sqor	Tacstd2	Tmem150a	Trim66	Vstm5
Ric3	Serpina3h	Slc2a6	Sqstm1	Taok3	Tmem154	Trim7	Vwa5a
Rin3	Serpina3i	Slc2a8	Srpx	Tap1	Tmem159	Trnp1	Wdr17
Ripk3	Serpinb6a	Slc2a9	Srrm4	Tapbpl	Tmem181a	Trp53cor1	Wdr81
Ripor1	Serpinb6c	Slc35a2	Srrm4os	Tbc1d2	Tmem198b	Trp53inp1	Wfs1
Rnase10	Serpinb8	Slc35f1	Ssc5d	Tbc1d9	Tmem202	Trp53inp2	Wipi1
Rnase4	Serpinb9b	Slc36a1	Sspn	Tbcel	Tmem37	Trpv2	Wisp1
Rnasek	Serpine1	Slc38a7	St14	Tbx18	Tmem53	Tshr	Wisp2
Rnf169	Sesn2	Slc41a2	Stard5	Tbx20	Tmem62	Tspan12	Wnt16
Rnh1	Setmar	Slc41a3	Stat4	Tbxa2r	Tmem63a	Tspan17	Wnt9a
Rrm2b	Sgca	Slc48a1	Stat5a	Tbxas1	Tmem63b	Tspo	Xaf1
Rsl1	Sgcd	Slc50a1	Steap3	Tcaf2	Tmem88	Tspyl4	Xdh
Rsph1	Sgsm2	Slc5a12	Stk10	Tchh	Tmem88b	Tstd3	Zbtb38
Rxfp1	Sh2d4a	Slc8b1	Stom	Tcirg1	Tnfaip2	Ttbk1	Zbtb4
Samd10	Sh3bgr	Slit1	Styk1	Tcn2	Tnfrsf1b	Ttc12	Zbtb42
Samd12	Sh3rf3	Slitrk3	Sulf1	Tcp11x2	Tnfrsf23	Ttc39b	Zbtb7b
Sash1	Shc4	Slitrk5	Sulf2	Tdrd7	Tnfsf12	Ttc7	Zc3h12a
Saysd1	Shisa5	Smim20	Sult6b1	Tdrp	Tnfsf18	Ttll9	Zfp296
Scg5	Shisa6	Smpd1	Sumf1	Terb1	Tns1	Ttyh2	Zfp3
Scn1b	Sidt2	Snta1	Susd2	Tes	Tor3a	Tuba4a	Zfp385a
Scn2a	Siglecg	Snx33	Susd5	Tex26	Tor4a	Tubb2a	Zfp389
Scn3b	Skap2	Soat2	Susd6	Tgtp1	Tox	Tuft1	Zfp456
Scpep1	Slc12a7	Sod3	Svep1	Tgtp2	Tpbgl	Uap1l1	Zfp52
Scrn1	Slc13a5	Sorbs2os	Svop	Thbd	Tpcn2	Ubtd1	Zfp677
Scube2	Slc16a3	Sorcs1	Syk	Them6	Tpd52	Ugt2b35	Zfp688
Scx	Slc16a5	Sord	Sync	Timp2	Tpp1	Unc5b	Zfp691
Sdsl	Slc17a9	Sp9	Syne1	Tlr4	Tradd	Unc5c	Zfp750
Sec14l5	Slc1a6	Spag4	Synm	Tlr5	Traf3ip2	Uprt	Zfp93
Sec16b	Slc24a3	Sparc	Synpo	Tlr6	Trib3	Usp20	Zfp994
Selenom	Slc25a35	Sphk1	Syt10	Tmbim4	Trim11	Vamp8	Zkscan4
Sema3c	Slc26a7	Spred3	Syt13	Tmem104	Trim25	Vat1	Znfx1
Sema3d	Slc29a3	Spsb2	Syt17	Tmem106a	Trim47	Vdr	Zswim6

Cluster 3 (1269)

37681	9330136K24Rik	Actg2	Agpat2	Anxa6	Arl5a	Atp6v0a2	Bcl7b
1110008F13Rik	9430037G07Rik	Actn1	Ahcyl1	Anxa7	Arl6ip5	Atp6v0e	Bdnf
1600002K03Rik	9930012K11Rik	Actn4	Ahnak	Anxa8	Arl8a	Atp6v1c1	Bicd2
1600012H06Rik	9930104L06Rik	Actr2	AI837181	Ap1s1	Arntl	Atxn1	Bloc1s2
1700007L15Rik	A530046M15Rik	Actr3	Aif1l	Ap1s2	Arpc1b	AU041133	Bmp4
1700009N14Rik	A630033H20Rik	Adam19	Ak6	Ap2m1	Arpc2	Avpr1a	Bnip2
1810055G02Rik	AA986860	Adam9	Akap12	Apaf1	Arpc4	AW209491	Bok
2010111I01Rik	Aacs	Adamts18	Alas1	Apbb1ip	Arxes2	Axl	Bpnt1
2200002D01Rik	Aars	Adamts6	Aldoa	Apeh	Asb6	B4galt4	Brat1
2210016F16Rik	Abca5	Adgra2	Alg3	Aph1a	Asb8	Bag1	Brf2
2310022B05Rik	Abcb10	Adgrf2	Als2cl	Apol10b	Ate1	Bag2	Btbd19
2610008E11Rik	Abcb1b	Adgrg5	Als2cr12	Apol8	Atg3	Bak1	Bves
3110021A11Rik	Abcc1	Adh7	Ammecr1	Apol9b	Atg4d	Bax	Bvht
4833412C05Rik	Abi1	Adm	Amotl2	Arfgef2	Atoh8	Bbs10	C1galt1c1
4930412O13Rik	Ablim1	Adora1	Angptl2	Arhgap1	Atp10b	BC037034	Cacna1s
4930426L09Rik	Acadl	Adora2b	Ankib1	Arhgap17	Atp10d	BC048403	Cacnb2
4930511M06Rik	Acot7	Adra1b	Ankrd1	Arhgdia	Atp13a3	Bcap29	Cactin
4931406P16Rik	Acot8	Aen	Ankrd52	Arhgef18	Atp1a1	Bcap31	Cald1
4933433H22Rik	Acot9	Aff1	Anxa1	Arhgef28	Atp1b1	Bcar1	Camk2g
8430423G03Rik	Acsl5	Aftph	Anxa2	Arhgef5	Atp2a2	Bcar3	Canx
9130008F23Rik	Acta1	Ago2	Anxa3	Arid5b	Atp2b1	Bcat1	Cap1
9130023H24Rik	Acta2	Agpat1	Anxa5	Arl14epl	Atp5b	Bcl2l1	Capn12

Capn2	Cd47	Chuk	Col8a1	Ctgf	Dcun1d3	Dscr3	Ell2
Capns1	Cd63	Cib1	Colq	Ctnnd1	Dda1	Dst	Elovl1
Capzb	Cdc34	Cisd1	Commd5	Cttn	Ddah1	Dstn	Emc4
Carmn	Cdc42ep3	Cited2	Comt	Cttnbp2nl	Ddb1	Dtna	Emc7
Carns1	Cdc42se1	Ckap2	Coq10b	Ctu1	Ddias	Dtnbp1	Emd
Casp14	Cdh26	Ckap4	Coq3	Cux1	Ddr1	Dubr	Emp3
Cast	Cdipt	Clcn5	Coro1c	Cx3cl1	Degs1	Duoxa1	Enc1
Cav1	Cenpt	Clcn7	Cox10	Cyb5d2	Dennd2d	Dusp10	Eno1
Cav2	Cep170b	Cldn22	Cox17	Cyb5r1	Depdc7	Dync1h1	Eno1b
Cav3	Cers6	Clic1	Cox18	Cyb5r3	Deptor	Dzip1l	Epb41l4a
Cavin1	Ces1g	Clic4	Cox5a	Cyfip1	Desi1	E030013I19Rik	Epha2
Cavin4	Cfap157	Clip1	Cpeb2	Cyld	Dgkh	Edem3	Ercc6
Ccdc129	Cfap70	Clptm1l	Cpn1	Cyp1a1	Dlat	Efemp2	Ereg
Ccdc130	Cfl2	Cmklr1	Cpox	Cyp20a1	Dlc1	Efnb2	Erich1
Ccdc51	Cflar	Cmtm7	Cpt2	Cyp4a12b	Dlgap4	Efr3a	Erlin2
Ccdc71	Cftr	Cndp2	Cptp	Cyr61	Dnah5	Egfr	Ero1l
Ccdc85b	Cgref1	Cnksr3	Crcp	D030025P21Rik	Dnajc13	Egln3	Esd
Ccdc92	Chac2	Cnn3	Creb3l1	D17H6S53E	Dnm2	Ehbp1l1	Esr2
Ccl17	Chfr	Coa4	Crim1	D630045M09Rik	Dok1	Ehd1	Esrra
Ccnd1	Chit1	Cobl	Cs	D6Wsu163e	Dolk	Ehd2	Esyt1
Ccng1	Chrm1	Cobll1	Csf1	Daam1	Dolpp1	Ehd4	Esyt2
Cd109	Chrna1	Cog1	Csnk1g1	Dact2	Dpagt1	Ei24	Ets1
Cd151	Chst11	Cog8	Csrp1	Dbt	Dpp9	Eid3	Etv6
Cd44	Chst7	Col5a2	Csrp2	Dcbld2	Dpysl3	Eif4ebp1	Eva1b

Exo5	Fat1	Flna	Gclc	Gm15217	Gprc5a	Hprt	Inppl1
Exoc8	Fblim1	Flnb	Gcnt2	Gm15694	Gprc5b	Hps6	Ipo13
Ext1	Fbln5	Flnc	Gcnt3	Gm16907	Gprc6a	Hras	Iqgap1
F2r	Fbxl18	Flrt2	Gdap2	Gm17746	Gprin3	Hspa4l	Itga11
Faap24	Fbxo4	Flt1	Gdpd5	Gm19689	Gpx1	Hspa9	Itga4
Fabp5	Fbxo46	Fmn1	Gdpgp1	Gm19705	Gskip	Hspb1	Itga5
Faf2	Fbxw17	Fn1	Gemin7	Gm20257	Gss	Hspb6	Itga7
Fam107b	Fbxw18	Fndc1	Gfer	Gm20324	Gsta1	Htr1b	Itga8
Fam118a	Fez2	Fndc9	Gfod1	Gm20939	Gsto1	Htt	Itgav
Fam120a	Fgd3	Foxg1	Ggta1	Gm2115	Gtf2f1	Id4	Itgb1
Fam129b	Fgf10	Foxp1	Gja3	Gm6498	Gtpbp8	Iffo2	Itpripl1
Fam13b	Fgf7	Frmd8	Glipr2	Gm6634	Gtse1	Ifitm10	Itpripl2
Fam173b	Fhl1	Fryl	Glrx3	Gm6654	Gypc	Ifngr1	Jade1
Fam174b	Fhl2	Fst	Glud1	Gm6712	Gys1	Ifngr2	Jag1
Fam198b	Fhl3	Furin	Glyat	Gm8801	Gzmd	Ift43	Jagn1
Fam207a	Fhl5	Fv1	Gm10033	Gmppb	Hacd1	Igf1r	Jam2
Fam20c	Filip1l	Fxyd5	Gm10548	Gne	Hacd4	Igfbp6	Jdp2
Fam222b	Fitm2	Fyb2	Gm12070	Gng12	Hcfc1r1	Il10rb	Jph2
Fam46b	Fiz1	Fzd5	Gm13446	Gnrh1	Hdac7	Il23r	Jrk
Fam71f1	Fkbp10	Gadd45g	Gm13985	Gorasp2	Hgfac	Il6st	Jrkl
Fam83g	Fkbp1a	Gale	Gm14005	Gp5	Hgs	Ildr2	Jup
Fam96b	Fkbpl	Galnt2	Gm14295	Gpd2	Hipk2	Inafm2	Kalrn
Farp1	Fkrp	Gapdh	Gm14326	Gpr107	Homez	Inf2	Kank2
Fastkd5	Flii	Gars	Gm14403	Gpr176	Hpdl	Inpp5a	Kcnab3

Kcnj6	Krt79	Lims1	Luzp1	Mcoln3	Mir221	Mybph	Nectin2
Kcnk2	Krtap1-5	Lims2	Ly75	Mcrip2	Mir22hg	Myh10	Nek7
Kctd10	Krtap6-2	Lipg	M6pr	Me1	Mir8112	Myh11	Nes
Kctd11	Lactb2	Lipt1	Maml2	Mecr	Mkl1	Myh9	Nexn
Kctd5	Lamc1	Lmf2	Mamld1	Med15	Mlc1	Myl12a	Nfkb1
Kdsr	Lamc2	Lmo7	Man1a	Med21	Mmd	Myl12b	Nfkb2
Khdrbs3	Lap3	Lmod1	Map10	Med8	Mmp10	Myl6	Ngf
Kif1c	Large1	Lox	Map1s	Med9	Mon1b	Myl9	Nhlrc3
Kif5b	Lasp1	Lpcat4	Map2k1	Mettl18	Mospd2	Mylk2	Nipal4
Kif5c	Lats2	Lpp	Map3k20	Mettl21a	Mpv17l2	Myo10	Nmt1
Kifc3	Lbh	Lrp2	Map4	Mettl6	Mrm1	Myo1c	Nol4
Klc2	Lcat	Lrrc14	Map4k5	Mfge8	Mrm2	Myo1d	Nomo1
Klf3	Lclat1	Lrrc15	Map6	Mfhas1	Mrpl51	Myo1e	Nploc4
Klf7	Ldha	Lrrc75a	Mapk14	Mfn2	Msln	Myo1h	Npnt
Klhl18	Ldlrad2	Lrrc8a	Mars2	Mfsd5	Msn	Myo9b	Nptn
Klhl21	Leprotl1	Lrrc8c	Masp1	Mgat2	Msrb3	Myocd	Nqo1
Klhl25	Lfng	Lrrc8d	Mast4	Mgll	Msto1	Myof	Nradd
Klhl5	Lgals1	Lrrfip1	Matn3	Mical2	Mt2	Nadk	Nrg1
Kpna4	Lgals9	Lrrk1	Mavs	Micu3	Mtap	Nanos1	Nsf
Kpna7	Lgalsl	Lsm10	Mblac1	Mid1	Mthfr	Nav2	Nsg1
Krcc1	Lhfp	Lsp1	Mbnl1	Mief2	Mtif3	Nceh1	Nt5c
Kremen1	Lig4	Ltbp1	Mbnl2	Mindy3	Mtpn	Ncln	Ntf3
Krt12	Lima1	Ltbp2	Mbp	Mir143	Myadm	Ndufb6	Ntn4
Krt7	Limch1	Lurap1l	Mcam	Mir145a	Mybl1	Neb	Nuak1

Nuak2	Pcdh7	Piezo1	Pmepa1	Prep	Pvt1	Rassf6	Rnf141
Nubp1	Pdcd6ip	Pigf	Pmm2	Prkaa1	Pxdc1	Rassf7	Rnf144b
Nupl2	Pdcl3	Pigg	Pnkp	Prkab2	Pxk	Rb1cc1	Rnf150
Nxn	Pde4a	Pigw	Polk	Prkag3	Qpctl	Rbm20	Rnf43
Ogfod1	Pdgfc	Pik3ip1	Polr2l	Prl	Qrfp	Rbm38	Rnf6
Optn	Pdgfrl	Pitpna	Polr3c	Prosc	Qsox1	Rbms1	Rock2
Orai2	Pdha1	Pkd1	Pomgnt1	Proser2	Rab21	Rcan2	Ros1
Osbpl5	Pdia5	Pkd2l2	Pop7	Prr33	Rab23	Rdh13	Rpp38
Osr1	Pdlim1	Pkm	Popdc3	Prss23	Rab27b	Rdh9	Rprm
Otud1	Pdlim5	Pkp2	Ppcs	Prss27	Rab3gap2	Reep4	Rps2
Otud3	Pdlim7	Pla2g15	Ppfibp1	Prx	Rabgef1	Rexo2	Rps27l
Otud7b	Pdrg1	Pla2g4a	Ppil3	Psmd8	Rad23a	Rgs12	Rragc
Oxsm	Pea15a	Plcb4	Ppme1	Ptchd4	Rad9a	Rgs16	Rras
P3h4	Peak1	Plcxd2	Ppp1r11	Ptges3l	Radil	Rgs17	Rrp36
P4ha1	Pfn1	Plec	Ppp1r12a	Ptpmt1	Ralgapb	Rgs20	Rsu1
P4ha2	Pgam1	Plekhf1	Ppp1r13l	Ptpn13	Rap1gds1	Rhoc	Rtn4
Pacsin2	Pgd	Plekhg2	Ppp1r14b	Ptpn14	Rap2a	Rhod	Rubcn
Pak3	Pgk1	Plekhg3	Ppp1r18	Ptpn21	Rap2b	Rhog	Rusc2
Palld	Pgs1	Plekho2	Ppp1r2-ps3	Ptpn23	Raph1	Ric8a	Ryk
Pappa	Phc2	Plod3	Ppp1r32	Ptprf	Rasa3	Rin1	S100a10
Paqr8	Phlda3	Plp2	Ppp2r5b	Ptrh1	Rasa4	Rit1	S100a11
Pars2	Phldb1	Plpp1	Pqlc3	Ptx3	Rasgrp3	Rnd1	S100a4
Parva	Phldb2	Pls3	Prdx6	Pura	Rassf1	Rnd3	S100a6
Pawr	Picalm	Plxna1	Prelid1	Pvr	Rassf5	Rnf128	S1pr2

Sac3d1	Sh3kbp1	Slc39a14	Snx30	Steap2	Tanc1	Tll1	Tmem9b
Sacs	Shisa4	Slc39a6	Snx7	Stmn2	Tax1bp3	Tln1	Tmppe
Samd4	Shoc2	Slc4a2	Snx9	Stmn4	Tbc1d10a	Tm4sf1	Tmsb4x
Samhd1	Shroom3	Slc4a4	Soat1	Ston1	Tbcc	Tmbim1	Tmtc3
Sap18	Sigmar1	Slc5a8	Socs5	Strn	Tcfl5	Tmed5	Tnfaip1
Sars	Sipa1l1	Slc6a6	Sorbs1	Stx11	Tcte2	Tmeff2	Tnfrsf10b
Sat1	Sirt7	Slc7a5	Sorbs2	Stx3	Tead3	Tmem115	Tnfrsf11a
Sbds	Slc10a3	Slco1a5	Sox30	Stxbp3-ps	Tefm	Tmem120a	Tnfrsf11b
Scamp4	Slc11a2	Slco3a1	Specc1	Styx	Tepsin	Tmem126a	Tnfrsf12a
Scd1	Slc12a2	Slco4a1	Sphk2	Sult4a1	Tg	Tmem128	Tnfsf15
Schip1	Slc12a4	Slit2	Spire2	Sun2	Tgfb1i1	Tmem129	Tnik
Scn10a	Slc19a2	Slmap	Spr	Suox	Tgfb2	Tmem151a	Tnks1bp1
Sdc4	Slc1a4	Slpi	Sprtn	Syde1	Tgfb3	Tmem160	Tnmd
Sec23ip	Slc20a1	Smad6	Spryd3	Syne3	Tgif1	Tmem177	Tnnc1
Sel1l	Slc20a2	Smg5	Spryd4	Syngr2	Thap7	Tmem192	Tnnt2
Selenof	Slc25a13	Smim12	Sptan1	Synj1	Thbs1	Tmem199	Tnrc18
Selenot	Slc25a3	Smim15	Sptbn1	Synj2	Thy1	Tmem245	Tom1
Senp5	Slc26a2	Smug1	Srxn1	Syt1	Tigar	Tmem38a	Tpm1
Senp8	Slc27a4	Smurf1	St3gal5	Syt12	Tigd4	Tmem43	Tpm2
Serpinf1	Slc30a1	Smyd1	Stambp	Sytl2	Timp1	Tmem47	Tpm4
Serpinh1	Slc33a1	Snhg15	Stard13	Tacc2	Timp3	Tmem5	Tppp
Sfxn3	Slc35c1	Sntg1	Stat6	Taf1c	Tinagl1	Tmem69	Tprn
Sh3bp4	Slc35f6	Snx11	Stbd1	Tagln	Tirap	Tmem70	Tpst2
Sh3glb1	Slc39a13	Snx16	Stc2	Taldo1	Tjap1	Tmem95	Traf2

Traf5	Tslp	Uggt1	Vmp1	Wtip	Zdhhc24	Zfp626	Zfp958
Tram2	Tspan2	Uhmk1	Vps18	Wwc2	Zdhhc7	Zfp658	Zfp960
Trappc2	Tstd2	Unc13b	Vps29	Xirp1	Zdhhc9	Zfp672	Zfp97
Trhde	Ttc1	Unc45a	Vps36	Yae1d1	Zfhx3	Zfp697	Zkscan6
Trim16	Ttll11	Upk1b	Vti1b	Yif1a	Zfp105	Zfp703	Zmat3
Trim17	Ttll7	Urgcp	Wars	Yif1b	Zfp113	Zfp719	Zmpste24
Trim3	Tuba1a	Uso1	Washc5	Ywhag	Zfp128	Zfp759	Znrd1as
Trim56	Tubb2a-ps2	Usp15	Wdr1	Zbtb3	Zfp143	Zfp78	Zscan20
Trim59	Tubb2b	Usp24	Wdr5b	Zbtb40	Zfp334	Zfp780b	Zscan22
Trip10	Tubb6	Usp32	Wdr62	Zbtb7a	Zfp35	Zfp790	Zswim1
Trmo	Twf1	Utp20	Whamm	Zbtb8b	Zfp365	Zfp804a	Zswim3
Trmt12	Txnrd1	Utrn	Wnk1	Zc2hc1a	Zfp51	Zfp809	Zxdc
Trmt1l	Uba6	Vangl1	Wnt10a	Zc3hav1	Zfp526	Zfp82	Zyx
Trmt61b	Ube2j1	Vasp	Wnt10b	Zdhhc12	Zfp53	Zfp930	Zzef1
Trp53rka	Ube2m	Vcl	Wnt4	Zdhhc13	Zfp54	Zfp947	
Trp53rkb	Ufsp1	Vgll3	Wnt5a	Zdhhc16	Zfp59	Zfp948	
Tsku	Ugdh	Vim	Wsb2	Zdhhc2	Zfp617	Zfp953	

Cluster 4 (689)

38231	5730405O15Rik	Acpp	Apc2	Atg10	C530044C16Rik	Ccpg1os	Cnp
1700020L24Rik	5730409E04Rik	Acyp1	Aph1b	Atl1	Cabp1	Cd55	Cnr1
1700042O10Rik	6430548M08Rik	Adamts12	Aplp1	AW011738	Cacna1a	Cd59a	Cnrip1
1700096K18Rik	6430571L13Rik	Adamtsl1	Apol6	B130024G19Rik	Calcoco1	Cd82	Col20a1
1810010H24Rik	9330102E08Rik	Adcy5	Apol7d	B3gnt9	Camk2a	Cd99l2	Col7a1
1810019D21Rik	9330133O14Rik	Adgrg2	Aqp11	Bambi-ps1	Camk2n1	Cdh18	Copz2
1810021B22Rik	A330023F24Rik	Adgrg6	Ar	BB218582	Capn5	Cdk15	Coq8b
1810044D09Rik	A330035P11Rik	AF357359	Arap1	BC028528	Capn9	Cela1	Cpa6
2010001A14Rik	A330048O09Rik	Agrp	Arhgap27	Bcl3	Car13	Celf5	Crabp2
2310001H17Rik	A4galt	AI197445	Arhgap45	Bcl6	Cass4	Celsr3	Creg1
2410004P03Rik	A530072M11Rik	AI427809	Arhgef6	Bco1	Catsperg1	Ces2e	Crip1
2610301B20Rik	A830018L16Rik	Aifm2	Arl5c	Bnip3	Cbln3	Cfap126	Csdc2
2810032G03Rik	A830082K12Rik	Aldh1b1	Armcx5	Borcs6	Cbr3	Cfap45	Csmd3
3632451O06Rik	AA543186	Aldh1l1	Arntl2	Bscl2	Ccdc122	Cfap54	Ctsf
3830406C13Rik	Aass	Aldh2	Arsa	Btbd11	Ccdc149	Chek2	Ctsh
4930528A17Rik	Abca7	Aldh3b1	Arsg	Btg2	Ccdc17	Chst13	Ctso
4930579K19Rik	Abcc3	Aldh6a1	Arsi	C1qtnf1	Ccdc181	Cited4	Cul9
4931406C07Rik	Abhd15	Amz1	Artn	C1qtnf6	Ccdc184	Clip3	Cyb5r2
4933411K16Rik	Abtb1	Angpt4	Arvcf	C1ra	Ccdc189	Clybl	Cyp2j6
5031425E22Rik	Acaa2	Ankrd13d	As3mt	C1rb	Ccdc28a	Cmbl	Cyp2j9
5033406O09Rik	Ackr4	Ankrd35	Asah2	C1rl	Ccl7	Cmtm5	Cyp4v3
5430405H02Rik	Acot2	Ano2	Asap3	C330013E15Rik	Ccpg1	Cngb1	D130017N08Rik

D330023K18Rik	Drc1	Fabp7	Fkbp7	Glrb	Grina	Hlx	Irx3
Dach2	Dusp18	Fahd2a	Fmo5	Gm10560	Grip1	Hmcn1	Isg15
Dact3	Dync2li1	Fam110b	Frmd4b	Gm10638	Gsap	Hmgcll1	Isoc2b
Dand5	Dyrk1b	Fam131a	Fuca2	Gm10814	Gsdmd	Hnmt	Itgb5
Dbp	E130311K13Rik	Fam181b	Fyco1	Gm15663	Gstm1	Hpn	Itm2b
Dcc	E230013L22Rik	Fam189b	Gaa	Gm16894	Gstm2	Hsd11b1	Itm2c
Ddah2	Ebpl	Fam19a2	Gabarapl1	Gm2a	Gstm4	Hsd17b11	Itpr2
Ddit4	Ech1	Fam210b	Gabra3	Gm5126	Gsto2	Htr1d	Jmjd8
Ddt	Ecscr	Fam213b	Gabrb1	Gm8615	Gstt2	Htr7	Katnal2
Dgka	Edil3	Fam214a	Gal3st1	Gna15	Gstt3	Icam4	Kcnc3
Dhrs4	Efcab12	Fam221b	Gal3st4	Gng7	Guca1a	Idnk	Kcnj15
Dhtkd1	Ell3	Fam53b	Galm	Gnpda2	Gucy1a3	Ifih1	Kcnk1
Dio3	Eno2	Fbln2	Galt	Gpr135	Gucy1b3	Ifit1	Kcnn1
Dmrt2	Enpp5	Fbxl20	Gamt	Gpr137b	H2-DMa	Ifit2	Kctd1
Dnah8	Entpd2	Fbxl21	Gatsl2	Gpr153	H2-Q4	Ift122	Kctd8
Dnaic2	Epas1	Fbxl7	Gca	Gpr45	H2-T-ps	Igf1	Kdm6b
Dnajb4	Ephb3	Fbxo17	Gdf9	Gpr85	Hacl1	Igfbp5	Kif13b
Dnajc12	Ephx2	Fbxo44	Gdpd1	Gpt2	Havcr2	Igsf1	Kif9
Dnal1	Etfbkmt	Fcgrt	Ggh	Gpx7	Hecw1	Ikbke	Kiss1r
Dnase1l1	Etfrf1	Fez1	Ggn	Gramd3	Hey2	Il1rl2	Kitl
Dnase2a	Etnk2	Fgd4	Gipc3	Grb14	Hic1	Il27ra	Klc4
Dok7	Extl1	Fggy	Gla	Grcc10	Hist1h2ac	Il2rg	Klf1
Dpep1	Ezh1	Fibin	Glb1l	Grik2	Hist1h2bg	Ip6k3	Klf9
Dpp4	F630042J09Rik	Fkbp14	Gldc	Grin2b	Hist1h3g	Irf7	Klhdc1

Kyat1	Manba	Mmp16	Nkain4	Pcdha5	Pisd-ps3	Procr	Rln1
L3hypdh	Map1lc3b	Mmp2	Nkiras1	Pcdhga10	Piwil4	Prox1	Rnaset2b
Lacc1	Mapk12	Mmp28	Nlrx1	Pcdhga12	Pkdrej	Prss12	Rnd2
Lama1	Mapk1ip1	Mppe1	Nme5	Pcdhga5	Plat	Psd3	Rnf165
Lama2	Mapre3	Mr1	Nol3	Pcdhga7	Plcg2	Ptger2	Robo3
Ldhb	Mapt	Mrc2	Nostrin	Pcdhga8	Plcxd1	Ptgir	Rom1
Lgals3bp	Mast1	Msc	Nox4	Pcdhgb2	Pld1	Ptpn7	Rragb
Lgmn	Mcee	Mxd4	Npr2	Pcdhgb4	Plekha4	Pxmp4	Rsph3b
Lhfpl1	Mcf2l	Myct1	Nqo2	Pcdhgb5	Plekhb1	Pxylp1	Rsph9
Lipa	Mcpt8	Myh14	Nr1h3	Pde10a	Plekhg6	Rab13	Rtp4
Lmbr1	Mctp2	Myl2	Nsun7	Pde4b	Plekhh3	Rab3a	Runx1
Lmcd1	Meg3	Myo18b	Ntng2	Pde8b	Plin2	Rab44	Rwdd3
Lpin1	Meis1	Myo5c	Nwd1	Pdpn	Plin3	Rad51ap2	S100a13
Lpin3	Mettl7a1	Mypop	Ociad2	Peli3	Plppr2	Ramp1	Sall1
Lrrc32	Mfsd4b4	Mzf1	Ogdhl	Per3	Pmp22	Rasgrp2	Scamp5
Lrrc4c	Mfsd6	Naga	Ogn	Perm1	Pnck	Rasl11b	Scand1
Lrrc9	Mfsd7c	Nap1l3	P2rx6	Pfkfb2	Podn	Rbl2	Scrn3
Lrriq3	Mfsd9	Naprt	Pabpc5	Pgam2	Pon3	Rcan3	Scube3
Lrrn4cl	Mgst1	Nbeal2	Pappa2	Pgf	Ppara	Rfx5	Sdhaf4
Ly6c1	Mgst3	Nbl1	Paqr7	Pik3r3	Ppargc1a	Rgma	Sdr42e1
Lyn	Mill2	Ndst4	Parp10	Pip5k1b	Ppp1r3d	Rgs3	Sec14l2
Mageh1	Mir3101	Nectin4	Parp12	Pip5kl1	Prcp	Rhag	Sema3b
Magix	Mir568	Nfkbie	Pcbd2	Pir	Prdm8	Rian	Sema4f
Man1c1	Mmp11	Nipal3	Pcdh9	Pisd-ps1	Prkcz	Rida	Serhl

Serpinb1a	Slc27a1	Snx32	Tec	Tmem173	Trappc6a	Unc93b1	Zfp219
Serpinb9	Slc2a5	Spata2l	Tef	Tmem176a	Trim12c	Usp18	Zfp300
Serpine2	Slc35d2	Speg	Tfec	Tmem200c	Trim13	Vamp5	Zfp442
Serping1	Slc35g2	Spock3	Tfr2	Tmem220	Trim2	Vipr2	Zfp459
Setbp1	Slc37a1	Ssh3	Tgfbi	Tmem45a	Trim21	Vmac	Zfp608
Sft2d2	Slc46a3	Sstr4	Tgm2	Tmem51os1	Trim34a	Vnn1	Zfp652os
Sgip1	Slc7a4	St6galnac6	Thbs3	Tmem74	Trim46	Vsir	Zfp874b
Sgsh	Slc7a7	Stat1	Thnsl2	Tmem86a	Trpv4	Wasf3	Zfp941
Sh3pxd2a	Slc9a3r1	Stat3	Tle6	Tmlhe	Tspan11	Wdr19	Zkscan14
Shisa3	Slc9a9	Synpo2	Tlr1	Tmtc1	Tspoap1	Wdr6	Zrsr1
Shpk	Slfn2	Syt11	Tlr2	Tnc	Ttc30b	Wnt2	
Shroom1	Smim1	Syt5	Tlr3	Tnfrsf18	Ttc38	Yipf2	
Slc19a3	Smpdl3a	Tap2	Tm7sf3	Tnfrsf26	Tubb4a	Ypel3	
Slc22a18	Sncg	Tapbp	Tmc6	Tnxb	Tubg2	Ypel5	
Slc25a21	Snph	Tcea3	Tmem117	Tob1	Txndc16	Zbtb20	
Slc25a45	Snx20	Tceal1	Tmem141	Toporsos	Ugt1a6a	Zfp133-ps	
Slc26a1	Snx31	Tctn2	Tmem14a	Trank1	Ugt1a6b	Zfp174	

Cluster 5 (461)

1700024F13Rik	Aox3	Car3	Dcp2	Fmnl1	Hck	Itih4	Mcm4
1700109H08Rik	Arglu1	Carmil1	Dctpp1	Fmr1	Hirip3	Ivns1abp	Mcm5
1700120K04Rik	Arl4a	Cbx1	Ddx39b	Fndc4	Hist1h2ag	Kcnb2	Mcm8
1810032O08Rik	Asap2	Ccdc24	Degs2	Fubp1	Hist1h2bk	Kcng2	Mdrl
2010204K13Rik	Asf1a	Ccdc34	Dek	G530011O06Rik	Hist1h2bm	Kcnh2	Mertk
2010300C02Rik	Asic4	Ccdc57	Dlgap1	Gabbr2	Hist1h4d	Kcnj14	Mgat3
2700099C18Rik	Atad5	Ccdc73	Dlk1	Gabpb2	Hjurp	Kcnk3	Miat
3010003L21Rik	Atg9b	Cd34	Dlx1as	Gas7	Hmgb1	Kcnq3	Miga1
4930404I05Rik	Atp11c	Cd5	Dlx2	Gcat	Hmgb2	Kif11	Mipol1
4930429F24Rik	AW551984	Cd84	Dmp1	Gcnt1	Hmgcs1	Kif15	Mir17hg
4930558J18Rik	AW554918	Cdc45	Dna2	Gins1	Hmgn2	Kl	Mir18
4933413G19Rik	B430212C06Rik	Cdc7	Dnd1	Gipc2	Hmgn5	Krt18	Mir1898
5930403L14Rik	Baalc	Cdca5	Dnmt3b	Gm11545	Hnrnpa1	Krt8	Mir19a
9130227L01Rik	Baat	Cdca7	Dnph1	Gm12504	Hnrnpa1l2-ps2	L1cam	Mir19b-1
9330182L06Rik	Bambi	Cdk3-ps	Dock8	Gm15421	Hnrnpa3	Lcor	Mir20a
9430015G10Rik	Bcl2	Ceacam1	Dpysl5	Gm15471	Hnrnpd	Lhx6	Mir25
A3galt2	Bcl7a	Cenpl	Dscc1	Gm16701	Hnrnpdl	Lig1	Mis18bp1
A530032D15Rik	Bean1	Cenpm	Duox1	Gm16897	Hnrnph1	Limd2	Mmp13
A630072M18Rik	Bex1	Cep126	Efcc1	Gm25500	Hnrnph3	Lingo2	Mnd1
A630089N07Rik	Bex2	Cep135	Elavl4	Gm2897	Hnrnpr	Lmnb1	Mns1
A830082N09Rik	Bex4	Chd3os	Elovl6	Gm5129	Homer1	LOC100862268	Msh3
Acat2	Bmp2	Chek1	Eml4	Gm5176	Hunk	Lpcat1	Mss51
Acp5	Brca2	Chga	Erbb4	Gm5643	Idh2	Lrrc19	Myc
Acsl3	Bsn	Chrna4	Espnl	Gm5796	Idi1	Lsr	Mycl
Adam21	Btbd18	Chrna6	Esyt3	Gm6277	Ifi211	Luc7l	Myod1
Adgrl1	Bzw2	Chst9	Ewsr1	Gmnn	Igsf9	Lypd6	Myot
Ak4	C130050O18Rik	Chsy3	Fam169a	Gnmt	Il12rb2	Mamdc4	Naaa
Aldh1a7	C3	Chtop	Fam60a	Gpr50	Il1rn	Map3k1	Naaladl2
Amhr2	C4b	Cmss1	Far1os	Greb1l	Ilf2	Map3k9	Naip5
Ank	Cables1	Cntf	Fdft1	Grk3	Iqgap2	Mapk11	Nampt
Ankrd61	Cacng5	Cort	Fgfr4	Grm7	Iqsec3	Marcksl1	Nasp
Ankrd66	Cadm1	Cpsf6	Fjx1	H19	Irs4	Matr3	Necab2
Anp32b	Cadps	Cxadr	Fkbp4	H2afx	Itga6	Mbd4	Nefm
Anp32e	Car10	Dcakd	Fkbp5	H2afy2	Itgam	Mcm3	Nespas

Nkain2	Pclaf	Ppid	Rpgr	Slc2a3	Snord47	Syce1	Traf1
Nlrc4	Pcna	Ppifos	Rph3al	Slc2a4rg-ps	Snord53	Sycp2l	Trib2
Nmt2	Pcp4l1	Ppih	Rpia	Slc35f2	Snord69	Syne2	Ttn
Npas3	Pcsk4	Ppp1r1a	Rpl22l1	Slc36a2	Snord72	Syt7	Ttyh1
Npw	Pcsk6	Prdm16	Rpl34	Slc5a5	Snord73a	Taf1d	Tube1
Nr1h5	Pdcd7	Prim1	Rps6ka6	Slc7a2	Snord91a	Taf4b	Tyms
Nrcam	Pde7a	Prodh	Rtbdn	Slc9b2	Snord98	Tceal7	Ube2ql1
Nrg2	Pdzd4	Prss16	Rtn4r	Smad9	Snrpd3	Tdp2	Unc79
Nrip2	Pecr	Prss8	Samd1	Smpdl3b	Snx22	Tex30	Ung
Nrp	Pgbd5	Psip1	Sclt1	Sncaip	Sost	Tfap2a	Usp1
Nsmce4a	Pgr	Psors1c2	Sel1l3	Snhg1	Sowahc	Tfap4	Usp37
Nudt10	Phf14	Ptbp2	Sephs1	Snhg6	Sp7	Tgfbr1	Vrk1
Nudt11	Phox2a	Ptma	Sfpq	Snora33	Spag17	Tgif2	Vwa3a
Nxf1	Piezo2	Rad54b	Sh2d3c	Snora41	Spc24	Timeless	Wasf1
Obox6	Pik3c2b	Rbpjl	Shisa8	Snora52	Spib	Tipin	Wfdc2
Ogfrl1	Pik3cg	Rexo5	Shtn1	Snora64	Srd5a1	Tm4sf19	Xist
Olfm2	Pim3	Rfc3	Siglec15	Snora69	Srek1	Tmem243	Zc3hav1l
Onecut1	Pla2g7	Rfc4	Slc11a1	Snora70	Srsf2	Tmem268	Zfp367
Opcml	Plekha8	Rif1	Slc16a1	Snord15b	Srsf7	Tmem86b	Zfp472
P2rx2	Pnn	Rims3	Slc16a14	Snord17	Sstr2	Tmpo	Zglp1
Paqr9	Poc1b	Ripk4	Slc22a14	Snord19	Stx19	Tnfaip3	Znrf3
Pard6b	Pold1	Rmi2	Slc23a4	Snord1c	Sub1	Tnfrsf13b	
Pate4	Poln	Rnf223	Slc24a5	Snord2	Suv39h2	Top2a	
Pcdh18	Pou2f1	Rpa2	Slc29a1	Snord22	Sybu	Tpd52l1	

Cluster 6 (927)

40787	Actc1	Arf2	Blm	Cdc6	Cpne1	Dhx37	Eif3c
1700012B09Rik	Actg1	Arhgap11a	Bmp8a	Cdca2	Cpsf2	Diaph3	Eif3d
1700015F17Rik	Actr8	Arhgap19	Bmp8b	Cdca4	Crabp1	Dimt1	Eif4g1
2310002F09Rik	Acvr1b	Arhgap32	Bmpr1b	Cdca8	Creld2	Dkc1	Eif5a
2310007B03Rik	Adam12	Arhgap36	Bop1	Cdh23	Crispld2	Dlk2	Eif5b
2310057M21Rik	Adarb1	Arhgdig	Brca1	Cdh3	Crybg1	Dlst	Eif6
2610028E06Rik	Adat1	Arhgef37	Brms1	Cdh4	Cse1l	Dnaaf2	Elac2
2700054A10Rik	Adpgk	Armc6	Btaf1	Cdk1	Csf3	Dnaaf5	Elof1
2810408I11Rik	Adsl	Arpc5	Bub1	Cenpe	Cstf1	Dnaja3	Eme1
3110082I17Rik	Afdn	Arv1	Bysl	Cenpi	Cstf3	Dnajb11	Eml5
3930402G23Rik	Afg3l1	Asap1	C1qbp	Cenpu	Ctdp1	Dnajc11	Enoph1
4930427A07Rik	Agps	Ascl1	C330027C09Rik	Cep192	Cthrc1	Dnmt1	Epb41l1
4930447F24Rik	Ahctf1	Asf1b	C530008M17Rik	Cep55	Ctnna1	Dock5	Epha1
4933404O12Rik	AI115009	Asns	Cad	Cep78	Ctnnal1	Dph2	Eps8
6030458C11Rik	AI506816	Atad3a	Cars	Cfap69	Ctps	Dph5	Erc1
6720468P15Rik	Aida	Atf6	Cavin3	Cfl1	Ctsw	Dqx1	Ercc1
6820408C15Rik	Aimp2	Atic	Cbx5	Chchd4	Cycs	Drd4	Ercc6l
9330188P03Rik	Ajuba	Atp10a	Ccdc110	Chordc1	D030028A08Rik	Dus4l	Eri2
9830107B12Rik	Ak5	Atp6v1c2	Ccdc134	Chtf18	Dapk3	Dusp4	Errfi1
9930014A18Rik	Akap1	Atp8b1	Ccdc86	Ciapin1	Dbf4	Dusp9	Esf1
A530064D06Rik	Akr1c18	Aunip	Cck	Cinp	Dcaf13	Dynap	Esm1
Aaas	Aldoart1	Aurka	Cckar	Cipc	Dclre1b	E2f7	Espl1
Aatf	Alg8	Aurkb	Ccm2	Cit	Ddx18	E330033B04Rik	Eva1a
Abce1	Als2	B3gnt5	Ccna2	Ckap2l	Ddx20	Ebna1bp2	Exo1
Abcf1	Anapc15	B430306N03Rik	Ccnb1	Cldn12	Ddx21	Ebp	Exosc1
Abcf2	Angptl7	Bach2	Ccnf	Clec4d	Ddx31	Ecel1	Exosc6
Abhd17c	Ankrd28	Baz1a	Ccnyl1	Cluh	Ddx39	Ect2	Exosc8
Abracl	Ankrd49	BC030867	Cct3	Cnih4	Ddx56	Edn1	Exosc9
Acaca	Anln	BC055324	Cct6a	Cnn2	Denr	Edn2	Ezr
Acan	Ap2a2	Bend6	Cct7	Cnst	Dgcr8	Eef1e1	F2rl1
Acot10	Ap5b1	Bend7	Cd300lb	Coch	Dhcr24	Eif1ad	Fam111a
Acsl4	Apln	Bicc1	Cd3eap	Col4a3bp	Dhfr	Eif2b3	Fam131b
Acsl6	Aqr	Birc5	Cdc20	Coq5	Dhrs9	Eif2s1	Fam19a5
Actb	Areg	Birc6	Cdc42bpa	Cpn2	Dhx29	Eif3b	Fam57a

Fam72a	Gemin6	Haspin	Ilk	Klk10	Mak16	Mphosph10	Nek11
Fam83d	Gen1	Hat1	Imp4	Klk8	Mal2	Mpp6	Nek2
Fam84a	Gfm1	Haus6	Inhba	Klk9	Map2k3	Mrpl12	Nemp1
Fam84b	Gjb2	Hbegf	Ints5	Kmt5a	Map2k3os	Mrpl47	Neto1
Fam98a	Gm12603	Hdgf	Ipo11	Knl1	Map2k4	Mrps10	Ngef
Fancb	Gm14137	Heatr1	Ipo4	Knop1	Map3k14	Mrps18b	Nhp2
Fancf	Gm15867	Heatr3	Ipo5	Kpna2	Mars	Mrps22	Nkain1
Far1	Gm15910	Heatr5a	Iqgap3	Kpnb1	Mast2	Mrto4	Nkrf
Farp2	Gm15915	Hells	Itga3	Kras	Mastl	Msmo1	Nln
Fasn	Gm26633	Hgh1	Itgae	Kri1	Mboat1	Mt3	Nmd3
Fastkd3	Gm29811	Hip1r	Jak2	Krt80	Mcm10	Mterf1a	Nme1
Fbxo48	Gm3636	Hipk4	Katnbl1	Krtdap	Mcph1	Mthfd1	Noc2l
Fbxo5	Gm5088	Hivep3	Kbtbd12	L3mbtl2	Mdn1	Mthfd1l	Noc3l
Fcrl1	Gm6756	Hmga1	Kbtbd8	Lad1	Me2	Mthfd2	Noct
Fdps	Gm7694	Hmga2	Kcnf1	Lamb3	Med14	Mtmr10	Nog
Fen1	Gm8773	Hmmr	Kcnip1	Lancl3	Med18	Mtmr4	Nol10
Fermt2	Gnl3	Homer2	Kcnk10	Larp1	Melk	Mum1l1	Nol12
Fgf5	Golim4	Hs3st3b1	Kcnk13	Larp1b	Met	Mvk	Nol8
Fhdc1	Got1	Hs6st3	Kcnk5	Larp4b	Metap1	Mybbp1a	Nol9
Fignl1	Gpat3	Hsd17b7	Kcnn4	Las1l	Metrnl	Mybl2	Nolc1
Fosl1	Gpat4	Hsp90aa1	Kcnq5	Lbr	Mettl14	Myl7	Nom1
Foxm1	Gpatch4	Hspbap1	Kctd9	Lgals3	Mfsd2a	Myo19	Nop14
Foxn2	Gphn	Hspd1	Kdm8	Lin54	Micalcl	Naa15	Nop2
Fscn1	Gpr1	Hsph1	Kif18b	Lin9	Mid1ip1	Naa25	Nop58
Fsip1	Grem2	Htra2	Kif20a	Llgl2	Mief1	Nanp	Nop9
Fstl4	Grik3	Hyls1	Kif20b	Llph	Mif	Nars	Nov
Ftsj3	Grk1	Iars	Kif22	Lrp8	Miga2	Nat10	Nova1
Fut8	Grk6	Ide	Kif2a	Lrr1	Mir155hg	Ncam1	Npas4
Gar1	Grp	Idh3a	Kif4	Lrrc59	Mir1949	Ncapg	Nppb
Gart	Grwd1	Ifrd1	Kifc1	Lrrd1	Mir6942	Ncapg2	Nptx2
Gatad1	Gspt1	Ifrd2	Kifc5b	Lrtm2	Mir7667	Nckap1	Nr1h4
Gchfr	Gsr	Igf2os	Kin	Lsm11	Mirt1	Ncl	Nras
Gclm	Gstcd	Ikzf2	Klc1	Lyar	Mis12	Ncs1	Nsl1
Gcnt4	Gzmk	Il15ra	Klf5	Mad2l1	Mmp3	Ndc80	Nsun2
Gemin4	Hacd2	Il1rl1	Klhdc8a	Magi3	Mob3a	Ndufaf4	Nudcd1
Gemin5	Hars	Il31ra	Klhl2	Magohb	Morc4	Nedd1	Nup107

Nup133	Pdgfb	Ppwd1	Rars	S100a7a	Slc29a2	Stip1	Tmem125
Nup155	Pdss1	Prc1	Rbm19	Sass6	Slc34a1	Stk32a	Tmem130
Nup160	Pdss2	Prkag2	Rbp4	Sbf2	Slc38a4	Strn3	Tmem144
Nup35	Pelp1	Prkar2a	Rbpj	Sbsn	Slc39a11	Supv3l1	Tmem171
Nup37	Pfas	Prkar2b	Rcc1	Sbspon	Slc44a4	Surf6	Tmem186
Nup43	Phgdh	Prkci	Rcl1	Scn5a	Slc5a6	Suv39h1	Tmem190
Nup85	Pif1	Prkg2	Relt	Sdad1	Slc6a12	Sv2c	Tmem200a
Nup93	Pik3cb	Prmt7	Rfwd3	Sdc2	Slc7a1	Swap70	Tmem238
Nutm1	Pinx1	Prr11	Rgs19	Sdf2l1	Slco2a1	Syde2	Tmem97
Nxph3	Pitrm1	Prr5l	Rhobtb3	Selenoi	Slf1	Syn1	Tnfsf13b
Odc1	Plaa	Prss2	Rhou	Sema3e	Smc2	Synpo2l	Tnk2
Ogdh	Plagl2	Prune2	Rilp	Sephs2	Smc4	Syt8	Tnk2os
Opn3	Plaur	Psat1	Rims2	Serpinb2	Smtn	Sytl5	Tnn
Orc1	Plk1	Psmc1	Riox2	Sertad2	Smurf2	Tacc3	Tns3
Orc2	Plk4	Psmd12	Ripor2	Sertad4	Smyd2	Tagln2	Tomm40
Ormdl2	Plscr2	Psmd14	Rnf126	Set	Smyd5	Tars	Tomm70a
Osbpl3	Pmch	Psme3	Rnf219	Sf3a2	Snora17	Tatdn2	Topbp1
Otud4	Pmp2	Psmg3	Rnf39	Sfn	Snora2b	Tbc1d10b	Tpm3
Otud7a	Pmpca	Ptgs2	Rnft1	Sgms1	Snora74a	Tbl3	Tpx2
Ovol1	Pno1	Ptgs2os	Rpf2	Sgms2	Snord12	Tbrg3	Traf3
Oxct2b	Poc1a	Ptpn22	Rpl29	Sgo1	Snord43	Tbrg4	Traip
Oxsr1	Podnl1	Ptprn	Rpl7l1	Sgo2a	Snord52	Tcof1	Tram1
Pa2g4	Polh	Pum3	Rpp30	Sh2d1b1	Snrpd1	Tead1	Trdmt1
Pabpc4	Polq	Pus1	Rps6ka4	Sh3bp5l	Spata5l1	Tead4	Trip13
Padi2	Polr1a	Pus7	Rras2	Shb	Spata9	Tfdp1	Trmt6
Pak2	Polr1b	Pusl1	Rrm1	Shcbp1	Spcs3	Tfpi2	Trmt61a
Pak7	Polr1e	Pwp1	Rrm2	Shmt1	Spdl1	Tfrc	Troap
Palb2	Polr3g	Pwp2	Rrp12	Shmt2	Spire1	Thoc5	Trpc6
Parl	Pop1	Qsox2	Rrp15	Ska2	Spop	Thumpd3	Tspan33
Parpbp	Ppa1	Rad18	Rrp1b	Slc14a1	Spp1	Ticrr	Tspan4
Pcdh19	Pparg	Rad51	Rrp7a	Slc17a8	Sptlc1	Timm10	Tsr1
Pcgf5	Ppargc1b	Rad51ap1	Rrp8	Slc19a1	Sqle	Timm17a	Ttk
Pcnt	Ppat	Rad54l	Rrp9	Slc1a5	Srf	Timm8a1	Ttll12
Pcolce2	Ppif	Ran	Rrs1	Slc25a22	Srm	Tjp2	Ttll4
Pcyox1l	Ppm1l	Rangap1	Rtkn2	Slc25a24	Srpk1	Tmcc3	Tuba1c
Pdcd11	Ppp2r1b	Rangrf	Ruvbl2	Slc25a5	Steap1	Tmem123	Tubb3

Tubb4b	Uchl3	Usp10	Vat1l	Wdr36	Wee1	Ybx3	Zfp568
Tut1	Uchl4	Usp14	Vav3	Wdr43	Wnt7a	Ydjc	Zfp689
Txn1	Uchl5	Usp31	Vcam1	Wdr46	Wnt7b	Ywhah	Zfp7
Txnrd3	Uck2	Uspl1	Vgf	Wdr55	Wrb	Zbed4	Zfp72
U90926	Ugcg	Ust	Vsig10	Wdr63	Wwc1	Zcchc2	Zfp850
Ubap2	Uhrf1bp1l	Utp15	Wbscr17	Wdr74	Xpo4	Zfp111	Zfp961
Ube2c	Ulbp1	Utp18	Wdfy1	Wdr75	Xpo5	Zfp202	Znhit6
Ube2t	Umps	Utp4	Wdr12	Wdr77	Xpot	Zfp354a	Zw10
Ubox5	Urb1	Uts2b	Wdr18	Wdr89	Yars	Zfp503	Zwilch
Uchl1	Urb2	Vars	Wdr3	Wdr95	Yars2	Zfp518b	

Journal of Dental Research
2017, Vol. 96(2) 186–191

DOI: 10.1177/0022034516682001
journals.sagepub.com/home/jdr

Mesenchymal Cell Community Effect in Whole Tooth Bioengineering

L. Yang[1], A. Angelova Volponi[1], Y. Pang[1], and P.T. Sharpe[1]

Abstract

In vitro expanded cell populations can contribute to bioengineered tooth formation but only as cells that respond to tooth-inductive signals. Since the success of whole tooth bioengineering is predicated on the availability of large numbers of cells, in vitro cell expansion of tooth-inducing cell populations is an essential requirement for further development of this approach. We set out to investigate if the failure of cultured mesenchyme cells to form bioengineered teeth might be rescued by the presence of uncultured cells. To test this, we deployed a cell-mixing approach to evaluate the contributions of cell populations to bioengineered tooth formation. Using genetically labeled cells, we are able to identify the formation of tooth pulp cells and odontoblasts in bioengineered teeth. We show that although cultured embryonic dental mesenchyme cells are unable to induce tooth formation, they can contribute to tooth induction and formation if combined with noncultured cells. Moreover, we show that teeth can form from cell mixtures that include embryonic cells and populations of postnatal dental pulp cells; however, these cells are unable to contribute to the formation of pulp cells or odontoblasts, and at ratios of 1:1, they inhibit tooth formation. These results indicate that although in vitro cell expansion of embryonic tooth mesenchymal cells renders them unable to induce tooth formation, they do not lose their ability to contribute to tooth formation and differentiate into odontoblasts. Postnatal pulp cells, however, lose all tooth-inducing and tooth-forming capacity following in vitro expansion, and at ratios >1:3 postnatal:embryonic cells, they inhibit the ability of embryonic dental mesenchyme cells to induce tooth formation.

Keywords: odontogenic capacity, tooth inducing cells, in vitro expansion, postnatal dental pulp cells, mixed cell recombination, root formation

Introduction

Whole tooth bioengineering has long been a goal of regenerative dentistry that, despite some recent progress, still has a number of difficult challenges to overcome. Tissue recombination experiments demonstrated sequential signaling between dental epithelium and mesenchyme (Mina and Kollar 1987; Lumsden 1988). This was followed by experiments that showed the ability of embryonic tooth germ cells to reaggregate following dissociation and form teeth (Yamamoto et al. 2003) and has since been used as a model to explore whole tooth bioengineering (Nakao et al. 2007; Nait Lechguer et al. 2008; Ikeda et al. 2009; Oshima et al. 2011). Thus, epithelium and mesenchyme tissues from E14.5- to E12.5-stage mouse tooth germs can be separated and the cells dissociated and recombined to form normal teeth. The reciprocal tissue induction that takes place during the early stages of tooth development, whereby the epithelium first induces tooth formation in the mesenchyme followed by a reciprocal induction from mesenchyme to epithelium, has been utilized to suggest a basis for whole tooth bioengineering that could employ adult cells (Jernvall and Thesleff 2000; Tucker and Sharpe 2004; Zhang et al. 2005). Thus, when mesenchyme cells derived from adult bone marrow are combined with inductive-stage embryonic dental epithelium, tooth formation is induced, and the adult mesenchymal cells respond and fully contribute to tooth development (Ohazama et al. 2004). To date, the only cells that have been shown to be capable of tooth-inductive capacity are embryonic cells (epithelium or mesenchyme) isolated from tooth germs (Ohazama et al. 2004; Angelova Volponi et al. 2013). Furthermore, in all experiments reported to date, the inductive cells, whether epithelial or mesenchymal, do not retain their inductive capacity following in vitro expansion (Zheng et al. 2016). This thus poses a major problem in tooth bioengineering. Clearly, the use of fresh (uncultured) embryonic tooth germ cells is not feasible in any clinical context. Generation of cell lines from embryonic inductive cells is also not feasible, since these cells lose their inductive capacity, in addition to any issues that use of such allogeneic cells may have for generation of nonessential organs such as teeth.

Adult cell populations have been shown to be capable of forming bioengineered teeth as recipient cells combined with inductive embryonic cell populations (Duailibi et al. 2004; Takahashi et al. 2010). Thus, as stated above, adult bone

[1]Department of Craniofacial Development and Stem Cell Biology, Dental Institute, King's College London, London, UK

A supplemental appendix to this article is available online.

Corresponding Author:
P.T. Sharpe, Department of Craniofacial Development and Stem Cell Biology, 27th floor, Tower Wing, Guy's Hospital, London SE1 9RT, UK.
Email: paul.sharpe@kcl.ac.uk

marrow mesenchymal cells can do this (Ohazama et al. 2004), as can adult gingival epithelial cells (Angelova Volponi et al. 2013). The challenge, therefore, is to identify adult cell populations that can be expanded in large numbers, ideally as autologous cells where one population, either mesenchyme or epithelium, has tooth-inducing capacity.

The rapid loss of tooth-inducing capacity by embryonic tooth germ cells, when expanded in vitro, is not understood, and as a way of beginning to understand this process, we investigated whether this ability might be rescued by embryonic cells. We found that uncultured embryonic tooth germ mesenchymal cells were able to rescue cultured cells and enable them to fully participate into bioengineered tooth development, forming pulp cells and odontoblasts. However, this rescue effect was not observed with postnatal dental pulp mesenchyme cells, despite these being of the same developmental origin as the embryonic cells. The rescue of cultured cells by the presence of fresh cells shows characteristics of the community effect identified during embryonic development as a process that enables mixtures of different cells to differentiate along the same pathway.

Materials and Methods

Experimental Mouse Strains

To trace the origins of the cells contributing to the tooth primordia formation in epithelium-mesenchyme recombination experiments, 3 strains of mice were used: wild-type mice (CD1 mice), transgenic mice expressing green fluorescent protein (GFP mice), and transgenic mice expressing membrane-targeted red fluorescent protein (tandem dimer Tomato) prior to Cre recombinase exposure (mTmG mice). All animal procedures conformed to the Animal Research: Reporting of In Vivo Experiments (ARRIVE) guidelines and in accordance with UK Home Office regulations.

Isolation of Embryonic Dental Epithelium and Mesenchymal Cells

Intact bilateral molar tooth germs were dissected from E12.5 (for epithelial tissue) and E14.5 (for mesenchymal embryonic cells) mouse embryos, utilizing sterile fine needles in Leibovitz's L-15 medium (21083-027; Gibco). After being trimmed from the surrounding tissue, tooth germs were transferred into 1.2 U/mL of Dispase and incubated at 37 °C for 40 min. After being washed in L-15 medium, epithelium and mesenchyme of the tooth germs were mechanically separated with fine needles. The embryonic mesenchymal cells were obtained by digesting the isolated mesenchymal tissue with Trypsin (TrypLE Express) and used as fresh (dissociated) cells from wild-type (CD1) mice or cultured from GFP (green) mice and recombined with epithelial tissue (mTmG mice). The embryonic dental mesenchymal cells were resuspended in complete alpha-minimum essential medium (BE02-002F; BioWhittaker) with 15% fetal bovine serum (10270-106; Gibco), 1% antibiotic-antimycotic (15240-062; Gibco), and 0.1mM L-ascorbic acid (49752; Sigma-Aldrich); plated in 6-well cell culture plates or 75-cm^2 cell culture flasks (CELLSTAR); and then incubated at 37 °C, 5% carbon dioxide, for 7 d. The embryonic mesenchymal cells were used at P0 (passage 0).

Postnatal dental pulp cells were obtained from molars of GFP (green) mice pups (7 d old). Postnatal molar pulp pieces were digested in a mixture of enzymes containing 2 mg/mL of Collagenase D (Roche) and 120 U/mL of Dispase (Roche) in phosphate-buffered saline (PBS) for 50 min, blocked with complete alpha-minimum essential medium, and filtered through a 70-µm cell strainer (352350; BD Falcon) to obtain a uniform single-cell suspension. These cells were cultured in a 6-well plate at a density of 1.2 to 1.5 × 10^5 cells/well. Medium was changed every 2 to 3 d, and passaging was performed when the cells were 70% confluent. These cells were used in recombination experiments with E12.5 embryonic tooth germ epithelium at P1 (passage 1).

Recombination of Epithelium and Mesenchymal Cells

Recombinations were carried out as previously described (Angelova Volponi et al. 2013). Briefly, mesenchymal cells (2 × 10^5) were centrifuged in a polymerase chain reaction tube (0.2 mL; STARLAB) to form a pellet and then injected on the top of 4 to 5 pieces of isolated E12.5 uncultured epithelium tissue with sharpened fine pipette tips (20 µL; GELoader) in a 25-µL gel drop of Cellmatrix Type I-A (Nitta Gelatin) and placed on a cell culture insert (4.0-µm pore size; BD). The recombination was cultured for 9 to 11 d on the cell culture insert containing 1.5 mL/well of complete alpha-minimum essential medium.

Renal Transfers

The surgical transfer of tissue explants (recombinations) into renal capsules was performed as previously described (Angelova Volponi et al. 2013). Samples were scanned with a Skyscan 1272 Bruker micro–computed tomography (micro-CT) and analyzed with Microview software (GE).

Imaging

Recombination samples were fixed in 4% paraformaldehyde for 20 min, washed 3 times for 5 min in 1× PBS, and mounted on slides via mounting medium with DAPI (H-1200; VECTASHIELD).

Coverslips on top of the specimen were sealed around the perimeter with nail polish. Fluorescent tomography scans were performed on processed samples with a z-stack imaging program on a confocal microscope (Leica TCS SP5).

Results

Cell Mixing of Embryonic Tooth Germ Cells

To develop a foolproof experimental protocol that could be used to test the contribution of mesenchymal cell populations to bioengineered tooth formation, we utilized genetically

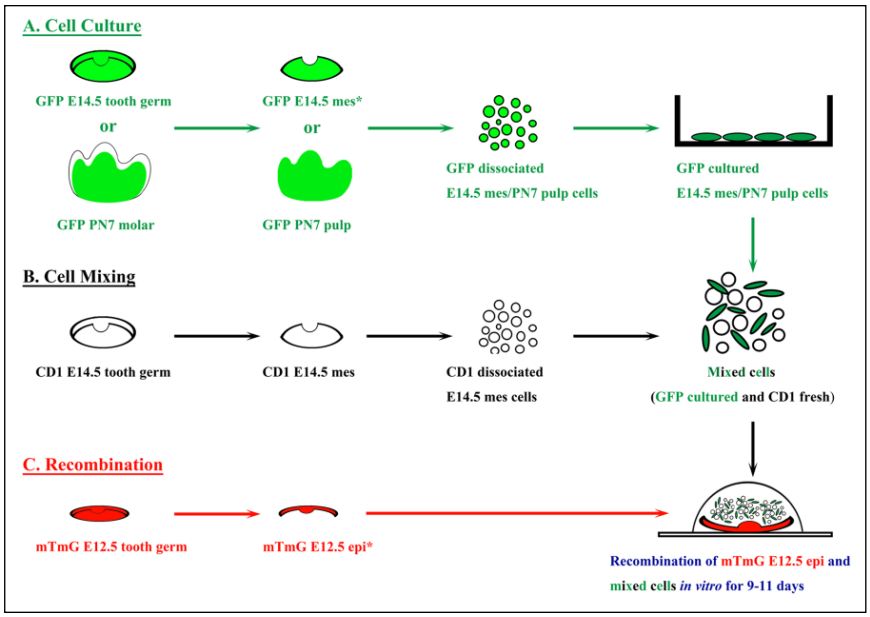

Figure 1. Schematic representation of recombinations through cell mixtures. (**A**) Cell culture: in vitro expansion of green fluorescent protein (GFP) mouse E14.5 molar tooth germ mesenchymal cells or PN7 molar pulp cells. (**B**) Cell mixing: cultured GFP cells (either E14.5 mesenchymal cells or PN7 pulp cells) were mixed with noncultured (fresh) CD1 E14.5 molar tooth germ mesenchymal cells at different ratios (cultured:fresh = 1:9, 1:3, 1:1, 3:1, 9:1). (**C**) Recombination: mixtures of cultured GFP cells and noncultured CD1 cells recombined with mTmG mouse E12.5 molar tooth germ epithelial tissue in vitro for 9 to 11 d. mes, mesenchyme; epi, epithelium.

marked mouse lines to follow cell fates. Since mesenchymal cell contamination is commonly observed following physical separation of embryonic dental epithelium from developing tooth germs, we used isolated epithelium at the E12.5 embryonic stage from a mouse reporter (mTmG mice) line where all cells are marked red, with fresh (dissociated) cells of wild-type mice (CD1, no fluorescent expression) and with cultured embryonic mesenchymal cells from transgenic mice expressing GFP (Fig. 1). In this way, any contamination with mesenchymal cells could be easily detected. We used a GFP reporter line for the isolation of mesenchymal cells whose fates were to be followed during bioengineered tooth formation, and we combined these with wild-type, uncultured mesenchymal cells.

We first verified the methodology by recombining fresh, dissociated (uncultured) E14.5 dental mesenchymal cells with E12.5 fresh epithelial tissue. In this recombination, the epithelial cells have not yet received inductive cells; thus, the mesenchymal cells are expected to induce tooth formation in the epithelial tissue. As expected, tooth germs were observed in 100% of the recombination experiments (Appendix Table). To determine if cultured embryonic E14.5 tooth mesenchyme cells could induce tooth formation, we combined GFP-positive (green) cells with E12.5 tooth germ epithelium, and in these combinations, no tooth germs were observed ($n = 11$; Appendix Table, Appendix Fig. 2B).

We next set out to investigate if the presence of uncultured E14.5 mesenchyme cells with cultured cells was sufficient to enable the cultured cells to participate in tooth formation. E14.5 cultured mesenchyme cells were mixed with fresh (dissociated) wild-type cells of E14.5 embryos in different ratios (Appendix Table). The mixtures of cells were recombined with embryonic epithelial tissue at stage E12.5 from mTmG mice, a reporter line where all cells are marked red. After 11 d in culture, we observed tooth germ formation in the experiments where the cultured embryonic mesenchymal cells constituted 10%, 50%, and 75% of the mesenchymal cell mixture (Appendix Table; Fig. 2), with clear participation of the cultured cells to the tooth pulp (Fig. 2A2, B2, C2). Cultured cells were also clearly visible (GFP positive, green) adjacent to epithelium, exhibiting an elongated appearance characteristic of odontoblasts (Fig. 2A3, B3, C3). When the embryonic mesenchymal cultured cells constituted 90% of the cells used in the mixture with 10% uncultured (fresh) cells, no formation of tooth germs was observed ($n = 10$; Appendix Table; Fig. 4A). Although there was variation in the numbers of GFP-positive cells observed in the tooth germs within a single experiment, there was a consistent general trend of increased cultured cell contribution with increased cell number. Significant variation in tooth germ shape was also observed in all recombinations regardless of the ratio of fresh:cultured cells. This is a usual phenomenon that we observe with this form of recombinations, and it is illustrated in Appendix Figure 3.

To study if the mixtures of cultured and fresh tooth cells could develop further to the mineralization stages and initiate root development, subcapsular transplantations of toothlike structures/tooth primordia in mouse kidney were performed. After 9 d of in vitro culture, toothlike structures/tooth primordia—formed in recombinations with cell mixtures consisting of 75% cultured GFP and 25% fresh CD1 E14.5 molar germ mesenchymal cells and mTmG E12.5 molar germ epithelial tissue—were transplanted under kidney capsules of adult (4 to 6 wk) CD1 mouse hosts. The host mice were sacrificed after 4 wk, and the implants were separated from the kidney capsules and fixed in 4% paraformaldehyde in PBS overnight at 4 °C. After being washed with PBS, specimens were scanned by a Skyscan 1272 Bruker micro-CT scanner. The specimens were scanned to produce 6.5-µm-voxel-size volumes, with an x-ray tube voltage of 80 kVp and a tube current of 125 µA. An aluminum filter (0.05 mm) was used to adjust the energy distribution of the x-ray source. The specimens were characterized further by 3-dimensional slice volumes, generated and measured with Microview software (GE). After micro-CT scan, specimens were embedded and mounted on slides for confocal fluorescent tomography scans, as in the procedure described in the "Imaging" section for recombination samples (Appendix Fig. 4, 5).

Cell Mixing of Postnatal Dental Pulp Cells

Postnatal dental pulp cells were isolated from molars of 7-d-old transgenic mice expressing GFP and expanded in culture for 10 d (passaged once; P1) prior to mixing with embryonic mesenchymal dissociated cells, and then the cell mixtures were recombined with epithelium (E12.5) of mTmG mice. Mixtures of 25%, 50%, and 100% of cultured postnatal dental pulp cells with nonlabeled (wild-type CD1 mice) dissociated embryonic mesenchymal cells (Appendix Table) were combined with E12.5 epithelium. After 11 d of culture, tooth germ formation was observed in the mixtures of 25% of cultured dental pulp cells (Fig. 3). Although a few individual cultured dental pulp cells could be seen in 25% mixtures (Fig. 3B–D), they did not contribute to tooth germ formation, and the majority of postnatal cells were excluded from the teeth formed in recombinations (Fig. 3A2). No tooth germ formation was observed in the mixture containing ≥50% cultured cells (Fig. 4B).

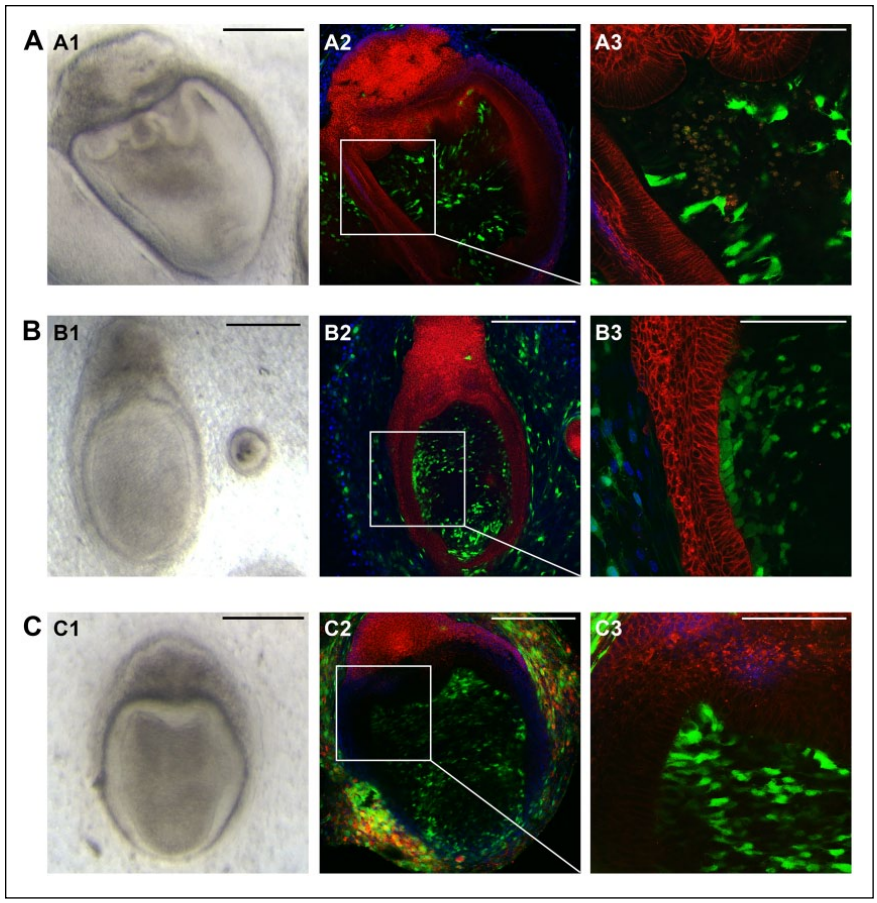

Figure 2. Recombinations of mTmG E12.5 molar germ epithelial tissue (red) and mixtures of cultured green fluorescent protein (GFP) molar tooth germ mesenchymal cells (green) and CD1 wild-type (nonlabeled) tooth germ dissociated cells: (**A**) 10% cultured GFP (green) and 90% fresh CD1 E14.5 molar germ mesenchymal cells, (**B**) 50% cultured GFP and 50% fresh CD1 E14.5 molar germ mesenchymal cells, (**C**) 75% cultured GFP and 25% fresh CD1 E14.5 molar germ mesenchymal cells. Toothlike structures formed in recombinations with cell mixtures consisting of no more than 75% cultured E14.5 tooth germ mesenchymal cells (A1, B1, C1: bright field). Green (GFP^+) cells could be seen adjacent to the epithelium (A2, B2, C2), exhibiting an elongated appearance (A3, B3, C3). Scale bars: 250 µm (A1-2, B1-2, C1-2); 100 µm (A3, B3, C3).

These results suggested that the presence of postnatal mesenchyme cells is inhibiting the ability of embryonic cells to induce tooth formation. An alternative explanation is that, since the postnatal cells are noninductive, the embryonic cells are the only inductive cells in the mixture, and their number may be below the threshold for induction. We thus repeated the 50% cultured postnatal cell mixture with 4 times the number of cells (4×10^5 embryonic and 4×10^5 postnatal cells). Since we know that the 75% cultured embryonic cell experiments (0.5×10^5 fresh and 1.5×10^5 cultured embryonic cells) can induce tooth formation (Fig. 2C), 4×10^5 fresh embryonic cells should be sufficient for induction. No tooth germ formation was observed with these increased cell numbers, suggesting that the postnatal cells are indeed inhibiting the tooth-inducing capacity of embryonic cells.

Discussion

The ability to reproduce embryonic tooth formation from combinations of dissociated cells in vitro forms a general concept for bioengineered tooth formation. In all such cell combinations, one of the cell populations, either epithelium or mesenchyme, needs to have tooth-inducing capacity. Thus, for example, embryonic tooth epithelium isolated from an embryonic stage where it is inductive can induce nondental cells, such as bone marrow stromal cells, to form teeth (Ohazama et al. 2004). Similarly, embryonic tooth mesenchymal cells from an inductive embryonic stage can induce formation in nondental epithelium from adult gingiva (Angelova Volponi et al. 2013). Since cells isolated from midgestation embryos are not usable in a clinical context, alternative inductive cell populations are required that can ideally be isolated from adult tissues and expanded in vitro to provide sufficient cell numbers. However, even embryonic tooth-inducing cells rapidly lose the inductive capacity following expansion in vitro, and until the basis for this loss is understood, further realistic progress toward a clinically usable bioengineered tooth system is not possible.

The use of a recombination of dissociated cells as an assay for cell-inductive capacity in organ formation relies on the ability to obtain populations of epithelial and mesenchymal cells

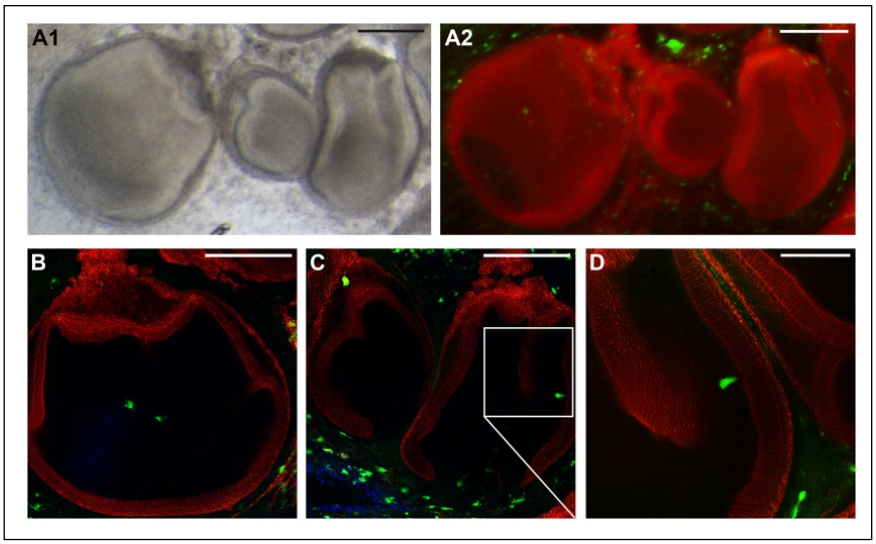

Figure 3. Toothlike structures formed in recombinations with cell mixtures consisting of 25% cultured green fluorescent protein–positive (GFP^+) postnatal (PN7) molar pulp cells. (**A**) In recombinations of mTmG E12.5 molar germ epithelial tissue (red) and 25% cultured GFP PN7 molar pulp cells (green) and 75% fresh wild-type (CD1) E14.5 molar germ mesenchymal cells (nonlabeled), toothlike structures were formed after 11 d in vitro (A1), and the majority of postnatal cells (green) were excluded from the toothlike structures (A2). Few cultured GFP^+ (green) cells could be seen inside the tooth primordia (**B–D**). Scale bars: 250 µm (A, B, C), 100 µm (D).

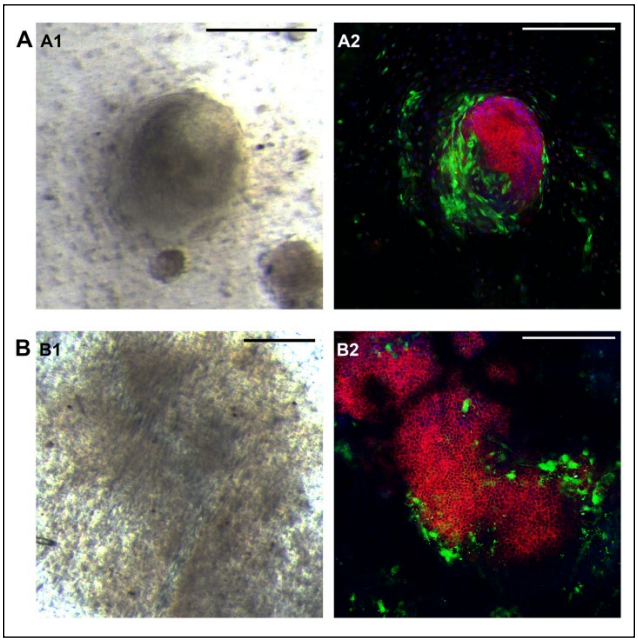

Figure 4. Failure of tooth formation in recombinations with cell mixtures consisting of 90% cultured E14.5 tooth germ mesenchymal cells or 50% cultured PN7 pulp cells. (**A**) Cystlike structures rather than teeth were formed in recombinations of mTmG E12.5 molar germ epithelial tissue (red) and 90% cultured green fluorescent protein (GFP) E14.5 molar germ mesenchymal cells (green) and 10% fresh CD1 E14.5 molar germ mesenchymal cells (nonlabeled), shown in bright field (A1) and confocal scan (A2). (**B**) 50% cultured GFP PN7 molar pulp cells (green) and 50% fresh CD1 E14.5 molar germ mesenchymal cells (nonlabeled) failed to form toothlike structures, shown in bright field (B1) and confocal scan (B2). Scale bar: 250 µm.

that are not cross-contaminated. Since cells proliferate in ex vivo tissue recombinations/reassociations, contamination of one population with even a small number of cells of the other population could lead to misleading results. We validated our cell dissociation methodology by using genetically labeled cell populations that can be easily distinguished by fluorescent markers.

The formation of tooth primordia from dissociated embryonic tooth epithelial and mesenchymal cells has been reported to require a minimum of $13.5 \pm 0.5 \times 10^4$ mesenchymal cells when recombined with epithelial cells (Nait Lechguer et al. 2008). We have also observed a minimum cell number requirement of $15.2 \pm 0.5 \times 10^4$ mesenchymal cells in our recombination experiments. In our cell-mixing experiments with cultured embryonic mesenchyme cells, we used a total mesenchyme cell number of 2.0×10^5. Tooth formation was observed with inductive mesenchyme cell numbers ranging from 5×10^4 to 1.8×10^5 in the mixture. Thus, in the mixture containing 5×10^4 (25%) inductive mesenchyme cells with 1.5×10^5 (75%) cultured cells, there are insufficient inductive cells alone for tooth formation. This suggests that the cultured cells are likely to be actively participating in tooth induction.

If current methods are to be used in any therapeutic context to generate bioengineered human teeth, the cell numbers needed will have to be obtained from in vitro cell expansion. However, it has been established that culture of inductive embryonic tooth primordia cells results in a rapid loss of inductive capacity (Zheng et al. 2016). In vitro cell expansion does not affect the ability of either epithelial or mesenchymal cells to participate in tooth formation; thus, obtaining sufficient cell numbers of a recipient cell population does not present a problem for bioengineering (Ohazama et al. 2004; Angelova Volponi et al. 2013).

During embryonic development, a process called the "community effect" can act to allow heterogeneous cell populations to differentiate down a common pathway by cells interacting with their immediate neighbors (Gurdon et al. 1993). To begin to understand the cellular basis for this rapid loss in inductive capacity in cell culture, we set out to investigate if an artificially generated community effect whereby inductive tooth mesenchymal cells (i.e., uncultured embryonic cells) might rescue the loss-inductive capacity following expansion in vitro. We showed that as few as 25% inductive tooth mesenchyme cells, when mixed with noninductive tooth mesenchyme cells, were sufficient to induce tooth formation and, for the noninductive cells, to fully participate in tooth formation, including differentiation into odontoblasts. At proportions ≥90% of noninductive cells, no tooth formation was observed. This observation is consistent with mathematical models of the

community effect that show that cell density must be above a critical threshold for the effect to occur (Saka et al. 2011). The embryonic community effect is most often described in terms of cell signaling regulating transcription to generate cell homogeneity (Gurdon et al. 1993). Implicit in this is the assumption that all cells in the community express common signaling receptors; thus, we assume that the most likely cause of the loss in tooth-inductive capacity is the loss of cell signal secretion rather than loss of receptors.

Dental pulp cells of adult teeth can be easily cultured in vitro as heterogeneous populations that contain cells with stem cell–like properties (Gronthos et al. 2000; Gronthos et al. 2002; d'Aquino et al. 2007; Jo et al. 2007; Huang et al. 2009; Koyama et al. 2009; Waddington et al. 2009; Balic et al. 2010; Volponi and Sharpe 2013). These cells have the same embryonic origin (cranial neural crest) as tooth primordia mesenchyme cells and are thus candidates for cells that might be used in tooth bioengineering. We therefore investigated whether postnatal tooth pulp cells are able to participate in the community effect provided by embryonic inductive cells. Proportions of postnatal pulp cells >25% in mixtures with inductive mesenchyme cells failed to form teeth. At ≤25%, although teeth formed, there was no contribution of postnatal cells to tooth formation. Tooth formation failure occurred with an inductive cell number of 1.0×10^5 (50%) that, in the absence of any postnatal cells in the mixture, is sufficient to induce tooth formation. We increased this number to 4.0×10^5 cells and still failed to observe any tooth formation when mixed with an equal number of postnatal pulp cells. The presence of adult tooth pulp cells thus appears to inhibit the ability of embryonic cells to induce tooth formation. Although this could be a simple dilution effect, we believe that this is unlikely, since even with increased numbers of inductive cells, there was still no evidence of tooth formation. Why postnatal pulp cells should have this effect is not currently understood. Adult mesenchyme cells are able to fully participate in bioengineered tooth formation as recipient cells for epithelial inductive signals, and so the inhibition of tooth formation that we observed in the mixtures is most likely prevention of inductive signals from the embryonic mesenchyme. One possible mechanism may be the secretion of signaling inhibitors by the postnatal pulp cells. Understanding the molecular basis of this phenomenon is important for future progress in tooth bioengineering.

Author Contributions

L. Yang, A. Angelova Volponi, Y. Pang, contributed to design and data interpretation, drafted the manuscript; P.T. Sharpe, contributed to conception and data interpretation, drafted the manuscript. All authors gave final approval and agree to be accountable for all aspects of the work.

Acknowledgments

L. Yang is supported by a China Scholarship Council award. We thank Yang Ma and Ana Caetano for their help. The authors declare no potential conflicts of interest with respect to the authorship and/or publication of this article.

References

Angelova Volponi A, Kawasaki M, Sharpe PT. 2013. Adult human gingival epithelial cells as a source for whole-tooth bioengineering. J Dent Res. 92(4):329–334.

Balic A, Aguila HL, Caimano MJ, Francone VP, Mina M. 2010. Characterization of stem and progenitor cells in the dental pulp of erupted and unerupted murine molars. Bone. 46(6):1639–1651.

d'Aquino R, Graziano A, Sampaolesi M, Laino G, Pirozzi G, De Rosa A, Papaccio G. 2007. Human postnatal dental pulp cells co-differentiate into osteoblasts and endotheliocytes: a pivotal synergy leading to adult bone tissue formation. Cell Death Differ. 14(6):1162–1171.

Duailibi MT, Duailibi SE, Young CS, Bartlett JD, Vacanti JP, Yelick PC. 2004. Bioengineered teeth from cultured rat tooth bud cells. J Dent Res. 83(7):523–528.

Gronthos S, Brahim J, Li W, Fisher LW, Cherman N, Boyde A, DenBesten P, Robey PG, Shi S. 2002. Stem cell properties of human dental pulp stem cells. J Dent Res Aug. 81(8):531–535.

Gronthos S, Mankani M, Brahim J, Robey PG, Shi S. 2000. Postnatal human dental pulp stem cells (DPSCs) in vitro and in vivo. Proc Natl Acad Sci U S A. 97(25):13625–13630.

Gurdon JB, Lemaire P, Kato K. 1993. Community effects and related phenomena in development. Cell. 75(5):831–834.

Huang GT, Gronthos S, Shi S. 2009. Mesenchymal stem cells derived from dental tissues vs. those from other sources: their biology and role in regenerative medicine. J Dent Res. 88(9):792–806.

Ikeda E, Morita R, Nakao K, Ishida K, Nakamura T, Takano-Yamamoto T, Ogawa M, Mizuno M, Kasugai S, Tsuji T. 2009. Fully functional bioengineered tooth replacement as an organ replacement therapy. Proc Natl Acad Sci U S A. 106(32):13475–13480.

Jernvall J, Thesleff I. 2000. Reiterative signalling and patterning during mammalian tooth morphogenesis. Mech Dev. 92(1):9-29.

Jo YY, Lee HJ, Kook SY, Choung HW, Park JY, Chung JH, Choung YH, Kim ES, Yang HC, Choung PH. 2007. Isolation and characterization of postnatal stem cells from human dental tissues. Tissue Eng. 13(4):767–773.

Koyama N, Okubo Y, Nakao K, Bessho K. 2009. Evaluation of pluripotency in human dental pulp cells. J Oral Maxillofac Surg. 67(3):501–506.

Lumsden AG. 1988. Spatial organization of the epithelium and the role of neural crest cells in the initiation of the mammalian tooth germ. Development. 103 Suppl:155–169.

Mina M, Kollar EJ. 1987. The induction of odontogenesis in non-dental mesenchyme combined with early murine mandibular arch epithelium. Arch Oral Biol. 32(2):123–127.

Nait Lechguer A, Kuchler-Bopp S, Hu B, Haïkel Y, Lesot H. 2008. Vascularization of engineered teeth. J Dent Res. 87(12):1138–1143.

Nakao K, Morita R, Saji Y, Ishida K, Tomita Y, Ogawa M, Saitoh M, Tomooka Y, Tsuji T. 2007. The development of a bioengineered organ germ method. Nat Methods. 4(3):227–230.

Ohazama A, Modino SA, Miletich I, Sharpe PT. 2004. Stem-cell-based tissue engineering of murine teeth. J Dent Res. 83(7):518–522.

Oshima M, Mizuno M, Imamura A, Ogawa M, Yasukawa M, Yamazaki H et al. 2011. Functional tooth regeneration using a bioengineered tooth unit as a mature organ replacement regenerative therapy. PloS One. 6(7):e21531.

Saka Y, Lhoussaine C, Kuttler C, Ullner E, Thiel M. 2011. Theoretical basis of the community effect in development. BMC Syst Biol. 5:54.

Takahashi C, Yoshida H, Komine A, Nakao K, Tsuji T, Tomooka Y. 2010. Newly established cell lines from mouse oral epithelium regenerate teeth when combined with dental mesenchyme. In Vitro Cell Dev Biol Anim. 46(5):457–468.

Tucker A, Sharpe P. 2004. The cutting-edge of mammalian development: how the embryo makes teeth. Nat Rev Genet. 5(7):499–508.

Volponi AA, Sharpe PT. 2013. The tooth: a treasure chest of stem cells. Br Dent J. 215(7):353–358.

Waddington RJ, Youde SJ, Lee CP, Sloan AJ. 2009. Isolation of distinct progenitor stem cell populations from dental pulp. Cells Tissues Organs. 189(1–4):268–274.

Yamamoto H, Kim EJ, Cho SW, Jung HS. 2003. Analysis of tooth formation by reaggregated dental mesenchyme from mouse embryo. J Electron Microsc (Tokyo). 52(6):559–566.

Zhang YD, Chen Z, Song YQ, Liu C, Chen YP. 2005. Making a tooth: growth factors, transcription factors and stem cells. Cell Res. 15(5):301–316.

Zheng Y, Cai J, Hutchins AP, Jia L, Liu P, Yang D, Chen S, Ge L, Pei D, Wei S. 2016. Remission for loss of odontogenic potential in a new micromilieu in vitro. PLoS One. 11(4):e0152893.